

**Implementation of the Mechanistic-Empirical Pavement
Design Guide in Mississippi**

**Implementation and Preliminary Local
Calibration of Pavement ME Design in
Mississippi
Volume I**

Report No. FHWA/MS-DOT-RD-017-284

[Task 15—Final Report]

**Prepared for:
Mississippi Department of Transportation
Research Division
P.O. Box 1850
Jackson, Mississippi 39215-1850**

**Prepared by:
Harold L. Von Quintus, P.E.
Chetana Rao, PhD
Biplab Bhattacharya, P.E.
Applied Research Associates, Inc.
100 Trade Centre Blvd., Suite #200
Champaign, Illinois**

May 15, 2017

DISCLAIMER STATEMENT

This document is disseminated under the sponsorship of the Mississippi Department of Transportation and the United States Department of Transportation in the interest of information exchange. The State of Mississippi and the United States Government assume no liability of its contents or use thereof.

The contents of this report reflect the views of the authors, who are responsible for the facts and accuracy of the data presented herein. The contents do not necessarily reflect the official policies of the Mississippi Department of Transportation or the United States Department of Transportation.

The State of Mississippi and the United States Government do not endorse products of manufacturers. Trademarks or manufacturers' names appear herein only because they are considered essential to the object of this document.

ACKNOWLEDGEMENTS

This report was prepared under sponsorship of the Mississippi Department of Transportation. The project team recognizes and appreciates the services provided by the Mississippi Department of Transportation. These services included complying traffic data and assistance with project activities to recover construction properties and performance/distress data from selected roadway segments. Specific individuals involved in the work and providing data for the validation/calibration study are listed below.

Bill Barstis, PE
Cindy Smith, PE
Jeff Wages, PE
James Watkins, PE
Randy Battey, PE
Trung Trinh
Alex Collum, EIT
DeMarco Harris

Technical Report Documentation Page

1. Report No. FHWA/MDOT-RD-17-284		2. Government Accession No.		3. Recipient's Catalog No.	
4. Title and Subtitle Update State Study No. 170 Deliverables with New PCC Test Data Revised final report for SS No. 170, "AASHTO 2002 Pavement Design Guide-Phase II" – Volume 1		5. Report Date May 15, 2017		6. Performing Organization Code	
		8. Performing Organization Report No.			
7. Author(s) Harold L. Von Quintus, PE, Chetana Rao, PhD, Biplab Bhattacharya, PE.		10. Work Unit No. (TRAIS)			
9. Performing Organization Name and Address Rao Research and Consulting, LLC 60 Hazelwood Dr. Champaign, IL 61820		11. Contract or Grant No. SPR-2017(023)/107552-101000			
		13. Type of Report and Period Covered Final Report May-May 2017			
12. Sponsoring Agency Name and Address Mississippi Department of Transportation PO Box 1850 Jackson, MS 39215-1850		14. Sponsoring Agency Code			
		15. Supplementary Notes The following final deliverables for SS No. 284 also constitute the corresponding final deliverables for SS No. 170 "AASHTO 2002 Pavement Design Guide –Phase II": Final Report, Mississippi DOT Pavement ME Design User Input Guide, Materials Database Explanation: MDOT funded State Study No. 177, "Inputs of Portland Cement Concrete Parameters needed for the Design of New and Rehabilitated Pavements in Mississippi," Project No. SPR-1 (45)/104323-120000 to provide PCC material inputs for design of rigid pavements using the MEPDG design methodology. The PCC material inputs from SS No. 177 were incorporated into the final deliverables for SS No. 170. After the completion of SS No. 177, FHWA discovered an issue with the coefficient of thermal expansion (CTE) test procedure. To ensure accurate CTE values for MDOT PCC mixes in AASHTOWare Pavement ME design procedure, Burns Cooley Dennis, Inc. (BCD) performed laboratory testing for MDOT using the same mix designs considered in SS No. 177. This testing was conducted under a work assignment with BCD entitled "Laboratory Data to Determine Impact of Coarse Aggregate Type and Cementitious Materials on Design Thickness of PCC Pavements," Project No. SP-9999-09(110)/106812-101000. The final deliverables for SS No. 284 are updated versions of select SS No. 170 deliverables; i.e., updated with the BCD test data and corresponding text related to PCC as revised by Dr. Rao.			
16. Abstract The objective of this research study was to develop performance characteristics of flexible and rigid pavements in Mississippi and to use these characteristics in the implementation of the Mechanistic-Empirical Pavement Design procedure that was developed under NCHRP Project 1-37A. Reliable transfer function and models will enable Mississippi Department of Transportation (MDOT) to more accurately quantify the pavement service and performance life for managing their roadway network. Calibration coefficients for all transfer functions in the Pavement ME Design software package were determined for both flexible and rigid pavements. Both Long Term Pavement Performance (LTPP) and non-LTPP test sections were used to estimate, for interim use, the local calibration coefficients. The inputs for the non-LTPP calibration sites were based on as-built records and construction files. Thus, these calibration coefficients are considered preliminary until the field investigations have been completed for the non-LTPP sites.					
17. Key Words Pavement Design, Pavement ME Design, Mechanistic-Empirical, Fatigue Cracking, Rutting, Thermal Cracking, IRI, Smoothness, Calibration, Transfer Functions, Distress Prediction Models.			18. Distribution Statement Unrestricted. This document is available through the National Technical Information Service, Springfield, VA 21161.		
19. Security Classification of this Report: Unclassified.		20. Security Classification of this Page: Unclassified.		21. No. of Pages 224	22. Price

SI* (MODERN METRIC) CONVERSION FACTORS				
APPROXIMATE CONVERSIONS TO SI UNITS				
Symbol	When You Know	Multiply By	To Find	Symbol
LENGTH				
In	Inches	25.4	Millimeters	mm
Ft	Feet	0.305	Meters	m
Yd	Yards	0.914	Meters	m
Mi	Miles	1.61	Kilometers	km
AREA				
in²	square inches	645.2	square millimeters	mm ²
ft²	square feet	0.093	square meters	m ²
yd²	square yard	0.836	square meters	m ²
Ac	Acres	0.405	Hectares	ha
mi²	square miles	2.59	square kilometers	km ²
VOLUME				
fl oz	fluid ounces	29.57	Milliliters	mL
Gal	Gallons	3.785	Liters	L
ft³	cubic feet	0.028	cubic meters	m ³
yd³	cubic yards	0.765	cubic meters	m ³
[NOTE: volumes greater than 1,000 shall be shown in m ³]				
MASS				
Oz	Ounces	28.35	Grams	g
Lb	Pounds	0.454	Kilograms	kg
T	short tons (2000 lb)	0.907	megagrams (metric tons)	Mg (or t)
TEMPERATURE (exact degrees)				
°F	Fahrenheit or (F-32)/1.8	5 (F-32)/9	Celsius	°C
ILLUMINATION				
Fc	foot-candles	10.76	Lux	lx
Fl	foot-Lamberts	3.426	candela/m ²	cd/m ²
FORCE and PRESSURE or STRESS				
Lbf	Pounds	4.45	Newtons	N
lbf/in² (psi)	pounds per square inch	6.89	kiloPascals	kPa
k/in² (ksi)	kips per square inch	6.89	megaPascals	MPa
DENSITY				
lb/ft³ (pcf)	pounds per cubic foot	16.02	kilograms per cubic meter	kg/m ³
APPROXIMATE CONVERSIONS FROM SI UNITS				
Symbol	When You Know	Multiply By	To Find	Symbol
LENGTH				
Mm	Millimeters	0.039	Inches	in
M	Meters	3.28	Feet	ft
M	Meters	1.090	Yards	yd
Km	Kilometers	0.621	Miles	mi
AREA				
mm²	square millimeters	0.0016	square inches	in ²
m²	square meters	10.764	square feet	ft ²
m²	square meters	1.195	square yards	yd ²
Ha	Hectares	2.47	Acres	ac
km²	square kilometers	0.386	square miles	mi ²
VOLUME				
mL	Milliliters	0.034	fluid ounces	fl oz
L	Liters	0.264	Gallons	gal
m³	cubic meters	35.314	cubic feet	ft ³
m³	cubic meters	1.307	cubic yards	yd ³
MASS				
G	Grams	0.035	Ounces	oz
Kg	Kilograms	2.202	Pounds	lb
Mg (or t)	megagrams (metric tons)	1.103	short tons (2000 lb)	T
TEMPERATURE (exact degrees)				
°C	Celsius	1.8C+32	Fahrenheit	°F
ILLUMINATION				
lx	Lux	0.0929	foot-candles	fc
cd/m²	candela/m ²	0.2919	foot-Lamberts	fl
FORCE and PRESSURE or STRESS				
N	Newtons	0.225	Pounds	Lbf
kPa	kiloPascals	0.145	pounds per square inch	lbf/in ² (psi)
Mpa	MegaPascals	0.145	kips per square inch	k/in ² (ksi)
DENSITY				
kg/m³	pounds per cubic foot	0.062	kilograms per cubic meter	lb/ft ³ (pcf)

*SI is the symbol for the International System of Units. Appropriate rounding should be made to comply with Section 4 of ASTM E 380. (Revised March 2003)

TABLE OF CONTENTS

LIST OF TABLES.....	ix
LIST OF FIGURES	xii
ABBREVIATIONS	xvi
CHAPTER 1—INTRODUCTION	1
1.1 BACKGROUND	1
1.2 PHASED IMPLEMENTATION APPROACH.....	2
1.3 SCOPE OF REPORT	3
1.4 DESIGN STRATEGIES INCLUDED IN CALIBRATION	4
1.4.1 New/Reconstructed Flexible Pavements and HMA Overlays	4
1.4.2 New/Reconstructed Rigid Pavements and PCC Overlays.....	5
1.5 DEFINITION OF TERMS	6
CHAPTER 2—OVERVIEW OF THE MEPDG DESIGN METHODOLOGY	8
2.1 INPUT CATEGORIES	8
2.2 HIERARCHICAL INPUT APPROACH.....	8
2.3 TRANSFER FUNCTIONS.....	12
2.3.1 Flexible and Semi-Rigid Pavements	13
2.3.2 Rigid Pavements.....	20
2.4 STANDARD ERROR OF ESTIMATE.....	23
2.5 DATA REQUIREMENTS	24
CHAPTER 3—CALIBRATION SAMPLING MATRIX	26
3.1 CALIBRATION OBJECTIVE AND OUTCOMES	26
3.2 CALIBRATION EXPERIMENTAL HYPOTHESIS.....	28
3.3 EXPERIMENTAL PLAN AND SAMPLING MATRIX.....	28
3.3.1 Experimental Factors	30
3.3.2 Number and Types of Calibration Sites.....	30
3.4 NUMBER AND TYPES OF CALIBRATION SITES	31
3.5 FIELD INVESTIGATIONS.....	31
CHAPTER 4—TRUCK TRAFFIC	35
4.1 TRUCK VOLUME—AVERAGE ANNUAL DAILY TRUCK TRAFFIC	35
4.2 TRUCK VOLUME FACTORS	35
4.3 NUMBER OF AXLES PER TRUCK CLASS.....	38
4.4 AXLE CONFIGURATION AND GEOMETRY AND OTHER TRUCK FACTORS	39
4.5 NORMALIZED AXLE LOAD DISTRIBUTION FACTORS.....	40
CHAPTER 5—CLIMATE	41
5.1 COUNTY WEATHER STATIONS	41
5.2 DEPTH TO WATER TABLE OR GROUND WATER.....	42
5.3 DEPTH TO BEDROCK OR RIGID LAYERS	44
CHAPTER 6—LAYER FEATURES.....	45
6.1 INITIAL INTERNATIONAL ROUGHNESS INDEX.....	45
6.2 STRUCTURAL LAYER FEATURES	45
6.2.1 Flexible Pavement Layers.....	45
6.2.2 Rigid Pavement Structural Layers: JPCP and CRCP	49

CHAPTER 7—MATERIAL PROPERTIES	53
7.1 ASPHALT CONCRETE MIXTURES	53
7.1.1 Volumetric Properties.....	54
7.1.2 Engineering Properties	56
7.2 PORTLAND CEMENT CONCRETE MIXTURES	57
7.2.1 PCC Mixture Properties	57
7.2.2 Existing PCC Slabs.....	64
7.2.3 Other PCC Layer Inputs.....	64
7.3 CEMENT TREATED BASE MIXTURES	64
7.4 UNBOUND AGGREGATE BASE AND SOIL LAYERS/MATERIALS	65
7.4.1 General Physical and Volumetric Properties	65
7.4.2 Resilient Modulus	66
7.4.3 Poisson’s Ratio	79
7.4.4 Hydraulic Properties.....	79
7.5 STABILIZED SUBGRADE FOR STRUCTURAL LAYERS	79
CHAPTER 8—VERIFICATION AND CALIBRATION OF FLEXIBLE PAVEMENT TRANSFER FUNCTIONS	81
8.1 FATIGUE ALLIGATOR CRACKING; BOTTOM-UP CRACKING	81
8.1.1 Verification of Calibration Coefficients.....	81
8.1.2 Local Calibration of Alligator Cracking Transfer Function	82
8.2 TOTAL RUTTING	89
8.2.1 Verification of the Global Calibration Coefficients.....	89
8.2.2 Mississippi Local Calibration Coefficients.....	91
8.3 TRANSVERSE THERMAL CRACKING	96
8.3.1 Verification of the Global Calibration Coefficients.....	96
8.3.2 Local Calibration Coefficient	96
8.4 SMOOTHNESS	98
8.4.1 Global MEPDG HMA Smoothness Model Verification.....	98
8.4.2 Local Calibration of the MEPDG HMA Smoothness Model for Mississippi	99
8.5 ESTIMATING DESIGN RELIABILITY FOR NEW HMA AND HMA OVERLAY PAVEMENT DISTRESS MODELS	102
CHAPTER 9—VERIFICATION AND CALIBRATION OF RIGID PAVEMENT TRANSFER FUNCTIONS	104
9.1 JPCP TRANSVERSE, MID-SLAB CRACKING	104
9.1.1 Global MEPDG Transverse Cracking Model Verification.....	104
9.1.2 Local Calibration of the MEPDG Transverse Cracking Model for Mississippi	105
9.2 JPCP TRANSVERSE JOINT FAULTING.....	109
9.2.1 Global MEPDG JPCP Transverse Joint Faulting Model Verification.....	109
9.2.2 Summary of JPCP Transverse Faulting Verification Results	110
9.3 JPCP SMOOTHNESS	114
9.3.1 Global MEPDG JPCP Smoothness Model Verification.....	114
9.3.2 Local Calibration of Mississippi JPCP IRI Model	114
9.4 ESTIMATING DESIGN RELIABILITY FOR NEW JPCP DISTRESS MODELS	118
CHAPTER 10—SUMMARY AND RECOMMENDATIONS	120
10.1 FINDINGS: ACCURACY AND PRECISION OF TRANSFER FUNCTIONS	120
10.2 RECOMMENDATIONS: MISSISSIPPI’S TRANSFER FUNCTIONS CALIBRATION COEFFICIENTS.....	123

REFERENCES	124
APPENDIX A—INPUT CHECKLIST FOR MISSISSIPPI	127
APPENDIX B—MATERIAL SAMPLING AND TESTING PLANS FOR NON-LTPP PROJECTS USED FOR LOCAL CALIBRATION	138
B.1 INTRODUCTION	138
B.1.1 Purpose of Document	138
B.1.2 Background	138
B.2 NEW CONSTRUCTION NON-LTPP PROJECTS WITH CRITICAL DATA MISSING	139
B.3 REQUIREMENTS FOR THE SAMPLING AND TESTING PLAN	140
B.4 PRIORITIZATION OF ROADWAY SEGMENTS INCLUDED IN THE FIELD MATERIAL SAMPLING AND TESTING PLAN	141
B.5 MATERIAL AND LAYER PROPERTIES FOR PAVEMENT ME DESIGN	142
B.5.1 HMA Inputs—Overlays and Existing Layers Prior to Overlay	142
B.5.2 Stabilized Layer Inputs—Overlays and Existing Layers Prior to Overlay	144
B.5.3 Unbound Aggregate Layers and Subgrade Material Property Inputs, Prior to Overlay Placement	144
B.5.4 PCC Inputs—Overlays and Surface Layers with PCC	145
B.6 SAMPLING AND FIELD TESTING PLAN FOR THE HMA, UNBOUND AGGREGATE LAYERS, EMBANKMENTS, SUBGRADES, AND PCC LAYERS	146
B.7 LABORATORY TESTING PLAN FOR THE HMA, UNBOUND AGGREGATE LAYERS, EMBANKMENTS, SUBGRADE, AND PCC LAYERS	146
B.8 SUGGESTED STEPS FOR PLANNING THE FIELD INVESTIGATIONS	147
ATTACHMENT B.1.....	152
MATERIALS SAMPLING & FIELD TESTING PLAN FOR NEW CONSTRUCTION & OVERLAY PROJECTS – NON-LTPP SECTIONS	152
APPENDIX C—MS-ATLAS: TRUCK TRAFFIC ANALYSIS TOOL	156
APPENDIX D—NORMALIZED AXLE LOAD DISTRIBUTION factors OR AXLE LOAD SPECTRA	160
APPENDIX E—GROUND WATER DEPTH TOOL	176
E.1 INTRODUCTION	176
E.2 TERMINOLOGIES AND CONCEPTS USED IN THE GWT TOOL	176
E.2.1 Water Table	177
E.2.2 Aquifers and Wells	177
E.2.3 Ground Water Table Depth	177
E.2.4 Time Dependent Changes to the Water Table Depth	178
E.2.5 Water Level in Wells from Confined Aquifers	178
E.3 DESCRIPTION OF GWT TOOL AND USER INTERFACE	180
E.3.1 Launching GWT Tool	180
E.3.2 User Interface and Definition of Terms	183
E.3.3 Find Location	183
E.3.4 Google Earth Layers	184
E.3.5 Information for Selected Area	184
E.3.6 Information for Selected Well	188
E.4 DETERMINATION OF WATER TABLE DEPTH	189
E.4.1 Setting Filters	189

E.4.2	Other Settings.....	190
E.4.3	Determining Water Table Depth for Project.....	190
APPENDIX F—DYNAMIC MODULUS TEST RESULTS.....		192
APPENDIX G—CALIBRATION OF RUT DEPTH TRANSFER FUNCTION.....		200
G.1	INTRODUCTION.....	200
G.2	TEST TEMPERATURE OPTION AND NUMBER OF TEST SPECIMENS.....	201
G.2.1	Option A – Multiple Test Temperatures.....	201
G.2.2	Option B – Equivalent Test Temperatures.....	201
G.3	TEST SPECIMEN PREPARATION.....	201
G.3.1	Short Term Aging of the Asphalt Concrete Mixture.....	202
G.3.2	Specimen Compaction.....	202
G.3.3	Grouping of Test Specimens.....	202
G.4	REPEATED LOAD TRIAXIAL TESTING.....	203
G.5	DETERMINATION OF PLASTIC STRAIN COEFFICIENTS.....	203
G.6	HMA MIXTURE EVALUATION PROCEDURE.....	204
G.6.1	Option A—Multiple Temperature Option.....	205
G.6.2	Option B—Equivalent Test Temperature Option.....	209
G.7	ESTIMATING THE PLASTIC STRAIN COEFFICIENTS FROM VOLUMETRIC PROPERTIES.....	212
G.7.1	Intercept of Transfer Function.....	212
G.7.2	m-Value of Transfer Functions.....	213
G.7.3	Temperature Term Exponent of Kaloush Transfer Function.....	213
G.8	HMA PROPERTIES USED IN DETERMINING LEVEL 2 INPUTS.....	213
G.8.1	Design Air Void Content to Select Target Asphalt Content, $V_{a(\text{design})}$	213
G.8.2	Saturation Asphalt Content by Weight, $P_{b(\text{sat})}$	214
G.8.3	Fine Aggregate Angularity Index, F_{Index}	215
G.8.4	Coarse Aggregate Angularity Index, C_{Index}	215
G.8.5	Estimation of Repeated Load Plastic Deformation Parameters—Input Level 2 ...	216
G.9	PROCEDURE FOR ADJUSTING THE PLASTIC STRAIN COEFFICIENTS FOR DIFFERENT EQUIVALENT TEST TEMPERATURES.....	216
APPENDIX H—CALIBRATION OF FATIGUE CRACKING (BOTTOM-UP CRACKING) TRANSFER FUNCTION.....		218
H.1	INTRODUCTION.....	218
H.2	RELATIONSHIPS TO DERIVE FATIGUE COEFFICIENTS.....	218
H.3	PROCEDURE TO DERIVE FATIGUE CRACKING MODEL COEFFICIENTS FROM THE INDIRECT TENSILE STRENGTH TEST.....	221

LIST OF TABLES

Table 1—Performance Indicators Predicted by Pavement ME Design Software	10
Table 2—Hierarchical Input Levels.....	10
Table 3—Predominant Source of Data Used for Transfer Function Verification and Initial Calibration in Mississippi.....	11
Table 4—Reflection Cracking Model Regression Fitting Parameters	19
Table 5—Standard Errors of the Estimate for each Transfer Function included in the Pavement ME Design Software	23
Table 6—Criteria for Determining Transfer Functions Accuracy for Mississippi Conditions	27
Table 7—Sampling Matrix for Flexible and Semi-rigid Pavements, Cell Numbers for New Construction and Rehabilitation	29
Table 8—Sampling Matrix for Rigid Pavements, Cell Numbers for New Construction and Rehabilitation.....	29
Table 9—Number of Test Sections: Flexible and Semi-rigid Pavements, New Construction and Rehabilitation.....	32
Table 10—Number of Test Sections: Rigid Pavements, New Construction and Rehabilitation ..	33
Table 11—Truck Traffic Classification Groups for Defining Mississippi’s Normalized Volume Distribution Factors.....	37
Table 12—Mississippi Monthly Distribution Factors	38
Table 13—Mississippi Hourly Distribution Factors.....	38
Table 14—Mississippi Number of Axles per Truck Class	38
Table 15—Mississippi Weather Stations Available in AASHTOWare	42
Table 16—Mississippi IR Values at Construction	47
Table 17—PCC Mix Designs Included in Laboratory Test Program	58
Table 18—Alternatives for level 2 correlations based on MDOT PCC test data.....	60
Table 19—Level 3 PCC Material Property Inputs Recommended for Use in Mississippi	61
Table 20—Recommended PCC CTE Values from MDOT Testing and MEPDG Defaults from LTPP Testing.....	62
Table 21—Resilient Modulus Values Derived for Selected Base Materials and Subgrade Soils Typical for Mississippi.....	70
Table 22—C-Factors Recommended for Use in Mississippi to Convert Backcalculated Layer Modulus Values to Laboratory Equivalent Modulus Values.....	70
Table 23—DCP Adjustment Factors Recommended for Use in Mississippi to Convert an Elastic Modulus from DCP Tests to a Laboratory Equivalent Resilient Modulus.....	72
Table 24—Poisson’s Ratio Suggested for Use for Unbound Layers.....	79
Table 25—Results of Statistical Goodness of Fit and Bias Evaluation of the MEPDG Alligator Cracking Global Model for Mississippi Conditions.....	82
Table 26—Description of HMA Fatigue Damage, HMA Alligator Cracking, and Reflection “Alligator” Cracking Models.....	83
Table 27—Summary of MEPDG Global and MDOT Local Calibration Coefficients for HMA Alligator Cracking and HMA Fatigue Damage Models.....	85
Table 28—Local Calibration Coefficients for HMA Overlay Reflection Cracking Model Developed using New HMA and HMA Overlaid HMA Pavement Projects.....	85
Table 29—Results of Statistical Bias Evaluation of MEPDG Reflection “Alligator” Cracking Local Model for Mississippi Conditions.....	85
Table 30—Results of Statistical Evaluation of MEPDG Total Rutting Global Sub-Models for Mississippi Conditions.....	90

Table 31—Description of Total Rutting Prediction Sub-Models	92
Table 32—Local Calibration Coefficients for HMA, Unbound Base, and Subgrade Soil Rutting Sub-Models	92
Table 33—Results of Statistical Evaluation of MEPDG Total Rutting using Local Rutting Sub-Models for Mississippi Conditions	92
Table 34. Results of Statistical Evaluation of MEPDG HMA IRI Global Regression Equation for Mississippi Conditions.....	98
Table 35. Local Calibration Coefficients for HMA Smoothness (IRI) Regression Equation	99
Table 36. Results of Statistical Evaluation of MEPDG HMA IRI Local Regression Equation Coefficients for Mississippi Conditions	100
Table 37. Results of statistical goodness of fit and bias evaluation of the MEPDG transverse cracking global model for Mississippi conditions.	106
Table 38. Summary of MEPDG global and MDOT local calibration coefficients for JPCP transverse cracking and JPCP fatigue damage models.	107
Table 39. Results of statistical bias evaluation of MEPDG JPCP transverse cracking local model for Mississippi conditions.	107
Table 40. Comparison of measured and predicted transverse joint faulting (percentage of all measurements).....	110
Table 41. Summary of MEPDG global coefficients for JPCP transverse joint faulting model. ...	111
Table 42. Goodness of fit and bias test statistics for JPCP IRI global model.	115
Table 43. Summary of MEPDG global and Mississippi local calibration coefficients for JPCP IRI model.....	115
Table 44. Results of statistical bias evaluation of MEPDG JPCP IRI local model for Mississippi conditions.	116
Table B.1—Non-LTPP Flexible Pavement New Construction, High Priority Projects.....	140
Table B.2—Non-LTPP Rigid Pavement Construction, High Priority Projects.....	140
Table B.3—Non-LTPP Rehabilitated Flexible Pavement, High Priority Projects.....	140
Table B.4—Properties for Local Calibration of the Pavement ME Design Software.....	143
Table B.5—Materials Sampling Plan for the Non-LTPP Projects.....	147
Table B.6—Materials Testing Plan for the Non-LTPP Projects.....	148
Table B.7—Checklist of Factors for Overall Pavement Condition Assessment and Problem Definition.....	149
Table B.8—Summary of Standard Test Procedures to be used for the Laboratory and Field Tests.....	151
Table D.1—Normalized Single Axle Load Spectra for TTC Group 3.....	161
Table D.2—Normalized Tandem Axle Load Spectra for TTC Group 3	162
Table D.3—Normalized Tridem Axle Load Spectra for TTC Group 3	163
Table D.4—Normalized Single Axle Load Spectra for TTC Group 6.....	164
Table D.5—Normalized Tandem Axle Load Spectra for TTC Group 6	165
Table D.6—Normalized Tridem Axle Load Spectra for TTC Group 6	166
Table D.7—Normalized Single Axle Load Spectra for TTC Group 7.....	167
Table D.8—Normalized Tandem Axle Load Spectra for TTC Group 7	168
Table D.9—Normalized Tridem Axle Load Spectra for TTC Group 7	169
Table D.10—Normalized Single Axle Load Spectra for TTC Group 12.....	170
Table D.11—Normalized Tandem Axle Load Spectra for TTC Group 12	171
Table D.12—Normalized Tridem Axle Load Spectra for TTC Group 12	172
Table D.13—Normalized Single Axle Load Spectra for TTC Group 15.....	173
Table D.14—Normalized Tandem Axle Load Spectra for TTC Group 15	174
Table D.15—Normalized Tridem Axle Load Spectra for TTC Group 15	175

Table G.1. Thickness Adjustment or Shift Factors for Determining the Field Matched Intercept Value of the Transfer Functions	209
Table G.2. Aggregate Properties for Determining the Mixture Adjustment Factors	213
Table H.1. Comparison of Fatigue Cracking Equation Model Coefficients	219
Table H.2. Model Coefficients Regressed Using Equation H.2	224

LIST OF FIGURES

Figure 1—Conceptual Flow Chart for the MEPDG Three-Stage Design-Analysis Process (AASHTO, 2008).....	9
Figure 2—Backcasting Process for Determining the AADTT for the Traffic Opening Dates	36
Figure 3—Comparison of Predicted Flexible Pavement Distress Values for the different Climate Libraries.....	43
Figure 4—Comparison of Predicted Rigid Pavement Distress Values for the different Climate Libraries.....	43
Figure 5—IRI Measured over Time for Two of the Mississippi LTPP Sections	46
Figure 6—Backcasting Process to Estimate the Initial IRI for Two of the Mississippi Sections ..	47
Figure 7—Illustration of the Process used to Backcast the Initial Air Voids of HMA Layers with Adequate Compaction	55
Figure 8—Initial Air Voids Compared to the Total Asphalt Content by Weight for the HMA Mixtures.....	55
Figure 9—Damage Index Derived through Backcalculation of Elastic Layer Moduli and Cracking	57
Figure 10—Relationship between Optimum Water Content and Maximum Dry Unit Weight for all Unbound Materials and Soils for the Mississippi LTPP Sites.....	66
Figure 11—Optimum Water Content and In Place Water Contents for the LTPP Sites	66
Figure 12—Resilient Modulus Test Results for Different Subgrade Soils	68
Figure 13—Resilient Modulus Test Results for Different Aggregate Bases	69
Figure 14—Backcalculated Elastic Modulus as a Function of In Place Water Content	71
Figure 15—Laboratory-Derived Resilient Modulus Values Compared to the Field-Derived Backcalculated Elastic Modulus Values for the Subgrade Soils – Mississippi LTPP Test Sections.....	72
Figure 16—Laboratory-Derived Resilient Modulus Values Compared to the Field-Derived Backcalculated Elastic Modulus Values for the Aggregate Bases – Mississippi LTPP Test Sections.....	73
Figure 17—Limiting Layer Modulus Ratio or Criterion of Unbound Aggregate Base Layers (Barker and Brabston, 1975).....	74
Figure 18—Resilient Modulus over Time for Different Moisture Contents; Example 1	76
Figure 19—Resilient Modulus over Time for Different Moisture Contents; Example 2.....	76
Figure 20—Sample Graph Illustrating the Method to Determine the Resilient Modulus at Construction; Sample 1.....	77
Figure 21—Sample Graph Illustrating the Method to Determine the Resilient Modulus at Construction; Sample 2.....	77
Figure 22—Sample Graph Illustrating the Method to Determine the Resilient Modulus at Construction; Sample 1 for Backcalculated Modulus	78
Figure 23—Sample Graph Illustrating the Method to Determine the Resilient Modulus at Construction; Sample 2 for Backcalculated Modulus	78
Figure 24. Verification of the HMA alligator cracking and fatigue damage models with MEPDG global coefficients, using Mississippi projects.	82
Figure 25—MDOT Local Calibration Coefficients for the Bottom-Up Fatigue Cracking Transfer Function.....	84
Figure 26. Plot showing measured HMA alligator cracking versus computed fatigue damage developed using MEPDG models with MDOT local coefficients.....	86

Figure 27. Plot showing measured HMA alligator cracking versus predicted HMA alligator cracking using MEPDG models with MDOT local coefficients.86

Figure 28. Plot showing progression of reflection cracking with HMA overlay age for different HMA overlay thicknesses.87

Figure 29. Plot of predicted alligator cracking versus age for MDOT pavement management system project 4784 (new HMA pavement).87

Figure 30. Plot of predicted alligator cracking versus age for LTPP project 1001 (HMA overlaid HMA pavement).88

Figure 31. Plot of predicted alligator cracking versus age for LTPP project 0806 (new HMA pavement).88

Figure 32. Plot of predicted alligator cracking versus age for LTPP project 0903 (HMA overlaid HMA pavement).89

Figure 33. Plot showing MEPDG global model predicted rutting versus measured rutting (HMA, unbound aggregate base, and subgrade).90

Figure 34. Plot showing predicted using MEPDG sub-models with MDOT local coefficients versus field-measured total rutting.93

Figure 35. Plot showing predicted rutting versus truck traffic for MDOT pavement management system project 1122 (New HMA pavement).93

Figure 36. Plot showing predicted rutting versus truck traffic for LTPP project 0959 (HMA overlaid HMA pavement).94

Figure 37. Plot showing predicted rutting versus truck traffic for LTPP project 0806 (New HMA pavement).94

Figure 38. Plot showing predicted rutting versus truck traffic for LTPP project 1802 (New HMA pavement).95

Figure 39. Plot showing predicted rutting versus truck traffic for MDOT pavement management system project 1122 (New HMA pavement).95

Figure 40. Plots of Transverse Cracking versus Age in Non-Freeze Areas of Yazoo and Covington, MS97

Figure 41. Predicted versus Measured IRI using Global MEPDG HMA IRI Regression Equation Coefficients98

Figure 42. Plot of Measured and Predicted IRI for New HMA and HMA-Overlaid HMA Pavements Developed using the Locally Calibrated MDOT HMA IRI Regression Equation100

Figure 43. Plot Showing Measured and Predicted IRI versus Time for MDOT Section 28-2202101

Figure 44. Plot Showing Measured and Predicted IRI versus Time for MDOT LTPP Test Section 28-0902101

Figure 45. Plot Showing Measured and Predicted IRI versus Time for MDOT LTPP Section 28-5618102

Figure 46. Verification of the JPCP transverse cracking and fatigue damage models with MEPDG global coefficients, using Mississippi JPCP projects.106

Figure 47. Plot showing predicted JPCP transverse cracking versus computed fatigue damage developed using MEPDG models with MDOT local coefficients.107

Figure 48. Plot of predicted and measured transverse cracking versus fatigue damage for LTPP 5_0213.108

Figure 49. Plot of predicted and measured transverse cracking versus fatigue damage for LTPP 5_0217.108

Figure 50. Plot of predicted and measured transverse cracking versus fatigue damage for LTPP 13_3020.109

Figure 51. Histogram showing distribution of measured JPCP transverse joint faulting for LTPP projects included in the analysis.	110
Figure 52. Plot showing predicted JPCP transverse joint faulting using MEPDG models with global coefficients versus measured joint faulting.	112
Figure 53. Predicted (using global calibration factors) and measured transverse joint faulting for LTPP 13_3016.....	112
Figure 54. Predicted (using global calibration factors) and measured transverse joint faulting for LTPP 13_3020.....	113
Figure 55. Predicted (using global calibration factors) and measured transverse joint faulting for LTPP 5_0219.....	113
Figure 56. Predicted (using global calibration factors) and measured transverse joint faulting for LTPP 5_0223.....	114
Figure 57. Predicted JPCP IRI versus measured Mississippi JPCP with global calibration coefficients.....	115
Figure 58. Plot showing predicted JPCP IRI using MEPDG models with MDOT local coefficients versus measured IRI.....	116
Figure 59. Predicted and measured JPCP IRI for Mississippi LTPP section 5_0224 over time.	117
Figure 60. Predicted and measured JPCP IRI for Mississippi LTPP section 13_3007 over time.	117
Figure 61. Predicted and measured JPCP IRI for Mississippi LTPP section 13_3020 over time.	118
Figure E.1. Ground Water Level (Source: USGS)	177
Figure E.2. Definition of Ground Water Table Depth and Results Displayed in the GWT Tool (Original Image Source: USGS, image labeled to explain terminologies).....	178
Figure E.3. Artesian Aquifer (Source: Environment Canada).....	179
Figure E.4. Secondary Aquifer Source	179
Figure E.5. Opening GWT Tool in Firefox Browser Window	180
Figure E.6. Selecting the html.file Index to Open the GWT Tool.....	181
Figure E.7. User Interface after Launching MDOT GWT Tool	181
Figure E.8. Loading the Data File to Import the Well Information and Water Table Depth Data	182
Figure E.9. Wells Displayed as Green Squares in the Region of Interest	182
Figure E.10. Location Tab to Select a Project Location by Name of Place	183
Figure E.11. Google Earth Layers Tab to Select the Topographical Features for Display	184
Figure E.12. Information for Selected Area Tab	184
Figure E.13. Warning to Alert the User that the Data used in Computing the Average has a Large Variability or Outliers that are Outside the Set Tolerance Level	186
Figure E.14. Update after User-Input Latitude and Longitude Inputs and Results Displayed ..	187
Figure E.15. Relocate Button to Manually Select the Project Location of Interest.....	187
Figure E.16. Graphical Display of Results by Season and over Time.....	188
Figure E.17. Data Displayed in the Information for Selected Well Tab	189
Figure G.1. Test Results from a Repeated Load Triaxial (Confined) Plastic Strain Test	203
Figure G.2. Accumulation of Plastic Axial Strain Measured in the Laboratory – Defined as Pattern A (Extracted from NCHRP Report #719)	205
Figure G.3. Accumulation of Plastic Axial Strain Defined as Pattern B (Extracted from NCHRP Report #719).....	206
Figure G.4. Accumulation of Plastic Axial Strain Defined as Pattern C (Extracted from NCHRP Report #719).....	206

Figure G.5. Determining the Field Matched Slopes from Laboratory-Derived m-Values from Repeated Load Triaxial Tests; Kaloush Transfer Function (Extracted from NCHRP Report #719. The data for this relationship is included in the NCHRP report.)	208
Figure G.6. Determining the Field Matched Intercept from Laboratory-Derived I_s -Values from Repeated Load Triaxial Tests; Kaloush Transfer Function (Extracted from NCHRP Report #719. The data for this relationship is included in the NCHRP report.)	208
Figure G.7. Graphical Relationship between the LTPPBind2.1 Pavement Temperature and the Equivalent Test Temperature.....	210
Figure G.8. Example of Rut Depths Predicted with MEPDG (Kaloush Transfer Function) using a Constant Temperature Environment to Estimate the Equivalent Test Temperature	211
Figure G.9. Graphical Example Determining the Design Air Void Content from the Laboratory Mixture Design Chart	214
Figure G.10. Graphical Example Determining the Saturation Asphalt Content from the Laboratory Mixture Design Chart for a Sensitive Mixture	215
Figure G.11. Graphical Example Determining the Saturation Asphalt Content from the Laboratory Mixture Design Chart for a Non-Sensitive Mixture.....	215
Figure G.12. Relationship of the Temperature Exponent (n-value) and Coefficient (d-value) for Different Repeated Load Tests (Extracted from NCHRP Report #719)	217
Figure H.1. Relationship between Dynamic Modulus and Tensile Strain at Failure for Estimating the Fracture Coefficients of Asphalt Concrete.....	220
Figure H.2. Comparison of Relationship between Dynamic Modulus and Tensile Strain at Failure for Three Fatigue Equations.....	221
Figure H.3. Estimating Fatigue Cracking Coefficients from the Indirect Tensile Strength and Modulus Tests; Michigan Mixture.....	222
Figure H.4. Estimating Fatigue Cracking Coefficients from the Indirect Tensile Strength and Modulus Tests; Texas Mixture	222
Figure H.5. Estimating Fatigue Cracking Coefficients from the Indirect Tensile Strength and Modulus Tests; Virginia Mixture	223
Figure H.6. Estimating Fatigue Cracking Coefficients from the Indirect Tensile Strength and Modulus Tests; Wyoming Mixture	223
Figure H.7. Fatigue Relationships from the Indirect Tensile Strength Test and Normalized to Equal Volumetric Properties.....	224

ABBREVIATIONS

AADTT	Average Annual Daily Truck Traffic
AASHTO	American Association of State and Highway Transportation Officials
AC	Asphalt Concrete
ARA	Applied Research Associates, Inc.
ATPB	Asphalt Treated Permeable Base
AVC	Automated Vehicle Classification
CAM	Cement Aggregate Mixtures
CRCP	Continuously Reinforced Concrete Pavement
CTB	Cement Treated Base
CTE	Coefficient of Thermal Expansion
DCP	Dynamic Cone Penetrometer
DDF	Directional Distribution Factor
DI	Damage Index (Fracture)
DOT	Department of Transportation
FHWA	Federal Highway Administration
FWD	Falling Weight Deflectometer
GPS	General Pavement Study and Global Positioning System
HDF	Hourly Distribution Factor
HMA	Hot Mix Asphalt
ICM	Integrated Climate Model
IRI	International Roughness Index
JPCP	Jointed Plain Concrete Pavement
LDF	Lane Distribution Factor
LFA	Lime-Fly Ash
LTPP	Long Term Pavement Performance
MAF	Monthly Adjustment Factor
MDF	Monthly Distribution Factor
MDOT	Mississippi Department of Transportation
ME	Mechanistic Empirical
MS-ATLAS	Mississippi Advanced Traffic Loading Analysis System
NALD	Normalized Axle Load Distribution
NALS	Normalized Axle Load Spectra
NCAT	National Center for Asphalt Technology
NCHRP	National Cooperative Highway Research Program
PCC	Portland Cement Concrete
PMA	Polymer Modified Asphalt
PMS	Pavement Management System
RAP	Recycled Asphalt Pavement
SEE	Standard Error of the Estimate
SHRP	Strategic Highway Research Program
SPS	Special Pavement Study
TTC	Truck Traffic Classification
VC	Vehicle Class
WIM	Weigh-In-Motion
WMA	Warm Mix Asphalt

IMPLEMENTATION AND PRELIMINARY LOCAL CALIBRATION OF PAVEMENT ME DESIGN IN MISSISSIPPI: VOLUME I

CHAPTER 1—INTRODUCTION

1.1 BACKGROUND

The Mississippi Department of Transportation (MDOT) currently uses the 1972 American Association of State Highway and Transportation Officials (AASHTO) Interim Guide for Design of Pavement Structures as its standard pavement design procedure (AASHTO, 1972). MDOT, however, plans to adopt the new Mechanistic-Empirical Pavement Design Guide (MEPDG) procedure (AASHTO, 2008). The new design procedure is a part of the AASHTO software Pavement ME Design and uses mechanistic-empirical (ME) principles. MDOT recognized the benefits and value of using the MEPDG and started the process of implementing the software package for new pavement and rehabilitation design in 2003.

The M-E based procedure is a significant departure from the existing AASHTO empirical procedure. The primary advantage of an ME-based design system is that it is based on pavement fatigue and deformation characteristics of all layers, rather than solely on the pavement's surface condition (ride quality). In addition, ME-based concepts allow the pavement design engineer to quantify the effect of changes in materials, load, climate, age, and construction practices on pavement performance. It also provides a more accurate and cost effective method of diagnosing pavement problems, optimizing new and rehabilitation designs, and forecasting maintenance and repair needs.

To facilitate a gradual transition from the current empirical pavement design methodology to the ME-based approach, MDOT assessed the MEPDG design inputs (traffic, materials and environment) as related to multiple factors, including: level of effort, procedures to measure the input values, availability of values from historical records, and other factors. Equally important was the verification of the distress prediction models or transfer functions with local data.

The MEPDG distress transfer functions and prediction methodology were calibrated using data from the Long Term Pavement Performance (LTPP) program under National Cooperative Highway Research Program (NCHRP) projects 1-37A and 1-40D. The global calibration effort, however, cannot be expected to consider all potential factors that can occur throughout all agencies, materials, design strategies, and climates found in the United States. For example, factors such as maintenance strategies, construction specifications, aggregate and binder type, mixture design procedures, and material specifications can result in performance differences – all other factors being equal. In fact, small differences in some of the above factors can cause large differences in performance.

Accordingly, the overall objective of MDOT's implementation process was to verify, re-calibrate, and validate the distress transfer functions and streamline a design process using the MEPDG for new and rehabilitation pavement design.

1.2 PHASED IMPLEMENTATION APPROACH

MDOT initiated a four-phased implementation approach to ensure all the inputs to the procedure can be accurately measured in day to day practice. In addition, MDOT evaluated the distress and smoothness prediction models or transfer functions to ensure they accurately predict the performance of MDOT roadways. The four phases are defined below.

1. Phase 1 included the development of an implementation plan for MDOT through State Study #163, “*Develop Mississippi DOT’s Plan to Implement the 2002 Design Guide.*” The 2002 Design Guide is the MEPDG and Pavement ME Design is the software package being distributed through AASHTOWare. The MEPDG procedure and methodology, as well as the transfer functions are described in the MEPDG Manual of Practice (*AASHTO, 2008*).
2. Phase 2 included two activities: (a) the verification and determination of the preliminary local calibration coefficients of the transfer functions, if found to be inadequate; and (b) the development of traffic and materials libraries for using the Pavement ME Design software in Mississippi.
3. Phase 3 includes an expanded local calibration of the MEPDG transfer functions and expanded inputs library based on an extensive field investigation of pavement test sections in Mississippi.
4. Phase 4 includes the training on the MEPDG procedure itself and use of the Pavement ME Design software.

Phases 1 and 2 have been completed. Phases 3 and 4 are future phases focused on enhancing the local calibration coefficients and training, respectively. This includes verifying and/or adjusting the local calibration coefficients of the distress transfer functions included in the MEPDG software and Manual of Practice (*AASHTO, 2008*).

The objective of Phase 1 was to develop a “road map” or plan for MDOT’s implementation of the MEPDG. Actual implementation of the new design procedure will take place in Phases 3 and 4. The road map (Phase 1) identified the steps to implement the MEPDG, and included the following tasks that are documented in report FHWA/MS-DOT-RD-03-163:¹

- Familiarize MDOT staff with the MEPDG – the procedure and software.
- Identify MDOT needs relative to the types of pavements of interest for new or reconstruction design and the types of rehabilitation for existing pavements.
- Develop a calibration and validation plan to revise the coefficients of the MEPDG transfer functions to accurately simulate Mississippi conditions, materials, and operational policies.
- Develop an experimental design and sampling matrix or factorial and select test sections for that matrix.
- Recommend technology transfer procedures and a training program to ensure proper use of the software, as well as proper determination of the input values.
- Prepare a detailed plan or “road map” for implementation of the MEPDG.

The objective of Phase 2 was to evaluate the MEPDG transfer functions and determine whether the global calibration coefficients reasonably predict distresses and smoothness for

¹ Phase 1 Report: FHWA/MS-DOT-RD-03-163, Mississippi DOT’s Plan to Implement the 2002 Design Guide; Authors Athar Saeed and Jim Hall, Mississippi DOT, Jackson, MS, September 2003.

LTPP and non-LTPP sites located in Mississippi. The outcomes from Phase 2 were preliminary sets of local calibration coefficients to ensure unbiased predictions of distress and roughness and a revised sampling and testing plan or template for finalizing the MDOT local calibration coefficients. Phase 2 also included preparation of a User Input Guide and Software Manual specific to MDOT, and some initial training in using the MEPDG software. The results from Phase 2 are documented in this report. Phases 3 and 4 are to be completed under a different project.

The objective of Phase 3 includes the field investigation and testing of the non-LTPP roadway segments and an updated local calibration of the MEPDG transfer functions, while Phase 4 includes continued training in using Pavement ME Design in day to day practice.

1.3 SCOPE OF REPORT

This report is volume I for the Phase 2 work. It provides a summary of all work completed under Phase 2 for verifying and completing a preliminary local calibration of the MEPDG transfer functions. Volume II of the Phase 2 work is a separate document and includes the MEPDG inputs and summary output files for all of the LTPP and non-LTPP roadway segments. The input files in Volume II can be used as a starting point for the final calibration effort to be completed after the field investigations of the non-LTPP roadway segments are completed.²

Volume I includes ten chapters. Chapter 1 is the introduction to the project, while Chapter 2 is an overview of the MEPDG design methodology and transfer functions used to predict pavement performance. Chapter 3 presents the experimental plan and sampling matrix used for the preliminary local calibration. The next four chapters are focused on describing the inputs used for the local calibration. Chapter 4 is on the truck traffic inputs, Chapter 5 is on Climate inputs, Chapter 6 is on the layer features, and Chapter 7 overviews the material properties. Chapters 8 and 9 provide the results from the local calibration process. Chapter 8 includes the results for the flexible pavement transfer functions, while Chapter 9 includes those for the rigid pavement transfer functions. Chapter 10 summarizes the conclusions and recommendations from the preliminary local calibration process and provides a brief discussion on specialty applications of the MEPDG in Mississippi.

These chapters are followed by multiple appendices that provide supporting documentation on various inputs and provide more detailed information and guidance for the expanded calibration of specific transfer functions that are based on the field investigations currently planned under Phase 3.

² Volume II Local Calibration Sections, Implementation of the Mechanistic-Empirical Pavement Design Guide in Mississippi, Report #FHWA/MS-DOT-RD-013-170, December 30, 2013.

1.4 DESIGN STRATEGIES INCLUDED IN CALIBRATION

1.4.1 New/Reconstructed Flexible Pavements and HMA Overlays

The new and reconstructed hot mix asphalt (HMA)³ surfaced pavements, as well as HMA overlays, included in the Pavement ME Design software are listed below and grouped by those verified using the LTPP sites and non-LTPP pavement management sections as well as those excluded from the verification process.⁴ The latter chapters in this research report provide more detailed discussion on the types of pavement included in the local calibration process as part of the sampling matrix or experimental factorial (see Chapter 3). The following identifies the flexible pavement types included, as well as excluded from the local calibration process in Mississippi.

- **Included in Verification-Local Calibration Process:**
 1. **Conventional flexible pavements:** thin HMA surfaces (less than 6 inches in thickness) and aggregate base layers (crushed gravel and soil-aggregate mixtures), greater than 8 inches in thickness with and without stabilized subgrades.
 2. **Deep strength flexible pavements:** thick HMA (a wearing surface and a dense-graded HMA base mixture exceeding 6 inches in thickness) placed over an aggregate base material with and without stabilized subgrades.
 3. **Full Depth flexible pavements:** HMA placed on the embankment soil or on a lime-stabilized soil. If the soil is stabilized with Portland cement (a soil-cement layer), the structure is classified as a semi-rigid pavement. A limited number of full-depth flexible pavement roadway segments were included in the calibration process, so these were combined with the deep strength strategy or family of flexible pavements. Chapter 3 discusses the sampling matrix and test sections included in the cells of the matrix.
 4. **Semi-Rigid pavements:** HMA mixtures placed over Cement Treated Base (CTB), Cement Aggregate Mixtures (CAM), soil-cement, or lime-fly ash stabilized base layers without an unbound aggregate layer. Semi-rigid pavements were not included in the original calibration completed under NCHRP Projects 1-37A (*ARA, 2004a,b,c,d*) and 1-40D (*NCHRP, 2006*). Although this type of pavement was included in the preliminary local calibration process, the material properties for the cementitious layer were unavailable from construction records, so the calibration coefficients were based on estimated material strength and stiffness properties.
 5. **HMA Overlays** of all conventional, deep strength, and full depth flexible pavements.

- **Excluded from the Verification-Local Calibration Process:**

³ HMA is used throughout this report as the standard notation for different dense-graded asphalt concrete mixtures produced in a drum mix or batch plant. Different dense-graded asphalt concrete mixtures include conventional mixtures, polymer modified asphalt mixtures, and warm mix asphalt mixtures.

⁴ HMA with and without recycled asphalt pavement (RAP) were the only bituminous mixtures included in the local calibration process. Thus, it is assumed that the local calibration coefficients to remove bias are also applicable to warm mix asphalt (WMA) and polymer modified asphalt (PMA) mixtures. This assumption, however, is probably incorrect.

1. **HMA Overlays** of jointed plain concrete pavements (JPCP) and continuously reinforced concrete pavements (CRCP), as well as HMA overlays of fractured (rubblized, crack and seat, and break and seat) JPCP and CRCP.
2. **Pavement Preservation** has a definite effect on pavement performance and should be considered in predicting pavement distresses and roughness.

It should be noted that pavement preservation treatments applied to the surface of HMA layers early in their life can have an impact on the structural performance and regional calibration coefficients (*Von Quintus and Moulthrop, 2007a and 2007b*). None of the roadway segments included within the local calibration process for MDOT included the use of pavement preservation strategies. Thus, the MDOT calibration values presented in Chapters 8 and 9 do not include any effect from pavement preservation.

The designer should consider whether a pavement preservation treatment applied early within the pavement's service life will be used as part of the pavement design strategy. The designer can consider the effect of a pavement preservation treatment only within the life cycle cost analysis by extending a pavement's expected service life related to the HMA mixture deterioration or materials-related distresses. If MDOT's policy changes so that pavement preservation treatments are used on a more routine basis, MDOT's calibration coefficients should be determined or verified for the different types of treatments used. The MEPDG and measured distress can be used to validate whether there is a reduction in the structural related distresses or an increase in the life of flexible pavements and HMA overlays, and if so, determine the increase in service life.

1.4.2 New/Reconstructed Rigid Pavements and PCC Overlays

The new and reconstructed Portland cement concrete (PCC) surfaced pavements, as well as PCC overlays, that were included or excluded from the local calibration refinement process are listed below.

- **Included in Verification-Local Calibration Process:**
 1. **Jointed Plain Concrete Pavements:** JPCP include transverse joints spaced to accommodate temperature gradient and drying shrinkage stresses to avoid cracking. The joints include dowels to complement the aggregate interlock in providing load transfer. MDOT JPCP sections used in the calibration had a thickness range of 9 to 10 inches and were placed on HMA, stabilized, and granular bases.
- **Excluded from the Verification-Local Calibration Process:**
 1. **Continuously Reinforced Concrete Pavements:** PCC slab cast with no transverse joints and containing longitudinal steel typically in the range of 0.5 to 0.8 percent of the cross-sectional area. The PCC surface develops transverse cracks and the design should ensure that the cracks remain tight and provide good load transfer during the service life of the pavement. Although a few CRCP sections were included in the verification process for MDOT, the thickness of the slab was confined to 8 inches. More sections are needed for adjusting the calibration coefficients. Until additional CRCP sections are included, the global calibration coefficients need to be used.
 2. **PCC Overlays** of all types of rigid pavements and HMA pavements, including bonded PCC overlay of rigid pavements, unbonded PCC overlay of rigid pavements,

and PCC overlay of flexible pavements. Similar to the CRCP sections, a few JPCP unbonded overlays of CRCP were included in the verification and local calibration process. More sections are needed to adjust the calibration coefficients. In the interim, the global calibration coefficients need to be used.

1.5 DEFINITION OF TERMS

The following provides a definition for some of the terms that are used within this report.

- **Accuracy** – The exactness of a prediction to the observed or “actual” value. The concept of accuracy encompasses both precision and bias.
- **Bias** – An effect that deprives predictions of simulating “real world” observations by systematically distorting it, as distinct from a random error that may distort on any one occasion but balances out on the average. A prediction model that is “biased” is significantly over or under predicting observed distress or roughness (as measured by the International Roughness Index [IRI]).
- **Calibration** – A systematic process to eliminate any bias and minimize the residual error between observed or measured results from the real world (e.g., the measured mean rut depth in a pavement section) and predicted results from the model (e.g., predicted mean rut depth from a permanent deformation model). This is accomplished by modifying empirical calibration parameters or transfer functions in the model to minimize the differences between the predicted and observed results. These calibration parameters are necessary to compensate for model simplification and limitations in simulating actual pavement and material behavior.
- **Precision** – The ability of a model to give repeated estimates that correlate strongly with the observed values. They may be consistently higher or lower but they correlate strongly with observed values.
- **Residual Error** – The difference between the observed or measured and predicted distress and IRI values (e.g., measured minus predicted values). The residuals explain how well the model predicts the observed distress and IRI.
- **Standard Error of the Estimate (s_e)** – The standard deviation of the residual errors for the pavement sections included in the validation and/or calibration data set for each prediction model. The standard error is usually obtained by taking the square root of the variance divided by the number of observations of the statistic.
- **Verification** – Verification of a model examines whether the operational model correctly represents the conceptual or statistical model that has been formulated. Verification can be done using both measured and predicted data, and if biased, then calibration was performed to remove bias. Verification can also be accomplished by entering typical materials, structural, environmental, and traffic data into the distress and performance models, and then determining through parameter studies whether the program operates rationally and provides outputs that meet the criterion of engineering reasonableness. If this criterion is not met, the computer code maybe erroneous or the conceptual model may be unsatisfactory. In either case, these problems must be remedied before the model enhancement process or

use continues. No field data are needed in either of the verification approaches described. Verification is primarily intended to confirm the internal consistency or reasonableness of the model. The issue of how well the model predicts reality is addressed during calibration and validation.

- **Statistical Model** – A model that is derived from data that are subject to various types of observations, experimental, and measurement errors. The statistical models in the MEPDG include the distress transfer functions, as well as the reflection cracking and IRI regression equations. The time-dependent material property models for HMA and PCC are also regression or statistical relationships. These models, however, are assumed to be correct in the MEPDG model formulation or computational methodology. Adjustments to the coefficients of these relationships are not permitted within the Pavement ME Design software.
- **Transfer Function** – A transfer function is a specific form of a statistical model and is defined as a mathematical relationship that transfers computed pavement responses (stresses, strains, and/or deflections) into what is observed or measured on the pavement surface. Transfer functions are included in the MEPDG software for bottom-up fatigue cracking, transverse cracking and rutting for flexible pavements and asphalt concrete overlays, as well as faulting, mid-slab cracking and punchouts of rigid pavements.
- **Validation** – A systematic process that reexamines the recalibrated model to determine if the desired accuracy exists between the calibrated model and an independent set of observed data. The calibrated model requires inputs such as the pavement structure, traffic loading, and environmental data. The simulation model must predict results (e.g., rutting, fatigue cracking) that are reasonably close to those observed or measured in the field. Separate and independent data sets should be used for calibration and validation (typically 10 percent of observations). Assuming that the calibrated models are successfully validated, the models can be recalibrated using the combined data sets (calibration and validation) without the need for additional validation to provide a better estimate of the residual error.

The terms validation and verification get used interchangeably in various documents. The process was to verify the global calibration coefficients and then calibrate and validate any changes needed for the transfer functions to accurately predict pavement distress and smoothness measured on Mississippi's roadways.

CHAPTER 2—OVERVIEW OF THE MEPDG DESIGN METHODOLOGY

The MEPDG is based on ME concepts and principles. This means that the procedure calculates pavement responses such as stresses, strains, and deflections, accumulates the incremental damage from these responses over time based on the material distress law, and relates that accumulated damage to measured pavement distress. In other words, the *mechanistic* aspect of the method uses an analytical model based on the principles of mechanics of materials to calculate pavement response from applied traffic and environmental loads. The *empirical* component relates the outputs from the mechanistic model (damage) to observed pavement performance using transfer functions. This ME based procedure is shown in flowchart form in Figure 1. Table 1 lists the performance indicators predicted by the Pavement ME Design software.

Complete discussion of the ME based concepts, procedure and transfer functions used to predict distress and smoothness is included in the *MEPDG—A Manual of Practice* that was published by AASHTO (AASHTO, 2008), as well as in the “HELP” manual that comes with the software and the NCHRP project 1-37A reports (ARA, 2004a,b,c,d). This chapter simply provides a summary of the transfer functions and factors used to predict the performance indicators. The material distress or damage law and related transfer functions are included in Section 5 of the MEPDG Manual of Practice (AASHTO, 2008). These relationships are repeated within this chapter for completeness.

2.1 INPUT CATEGORIES

The inputs to the program are grouped into five categories: (1) General Project Information (including the design criteria), (2) Traffic, (3) Climate, (4) Design Features, and (5) Structure (including material properties). Appendix A (*Checklist and Input Worksheets for the MEPDG in Mississippi*) includes a listing of all inputs within each of these categories. It is essential that the inputs are adequately determined to quantify the accuracy of the transfer functions relative to MDOT’s operational policies, material and construction specifications, truck traffic, and climate. Each input category relative to calibration is discussed separately in latter chapters of this report.

2.2 HIERARCHICAL INPUT APPROACH

The MEPDG uses a hierarchical approach for determining the inputs. Data are classified as input levels 1, 2, or 3 depending upon the importance of the project. For example, low-volume roads may use input level 3 data, whereas high-volume roads would use input level 1 data because a more precise design is required. The standard error, however, is the same for all transfer functions regardless of the input level used, except for transverse cracking of flexible pavements.

Table 2 defines each level, while the hierarchical approach for the inputs is explained in detail in Section 6 of the 2008 MEPDG Manual of Practice. As noted above, input level has no effect other than knowledge of the input parameter except for low-temperature transverse cracking of HMA wearing surfaces (see Table 1). For low-temperature transverse cracking, the standard error of the transfer function is dependent on the input level.

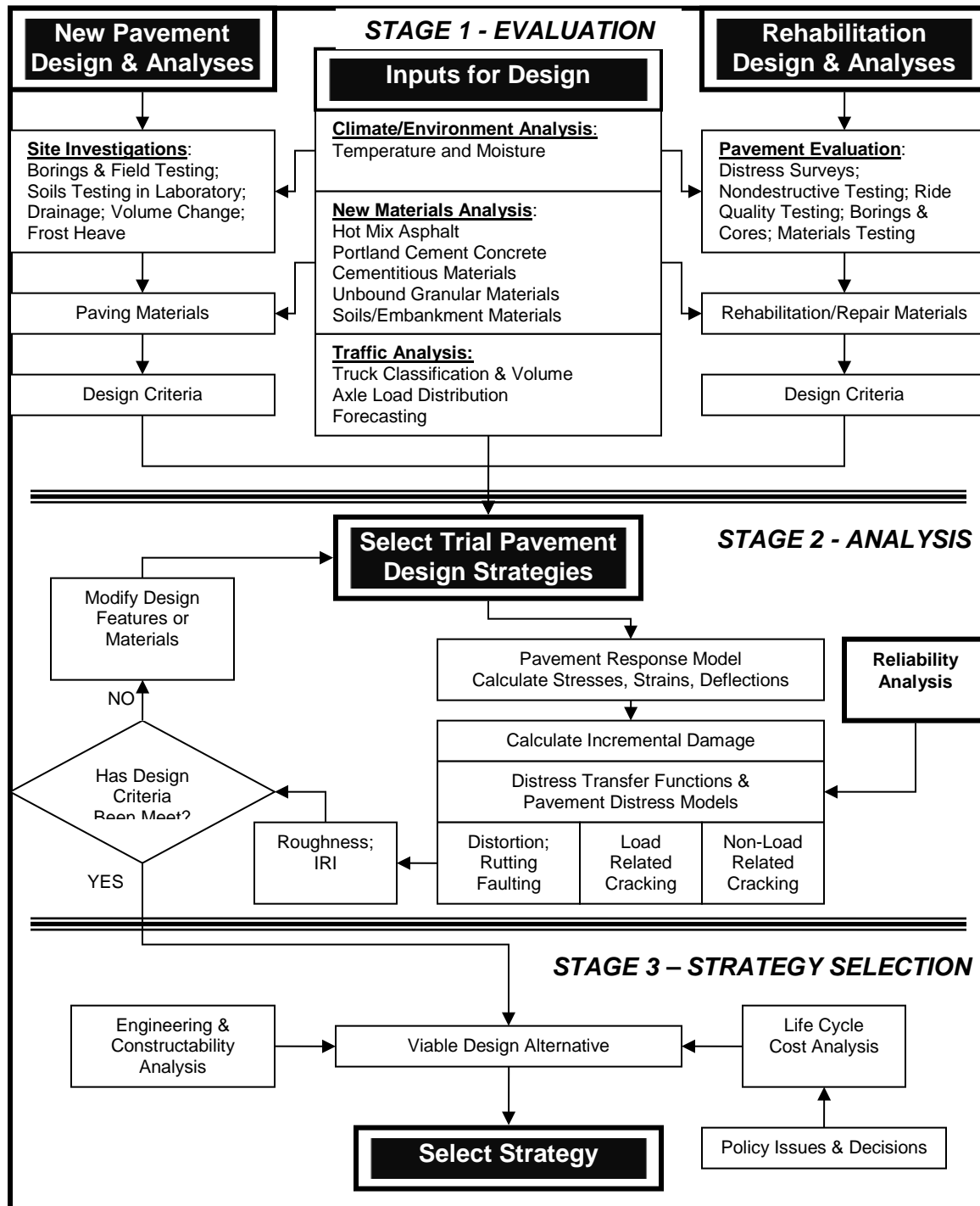


Figure 1—Conceptual Flow Chart for the MEPDG Three-Stage Design-Analysis Process (AASHTO, 2008)

Table 1—Performance Indicators Predicted by Pavement ME Design Software

Type of Pavement		Performance Indicator	Type of Model	Standard Error Tied to Input Level
Flexible Pavement and HMA Overlays	HMA Rutting		ME Transfer Function	No
	Unbound Aggregate Base and Subgrade Rutting		ME Transfer Function	No
	Fatigue Cracking	Alligator Area Cracking; Bottom-Up Cracking	ME Transfer Function	No
		Longitudinal Cracking; Top-Down Cracking	ME Transfer Function	No
	Thermal, Low-Temperature Cracking (Transverse)		ME Transfer Function	Yes
	International Roughness Index		Regression Equation	No
	Reflection Cracking; confined to HMA overlays		Regression Equation	No
Semi-Rigid Pavement	Fatigue Cracking of Cementitious Layer		ME Transfer Function	No
	HMA Rutting, Fatigue Cracking, and Low-Temperature Cracking; same as for flexible pavements		ME Transfer Functions	No
	International Roughness Index		Regression Equation	No
Rigid Pavements	JPCP & JPCP Overlays	Faulting	ME Transfer Function	No
		Fatigue Mid-Slab Cracking	ME Transfer Function	No
		International Roughness Index	Regression Equation	No
	CRCP & CRCP Overlays	Punchouts	ME Transfer Function	No
		International Roughness Index	Regression Equation	No

Table 2—Hierarchical Input Levels

Input Level	Definition of the Level
1	Input parameter based on site specific data and information. Level 1 represents the greatest knowledge about the input parameter for the specific project. This input level would be limited to designs having unusual site features, materials, or traffic conditions, and it has the highest testing or data collection costs for determining the input value.
2	Regression equations are used to determine the input value. The data collection and testing for this input level is much simpler and less costly. This level is typically used for the more routine pavement designs.
3	Level 3 inputs are “best-guessed” (default) values that represent global or regional average values. This input level has the least knowledge about the input parameter for the specific project. Initially, it is expected that this level will be the one more commonly used until MDOT becomes familiar with the MEPDG and its multiple inputs.

One of three levels can be used to estimate the value for each input, and the three levels can be combined for different inputs. The procedure does not require that all inputs have the same hierarchical level. The three levels allow MDOT’s users with minimal experience in ME based procedures and no advanced materials test equipment to use the MEPDG with little initial investment. The highest level of input or “best available data” was used in verifying and calibrating the MEPDG transfer functions, both at the global and local level. Table 3 identifies the input levels used for verification and local calibration. The three levels as used in MDOT’s verification and local calibration process are defined below.

Table 3—Predominant Source of Data Used for Transfer Function Verification and Initial Calibration in Mississippi

Input Group		Input Parameter	Input Level Used for Calibration	Data Source		
Truck Traffic		Initial Average Annual Daily Truck Traffic	Level 1	LTPP & MDOT Traffic Databases (backcast value)		
		Axle load distributions (single, tandem, tridem)	Level 1	LTPP & MDOT WIM Databases		
		Truck volume distribution	Level 1	LTPP & MDOT Traffic Databases		
		Lane & directional truck distributions	Level 1	LTPP & MDOT Databases		
		Tire pressure	Level 3	MEPDG defaults		
		Axle configuration, tire spacing	Level 3			
Truck wander	Level 3					
Climate		Temperature, wind speed, cloud cover, precipitation, relative humidity	Level 1	Expanded Historical Weather Station Database (Truax, et. al., 2011)		
Material Properties		Unbound Layers & Subgrade		LTPP; Lab & Backcalculated Values/Constr. Files		
		Resilient modulus – subgrade	Levels 1 & 2			
		Resilient modulus – unbound aggregate base/subbase	Levels 1 & 2	LTPP Database/Constr. Files		
		Classification & volumetric properties	Level 1			
		Moisture-density relationships	Level 1			
		HMA		Soil-water characteristic relationships	Level 3	MEPDG defaults
				Saturated hydraulic conductivity	Level 3	
				HMA dynamic modulus	Level 3	MEPDG E* Equation
				HMA creep compliance & indirect Tensile strength	Level 3	MEPDG defaults
		PCC		Volumetric properties	Level 1	LTPP Database/Constr. Files
HMA coefficient of thermal expansion	Level 3			MEPDG defaults		
PCC elastic modulus	Level 1 & 2			LTPP & MDOT Databases		
All Materials		PCC flexural strength	Level 1 & 2	LTPP & MDOT Databases		
		PCC coefficient of thermal expansion	Level 1 & 3	LTPP & MDOT Databases		
		Unit weight	Level 1	LTPP Database/Constr. Files		
		Poisson’s ratio	Level 3	MEPDG defaults		
Surface Condition (Distress Measurements)		Other thermal properties; conductivity, heat capacity, surface absorptivity	Level 3	MEPDG defaults		
		Initial IRI	Level 1	LTPP & MDOT Databases (backcast value)		
		Average rut depth and fatigue cracking	Level 1	LTPP Database & MDOT PMS Database		

1. Input level 1 data are used to design high-volume roads where there is safety or economic consequences of early failure. Obtaining level 1 inputs requires more resources and time than other levels. Level 1 uses site-specific data such as laboratory test data on soils or materials. Other examples would be Falling Weight Deflectometer (FWD) testing and backcalculation of pavement characteristics for a rehabilitation project or site-specific weigh-in-motion (WIM) traffic data.
2. Input level 2 data generally represent the inputs used in the current State Department of Transportation (DOT) design procedures when resources or testing equipment are not available for tests required for level 1. These are usually user-selected inputs selected from experience or from a database of earlier test results. These could also be estimated through correlations with simpler tests. Examples of such data include estimating asphalt concrete dynamic modulus from binder, aggregate, and mix properties, or using site-specific traffic volume and traffic classification data in conjunction with agency-specific axle load spectra.
3. Input level 3 inputs are used where there are minimal consequences of early failure (e.g., lower volume roads). These are usually user-selected default values or “best-guessed” values and represent typical averages for a particular part of the state.

This hierarchical approach provides the designer with flexibility in obtaining the design inputs based on the criticality of the project and available resources. For a given design project, inputs from a mix of input levels can be used. No matter what input levels are used, the computational algorithm for damage in the design procedure remains the same. Stated differently, the same models, transfer functions, and procedures are used to predict distress and smoothness no matter what input levels are used.

A notable exception to this general rule is the thermal fracture model which has three different formulations of the design reliability equation corresponding to each of the three input levels. Future calibration of the MEPDG software, however, will attempt to link input accuracy level to design reliability for the other prediction models. This will provide a powerful tool to show the advantages of good engineering design (using Level 1 inputs) for improving the reliability of a design and the possibility to reduce pavement construction and rehabilitation costs. As an example, Von Quintus, et al under NCHRP project 9-30A found the use of repeated load plastic deformation tests were cost effective in reducing the standard error of the estimate in comparison to using the default coefficients of the rut depth transfer function (*Von Quintus, et al., 2012*). In general, the highest input level was used in the local calibration process for Mississippi. It is recommended that MDOT continue using the results from testing (input level 1), rather than just using “best guessed” or default values (input level 3).

2.3 TRANSFER FUNCTIONS

Chapter 5 in the *MEPDG—A Manual of Practice* includes a summary of the transfer functions for all types of pavements that are included in the MEPDG design and analysis methodology. Table 1 listed the performance indicators and the type of model or equation used to predict performance for each family of pavements included in the Pavement ME Design software. This section of Chapter 2 provides a summary of the distress transfer functions and describes how the distress or performance indicators are predicted. As noted above, a summary of the transfer functions is provided in this section for completeness.

2.3.1 Flexible and Semi-Rigid Pavements

2.3.1.1 Rutting or Permanent Deformation Transfer Function

Two transfer functions are used to predict the total rut depth of flexible pavements and HMA overlays of flexible pavements: one for the HMA layers and the other one for all unbound aggregate base layers and subgrades. For semi-rigid pavements, it is assumed no plastic deformation accumulates in the unbound layer or subgrade.

The HMA calibrated transfer function was based on laboratory repeated load plastic deformation tests and is shown below.

$$\Delta_{p(HMA)} = \varepsilon_{p(HMA)} h_{HMA} = \beta_{1r} k_z \varepsilon_{r(HMA)} 10^{k_{1r}} n^{k_{2r} \beta_{2r}} T^{k_{3r} \beta_{3r}} \quad (1)$$

Where:

- $\Delta_{p(HMA)}$ = Accumulated permanent or plastic vertical deformation in the HMA layer/sublayer, in.
- $\varepsilon_{p(HMA)}$ = Accumulated permanent or plastic axial strain in the HMA layer/sublayer, in/in.
- $\varepsilon_{r(HMA)}$ = Resilient or elastic strain calculated by the structural response model at the mid-depth of each HMA sublayer, in/in.
- $h_{(HMA)}$ = Thickness of the HMA layer/sublayer, in.
- n = Number of axle load repetitions.
- T = Mix or pavement temperature, °F.
- k_z = Depth confinement factor.
- $k_{1r, 2r, 3r}$ = Global field calibration parameters (from the NCHRP 1-40D recalibration; $k_{1r} = -3.35412$, $k_{2r} = 0.4791$, $k_{3r} = 1.5606$).
- $\beta_{1r}, \beta_{2r}, \beta_{3r}$ = Local or mixture field calibration constants; for the global calibration, these constants were all set to 1.0.

$$k_z = (C_1 + C_2 D) 0.328196^D \quad (2)$$

$$C_1 = -0.1039(H_{HMA})^2 + 2.4868H_{HMA} - 17.342 \quad (3)$$

$$C_2 = 0.0172(H_{HMA})^2 - 1.7331H_{HMA} + 27.428 \quad (4)$$

D = Depth below the surface, in.

H_{HMA} = Total HMA thickness, in.

It should be understood that the global calibration coefficients for HMA mixtures take into account the shift between the laboratory and field-derived coefficients. This shift factor is discussed in more detail in Chapter 8 relative to MDOT's mixtures, climates, and operational policies.

Equation 5 shows the field-calibrated transfer function for the unbound layers and subgrade.

$$\Delta_{p(soil)} = \beta_{s1} k_{s1} \varepsilon_v h_{soil} \left(\frac{\varepsilon_o}{\varepsilon_r} \right) e^{-\left(\frac{\rho}{n} \right)^\beta} \quad (5)$$

Where:

- $\Delta_{p(Soil)}$ = Permanent or plastic deformation for the layer/sublayer, in.
- n = Number of axle load applications.

- ϵ_o = Intercept determined from laboratory repeated load permanent deformation tests, in/in.
 ϵ_r = Resilient strain imposed in laboratory test to obtain material properties ϵ_o , β , and ρ , in/in.
 ϵ_v = Average vertical resilient or elastic strain in the layer/sublayer and calculated by the structural response model, in/in.
 h_{Soil} = Thickness of the unbound layer/sublayer, in.
 k_{s1} = Global calibration coefficients; $k_{s1}=2.03$ for granular materials and 1.35 for fine-grained materials.
 β_{s1} = Local calibration constant for the rutting in the unbound layers; the local calibration constant was set to 1.0 for the global calibration effort.

$$\text{Log} \beta = -0.61119 - 0.017638(W_c) \quad (6)$$

$$\rho = 10^9 \left(\frac{C_o}{1 - (10^9)^\beta} \right)^{\frac{1}{\beta}} \quad (7)$$

$$C_o = \text{Ln} \left(\frac{a_1 M_r^{b_1}}{a_9 M_r^{b_9}} \right) = 0.0075 \quad (8)$$

- W_c = Water content, percent.
 M_r = Resilient modulus of the unbound layer or sublayer, psi.
 $a_{1,9}$ = Regression constants; $a_1=0.15$ and $a_9=20.0$.
 $b_{1,9}$ = Regression constants; $b_1=0.0$ and $b_9=0.0$.

2.3.1.2 Alligator, Fatigue (Bottom-Up) Cracking Transfer Function

Two types of load-related cracks are predicted by the MEPDG, alligator cracking and longitudinal cracking. The MEPDG assumes alligator or area cracks initiate at the bottom of the HMA layers and propagate to the surface with continued truck traffic, while longitudinal cracks are assumed to initiate at the surface and propagate downward (top-down cracking).

The MEPDG Manual of Practice recommends the top-down or longitudinal cracking transfer function not be used to make design revisions. The debate and controversy on the appropriateness of the mechanism for surface initiated cracks has yet to be resolved. More importantly, field investigations were not used as part of the global calibration to confirm if the longitudinal cracks actually initiated at the surface. MDOT should revisit use of the top-down cracking transfer function after the field investigations of the non-LTPP sites has been completed.

The allowable number of axle load applications needed for the incremental damage index approach to predict both types of load related cracks (alligator and longitudinal) is shown below.

$$N_{f-HMA} = k_{f1} (C) (C_H) \beta_{f1} (\epsilon_t)^{k_{f2} \beta_{f2}} (E_{HMA})^{k_{f3} \beta_{f3}} \quad (9)$$

Where:

- N_{f-HMA} = Allowable number of axle load applications for a flexible pavement and HMA overlays.
 ϵ_t = Tensile strain at critical locations and calculated by the structural response model, in/in.
 E_{HMA} = Dynamic modulus of the HMA measured in compression, psi.
 k_{f1}, k_{f2}, k_{f3} = Global field calibration parameters (from the NCHRP 1-40D re-calibration; $k_{f1} = 0.007566$, $k_{f2} = -3.9492$, and $k_{f3} = -1.281$).
 $\beta_{f1}, \beta_{f2}, \beta_{f3}$ = Local or mixture specific field calibration constants; for the global calibration effort, these constants were set to 1.0.

$$C = 10^M \quad (10)$$

$$M = 4.84 \left(\frac{V_{be}}{V_a + V_{be}} - 0.69 \right) \quad (11)$$

- V_{be} = Effective asphalt content by volume, percent.
 V_a = Percent air voids in the HMA mixture.
 C_H = Thickness correction term, dependent on type of cracking.

$$C_H = \frac{1}{0.000398 + \frac{0.003602}{1 + e^{(11.02 - 3.49H_{HMA})}}} \quad (12)$$

H_{HMA} = Total HMA thickness, in.

The cumulative damage index (DI) is determined by summing the incremental damage indices over time, as shown below.

$$DI = \sum (\Delta DI)_{j,m,l,p,T} = \sum \left(\frac{n}{N_{f-HMA}} \right)_{j,m,l,p,T} \quad (13)$$

Where:

- n = Actual number of axle load applications within a specific time period.
 j = Axle load interval.
 m = Axle load type (single, tandem, tridem, quad, or special axle configuration).
 l = Truck type using the truck classification groups included in the MEPDG.
 p = Month.
 T = Median temperature for the five temperature intervals or quintiles used to subdivide each month, °F.

The area of alligator cracking and length of longitudinal cracking are calculated from the total damage over time using different transfer functions. The relationship used to predict the amount of alligator cracking on an area basis, FC_{Bottom} , is shown below.

$$FC_{Bottom} = \left(\frac{1}{60} \right) \left(\frac{C_4}{1 + e^{(C_1 C_1^* + C_2 C_2^* \text{Log}(DI_{Bottom} * 100))}} \right) \quad (14)$$

Where:

- FC_{Bottom} = Area of alligator cracking that initiates at the bottom of the HMA layers, percent of total lane area.
 DI_{Bottom} = Cumulative damage index at the bottom of the HMA layers.

$C_{1,2,4}$ = Transfer function regression constants; $C_4=6,000$; $C_1=1.00$; and $C_2=1.00$

$$C_1^* = -2C_2^* \quad (15)$$

$$C_2^* = -2.40874 - 39.748(1 + H_{HMA})^{-2.856} \quad (16)$$

H_{HMA} = Total HMA thickness, in.

2.3.1.3 Fatigue Cracking Transfer Function, Semi-Rigid Pavements

The extent of fatigue cracks in the CTB and other cementitious or pozzolonic layers is calculated using a similar process to the alligator fatigue cracks for the HMA mixtures. The allowable number of load applications for the CTB and other cementitious layers, N_{f-CTB} , is determined in accordance with equation 17. The amount or area of fatigue cracking is calculated in accordance with equation 18 using the CTB damage calculated similar to equation 13.

$$N_{f-CTB} = 10^{\left[\frac{k_{c1}\beta_{c1}\left(\frac{\sigma_t}{M_R}\right)}{k_{c2}\beta_{c2}} \right]} \quad (17)$$

$$FC_{CTB} = C_1 + \frac{C_2}{1 + e^{(C_3 - C_4 \text{Log}(DI_{CTB}))}} \quad (18)$$

Where:

- N_{f-CTB} = Allowable number of axle load applications for a semi-rigid pavement.
- σ_t = Tensile stress at the bottom of the CTB layer, psi.
- M_R = 28-day Modulus of rupture for the CTB layer, psi.
- DI_{CTB} = Cumulative damage index of the CTB or cementitious layer.
- $k_{c1,c2}$ = Global calibration factors – Undefined because prediction equation was never calibrated; these values are set to 1.0 in the software. From other studies, $k_{c1}=0.972$ and $k_{c2}=0.0825$.
- $\beta_{c1,c2}$ = Local calibration constants; these values are set to 1.0 in the software.
- FC_{CTB} = Area of fatigue cracking, sq ft.
- $C_{1,2,3,4}$ = Transfer function regression constants; $C_1=1.0$, $C_2=1.0$, $C_3=0$, and $C_4=1,000$, however, this transfer function was never calibrated and these values will likely change once the transfer function has been calibrated.

These damage and distress transfer functions were never calibrated under any of the NCHRP projects. Montana DOT, however, completed a local calibration study of fatigue cracking in semi-rigid pavements (*Von Quintus and Moulthrop, 2007*). The calibration coefficients were found to be highly dependent on the strength of the CTB layer. The following lists the coefficients derived from Montana using a much earlier version of the MEPDG software (version 0.9).

- For High Strength CAM Mixtures (intact cores recovered with cement content greater than 6 percent; compressive strength generally greater than 1,000 psi):
 - $B_{c1} = 0.85$
 - $B_{c2} = 1.10$

- For Moderate Strength CAM Mixtures (intact cores recovered with cement contents greater than 4 percent but less than 6 percent; compressive strength generally greater than 300 psi but less than 1,000 psi):
 - $B_{c1} = 0.75$
 - $B_{c2} = 1.10$
- For Low Strength CAM Mixtures (intact cores cannot be recovered with cement content generally less than 4 percent; compressive strength generally less than 300 psi):
 - $B_{c1} = 0.65$
 - $B_{c2} = 1.10$

The local calibration coefficients from the Montana DOT study were used as the starting point to evaluate the semi-rigid transfer function in Mississippi. CTB strengths, however, were generally unavailable from the MDOT construction files or from the LTPP database for the calibration sites (see Chapter 8).

The computational analysis of incremental fatigue cracking for a semi-rigid pavement uses the damaged modulus approach. In summary, the elastic modulus of the CTB layer decreases as the damage index, DI_{CTB} , increases. The following equation is used to calculate the damaged elastic modulus within each season or time period for calculating critical pavement responses in the CTB and other pavement layers.

$$E_{CTB}^{D(t)} = E_{CTB}^{Min} + \left(\frac{E_{CTB}^{Max} - E_{CTB}^{Min}}{1 + e^{(-4+14(DI_{CTB}))}} \right) \quad (19)$$

Where:

- $E_{CTB}^{D(t)}$ = Equivalent damaged elastic modulus at time t for the CTB layer, psi.
- E_{CTB}^{Min} = Equivalent elastic modulus for total destruction of the CTB layer, psi.
- E_{CTB}^{Max} = 28-day elastic modulus of the intact CTB layer, no damage, psi.

2.3.1.4 Thermal (Low Temperature) Cracking Transfer Function

The degree of thermal cracking predicted by the MEPDG uses an assumed relationship between the probability distribution of the log of the crack depth to HMA layer thickness ratio and the percent of cracking. The following equation is used to determine the extent of thermal cracking.

$$TC = \beta_{t1} N \left[\frac{1}{\sigma_d} \text{Log} \left(\frac{C_d}{H_{HMA}} \right) \right] \quad (20)$$

Where:

- TC = Observed amount of thermal cracking, ft/mi.
- β_{t1} = Regression coefficient determined through global calibration (400).
- $N[z]$ = Standard normal distribution evaluated at $[z]$.
- σ_d = Standard deviation of the log of the depth of cracks in the pavement (0.769), in.
- C_d = Crack depth, in.

H_{HMA} = Thickness of HMA layers, in.

The crack depth or amount of crack propagation induced by a given thermal cooling cycle is predicted using the Paris law of crack propagation in accordance with fracture mechanics.

$$\Delta C = A(\Delta K)^n \quad (21)$$

Where:

ΔC = Change in the crack depth due to a cooling cycle.
 ΔK = Change in the stress intensity factor due to a cooling cycle.
 A, n = Fracture parameters for the HMA mixture, which are obtained from the indirect tensile creep-compliance and strength of the HMA in accordance with the following equations.

$$A = 10^{k_t \beta_t (4.389 - 2.52 \text{Log}(E_{HMA} \sigma_m^n))} \quad (22)$$

Where:

$$\eta = 0.8 \left[1 + \frac{1}{m} \right] \quad (23)$$

k_t = Coefficient determined through global calibration for each input level (Level 1 = 1.5; Level 2 = 0.5; and Level 3 = 1.5).
 E_{HMA} = HMA indirect tensile modulus, psi.
 σ_m = Mixture tensile strength, psi.
 m = The m-value derived from the indirect tensile creep compliance curve measured in the laboratory.
 β_t = Local or mixture calibration factor.

The stress intensity factor, K , is defined or estimated using the following simplified equation.

$$K = \sigma_{tip} (0.45 + 1.99(C_o)^{0.56}) \quad (24)$$

Where:

σ_{tip} = Far-field stress from pavement response model at depth of crack tip, psi.
 C_o = Current crack length, feet.

2.3.1.5 Reflection Cracking Regression Equation

The MEPDG predicts reflection cracks in HMA overlays or HMA surfaces of semi-rigid pavements using an empirical equation. The empirical equation is used for estimating the amount of fatigue and thermal cracks from a non-surface layer that has reflected to the surface after a certain period of time. This empirical equation predicts the percentage of area of cracks that propagate through the HMA as a function of time using the relationship shown below. This empirical equation, however, was never calibrated under any of the NCHRP projects.

$$RC = \frac{100}{1 + e^{a(c)+bt(d)}} \quad (25)$$

Where:

RC = Percent of cracks reflected. [NOTE: The percent area of reflection cracking is output with the width of cracks being 1 ft.]

- t = Time, years.
- a, b = Regression fitting parameters defined through calibration process.
- c, d = User-defined cracking progression parameters.

The regression fitting parameters of the above equation (a and b) are a function of the effective HMA overlay thickness (H_{eff}), the type of existing pavement, and for PCC pavements, load transfer at joints and cracks, as shown below. The effective HMA overlay thickness is provided in Table 4. The user-defined cracking progression parameters can be used by the user to accelerate or delay the amount of reflection cracks, which also are included in Table 4. Non-unity cracking progression parameters (c and d) could be used with caution, after they have been calibrated locally.

$$a = 3.5 + 0.75(H_{eff}) \tag{26}$$

$$b = -0.688684 - 3.37302(H_{eff})^{-0.915469} \tag{27}$$

The MEPDG predicts the total amount of cracking by combining the reflection cracks with the fatigue cracks predicted in the HMA overlay. Thus, the reflection cracking regression equation is not calibrated separately, but is calibrated concurrently with the other cracking transfer functions based on total cracking measured at the surface of the overlay.

Table 4—Reflection Cracking Model Regression Fitting Parameters

Pavement Type	Fitting and User-Defined Parameters (equation 25)			
	a and b	c	D	
	H_{eff} of Equations 26 and 27		Delay Cracking by 2 years	Accelerate Cracking by 2 years
Flexible	$H_{eff} = H_{HMA}$	---	---	---
Rigid-Good Load Transfer	$H_{eff} = H_{HMA} - 1$	---	---	---
Rigid-Poor Load Transfer	$H_{eff} = H_{HMA} - 3$	---	---	---
Effective Overlay Thickness, H_{eff}, inches	---	---	---	---
<4	---	1.0	0.6	3.0
4 to 6	---	1.0	0.7	1.7
>6	---	1.0	0.8	1.4
NOTES:				
1. Minimum recommended H_{HMA} is 2 inches for existing flexible pavements, 3 inches for existing rigid pavements with good load transfer, and 4 inches for existing rigid pavements with poor load transfer.				

2.3.1.6 Asphalt Concrete Smoothness Regression Equation

The following equations were developed from data collected within the LTPP program and are used to predict IRI over time for HMA-surfaced pavements.

Equation for New HMA Pavements and HMA Overlays of Flexible Pavements:

$$IRI = IRI_o + 0.0150(SF) + 0.400(FC_{Total}) + 0.0080(TC) + 40.0(RD) \quad (28)$$

Where:

- IRI_o = Initial IRI after construction, in/mi.
- SF = Site factor; as defined below.
- FC_{Total} = Area of fatigue cracking (combined alligator, longitudinal, and reflection cracking in the wheel path), percent of total lane area. All load related cracks are combined on an area basis – length of cracks is multiplied by 1 foot to convert length into an area basis.
- TC = Length of transverse cracking (including the reflection of transverse cracks in existing HMA pavements), ft/mi.
- RD = Average rut depth, in.

The site factor (SF) is calculated in accordance with the following equation.

$$SF = Age(0.02003(PI + 1) + 0.007947(Precip + 1) + 0.000636(FI + 1)) \quad (29)$$

Where:

- Age = Pavement age, years.
- PI = Percent plasticity index of the soil.
- FI = Average annual freezing index, degree F days.
- $Precip$ = Average annual precipitation or rainfall, in.

Equation for HMA Overlays of Rigid Pavements:

$$IRI = IRI_o + 0.00825(SF) + 0.575(FC_{Total}) + 0.0014(TC) + 40.8(RD) \quad (30)$$

2.3.2 Rigid Pavements

2.3.2.1 JPCP Fatigue Mid-Slab Cracking

Two key models are involved with the verification of transverse slab cracking. The following equation estimates the fatigue life (N) of PCC in terms of the number of axle applications when subjected to repeated stress for a given flexural strength. Calibration factors C_1 and C_2 could be modified, but the MEPDG Manual of Practice does not recommend changing these coefficients because they are based on extensive field data (substantial laboratory and field testing data).

$$\log(N_{i,j,k,l,m,n}) = C_1 \cdot \left(\frac{MR_i}{\sigma_{i,j,k,l,m,n}} \right)^{C_2} \quad (31)$$

The transfer function with appropriate coefficients is the S-shaped curve giving the relationship between field measured cracking and accumulated fatigue damage index (DI) at the top and bottom of the JPCP slabs. Parameters C_4 and C_5 in the following equation are the ones to adjust to remove bias and improve the goodness of fit with field data.

$$CRK = \frac{1}{1 + C_4(DI_F)^{C_5}} \quad (32)$$

2.3.2.2 JPCP Faulting Transfer Function

The mean transverse joint faulting is predicted using a complex incremental approach. A detailed description of the faulting prediction process is presented in the MEPDG Manual of Practice. MEPDG faulting is predicted using the models presented below:

$$Fault_m = \sum_{i=1}^m \Delta Fault_i \quad (33)$$

$$\Delta Fault_i = C_{34} * (FAULTMAX_{i-1} - Fault_{i-1})^2 * DE_i \quad (34)$$

$$FAULTMAX_i = FAULTMAX_0 + C_7 * \sum_{j=1}^m DE_j * \text{Log}(1 + C_5 * 5.0^{EROD})^{C_6} \quad (35)$$

$$FAULTMAX_0 = C_{12} * \delta_{curling} * \left[\text{Log}(1 + C_5 * 5.0^{EROD}) * \text{Log}\left(\frac{P_{200} * WetDays}{P_s}\right) \right]^{C_6} \quad (36)$$

Where:

- $Fault_m$ = mean joint faulting at the end of month m , in
- $\Delta Fault_i$ = incremental change (monthly) in mean transverse joint faulting during month i , in
- $FAULTMAX_i$ = maximum mean transverse joint faulting for month i , in
- $FAULTMAX_0$ = initial maximum mean transverse joint faulting, in
- $EROD$ = base/subbase erodibility factor
- DE_i = differential deformation energy accumulated during month i . computed using various inputs including joint LTE and dowel damage.
- $\delta_{curling}$ = maximum mean monthly slab corner upward deflection due to temperature curling and moisture warping.
- P_s = overburden on subgrade, lb.
- P_{200} = percent subgrade soil material passing No. 200 sieve
- $WetDays$ = average annual number of wet days (greater than 0.1 in rainfall)

$$C_{12} = C_1 + C_2 * FR^{0.25} \quad (37)$$

$$C_{34} = C_3 + C_4 * FR^{0.25} \quad (38)$$

- FR = base freezing index defined as percentage of time the top base temperature is below freezing (32°F) temperature.

Dowel joint damage accumulated for the current month is determined from the following equation:

$$\Delta DOWDAM_{tot} = \sum_{j=1}^N C_8 * F_j \frac{n_j}{d f_c^*} \quad (39)$$

Where:

- $\Delta DOWDAM_{tot}$ = Cumulative dowel damage for the current month
- N_j = Number of axle load applications for current increment and load group j

- N = Number of load categories
- f_c^* = PCC compressive stress estimated
- C_8 = Calibration constant
- F_j = Effective dowel shear force induced by axle loading of load category j.
- C_1 through C_8 are calibration constants established from field performance.

Calibration of the faulting model involved deriving the calibration parameters C_1 through C_7 (equations 33 to 38) and the rate of the dowel deterioration parameter C_8 (equation 39), which minimize the error function, ERR, defined as:

$$ERR(C_1, C_2, \dots, C_8) = \sum_{ob=1}^{Nob} (FaultPredicted_{ob} - FaultMeasured_{ob})^2 \quad (40)$$

Where:

- ERR = error function
- C_1, C_2, \dots, C_8 = calibration parameters
- $FaultPredicted_{ob}$ = predicted faulting for observation ob in the calibration database
- $FaultMeasured_{ob}$ = measured faulting for observation ob in the calibration database
- Nob = Number of observation in the calibration database

Global calibration coefficients from NCHRP project 20-07 are listed below:

- C1 = 0.51040
- C2 = 0.00838
- C3 = 0.00147
- C4 = 0.008345
- C5 = 5999
- C6 = 0.8404
- C7 = 5.9293
- C8 = 400

2.3.2.3 JPCP Smoothness Regression Equation

The IRI for JPCP is significantly affected by mid-slab cracking, faulting, spalling, and site factor. The smoothness degradation regression equation is as follows:

$$IRI = IRI_i + J1*CRK + J2*SPALL + J3*FAULT + J4*SF \quad (41)$$

Where:

- IRI_i = Initial IRI
- CRK = JPCP transverse cracking
- SPALL = JPCP joint spalling
- FAULT = JPCP mean joint faulting
- SF = Site factor

2.3.2.4 CRCP Punchout Transfer Function

The CRCP transfer function for punchouts is a function of accumulated fatigue damage due to top-down stresses in the transverse direction. A complete explanation and discussion of the punchout transfer function is included in the MEPDG Manual of Practice.

$$PO = \frac{A_{PO}}{1 + \alpha_{PO} \cdot DI_{PO}^{\beta_{PO}}} \quad (42)$$

Where:

- PO = Total predicted number of medium and high severity punchouts per mile.
- DI_{PO} = Accumulated fatigue damage (due to slab bending in the transverse direction) at the end of y^{th} year.
- $A_{PO}, \alpha_{PO}, \beta_{PO}$ = Calibration constants (85, 1.4149, -0.8061, respectively) from NCHRP project 20-07.

2.3.2.5 CRCP Smoothness Regression Equation

Key distresses affecting the IRI for CRCP include punchouts and site factors. The CRCP IRI regression equation is given as follows:

$$IRI = IRI_i + C_1 \cdot PO + C_2 \cdot SF \quad (43)$$

Where:

- IRI_i = Initial IRI, in/mi.
- PO = Number of medium and high severity punchouts per mile.
- C_1 = 3.15
- C_2 = 28.35
- SF = Site factor

$$SF = AGE \cdot (1 + 0.556 FI) \cdot (1 + P_{200}) \cdot 10^{-6} \quad (44)$$

Where:

- AGE = Pavement age, yr.
- FI = Freezing index, °F days.
- P_{200} = Percent subgrade material passing No. 200 sieve.

2.4 STANDARD ERROR OF ESTIMATE

The MEPDG uses a different methodology in determining the reliability of a design. The standard error of the estimate (SEE) for each transfer function is used to determine the predicted performance indicators at different reliability levels. Table 5 summarizes the SEE for each transfer function. The calibration completed under NCHRP projects 1-37A and 1-40D eliminated bias at the global level using LTPP test sections. The SEEs from the local calibration process need to be compared with the global values to determine whether there is an improvement in the predictive capability of the transfer functions in Mississippi.

Table 5—Standard Errors of the Estimate for each Transfer Function included in the Pavement ME Design Software

Type of Pavement	Performance Indicator	Standard Error	Type of Model
Flexible Pavement and HMA Overlays	Total Rutting, inches	0.107	ME Transfer Function
	HMA Rutting	$= 0.1587(\Delta_{HMA})^{0.4579} + 0.001$	
	Unbound Aggregate Base and Coarse-Grained Soils Rutting	$= 0.1169(\Delta_{Gran})^{0.5303} + 0.001$	

	Fine-Grained Soils Rutting	$= 0.1724(\Delta_{Fine})^{0.5516} + 0.001$	
	Alligator Area Cracking; Bottom-Up Cracking, %	5.01	ME Transfer Function
		$= 32.7 + \frac{995.1}{1 + e^{2-2\text{Log}(FC_{Bottom} + 0.0001)}}$	
	Thermal, Low-Temperature Cracking (Transverse); ft./mi.	850 (input level 3)	ME Transfer Function
		$= -0.0869(TC + 453.98)$	
	International Roughness Index; New & Overlays, in./mi.	18.9	Regression Equation
IRI, HMA Overlays of JPCP	9.6		
Reflection Cracking; confined to HMA overlays	Standard error not defined because cracks were not segregated.	Regression Equation	
Semi-Rigid Pavement	Fatigue Cracking of Cementitious Layer	Was not calibrated, so standard error was not determined.	ME Transfer Function
	HMA Rutting, Fatigue Cracking, and Low-Temperature Cracking; same as for flexible pavements	Same as for flexible pavements and HMA overlays, but calibration not completed to verify concept.	ME Transfer Function
Rigid Pavement	JPCP Faulting	0.033	ME Transfer Function
		$= (0.00761(Fault) + 0.000081)^{0.445}$	
	JPCP Fatigue Mid-Slab Cracking, New, %	$= -0.00198(CK)^2 + 0.56857(CK) + 2.76825$	ME Transfer Function
	International Roughness Index, New JPCP, in./mi.	17.1	Regression Equation
	CRCP Punchouts; #/mi.	$= 0.00609(PO)^2 + 0.58242(PO) + 3.36783$	ME Transfer Function
CRCP International Roughness Index	14.6	Regression Equation	

2.5 DATA REQUIREMENTS

The data needed for the local calibration-validation process are dictated by the input requirements of the MEPDG procedure. Traffic, climate, materials and distress data are needed for each test section, which are summarized in Appendix A. The forms in Appendix A can be used by the MDOT pavement designers (staff and consultants) in setting up the runs with the MEPDG at least until MDOT becomes familiar with the inputs. Additional details about traffic, climate, and materials are provided in the following chapters.

The test sections included in the calibration sampling matrix (discussed in Chapter 3) represent a wide range of pavement strategies, layer properties, and surface conditions that are encountered in Mississippi. Chapters 4 (truck traffic), 5 (climate), and 6 (layer features), and 7 (material properties) discuss and overview the inputs used in the preliminary local calibration process.

CHAPTER 3—CALIBRATION SAMPLING MATRIX

Actual distress mechanisms are far more complex than can be predicted reliably using the performance models. Hence, the performance models are calibrated using measured performance data to obtain accurate performance prediction. The pavement distress models or transfer functions presented in Chapter 2 were calibrated at the global level using data from the LTPP program. As such, the current design procedure is based on the global averages in terms of performance, as well as input values, but may be inaccurate for all conditions and regions of the country. Thus, these global averages need to be verified at the local or state-level.

The intent of this chapter is to discuss the process used to develop the sampling matrix and experimental plan for verification and local calibration.

3.1 CALIBRATION OBJECTIVE AND OUTCOMES

The purpose of the global, as well as local, calibration process is to determine whether a conceptual model or transfer function is a reasonable representation of the real-world, and if the desired correspondence (accuracy) exists between the model simulations and real-world conditions. The transfer functions to predict these performance indicators were calibrated and validated using some of the LTPP test sections under NCHRP project 1-37A, but only a few of the MDOT LTPP test sections were used in that global calibration.

A global calibration cannot be expected to consider all potential factors that affect pavement performance. For example, factors such as maintenance strategies, construction specifications, aggregate and binder type, mixture design procedures, and material specifications can result in differences in performance. In fact, small differences in some of the above factors can cause large differences in performance. As such, the MEPDG transfer functions were verified and re-calibrated using Mississippi's roadway segments (LTPP and non-LTPP test sections).

The success of this process can be gauged on the biases of predicted values and the SEE. Reasonable goodness of fit was determined using the diagnostic statistics R^2 and SEE, while the presence or absence of bias was determined based on the hypothesis test described below. The criteria used to determine the adequacy of the global models for Mississippi conditions are presented in Table 6.

The SEE for the validation may not be equal to the SEE for calibration; generally, it is higher. To test if it is significantly higher, which would suggest that the validation failed, a chi-square test was used. Conversely, an operational definition of "reasonable correlation" is that the null hypothesis is accepted when the student and/or paired t-tests are used to compare the observed and predicted responses at a confidence interval of 95 percent ($\alpha = 0.05$). The MEPDG transfer functions were evaluated to determine if the global calibration coefficients are adequate for the construction practices, materials, climate, and traffic prevalent in Mississippi.

The MDOT verification and local calibration of the transfer functions followed the procedures and steps included in the 2010 Local Calibration Guide (*AASHTO, 2010*) relative to two objectives or outcomes. The first and primary outcome is verifying and making revisions to

the global calibration coefficients. The second outcome is equally important but ignored by some agencies implementation plans. The outcome verifies or revises the default values for some of the inputs and ensures the inputs are being properly determined. Inputs are equally important as the difference between the predicted and measured values.

Table 6—Criteria for Determining Transfer Functions Accuracy for Mississippi Conditions

Criterion of Interest	Test Statistic	Range of R ² & Model SEE	Rating
Goodness of fit	R ² , percent (all models)	81 to 100	Very good (strong relationship)
		64 to 81	Good
		49 to 64	Fair
		< 49	Poor (weak relationship)
	Global HMA alligator cracking model SEE	< 5 percent	Good
		5 to 10 percent	Fair
		> 10 percent	Poor
	Global HMA transverse cracking model SEE	—	N/A
	Global HMA total rutting model SEE	< 0.1 in	Good
		0.1 to 0.2 in	Fair
		> 0.2 in	Poor
	Global JPCP transverse cracking model SEE	< 4.5 percent	Good
		4.5 to 9 percent	Fair
		> 9 percent	Poor
	Global JPCP transverse joint faulting model SEE	< 0.033 in	Good
		0.033 to 0.066 in	Fair
> 0.066 in		Poor	
Global HMA IRI model SEE	< 19 in/mi	Good	
	19 to 38 in/mi	Fair	
	> 38 in/mi	Poor	
Bias	Hypothesis testing of slope of the linear measured vs. predicted distress/IRI model (b1 = slope) H0: b1 = 0	p-value	Reject if p-value is < 0.05 (i.e., 5 percent significant level)
	Paired t-test between measured and predicted distress/IRI	p-value	Reject if p-value is < 0.05 (i.e., 5 percent significant level)

The verification and local calibration process was focused more on the first outcome, because the field investigation for the non-LTPP roadway segments is planned for Phase 3. The project specific layer/material properties for the LTPP sites are included in the LTPP database. The layer/material properties for the non-LTPP sites were estimated from construction records. The field investigations planned for the non-LTPP sites are discussed in a latter section of this chapter.

3.2 CALIBRATION EXPERIMENTAL HYPOTHESIS

As stated above, it is impossible to account for all factors in developing a global distress/performance simulation model. All models have errors because of simplifying assumptions, so it is good practice to evaluate the applicability of any conceptual and/or statistical model on a limited basis prior to full-scale use. The LTPP test sections were selected to determine if there are significant differences between the measured and predicted distresses using the global calibration factors of the MEPDG conceptual model. The global calibration factors for each transfer function are included in Section 5 of the MEPDG Manual of Practice (AASHTO, 2008), as well as in Chapter 2 of this report.

The following experimental hypothesis was used to evaluate the accuracy and applicability of the MEPDG transfer functions and global calibration coefficients in predicting pavement distresses and smoothness for the materials, climate, and operational policies used in Mississippi. The null hypothesis is:

Null Hypothesis: There is no significant error and no bias (i.e.; as stated above, reasonable correlation and accuracy and no overall over or under prediction) between the predicted and measured values for each performance indicator for flexible and rigid pavements and overlays for roadways within MDOT's jurisdiction.

The criteria for performing local calibration were based on: (1) whether the given global transfer function exhibited a reasonable goodness of fit (between measured and predicted outputs), and (2) whether distresses/IRI were predicted without significant bias. Tables 1 and 5 included the transfer functions evaluated as part of the MEPDG implementation in Mississippi. Chapter 2 provided a detailed description of the transfer functions.

3.3 EXPERIMENTAL PLAN AND SAMPLING MATRIX

The experimental plan and sampling matrix were prepared at the beginning of Phase 1 to evaluate and determine the cause for performance differences so that adjustments can be made to the global calibration coefficients.⁵ The MEPDG software version 1.1 was initially used to predict the performance of the LTPP sites in Mississippi. The predicted values were compared to the measured distresses in making revisions to the sampling matrix, as well as for selecting test sections to fill the cells in the matrix. In addition, comparative designs were completed for projects with selected sites features. Results from those comparative designs were also used in revising the initial or Phase 1 sampling matrix.

Tables 7 and 8 show the primary tier factors in the final sampling matrix for flexible and rigid pavements, respectively. The rigid pavement matrix is smaller than the flexible pavement matrix because there are fewer rigid pavement strategies or family of pavements built in Mississippi in comparison to flexible pavement strategies. Cell numbers are also included in the sampling matrix and are used to evaluate the residual error as a function of the different factors.

⁵ Phase 1 Report: FHWA/MS-DOT-RD-03-163, Mississippi DOT's Plan to Implement the 2002 Design Guide; Authors Athar Saeed and Jim Hall, Mississippi DOT, Jackson, MS, September 2003.

Table 7—Sampling Matrix for Flexible and Semi-rigid Pavements, Cell Numbers for New Construction and Rehabilitation

Asphalt Binder Type	HMA Mixture Type	Subgrade Treatment	Pavement or Analysis Type							
			Conventional	Deep-Strength	Full-Depth	Semi-Rigid	HMA Overlays			
							Flexible Pavements		Rigid Pavements	
							HMA	Semi-Rigid	JPCP	CRCP
Unmodified	Dense	Untreated or Not Stabilized	1A	5A	9A	20A	30	40	50	54
		Stabilized	1B	5B	9B	20B				
	Superpave	Untreated or Not Stabilized	2A	6A	10A	21A	31	41	51	55
		Stabilized	2B	6B	10B	21B				
Modified	Dense	Untreated or Not Stabilized	3A	7A	11A	22A	32	42	52	56
		Stabilized	3B	7B	11B	22B				
	Superpave	Untreated or Not Stabilized	4A	8A	12A	23A	33	43	53	57
		Stabilized	4B	8B	12B	23B				

Notes:

1. The deep-strength pavement structures will generally include more than 6 inches of total HMA thickness.
2. Full-depth is whatever the HMA thickness is above the unmodified or modified subgrade.
3. Semi-Rigid pavement structures can include lime-fly ash (LFA) or Portland cement additive for the pozzolonic-stabilized layer.
4. Additional LTPP test sections in adjacent states will be used where applicable.

Table 8—Sampling Matrix for Rigid Pavements, Cell Numbers for New Construction and Rehabilitation

Subgrade	Design Features				Pavement Types; New Construction		Overlays
	Graunlar Base	Dowels	Shoulder	Drainage	JPCP	CRCP	Unbonded PCC of JPCP
Stablized Subgrade Soil	Aggregate	Yes	Widened	None & PATB	1.a to 1.f	There are relatively few CRCP pavements, use as many as exists in the database with sufficient & adequate data.	There are relatively few unbonded PCC overlays, use as many as exists in the database with sufficient & adequate data.
			PCC				
			HMA				
		No	Widened	None & PATB	2.a to 2.f		
	PCC						
	HMA						
	None Present	Yes	Widened	None & PATB	3.a to 3.f		
			PCC				
HMA							
No		Widened	None & PATB	4.a to 4.f			
	PCC						
	HMA						
Soil unstablized	Aggregate	Yes	Widened	None & PATB	5.a to 5.f		
			PCC				
			HMA				
		No	Widened	None & PATB	6.a to 6.f		
	PCC						
	HMA						
	None Present	Yes	Widened	None & PATB	7.a to 7.f		
			PCC				
HMA							
No		Widened	None & PATB	8.a to 8.f			
	PCC						
	HMA						

3.3.1 Experimental Factors

The levels for the primary factors were established based on the previous discussion and in consultation with the Research, Roadway Design, and Materials Divisions of Mississippi DOT during Phase 1. Traffic and thickness were excluded as primary factors in the factorial experiment, because they represent definitive or well-defined input values. Material design features were included as the primary factors. Similarly, soil type (classification) and resilient modulus were also excluded as a primary factor because they represent well-defined, definitive input values. Soil stabilization is common practice in Mississippi for both flexible and rigid pavements. Thus, the primary factor included in the sampling matrix was stabilized and unstabilized subgrade soils.

3.3.2 Number and Types of Calibration Sites

The total number of sites required for the flexible and rigid pavement sampling matrices was estimated in accordance with the 2010 AASHTO Local Calibration Guide. MDOT recognized the value of their pavement performance and construction databases and LTPP sites towards validating the distress transfer functions and design tools. Both LTPP and non-LTPP sites were used to estimate the precision and eliminate any bias of the MEPDG transfer functions relative to Mississippi's materials, local conditions, and operational policies. The following describes the specific use of each set of sites (LTPP and non-LTPP).

- The Mississippi LTPP test sections were identified as priority sites, because the time-series performance, materials, traffic, and other data was readily available for these test sections. These sites were used for the verification and local calibration of the transfer functions. The LTPP sites in adjoining States were also reviewed for use in Mississippi's experimental plan and factorials to supplement the Mississippi LTPP sites, especially for the rigid pavement sampling matrix.
- Roadway segments from Mississippi DOT's pavement management system (PMS) were used to fill in the gaps of the sampling matrix. The Mississippi construction database was queried by MDOT staff to identify projects with design and site features included in the sampling matrix for flexible and rigid pavements (refer to Tables 7 and 8). The construction database was also used to identify those projects for which the majority of the layer/material properties were available in the project files. Non-LTPP sites were selected for each cell at random based on the following criteria.
 - Distress magnitude was considered in selecting the test sections for the individual cells. Two test sections were selected for each cell—one with a low level of distress and the second with a high level of distress.
 - Two sets of test sections were selected for each cell: one set for fatigue cracking and ride quality, and the second set for rutting and thermal cracking. These two sets were initially developed because of different factors influencing fatigue cracking and ride quality (more structural related factors) versus rutting and thermal cracking (more mixture related factors). The two test sections in each cell have different performance measures but are about the same age.
 - Availability of as-built construction data. Based on a review of the files, many of the projects were removed from the sampling matrix because of missing data, such that there were too many cells without any projects. It became obvious that a field investigation program was needed to confirm the as-built data and

- determine level 1 inputs. The verification and preliminary local calibration discussed in Chapters 8 and 9 were completed using the available data collected under Phase 2 using mostly input level 3 for the layer properties.
- Maintaining a balanced experimental factorial or sampling matrix with the assumption that the LTPP and non-LTPP sites can be combined.

3.4 NUMBER AND TYPES OF CALIBRATION SITES

Tables 9 and 10 list the sites included in the sampling matrix for evaluating bias or residual error (predicted minus measured values) throughout the sampling matrix. The number of sites exceeds the minimum number stated in the 2010 AASHTO Local Calibration Guide. All roadway segments included in the flexible and semi-rigid pavement sampling matrix are located in Mississippi (see Table 9). There were fewer rigid pavement segments available in Mississippi, so some of the LTPP rigid pavement sections located in adjacent states were included in the rigid pavement sampling matrix (see Table 10).

The flexible and rigid pavement sampling matrices are fractional factorials designed to be grouped into new construction and overlays (HMA and PCC) of flexible pavements for all of the performance indicators. The fractional factorials are unbalanced, which will need to be considered in deriving the local calibration coefficients. The reason for the unbalanced sampling matrices is a result of MDOT operational and design policies (many more roadway projects have specific features). The use of an unbalanced sampling matrix or fractional factorial is common and does not prevent the determination of the calibration coefficients.

The semi-rigid new construction pavements were combined with the HMA overlays to evaluate the calibration coefficients of the reflection cracking transfer function. The semi-rigid pavements were used by themselves in terms of determining the local calibration coefficients for the fatigue cracking transfer function of the CTB layer. The Montana DOT local calibration study was used as the starting point for the Mississippi local calibration process (*Von Quintus and Moulthrop, 2007*).

The fractional factorial for new construction was designed to be grouped into three types of flexible pavements which were collapsed into two groups in the final sampling matrix (conventional and deep-strength flexible pavements). There are only two full-depth non-LTPP sections in the sampling matrix, so these were combined with the deep-strength flexible pavement groups. In addition, the flexible pavement sampling matrix includes a higher number of sites with neat (unmodified) asphalt in comparison to polymer modified asphalt (PMA) and a higher number of sites with stabilized soils in comparison to untreated soils.

3.5 FIELD INVESTIGATIONS

Just about all agencies that have completed a local calibration study recognized the importance of field investigations. Some agencies initially excluded field investigations from their implementation and calibration plan, but quickly realized its value in reducing the SEE of the transfer functions, because level 1 inputs are being used rather than “best-guessed” values and/or the average value from an entire construction project.

Table 9—Number of Test Sections: Flexible and Semi-rigid Pavements, New Construction and Rehabilitation

Asphalt Binder Type	HMA Mixture Type	Subgrade Treatment	Pavement or Analysis Type								
			Conventional	Deep-Strength	Full-Depth	Semi-Rigid	HMA Overlays				
							Flexible Pavements		Rigid Pavements		
							HMA	Semi-Rigid	JPCP	CRCP	
Unmodified	Dense	Untreated or Not Stabilized		L805, 806; L1001, L1016, L1802, LA310, LA330, LA350	2202; L3091	L2807, L3081, L3087, L3089, L3090	1822 1823 222 1463	1708 2358 1125 1703;	L3097, L7012	L3099, L9030	
		Stabilized	4776 4834	1122	L501-560; L3093	4527; L902, L903, L959; L3082, L3083, L3085, L3089, L3090, L3094	L502-560; L1001, L1802, L3091, L3093, LA310, LA320, LA330, LA350	L902; L2807, L3081, L3085, L3087, L3094			
	Superpave	Untreated or Not Stabilized	4816 4894 5618 5688 5849	5105 5500	4602	3163 5210 5244 5249 5627					
		Stabilized	4784 4865 4902 5230 5628	1123 2580 3144 4864 5280 5310 5318 6015		4588 4669 4782 5506 5511 5526 5554 5828	3868 1351	2108 3512; L959			
		Untreated or Not Stabilized				1797 1799					
		Stabilized	5616			3038					
Modified	Superpave	Untreated or Not Stabilized			4742	2824 2830					
		Stabilized		3204 4580 4933	4889 5446	3699 3686	2833 2851 L903				
Total Number of Calibration Sites			13	22	5	29	22	18	2	2	

L – Identifies the LTPP test sections.

A sampling and testing plan was prepared under Phase 2, based on the review of as-built and construction files. Appendix B includes the “*Materials Sampling and Testing Plan and Guidelines for Projects Used for Local Calibration.*” This plan is to be executed under Phase 3 for the final calibration. The following are the primary issues and points that were used in preparing that field investigation plan.

- Pavement distress data from the LTPP database and the MDOT PMS database were used for the preliminary calibration of the transfer functions. MDOT distress database includes detailed distress data believed to be consistent with the Federal Highway Administration (FHWA) Distress Identification Manual that was used and is being used on all of the LTPP test sections (FHWA, 1993). As such, the distress surveys are to be completed in accordance with the FHWA Distress Identification Manual to confirm the consistency in observed values between the LTPP and non-LTPP sections.

Table 10—Number of Test Sections: Rigid Pavements, New Construction and Rehabilitation

Design Features					Pavement Types; New Construction		Overlays
Subgrade	Graunlar Base	Dowels	Shoulder	Drainage	JPCP	CRCP	Unbounded PCC of JPCP
Stablized Subgrade Soil	Aggregate	Yes	Widened	None & PATB	960; 1682; 2302; 2389; 5764		903-PCC overlay of HMA; 2258-PCC overlay of HMA; 6023-PCC overlay of CRCP
			PCC				
			HMA				
		No	Widened	None & PATB		6023; L3099	
	PCC						
	HMA						
	None; CTB or Lime Stab.	Yes	Widened	None & PATB	903; 2258; 2838; L3018; L3019		987-PCC overlay of CRCP; 989-PCC overlay of CRCP; 991-PCC overlay of CRCP
			PCC				
HMA							
No		Widened	None & PATB	L4024	987; 989; 991; L5006		
	PCC						
	HMA						
Soil unstablized	Aggregate	Yes	Widened	None & PATB	2789; 2826		L7012
			PCC				
			HMA				
		No	Widened	None & PATB			
	PCC						
	HMA						
	None; CTB or Lime Stab.	Yes	Widened	None & PATB	2797; 2798; 2868; 2869		
			PCC				
HMA							
No		Widened	None & PATB	2826; 2382; 2383	L5025; L5803; L5805		
	PCC						
	HMA						
Total Number of Calibration Sites					20	9	7

L – Identifies the LTPP test sections.

- Cores are needed for the flexible pavement test sections to determine whether the cracks started at the surface or bottom of the HMA layers. The cores and borings will also be used to confirm the as-built layer thickness. More importantly, the cores are used to determine whether all layers in the flexible pavement are bonded and if any material defects like stripping have occurred.
- Cores of any CTB layer in a semi-rigid pavement are also required for measuring the in place compressive strength of that layer. The 28-day strengths will be estimated by backcasting the current strength for the time of construction using a similar procedure for backcasting as for the 28-day PCC strength.
- Laboratory tests are included in the plan to measure the in place volumetric properties. This data is needed to backcast the air voids at construction which are unavailable for many of the non-LTPP and LTPP projects, especially for the older projects.
- The in place water content and density of the unbound layers are also important. Samples of the unbound aggregate base layers and embankment soils will be recovered for testing. The strength of the unbound layers should be measured using the dynamic cone penetrometer (DCP). The DCP can be used to estimate the transition between different unbound layers in support of the backcalculated elastic layer modulus values.

- One of the more important activities of the field investigations is to measure the deflection basins along the segment identified for use in local calibration. The deflection basin data are used to backcalculate the elastic modulus of all structural layers. The backcalculated elastic layer modulus can be used to estimate the in place damage and independently determine the coefficients of the fatigue cracking transfer function (see equation 14).
- The fatigue cracking transfer function is applicable to both bottom- and surface-initiated fatigue cracks. Because two types of fatigue cracking mechanisms are considered, the field investigation includes cores to determine the direction of crack propagation. Classical fatigue or “alligator cracking” starts at the bottom under the wheel load due to limiting tensile strains being exceeded at the bottom of the HMA layer. At the edge of the tire, the tension in the HMA is at the top, hence a longitudinal crack appears.

CHAPTER 4—TRUCK TRAFFIC

This chapter summarizes and explains how the truck traffic inputs were determined and used in the local calibration process and in developing the default values for selected truck traffic inputs. Appendices A and C show the traffic data used for calibration. MDOT research study SS 165 provided a lot of the data that was used to determine the default values when sufficient traffic data were unavailable (*Buchanan, 2004*).

The Planning Division used a truck traffic tool called *Mississippi's Advanced Traffic Loading Analysis System (MS-ATLAS)* to generate many of the traffic inputs for a specific roadway segment. Appendix C (*MS-ATLAS Truck Traffic Analysis Tool for Mississippi*) provides a brief discussion on the software and how that software is used to determine some of the truck traffic input values required for the Pavement ME Design software. This chapter defines and explains the truck traffic parameters and values used in the preliminary local calibration effort.

4.1 TRUCK VOLUME—AVERAGE ANNUAL DAILY TRUCK TRAFFIC

Average annual daily truck traffic (AADTT) is an important input. AADTT is the weighted average between weekday and weekend truck traffic. A project specific AADTT at the beginning of the design analysis period is required for every roadway segment, which was obtained from the Planning Division for all non-LTPP roadway segments. The AADTT values for the LTPP sites were obtained from the LTPP database.

Truck volumes were available for all roadway segments included in the verification-local calibration study for multiple years. In some cases, however, the AADTT was unavailable for the traffic opening date needed by the software. For those cases, the historical AADTT values were used to backcast the AADTT for the traffic opening data. Figure 2 shows an example of the backcasting process used for some of the LTPP test sections. The AADTT for the traffic opening date is included in the project files included in the Volume II report for all LTPP and non-LTPP roadway segments.

4.2 TRUCK VOLUME FACTORS

The truck volume factors include the directional, lane, monthly and hourly distribution factors. Each is defined below along with the default values. In addition, all of the truck volume factors are included in the project files for all LTPP and non-LTPP roadway segments (Volume II report).

- **Directional Distribution Factors (DDF)**: DDF is the percent trucks in the design direction, and is defined by the primary truck class for the roadway. For the calibration sites where sufficient truck volume data was unavailable, the following default values were used.

Primary Vehicle/Truck Class	Directional Distribution Factor
4	0.50
5 through 7	0.62
8 through 10	0.55
11 through 13	0.50

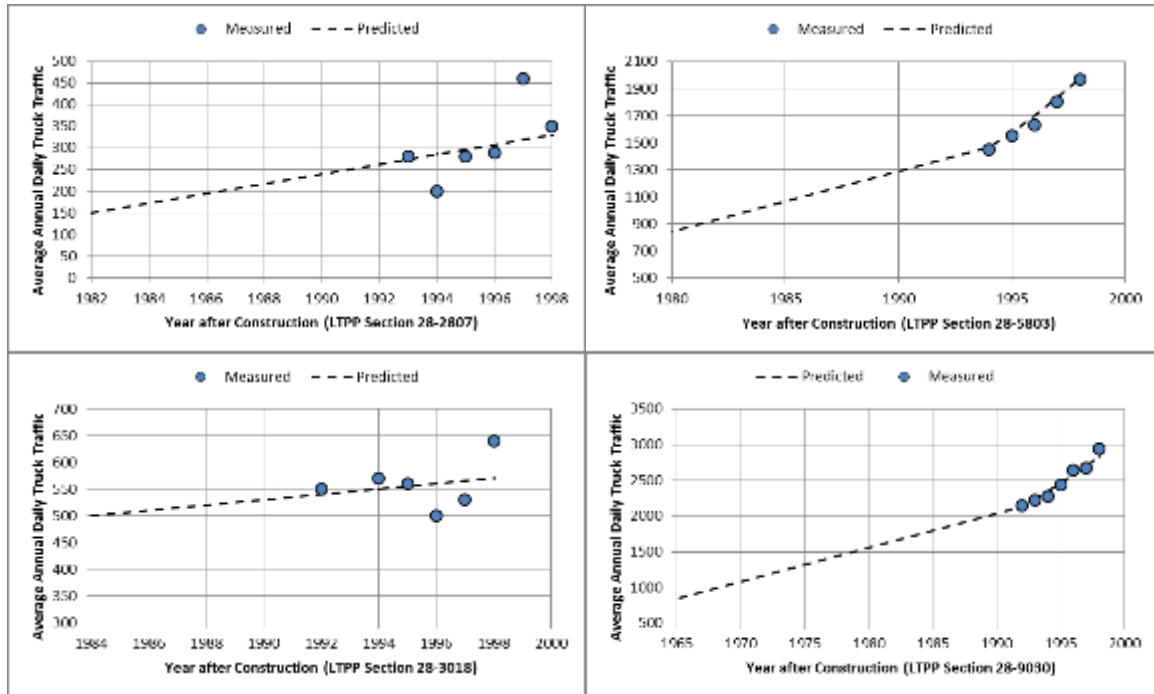


Figure 2—Backcasting Process for Determining the AADTT for the Traffic Opening Dates

- **Lane Distribution Factors (LDF):** LDF is the percent of trucks in the design lane, and is defined by the primary truck class for the roadway. For the calibration sites where sufficient truck volume data was unavailable, the following default values were used.

Number of Lanes	Lane Distribution Factor
4	0.90
6	0.60
8	0.45

- **Normalized truck volume distribution factors.** The percentage of each truck class within the mixed truck traffic (vehicle class 4 through 13 as defined by FHWA). These percentages represent the normalized truck volumes or truck volume distribution and are determined from the truck traffic software—MS-ATLAS, as discussed in Appendix C.

Three truck class categories were used to select the truck traffic classification (TTC) group included in the Pavement ME Design software for a specific roadway segment: single unit trucks (vehicle class [VC] 5 to 7), combination trucks or single trailers (VC 8 to 10), and multi-trailer trucks (VC 11 to 13). These three categories were used within the Mississippi State University traffic study to identify the more common TTC groups exhibited on Mississippi’s roadways (*Buchanan, 2004*).

Table 11 summarizes the TTC groups that were used in the verification and preliminary local calibration effort for the roadway segments with insufficient volume data.

Table 11—Truck Traffic Classification Groups for Defining Mississippi’s Normalized Volume Distribution Factors

Roadway Description	Type of Truck	Percentage of Trucks in That Class	Applicable TTC Group
Interstate Highways, 4-Lane Divided Highways, Heavier Truck Volumes	Single Units	12.0	TTC-3
	Single Trailers	81.0	
	Multi-Trailers	5.0	
Principal Roadways, 4-Lane Divided Highways, Heavy Truck Volumes	Single Units	27.0	TTC-7
	Single Trailers	67.0	
	Multi-Trailers	2.0	
Primary & Secondary Arterials; Moderate Truck Volumes	Single Units	27.0	TTC 6
	Single Trailers	62.0	
	Multi-Trailers	4.0	
Minor Arterials and Major Collector Routes	Single Units	65.0	TTC 12
	Single Trailers	27.0	
	Multi-Trailers	1.1	
Local Two-Lane Routes with Low Truck Volumes	Single Units	63.0	TTC-15
	Single Trailers	31.0	
	Multi-Trailers	2.2	

NOTE: The values in this table exclude the percentage of buses. The percent bus traffic is simply 100 minus the cumulative total of the other truck classes.

- **Monthly distribution factors (MDF):** MDFs are the relative amount of annual trucks for each truck class within each month. The MDFs are determined using the truck traffic software discussed in Appendix C. For the calibration sites where sufficient truck volume data was unavailable, the values included in Table 12 were used.

The monthly distribution factors for the truck traffic data evaluated on Mississippi’s roadways significantly deviated from the default values that are included in the MEPDG software, with the exception of TTC 3. The default MDFs are included in the Mississippi truck traffic libraries.

- **Hourly Distribution Factors (HDF):** HDFs are only required for rigid pavement analyses; they are not used for predicting distresses of flexible pavements and HMA overlays of flexible pavements. These factors were determined from the Mississippi State project for the TTC values that are representative of many roadways in Mississippi (*Buchanan, 2004*). For the calibration sites where sufficient truck volume data was unavailable, the default values listed in Table 13 were used which were found to be dependent on the TTC group.

Table 12—Mississippi Monthly Distribution Factors

Month	Average Monthly Distribution Factor				
	TTC 3	TTC 6	TTC 7	TTC 12	TTC 15
January	0.90	0.80	0.82	0.96	0.69
February	0.96	0.97	0.91	1.06	0.70
March	1.01	1.02	0.97	0.99	0.79
April	1.00	0.97	1.00	0.89	0.93
May	0.99	0.96	1.04	1.05	0.84
June	1.01	1.09	1.04	1.05	0.90
July	0.98	0.96	0.98	1.11	0.86
August	1.06	1.07	1.03	1.07	1.15
September	1.04	1.08	1.05	1.28	1.21
October	1.08	1.12	1.11	1.03	1.46
November	1.00	1.08	1.06	0.80	1.23
December	0.96	0.88	0.99	0.70	1.25

Table 13—Mississippi Hourly Distribution Factors

Time of Day	Hourly Distribution of Truck Traffic, %					
	TTIC 3	TTC 6	TTC 7	TTC 12	TTC 15	Average
Midnight to 6 a.m.	16.9	12.9	11.5	7.3	6.1	11.0
6 a.m. to 10 a.m.	18.9	26.1	22.4	23.8	33.1	24.8
10 a.m. to 4 p.m.	33.1	40.5	40.0	42.2	36.5	38.4
4 p.m. to 8 p.m.	18.3	14.2	18.2	18.8	20.1	18.0
8 p.m. to Midnight	12.8	6.3	7.9	7.9	4.2	7.8

4.3 NUMBER OF AXLES PER TRUCK CLASS

The average number of axles per truck class was determined from an analysis of the MDOT's WIM data as part of the Mississippi State traffic study. The default number of axles per truck class is listed in Table 14, and was assumed for each calibration site with insufficient WIM data.

Table 14—Mississippi Number of Axles per Truck Class

Vehicle/Truck Class	Type of Axle			
	Single	Tandem	Tridem	Quads
4	1.53	0.45	0.0	0.0
5	2.62	0.16	0.02	0.0
6	1.12	0.93	0.0	0.0
7	1.19	0.07	0.45	0.02
8	2.41	0.56	0.02	0.0
9	1.16	1.88	0.01	0.0
10	1.05	1.01	0.93	0.02
11	4.35	0.13	0.0	0.0
12	3.15	1.22	0.09	0.0
13	2.77	1.40	0.51	0.04

4.4 AXLE CONFIGURATION AND GEOMETRY AND OTHER TRUCK FACTORS

Many other truck traffic input parameters are required for predicting the distresses of flexible and rigid pavements. Some of these inputs are difficult to determine and are unavailable within MDOT's truck traffic database. Thus, the global default values were used in the verification and local calibration work. The global default values are defined and discussed within the NCHRP Project 1-37A reports (*ARA, 2004a*). The following values were used in the preliminary local calibration for Mississippi.

- Axle spacing:
 - Tandem axle spacing: The average distance between the two axles of a tandem axle; 51.6 inches, the MEPDG default value.
 - Tridem axle spacing: The average distance between the three axles of a tridem axle; 49.2 inches, the MEPDG default value.
- Dual tire spacing: The average distance between the center of the two tires; 12 inches, the MEPDG default value.
- Other Truck and Tire Factors:
 - Hot tire inflation pressure: An average hot tire pressure of 120 psi was assumed for both single and dual tires.
 - Truck traffic wander standard deviation: The lateral distribution of trucks traveling down the roadway; 10 inches, the MEPDG default value.
 - Operational Speed: This input parameter was taken as the posted speed limit or the average truck speed of the heavier or larger trucks through the project segment. For most of the calibration sites, 50 to 60 mph was used.

The following truck axle configuration and axle location inputs are only required for rigid pavement analyses; these are not used for predicting distresses in flexible pavements and in HMA overlays of flexible pavements.

- Wheelbase Information: Axle spacing and percentage of trucks with that spacing; the Mississippi default values recommended for use in Mississippi are:
 - 17 percent for 12 ft. spacing.
 - 22 percent for 15 ft. spacing.
 - 61 percent for 18 ft. spacing.
- Mean Wheel Location: The average distance from the outer edge of the wheel to the pavement edge marking; 18 inches, the Pavement ME Design default value.
- Average Axle Width: The average distance between the outside edge of the tires of an axle; 8.5 feet, the Pavement ME Design default value.
- Design Lane Width: The width of the lane between the pavement lane designation markings and not the slab width. This input is a design feature and not a traffic input. It is included with the other traffic inputs because it has a significant impact on the stresses in the PCC slab based on the location of the wheel load relative to the edge of the pavement. The value assumed for most of the sites was 12 feet.

4.5 NORMALIZED AXLE LOAD DISTRIBUTION FACTORS

The default normalized axle load distributions (NALD) or normalized axle load spectra (NALS) were determined within the Mississippi State project to validate the MEPDG design methodology default values (*Buchanan, 2004*). Buchanan found some of the TTC groups were similar to the default values, but significant deviation was found in some of the other groups. The values used for the verification and local calibration work when axle weight data were unavailable are provided in Appendix D (*Normalized Axle Load Distribution Factors or Axle Load Spectra*) and included in Mississippi's truck traffic library.

The MS-ATLAS program was originally developed to process, store, and analyze raw WIM data so that traffic input files can be generated for the MEPDG. Under MDOT State Study 188, the MS-ATLAS software program was developed and customized specifically for MDOT traffic data and conditions. A description of MS-ATLAS is included in Appendix C. MDOT provided all of the NALD factors for each calibration site which are included in the Volume II report. MDOT is one of the few agencies that generate specific NALS from their WIM stations. The NALD factors used in the preliminary calibration are considered level 2 inputs, except when the calibration site is located near one of the WIM stations in which case the NALD is considered a level 1 input.

CHAPTER 5—CLIMATE

Detailed climate data are used to predict the temperature and moisture distribution in each of the pavement layers over time for estimating time-dependent layer stiffness. In addition, the climate data provides some of the inputs to the site factor parameter for the JPCP joint faulting as well as the smoothness or roughness regression equations for all pavement types. Climate data include hourly temperature, precipitation, wind speed, relative humidity, and cloud cover. All of these climate data are available from weather stations, generally located at airfields around the United States (U.S.). Most agencies, including MDOT, however, have relatively few weather stations included in the MEPDG software.

Two site feature inputs required by the MEPDG but excluded from the weather station data are: (1) the water table depth, and (2) the depth to a rigid layer. All climate data and inputs relative to the calibration sites are discussed in this chapter of the report.

5.1 COUNTY WEATHER STATIONS

The MEPDG requires the location of a project described in terms of longitude, latitude, and elevation in order to develop project specific climate data (refer to Table 3 and Appendix A). The climate specific data for each project are generated using the closest weather station. Table 15 lists the 12 weather stations within Mississippi and near the state lines of adjacent States.

Two or more of these weather stations were to be selected as close to the calibration site as possible to provide hourly temperature, precipitation, wind speed, relative humidity, and cloud cover information. Table 15 also lists the number of months with data for those weather stations, and identifies the stations with missing data. MDOT considered these weather stations to be insufficient, so additional stations were added to Mississippi's climate library.

An expanded historical climate database was created by the National Center for Asphalt Technology (NCAT) for use in verifying and calibrating the MEPDG design methodology in Mississippi (*Truax, et al., 2011*). At least one weather station for each county in Mississippi was added to Mississippi's climate database. These additional weather stations include data over a much longer period of time than those listed in Table 15.

A second climate database was created by NCAT. This second database also includes one weather station in each county in Mississippi, but includes weather projections, rather than historical data (*Truax, et al., 2011*). The library of weather stations with the projected climate data is used in design, while the expanded historical weather station database was used for local calibration. Different runs were made for one of the calibration sites located near Tupelo, Mississippi to demonstrate the impact of county specific weather stations with an expanded climate database.

Figures 3 and 4 includes the predicted levels of distress over time using 1) the closest weather station included in the Pavement ME Design software, 2) a virtual weather station from those included in the Pavement ME Design software, and 3) the expanded historical weather data for the specific county. The Tupelo weather station was used for the station closest to the project location. The virtual weather station was created using the Tupelo,

Muscle Shoals (Alabama), Tuscaloosa (Alabama), Greenwood (Mississippi), and Memphis (Tennessee) stations. Figure 3 includes the results from one of the LTPP flexible pavement sites, while Figure 4 includes the results for one of the LTPP rigid pavement sites.

Table 15—Mississippi Weather Stations Available in AASHTOWare

City	Latitude (Degrees.Minutes)	Longitude (Degrees.Minutes)	Elevation, ft.	Number of Months Available
Greenville	33.29	-90.59	150	55*
Greenwood	33.30	-90.05	149	103
Gulfport	30.25	-89.05	51	91
Hattiesburg	31.16	-89.15	147	70*
Jackson International	32.19	-90.05	296	116
Hawkins Field Airport, Jackson	32.20	-90.13	312	68
McComb	31.11	-90.28	410	66
Meridian/McCain Field	32.33	-88.34	293	116*
Key Field Airport, Meridian	32.20	-88.45	292	116
Pascagoula	30.28	-88.32	22	102*
Tallulah/Vicksburg	32.21	-91.02	88	116*
Tupelo	34.16	-88.46	350	116
*The highlighted weather stations have missing data within the database.				

As shown, the predicted distresses using the closest and virtual weather stations are almost identical for both flexible and rigid pavements, while the predicted distresses using the weather station in Lee County created from the expanded historical climate data are significantly different. As such, the weather stations with limited data were not combined with the stations added on a county wide basis in creating a virtual weather station for a specific project location. MDOT is the only agency to date that has generated county specific virtual weather stations with an expanded historical and forecast climate database to be used in calibration and design.

5.2 DEPTH TO WATER TABLE OR GROUND WATER

The depth to the water table or “free” water is the average distance between the pavement surface and the depth at which free water is encountered. This depth is representative of cuts and fills or perched water tables along the project location.

The 20-foot boring drilled in the shoulder area at each LTPP site was reviewed to estimate the depth to a rigid layer, a saturated layer, or free water. Wet soil strata or water was observed during the drilling process and recorded on the boring log for some of the sites. The depth to water table is included in the MEPDG project files (refer to Volume II).

The water table depth entered in the Pavement ME Design software was the shallower depth to: free water, perched water, or the lateral flow of water. The following was used in determining the depth to the water table or free water for the calibration sites.

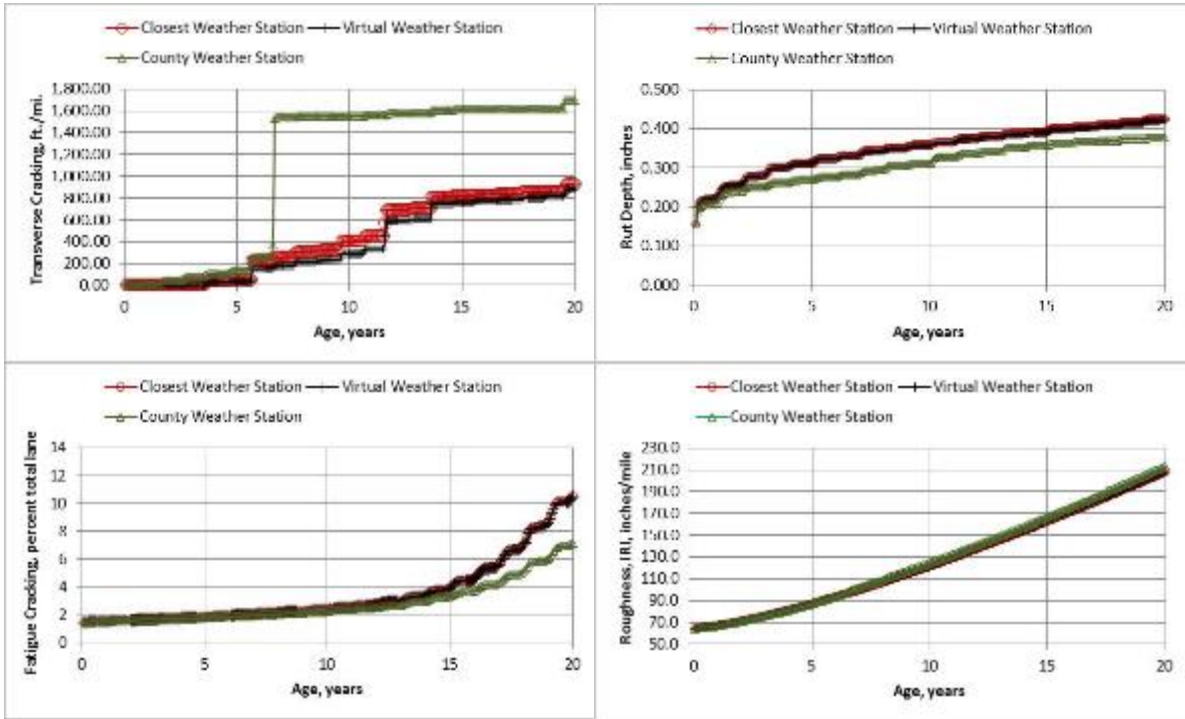


Figure 3—Comparison of Predicted Flexible Pavement Distress Values for the different Climate Libraries

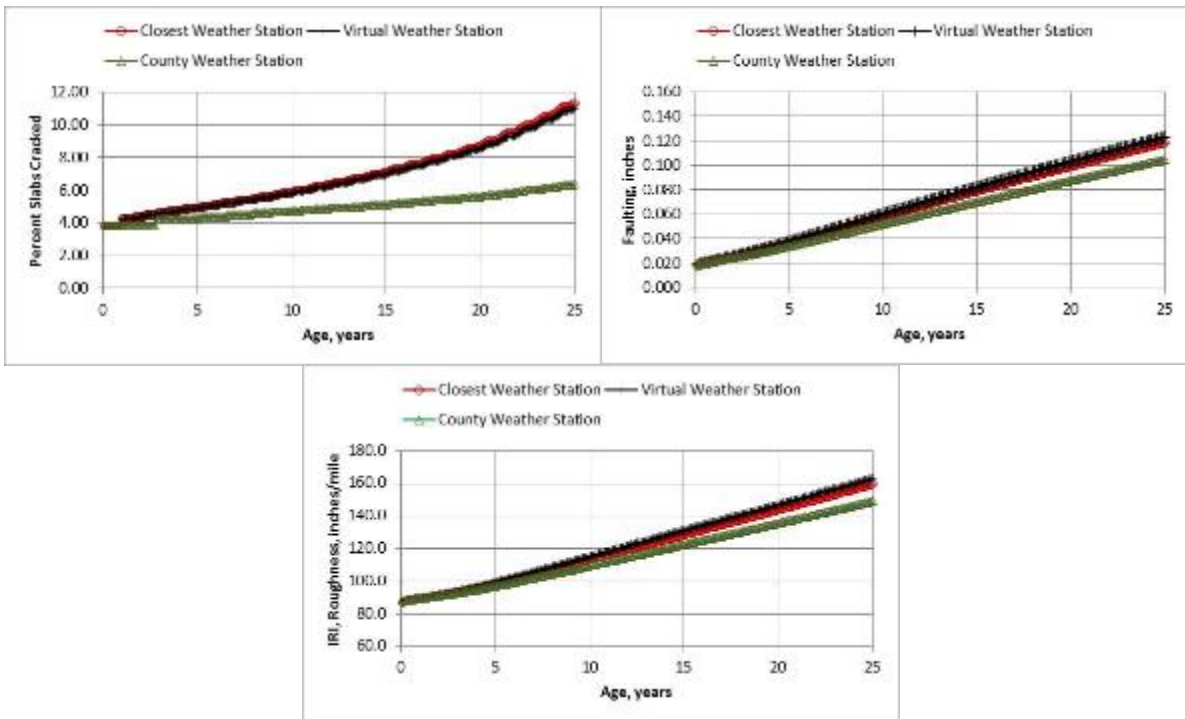


Figure 4—Comparison of Predicted Rigid Pavement Distress Values for the different Climate Libraries

1. Borings were not monitored or left open over a sufficient amount of time to measure the depth to water. If seasonal or perched water table depths are known to exist along the project site, these seasonal values were used.
2. If the water table depth was unknown for a specific location, the water depth tool was used to estimate that depth. Use of this tool is described in Appendix E (*Ground Water Depth Tool or Software*). It should be noted that the depth to the water table estimated from this tool is the depth to the actual water table and not the depth to perched water or the lateral flow of water across an area.

If water or wet soils was not recorded on the boring log, the depth to the water table was assumed to be 20 feet in setting up the pavement structure in the MEPDG for most of the calibration sites. The Volume II report includes the depth to the water table assumed for each calibration site.

5.3 DEPTH TO BEDROCK OR RIGID LAYERS

The 20-foot boring drilled in the shoulder area at each LTPP site was reviewed to estimate the depth to a rigid layer. Refusal or presence of weathered rock was recorded on the boring log for some of the sites. In addition, the deflection basin data measured along all LTPP sections was used to estimate and/or confirm the depth to a hard layer from the backcalculation of elastic layer modulus values. The depth to a hard or rigid layer is included in the MEPDG project files (refer to Volume II). In most cases, the depth to bedrock exceeded 10 feet, so the subgrade thickness was assumed to be infinite.

For the non-LTPP sites, the subgrade thickness was assumed to be infinite for the preliminary local calibration. The deflection basin data measured during the field investigations will be used to estimate the depth to a hard layer from the backcalculation of elastic layer modulus values.

CHAPTER 6—LAYER FEATURES

Different features are required by the Pavement ME Design software for different pavement types or materials. The global default values were used for some of the parameters. Appendix A lists and identifies the layer features and materials properties for which input level 3 default values were used in the local calibration process for the flexible and rigid pavements. This chapter discusses the features required for specific pavement types in terms of the values used in the local calibration process.

6.1 INITIAL INTERNATIONAL ROUGHNESS INDEX

The initial IRI represents the average value measured after construction. This initial value was determined from construction records of previously placed HMA or PCC surfaces under comparable conditions. The initial IRI was only available for a few of the Mississippi LTPP test sections. Thus, the initial value was backcast from the monitored IRI data, similar to the backcasting procedure used for the initial AADTT, with one major exception. Unlike for AADTT, IRI does not change significantly until distresses begin to occur, as illustrated in Figure 5 for some SPS-5 test sections. The IRI-time relationship for some time after construction is relatively flat, and only starts to increase after the occurrence of surface distress. The following equation was used to backcast the initial IRI, which has been used in other studies (*Von Quintus and Perera, 2011*).

$$IRI_t = IRI_i \left(e^{\left(\frac{t}{20} \right)^{g_2}} \right)^{g_1} \quad (45)$$

Where:

- IRI_t = IRI measured at time t.
- IRI_i = Initial IRI measured or estimated at time of construction.
- t = Time or age of pavement, years.
- g₁, g₂ = Regression constants determined from the monitored IRI-time values.

Figure 6 includes examples of using the empirical IRI-time relationship to estimate the initial IRI for a couple of the LTPP sites. The measured IRI values with none to minimal amounts or levels of distress were used to estimate the initial IRI for a specific test section. If the starting value was unknown and there was insufficient data to backcast the initial IRI for a site, the values in Table 16 were used. The initial IRI used for each LTPP and non-LTPP site is included in the Volume II report.

6.2 STRUCTURAL LAYER FEATURES

6.2.1 Flexible Pavement Layers

The inputs to define the structure are straightforward and include the material type and thickness of each layer included in the design strategy. The material type and layer thickness for each LTPP and non-LTPP site included in the local calibration process are included in the Volume II report. The following provides a listing of points creating the pavement structure used in a new or rehabilitated flexible pavement analysis to determine the local calibration coefficients.

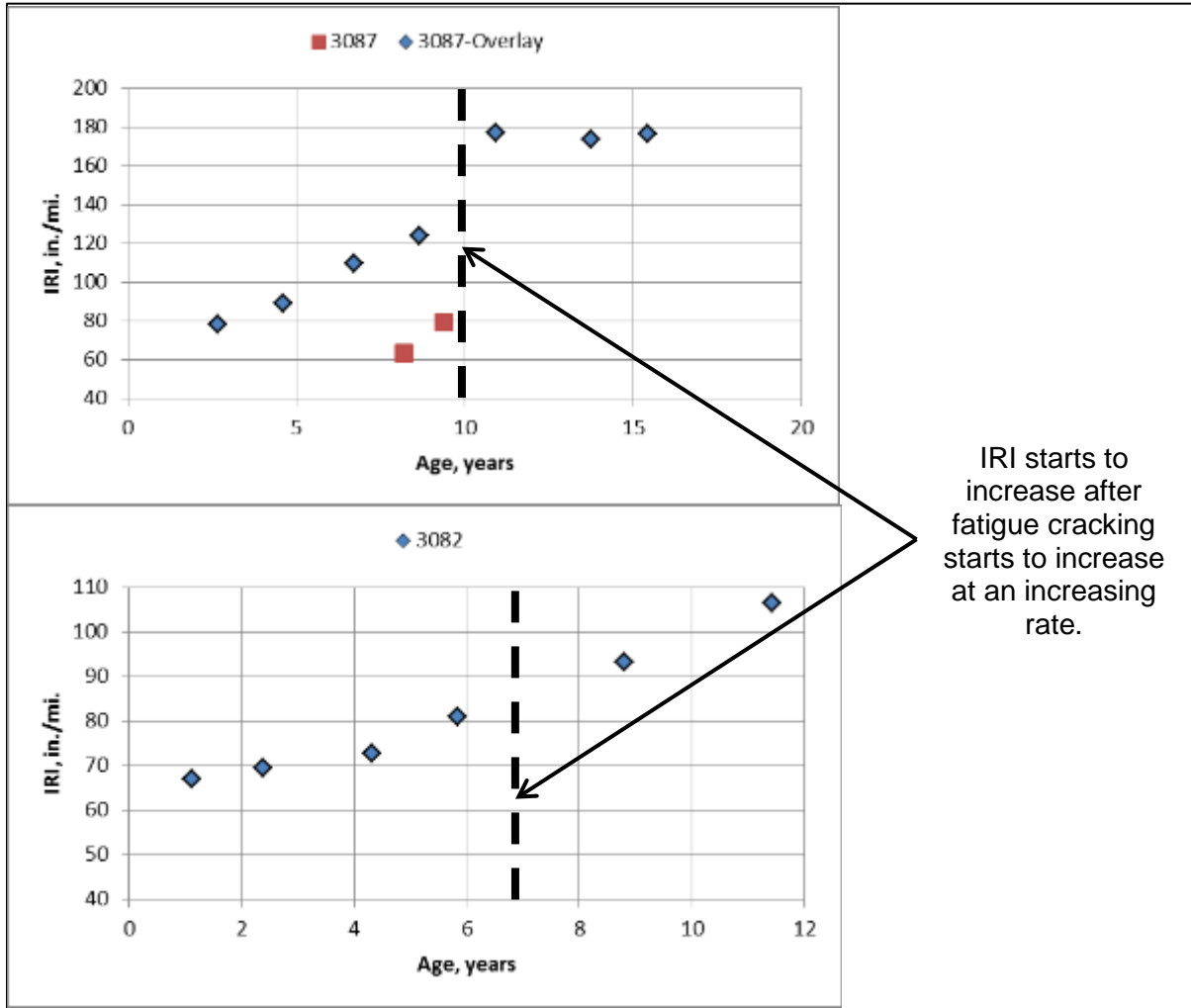


Figure 5—IRI Measured over Time for Two of the Mississippi LTPP Sections

- HMA and Asphalt Stabilized Base Layers:** For new construction or reconstruction, the number of HMA layers was limited to three. The lower layer controls bottom-up or alligator cracking, while the upper layers have more control on the predictions of rut depth and thermal cracking. For HMA overlays over flexible pavements, the existing HMA and overlay layers were also limited to three layers. When two layers were used to represent the existing HMA, only one overlay layer was used. Conversely, if two overlay layers were used, only one layer was used for the existing HMA layers. For the LTPP sites, results from deflection basin testing and the backcalculation of elastic layer modulus values were used to determine whether the existing HMA layers should be confined to one or two layers. For the non-LTPP sites, deflection basins were unavailable so input level 3 was used to estimate the layer properties. A more refined pavement structure will be included after the field investigations have been completed. For both new construction and rehabilitation designs, thin HMA layers (less than 1.0 inch in thickness) were combined with the adjacent structural layer.

An important assumption used in the preliminary local calibration process is that all HMA layers do not exhibit moisture damage. This assumption is probably incorrect, even for some of the LTPP sections. As an example, the SPS-5 test sections exhibited stripping, resulting in extensive rutting. The field investigation planned for Phase 3 should quantify material defects and reduce the SEE for the transfer functions.

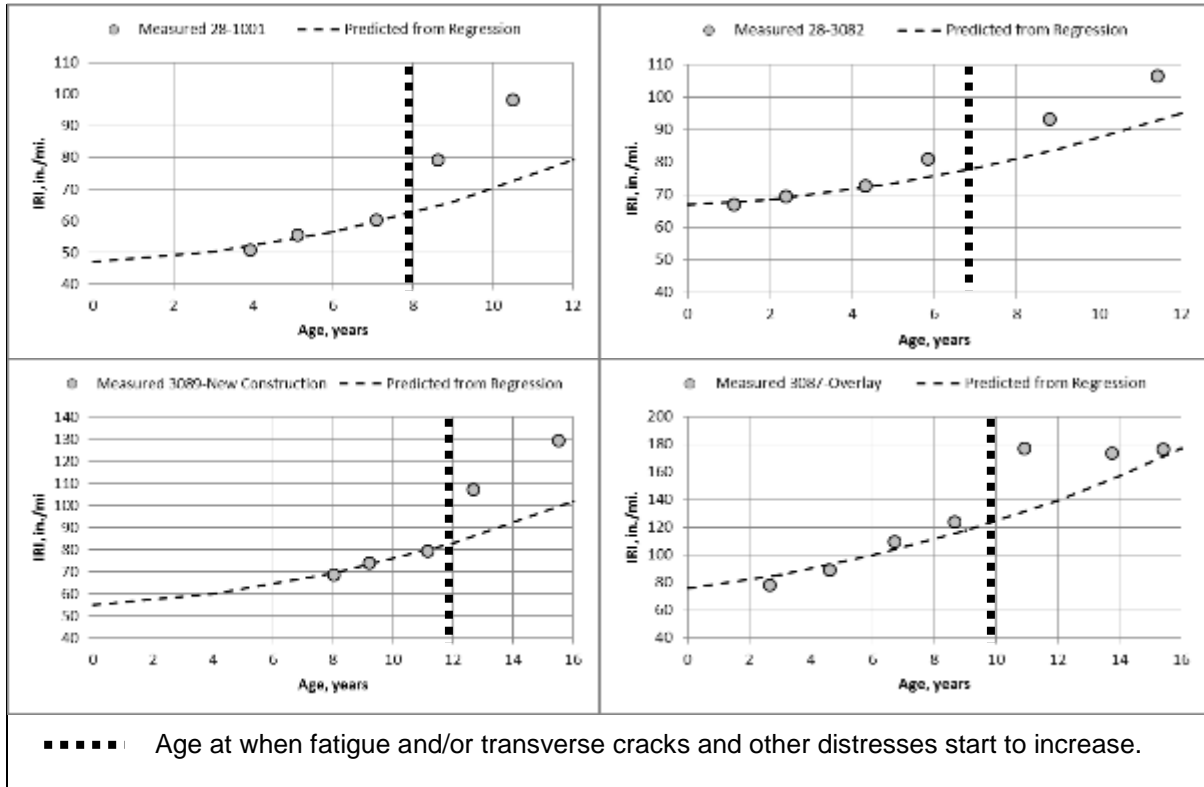


Figure 6—Backcasting Process to Estimate the Initial IRI for Two of the Mississippi Sections

Table 16—Mississippi IR Values at Construction

Type of Surface	Type of Design		Initial IRI, in./mi.
HMA Mixtures	New Design		50
	Overlays		60
PCC Mixtures	JPCP	New Design	65
		Overlays	65
	CRCP	New Design	50
		Overlays	50

- Asphalt Treated Permeable Base (ATPB) Layers:** ATPB mixtures placed below dense-graded HMA layers typically have air voids at construction ranging from 15 to 20 percent. The Pavement ME Design software significantly over predicts bottom-up fatigue cracks because of the higher air voids and low asphalt content for the ATPB (*Von Quintus and Moulthrop, 2007a*). The fatigue life calculated for these bituminous mixtures is very low resulting in excessive and accelerated fatigue cracking (see

equation 11 in Chapter 2). The measured amount of alligator cracking, however, does not support this prediction on most of the LTPP SPS-1 projects. As such, ATPB layers were simulated as a high quality unbound base layer with a constant elastic modulus throughout the year. This assumption forces the bottom-up fatigue cracking to be controlled by the lower dense-graded HMA layer.

- **Cement Treated Base or Cementitious Layers:** No more than one layer of cement, lime, or lime-fly ash stabilized base layer was included in the analysis. This does not include stabilized subgrade soils. When the cementitious layer is placed directly below the HMA layer, even if this layer is soil cement, the pavement structure is defined as a semi-rigid pavement. As stated previously, none of the MDOT LTPP sites included compressive strengths in the LTPP database. Either the layer was too thin or a test specimen was not recovered through the coring process. As such, the backcalculated elastic layer moduli were used to estimate the in place strength.

For the non-LTPP sites, it was assumed that the minimum compressive strengths of the CTB and soil-cement layers were met at construction and represents a good quality material. The field investigations should confirm the 28-day strengths to be used in the final calibration.

- **Unbound Granular Base Layers:** In most cases, only one unbound aggregate base layer was used for both new and rehabilitation design. The number and thickness of the unbound granular aggregate base layers of the existing pavement structure coincided with the pavement structure used to backcalculate elastic layer modulus values from deflection basin data for the LTPP test sections. For the non-LTPP sites, the as-built records and plans were used to define the thickness of any unbound aggregate base layer.
- **Stabilized Subgrade:** No more than one layer of a stabilized subgrade was used in the analysis. If the stabilized subgrade was used as a construction platform with only minimum additive for improving the strength, the layer was still treated as a separate layer.
- **Embankment/Foundation Layers or Subgrade:** Two subgrade layers were used for all calibration sites: a compacted embankment layer (defined as a weathered layer), and the natural or undisturbed soil. The exception to this recommendation is when a water table is located near the surface (less than 10 ft.) and the type of soil changes significantly between the water table and lower pavement layer because the properties of the soils can have a significant effect on the amount of water being moved through the subgrade—lowering the resilient modulus of the upper soil strata.

6.2.1.1 *Interface Friction*

The layer interface friction was difficult to define without any destructive sampling (coring program). Full friction was assumed between each layer. An interface friction value of 1.0 represents full friction in the MEPDG design methodology. The assumption is that at construction all layers are fully bonded. The MEPDG does not predict or account for a loss of bond or interface friction over time.

6.2.1.2 Condition of Existing HMA Surface for HMA Overlay Design

The condition of the existing surface is determined from the distress measurements (condition surveys [input levels 2 or 3]) or determined from backcalculated elastic modulus (input level 1). Although each can be used, MDOT's policy is to measure deflection basins along the project for rehabilitation design. Thus, rehabilitation input level 1 was used for those sites when deflection basin data were available. For the non-LTPP sites, input level 2 was used because deflection basins are to be measured in Phase 3 as part of the field investigations.

6.2.1.3 Rut Depth in Each Structural Layer

The other input required for rehabilitation input level 1 is the rutting within each pavement layer and subgrade. The average rut depth in each pavement layer and in the subgrade is measured through the use of trenches. Trenches, however, are normally not included in the pavement evaluation process for rehabilitation design. The following percentages were used to distribute the total rut depth measured at the surface to each pavement layer and subgrade in calibrating the rut depth transfer function for HMA overlays of flexible pavements.

- HMA Layer—75 percent of the measured rut depth.
- Aggregate Base Layer—10 percent of the measured rut depth.
- Subgrade Layer—15 percent of the measured rut depth.

These percentages were determined through the global calibration process under NCHRP projects 1-37A and 1-40D and revised based on the local calibration study for MDOT using the LTPP and non-LTPP roadway segments located in Mississippi. The assumption is that the unbound aggregate base layers and embankment soils were compacted to optimum conditions at construction.

6.2.2 Rigid Pavement Structural Layers: JPCP and CRCP

6.2.2.1 Layer Type

The layer types and thickness for each LTPP and non-LTPP rigid pavement section used in the local calibration process are included in the Volume II report. The following provides a listing of points considered in creating the rigid pavement structure for both new construction and rehabilitated pavement analysis to determine the local calibration coefficients.

- **HMA or Asphalt Stabilized Base Layers:** For new construction, HMA or stabilized base layers are placed below the PCC slabs and were limited to one layer. For the non-LTPP sites, the thickness was extracted from the as-built plans and construction records.
- **Asphalt Treated Permeable Base (ATPB) Layers:** ATPB mixtures have high air voids (generally greater than 20 percent for a well-draining mixture). Pavement ME Design does not predict the fatigue cracking or damage of this layer below PCC slabs. The high air voids have no impact on the damage of this layer. Thus, this layer can be treated as an asphalt layer.

- **Cement Treated Base Layers:** No more than one layer of cement, lime, or lime-fly ash stabilized base layer was used in the rigid pavement analysis.
- **Unbound Granular Base Layers:** The compacted unbound aggregate base was limited to one layer. If more than one layer was identified in the as-built plans the unbound aggregate base layers were combined, especially if one of the layers was relatively thin (less than 4 inches).
- **Stabilized Subgrade:** Only one layer of a stabilized subgrade was used in the analysis. A stabilized aggregate base layer and stabilized subgrade were included when both were identified in the as-built plans.
- **Embankment/Foundation Layers or Subgrade:** The subgrade was limited to two layers; a compacted embankment layer and the natural or undisturbed soil. The exception to this recommendation is when a water table is located near the surface (less than 10 ft.) and the type of soil changes significantly between the water table and lower pavement layer because the properties of the soils can have a significant effect on the amount of water being moved through the subgrade—lowering the resilient modulus of the upper soil strata.

6.2.2.2 Joint Spacing

Pavement ME Design allows two options for the joint spacing of JPCP: a constant or random joint spacing. MDOT only permits the use of a constant joint spacing; a random joint spacing has not been used or allowed by MDOT. The joint spacing used on most projects in Mississippi is 15 to 20 feet. The input spacing for each project are included in the Volume II report.

6.2.2.3 Erodibility Index

The erodibility index for JPCP is defined by the type of base material for the specific project trial design, and is classified through five categories, which are listed below. The more erosion resistant the base material, the lower the PCC stresses and the less cracking and faulting.

Erodibility Category		Recommendation Based on Type of Base Material
1	Extremely Erosion Resistant	Asphalt Stabilized Layer or HMA.
2	Very Erosion Resistant	Cement Treated Base Layer
3	Erosion Resistant	Dense-graded crushed stone materials with less than 10 percent fines.
4	Fairly Erodible	Dense-graded aggregate base materials with more than 10 percent fines.
5	Very Erodible	Silts and other non-cohesive fine-grained soils and cohesive soils.

6.2.2.4 **PCC-Base Contact or Interface Friction**

The following lengths of time for full contact friction between the PCC slab and base course were used, which represent the values reported from the national or global calibration.

- Asphalt Stabilized Base: Full design analysis period.
- Cement Stabilized Base: 120 months after which there is a good chance of debonding.
- Lean Concrete Base: Finished smooth and cured with wax-based curing compound: zero months.
- Unbound Aggregate Base: Full design analysis period.

6.2.2.5 **Condition of Existing PCC Surface for JPCP Rehabilitation Design**

Two inputs are required for the existing PCC layer when designing an overlay of an existing JPCP: (1) the percentage of slabs that are distressed or have been replaced prior to rehabilitation or restoration, and (2) the percentage of slabs that will be replaced as part of the rehabilitation project after restoration. These two inputs are important because they relate to determining the in place damage of the JPCP for predicting future damage and cracking of the PCC slabs. The input values used for the calibration sites were estimated based on the available information.

6.2.2.6 **CRCP: New and Existing Layers**

The inputs for CRCP layer features are mostly specific to the CRCP design philosophy and are as follows:

- Percent longitudinal steel in PCC slab, which is a project specific design input.
- Bar diameter of the longitudinal steel reinforcement, also a project specific input.
- Depth of the longitudinal steel reinforcement is a project specific design input. The longitudinal steel is generally assumed to be placed at the mid-depth of the PCC slab or within the top half of the slab with minimum steel cover specified by the agency.
- Base/Slab friction coefficient or the coefficient of friction at the interface of the CRCP and layer supporting the CRCP. This parameter defines the degree of frictional restraint offered by the underlying base layer and impacts the spacing of shrinkage cracking. There is not specific test method for measuring the coefficient of friction between two pavement layers. The following summarizes the default values recommended for design which are included in the MEPDG Manual of Practice (AASHTO, 2008). These recommended values, however, were not confirmed through the verification process.

Subbase/Base Material Type	Friction Coefficient
Lean Concrete Base	8.5
Cement Treated Base	8.9
Soil Cement	7.9
Asphalt Treated Base or HMA	7.5
Lime-Stabilized Soil	4.1
Crushed Stone or Aggregate	2.5
Sand and Coarse-Grained Soil	0.8
Fine-Grained Soil	1.1

6.2.2.7 *Other Rigid Pavement Layer Features*

The other inputs for rigid pavement layer features include parameters specific to JPCP design, which are: dowel size and spacing, presence of a widened slab, slab width, shoulder type, and tied shoulders. These features are all project specific. The project specific values for each of these are included in Volume II for each calibration site.

CHAPTER 7—MATERIAL PROPERTIES

For all layers or material groups, detailed information was obtained from the LTPP database to determine the layer properties. Appendix A includes a listing of all material or layer properties.

Most of the key material properties in the LTPP database were obtained through laboratory testing of material samples or extracted cores. For other material properties such as PCC zero stress temperature, thermal conductivity, dynamic modulus of HMA, and so on, MEPDG or Mississippi-specific defaults were assumed. The sources of key material properties to estimate the MEPDG inputs are described in the following subsections for each material. The material properties used for each layer are discussed in separate sections of this chapter, which are grouped into the following categories:

- Asphalt Concrete (AC) materials
- PCC materials
- Cement stabilized aggregate base materials and stabilized soils
- Unbound granular materials and subgrade soils
- Bedrock

7.1 ASPHALT CONCRETE MIXTURES

Volumetric, engineering, and thermal properties are required for each HMA layer (see Appendix A). The volumetric and engineering properties represent the mixture after compaction at the completion of construction, while the thermal properties are assumed to be constant throughout the analysis period. The volumetric properties include air voids, effective asphalt content by volume, aggregate gradation, mix density, and asphalt grade.

Most of the HMA mixture inputs were extracted from the LTPP database or from other MDOT sponsored projects and/or construction records, so input levels 1 and 2 were used for the local calibration of the flexible pavement transfer functions. The sources of data were presented in Table 3. Key inventory, design, materials, and construction data were assembled for each calibration site for review, identification and/or elimination of outliers and anomalies. The HMA mixture input values are included in the Volume II report for each calibration site.

For the LTPP sites, the volumetric properties were measured for all structural layers. The asphalt content, aggregate gradation and maximum specific gravity at the time of sampling were assumed to be unchanged or the same value at the time at construction. Air voids decrease over time and were only available at construction for some of the Special Pavement Study (SPS) projects. The engineering and thermal properties, however, were unavailable for all of the LTPP and non-LTPP test sections.

The following summarizes the input values selected or assumed for the HMA mixtures. For all other properties (including the thermal properties), the global default values were assumed for the HMA mixtures (see Appendix A).

7.1.1 Volumetric Properties

- **Aggregate gradation and density:** For the LTPP sections, the average value from the test results stored in the LTPP database were used. For the non-LTPP sites, the mid-range value for the project specifications of a particular type of mix was used for gradation. For density, the average value reported in the construction files for the entire project was used, but if density was not included in the files, it was assumed that the mixture was compacted in accordance with the project specifications.
- **Air voids:** The bulk and maximum specific gravities are used to calculate the air voids but are only available at the time of sampling for the General Pavement Study (GPS) sites. For the SPS sites, the values at the time of construction are included in the LTPP database. The air voids at construction (calculated from bulk and maximum specific gravities) change over time and the values at construction are unavailable for most of the flexible pavement sites. The maximum specific gravity of the HMA mixtures was measured as part of the LTPP test program and is available in the LTPP database. This value was assumed to be constant over time. Thus, the air void at construction was backcasted using the average air voids measured at the pavement's age of sampling using the densification function shown below.

$$V_a(t) = (D + V_d)10^{-a\left(\frac{t}{5}\right)^b} \quad (46)$$

Where:

- $V_a(t)$ = Air voids at time or age t.
- V_d = Design air voids for selecting the asphalt content, %
- t = Time or age of HMA mixture after construction, years.
- D = Regression constant; expected maximum change or decrease in air voids and defined at the age or time of sampling.
- a, b = Regression constants fitting the decrease in air voids over time (a=0.15 and b=0.25). These regression coefficients for typical dense graded mixtures (estimated from previous projects).

Figure 7 illustrates use of the densification function for backcasting the initial HMA air voids for four LTPP sections. This same process will be used for all of the non-LTPP sites included in the field investigation. For the non-LTPP sites where the initial air voids were unavailable from the MDOT construction materials database a default value of 7.0 percent was used. The air voids after construction are included in the Volume II report for all flexible test sections.

- **Effective asphalt content by volume:** For the LTPP sites, the average value reported in the LTPP database was used. However, the total asphalt content by weight is included in the LTPP and MDOT construction databases, while the effective asphalt content by volume is required but not included in the databases. The effective asphalt content by volume was calculated using assumed aggregate specific gravity and other volumetric properties (bulk specific gravity of compacted mix, asphalt specific gravity, and total asphalt content by weight).

Figure 8 shows a comparison of the asphalt content and air voids at construction for the LTPP sites. As shown, there is extensive dispersion between the asphalt content and air voids; no relationship was found. However, this information can be used to

judge the cracking and rutting resistance of different mixtures. Mixtures that exhibit lower air voids at construction in comparison to sites with higher air voids for similar design asphalt contents should have greater resistance to rutting and cracking. After the field investigation, the data for the non-LTPP sites will be added to Figure 8.

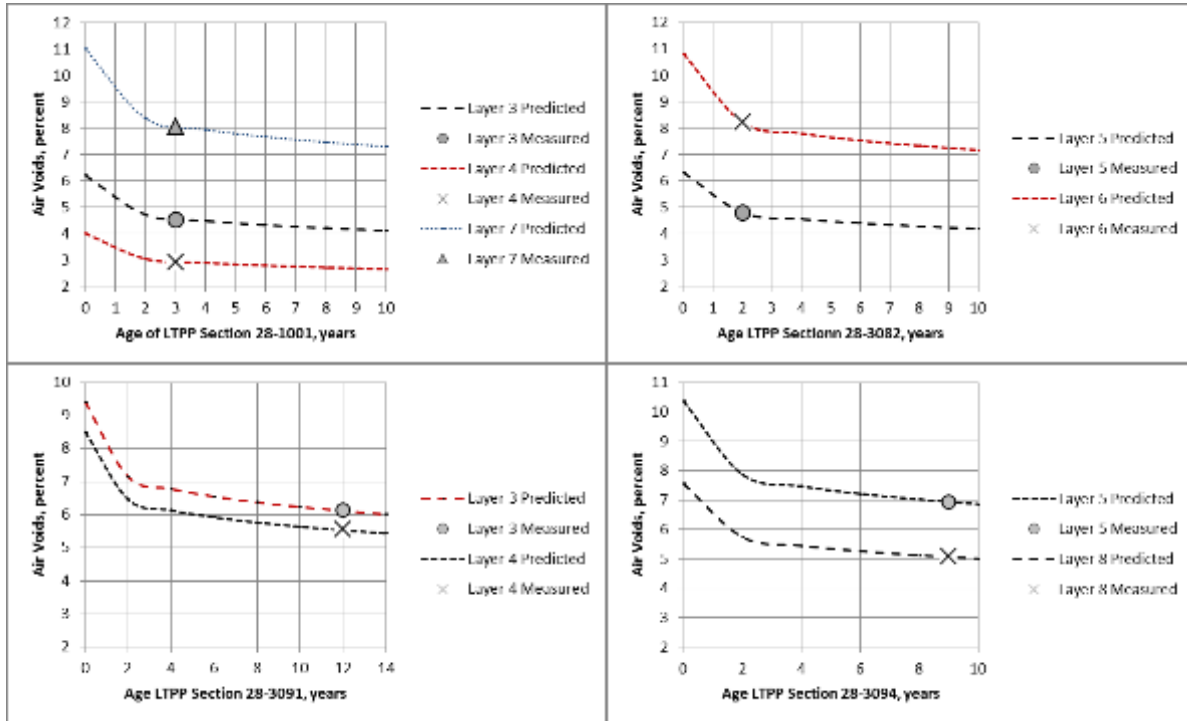


Figure 7—Illustration of the Process used to Backcast the Initial Air Voids of HMA Layers with Adequate Compaction

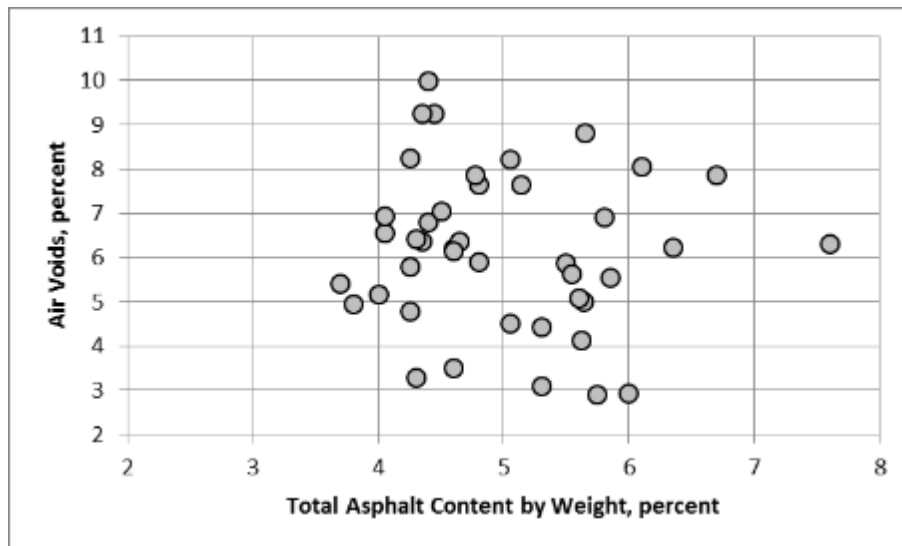


Figure 8—Initial Air Voids Compared to the Total Asphalt Content by Weight for the HMA Mixtures

7.1.2 Engineering Properties

- **Poisson's ratio:** The temperature calculated values from the regression equation included in Pavement ME Design was used for all HMA layers.
- **Dynamic modulus:** Mississippi State University conducted dynamic modulus test on multiple HMA mixtures. The test results are included in the material testing library and were imported into the Pavement ME Design software (*White, et al., 2007*). The test results and mixtures tested are summarized in Appendix F (*Dynamic Modulus Test Results*).
 - New HMA Mixtures for new construction: Dynamic modulus and the asphalt binder properties are unavailable at the time of construction for all LTPP and non-LTPP sites. If an HMA mixture was included in the pavement structure that was not included in the HMA materials library, level 2 inputs were used to estimate the dynamic modulus values using the viscosity based model. The dynamic modulus is calculated by the Pavement ME Design software using the aggregate gradation, asphalt content, air void content, and binder grade. The gradation and volumetric inputs were either obtained from HMA mix designs or measured using cores recovered during sampling, while the binder grade is included in the LTPP database and construction files.
 - Existing HMA Mixtures for rehabilitation of flexible pavements: For rehabilitation input level 1, the backcalculated elastic modulus represents the dynamic modulus of the existing HMA layer. Deflection basins were measured on all of the LTPP test sections and used to backcalculate the elastic modulus values. The two other inputs that are needed include: (1) the frequency of deflection testing—a default value of 20 Hz was used; and (2) the temperature representative of the average backcalculated elastic modulus value—the mid-depth temperature of the layer used in the backcalculation process measured during deflection testing. Figure 9 includes a comparison of the damage index based on the backcalculated elastic layer modulus and laboratory measured dynamic modulus in comparison to the amount of fatigue cracking. As the backcalculated elastic layer moduli decrease (increasing damage index) the area of cracking increases. The impact of this relationship will be discussed in greater detail in Chapter 8.

Two data points in Figure 9 are considered anomalous or outliers. These two data points are from LTPP test sections 28-1001 and 28-A320. The reason for the high amounts of cracking relative to the in-place damage index is unknown at this time.

For the non-LTPP sites, input level 2 was used for the preliminary local calibration because deflection data were unavailable. After the field investigation, the deflection basins measured on the non-LTPP sites will be used to backcalculate the in place elastic modulus values for the existing HMA layers and used in the local calibration process as for the LTPP sites. These data will be added to Figure 9 and used in the final calibration.

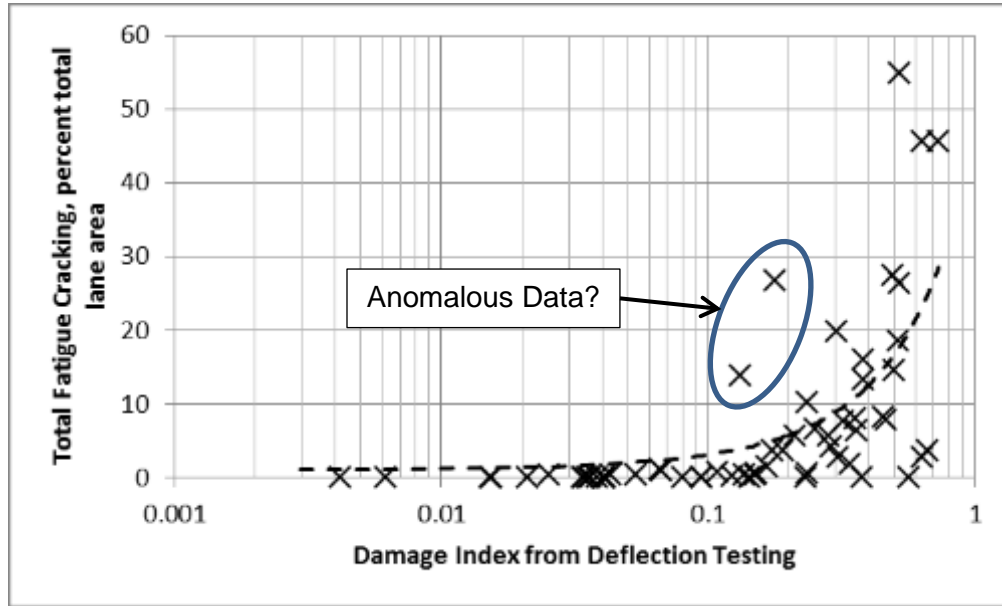


Figure 9—Damage Index Derived through Backcalculation of Elastic Layer Moduli and Cracking

- **Creep compliance and indirect tensile strength:** Creep compliance and the indirect tensile strength are needed for the low temperature cracking transfer function, but were not measured on typical HMA mixtures placed in Mississippi or included in the LTPP database. Transverse cracking was not believed to be that prevalent on Mississippi’s roadways, so MDOT decided to not expend the same effort as for the load related distresses. Default values (input level 3) from the regression equations included in Pavement ME Design were used in estimating the mixture specific properties for the thermal cracking transfer function.

7.2 PORTLAND CEMENT CONCRETE MIXTURES

Similar to HMA mixtures, volumetric, engineering, and thermal properties are required for the PCC layer. Most of the input level 1 properties, however, were unavailable for the LTPP test sections or were measured at the time of sampling – many years after construction. The MEPDG does include global material correlations through input level 2 and default values when site project PCC properties are unavailable. The sources of data were presented in Table 3.

The following summarizes the input values selected or assumed for the PCC mixtures and existing PCC slabs. For all other properties (including the thermal properties), the global default values (input level 3) were assumed for the PCC mixtures (see Appendix A).

7.2.1 PCC Mixture Properties

MDOT conducted a comprehensive laboratory test program to characterize PCC mixtures for use in MEPDG for a rigid pavement analysis (Varner, 2016). This study was followed by

a subsequent data analyses effort to provide recommendations for use of PCC inputs in the hierarchical levels 1, 2 and 3 in MEPDG (Rao, 2014)

The laboratory test program (Varner, 2016) was performed to test twenty different mix designs using five different aggregate types and four different blends of cementitious materials, covering statewide materials. These mix designs can be considered typical of paving mixes in MDOT using materials local to Mississippi and are identified in Table 17.

Table 17—PCC Mix Designs Included in Laboratory Test Program

MIX_ID	Cement (lb/yd ³)	Class F Fly Ash (lb/yd ³)	Class C Fly Ash (lb/yd ³)	Slag (lb/yd ³)	Total cementitious (lb/yd ³)	Coarse Aggregate Type	w/c ratio
1	548	0	0	0	548	High Absorption Gravel	0.42
2	411	137	0	0	548		0.41
3	411	0	137	0	548		0.38
4	274	0	0	274	548		0.42
5	548	0	0	0	548	Crushed Limestone	0.42
6	411	137	0	0	548		0.43
7	411	0	137	0	548		0.41
8	274	0	0	274	548		0.43
9	548	0	0	0	548	Low Absorption Crushed Limestone	0.42
10	411	137	0	0	548		0.43
11	411	0	137	0	548		0.40
12	274	0	0	274	548		0.43
13	548	0	0	0	548	Low Absorption Gravel	0.38
14	411	137	0	0	548		0.38
15	411	0	137	0	548		0.36
16	274	0	0	274	548		0.40
17	548	0	0	0	548	Small Maximum Size Gravel	0.42
18	411	137	0	0	548		0.43
19	411	0	137	0	548		0.40
20	274	0	0	274	548		0.42

Materials properties considered critical for performance prediction of JPCP were determined. The test results included both mechanical properties as well as those properties that influence volumetric changes in the PCC slab due to thermal and moisture changes. PCC material inputs added to the MDOT's PCC material library are as follows:

- Modulus of Rupture or Flexural Strength @ 7,14, 28, and 90 days in accordance with AASHTO T97
- Compressive Strength @ 7, 14, 28, and 90 days in accordance with AASHTO T22

- Modulus of Elasticity @ 7, 14, 28, and 90 days in accordance with ASTM C 469
- Poisson's Ratio in accordance with ASTM C 469
- Coefficient of Thermal Expansion (CTE) in accordance with AASHTO T336
- Concrete Shrinkage in accordance with ASTM C 157
- Unit Weight in accordance with AASHTO T 121

The mix designs included in the PCC materials library represent PCC mixtures that can be applied to future designs or non-LTPP sections that can be used in future recalibration efforts. State Study 260 (Rao, C., 2014), developed recommendations for PCC inputs to MEPDG procedure based on the laboratory testing of mixes reported in Table 17. The study developed level 2 correlation models to estimate design inputs, as well as level 3 defaults using test data.

PCC level 2 correlations were derived for flexural strength and elastic modulus estimation based on compressive strength test results and other mix design index properties, which is the approach used for level 2 estimates in the MEPDG procedure. The level 2 models derived with MDOT test data of mixes reported in Table 17, showed a deviation from the national level 2 equations. Additionally, because of the controlled nature of the experimental program and the aggregate types included in the experimental matrix, it was possible to improve the level 2 correlations to account for the aggregate type. Recommendations for level 2 models as provided in the State Study 260 (Rao, C., 2014) are summarized in Table 18. Note that the recommendations are based on the knowledge of aggregate type.

Level 3 defaults developed from the MDOT test data are shown in Table 19 for the critical material properties as well as mix design properties. State study 260 recommends that for the use of level 3 values, material source information for the intended design project should be compared with that of the 20 mix designs from the experimental program (shown in Table 17). The user should identify the MIX_ID that aligns with the selected coarse aggregate and the cementitious material blend from Table 17. If the mix design and materials of the project closely align with a MIX_ID in Table 17, level 1 mix design data for the corresponding mix design available from the MDOT Materials library is recommended. If the mix design does not fully align with the mixes in Table 17, level 3 default values in Table 19 for the closest mix design is recommended.

Additionally, CTE values for the different aggregate sources from MDOT testing are summarized in Table 20. The averages are reported for specific aggregate sources as well as for the two primary aggregate types — limestone and chert. Table 20 also lists the average values recommended by AASHTO for different aggregate types based on averages from LTPP database. Clearly the CTE values for the two aggregate types—limestone and chert are higher for MDOT aggregate sources compared to national averages. Therefore, the use of national defaults is NOT recommended for CTE inputs.

Table 18—Alternatives for level 2 correlations based on MDOT PCC test data.

Knowledge of aggregate	Flexural strength	Elastic modulus																																																
No	MDOT Model 2: $MR = 4.5912 * f'_c{}^{0.5894}$	MDOT Model 5: $E = 73360 * f'_c{}^{0.5}$ MDOT Model 6: $E = 409110 * f'_c{}^{0.305}$ MDOT Model 7: $E = 4.91 * w^{2.41} * f'_c{}^{0.23}$																																																
Yes	MDOT Model 3: $MR = a * f'_c{}^{0.5}$ where a has the values: <table border="1" data-bbox="542 821 813 1031"> <thead> <tr> <th>CA_ID</th> <th>a</th> </tr> </thead> <tbody> <tr><td>1</td><td>9.7816</td></tr> <tr><td>2</td><td>9.4012</td></tr> <tr><td>3</td><td>11.0280</td></tr> <tr><td>4</td><td>10.805</td></tr> <tr><td>5</td><td>9.6891</td></tr> </tbody> </table> MDOT Model 4: $MR = a * f'_c{}^b$ where a and b have the values: <table border="1" data-bbox="464 1188 885 1398"> <thead> <tr> <th>CA_ID</th> <th>a</th> <th>b</th> </tr> </thead> <tbody> <tr><td>1</td><td>7.5366</td><td>0.5297</td></tr> <tr><td>2</td><td>7.6295</td><td>0.5235</td></tr> <tr><td>3</td><td>2.2333</td><td>0.6801</td></tr> <tr><td>4</td><td>1.7049</td><td>0.7090</td></tr> <tr><td>5</td><td>6.9302</td><td>0.5376</td></tr> </tbody> </table>	CA_ID	a	1	9.7816	2	9.4012	3	11.0280	4	10.805	5	9.6891	CA_ID	a	b	1	7.5366	0.5297	2	7.6295	0.5235	3	2.2333	0.6801	4	1.7049	0.7090	5	6.9302	0.5376	MDOT Model 9: $E = a * f'_c{}^b$ where a and b have the values: <table border="1" data-bbox="964 821 1385 1031"> <thead> <tr> <th>CA_ID</th> <th>a</th> <th>b</th> </tr> </thead> <tbody> <tr><td>1</td><td>229467</td><td>0.3652</td></tr> <tr><td>2</td><td>523594</td><td>0.2693</td></tr> <tr><td>3</td><td>2000000</td><td>0.1585</td></tr> <tr><td>4</td><td>654322</td><td>0.2627</td></tr> <tr><td>5</td><td>203805</td><td>0.3768</td></tr> </tbody> </table>	CA_ID	a	b	1	229467	0.3652	2	523594	0.2693	3	2000000	0.1585	4	654322	0.2627	5	203805	0.3768
CA_ID	a																																																	
1	9.7816																																																	
2	9.4012																																																	
3	11.0280																																																	
4	10.805																																																	
5	9.6891																																																	
CA_ID	a	b																																																
1	7.5366	0.5297																																																
2	7.6295	0.5235																																																
3	2.2333	0.6801																																																
4	1.7049	0.7090																																																
5	6.9302	0.5376																																																
CA_ID	a	b																																																
1	229467	0.3652																																																
2	523594	0.2693																																																
3	2000000	0.1585																																																
4	654322	0.2627																																																
5	203805	0.3768																																																
Where, in all equations above MR is the flexural strength in psi f'c is the compressive strength in psi E is the modulus of elasticity in psi, and w is the unit weight of concrete in lb/ft ³ CA_ID is the coarse aggregate source, 1(High Absorption Gravel), 2(Crushed Limestone), 3(Low Absorption Crushed Limestone), 4(Low Absorption Gravel), and 5(Small Maximum Size Gravel)																																																		

Table 19—Level 3 PCC Material Property Inputs Recommended for Use in Mississippi

MIX_ID	Coarse Aggregate Source	Cementitious Materials*	Flexural strength (psi)	Modulus of elasticity (psi)	Poisson's ratio	CTE, x10 ⁻⁶ /degF
1	High Absorption Gravel	1	786	5883333	0.17	6.575
2		2	752	5233333	0.16	6.475
3		3	783	6333333	0.14	6.94
4		4	843	5933333	0.15	6.82
5	Crushed Limestone	1	736	5483333	0.19	5.025
6		2	721	5400000	0.20	4.99
7		3	816	6366667	0.23	5.19
8		4	913	5416667	0.19	5.25
9	Low Absorption Crushed Limestone	1	928	6683333	0.21	4.65
10		2	933	6583333	0.22	4.86
11		3	973	6650000	0.21	5.14
12		4	1047	6550000	0.23	5.29
13	Low Absorption Gravel	1	858	6583333	0.17	6.82
14		2	850	6566667	0.14	6.745
15		3	901	6666667	0.18	6.795
16		4	1004	7533333	0.15	6.935
17	Small Maximum Size Gravel	1	811	5833333	0.14	6.66
18		2	764	5700000	0.15	6.565
19		3	844	6250000	0.15	6.73
20		4	928	5816667	0.15	6.84
<p>*Cementitious Materials – 1 (type 1 cement), 2 (type 1 cement + class F fly ash), 3 (type 1 cement + class C fly ash) and 4 (type 1 cement + slag)</p> <p>Other PCC Default Inputs</p> <p>Unit weight = 145 pcf</p> <p>Poisson's ratio = 0.18</p> <p>Surface shortwave absorptivity = 0.85</p> <p>Thermal conductivity, BTU/hr-ft-°F = 1.25</p> <p>Heat capacity, BTU/lb-oF = 0.28</p> <p>Cement type = Type 1</p> <p>Cementitious material (PCC + pozzolans) = 548 lb/yd³</p> <p>Water to cement ratio (w/c) = 0.43</p> <p>PCC zero stress temperature, oF – Computed by the software program</p> <p>Ultimate shrinkage, microstrain – Computed by the software program</p> <p>Reversible shrinkage – 50%</p> <p>Time to develop 50% of ultimate shrinkage – 35 days</p> <p>Curing method – Curing compound</p>						

Table 20—Recommended PCC CTE Values from MDOT Testing and MEPDG Defaults from LTPP Testing

MDOT CTE Test Result Defaults			LTPP Default CTE Values	
Coarse Aggregate Description	Aggregate type	CTE (10 ⁻⁶ /°F)	Coarse Aggregate Type	CTE (10 ⁻⁶ /°F)
High Absorption Gravel	Chert	6.70	Basalt	4.4
Crushed Limestone	Limestone	5.11	Diabase	5.2
Crushed Limestone	Limestone	4.99	Granite	4.8
Low Absorption Gravel	Chert	6.82	Schist	4.4
Small Maximum Size Gravel	Chert	6.70	Chert	6.1
Average for Chert Gravels		6.7	Dolomite	5.0
Average for Limestone		5.1	Limestone	4.4
			Quartzite	5.2
			Sandstone	5.8

In summary, for any given PCC mixture to be used in a future MEPDG design, a user has the option of using one of the following input levels (as is also described in detail by Rao, C., 2014):

- Level 1 inputs if project specific testing can be performed and test data are available at the time of design.
- MDOT-specific level 2 correlation models in Table 18 from State Study 260 if level 2 tests data are available. Note that the recommendations provide different level 2 correlation equations for modulus of rupture and elastic modulus depending on whether the aggregate type is known.
- MDOT-specific level 3 defaults in the absence of laboratory test data (from Table 19 and 20)

For the LTPP sections used in local calibration, all data were obtained from the LTPP database. The sources of data were presented in Table 3. Key inventory, design, materials, and construction data were assembled for each calibration site for review, identification and/or elimination of outliers and anomalies. Therefore, input levels 1, 2, and 3 were used for the local calibration of the rigid pavement transfer functions. The PCC mixture input values are included in the Volume II report for each calibration site.

For the LTPP sections used in calibration, the PCC mixture properties or inputs were assumed as follows when project specific properties were unavailable:

- 28-day flexural strength and elastic modulus. The modulus of rupture and elastic modulus are critical for both the AASHTO 1993 rigid pavement design procedure and the MEPDG. The modulus of elasticity has a much greater effect on performance with the MEPDG than with the AASHTO 1993 procedure. For the GPS sections, only the long-term (mostly 5 years or more) compressive and tensile strength and elastic modulus was tested. The initial flexural or compressive strength and elastic modulus were backcast to the time of

- construction using the laboratory test values at the age of the pavement when the samples were recovered for testing. The strength-modulus gain or growth model included in the MEPDG was used to backcast the strength and modulus of the Mississippi LTPP PCC mixtures. The following are the assumed values when no information or data were available for the calibration sites:
- 28-day PCC mean flexural strength: 700 psi.
 - 28-day PCC mean elastic modulus: 4,200,000 psi.
 - Compressive strength ratio at 7, 14, 28, and 90 days. Long-term to 28-day PCC compressive strength of 1.44 is recommended and was used for all calibration sites.
 - CTE: The CTE value was determined based on the amount of information available for each calibration test section, as follows:
 - When no information on the PCC mixture and/or aggregate source was available, 4.7×10^{-6} in/in/degrees Fahrenheit was used.
 - When the PCC coarse aggregate geological class was known, the appropriate CTE values was selected from Table 20; default CTE values. However, characterizing the aggregate by its mineralogy or class is inadequate to estimate CTE of the concrete. It is also dependent on the aggregate hardness and the aggregate source. For example, a limestone coarse aggregate from Mississippi may produce a different PCC CTE than a limestone from elsewhere in the Midwest. This was one of the reasons CTE was included in the SS 177 test program (Varner, 2016).

7.2.2 Existing PCC Slabs

Existing intact PCC properties are required only for HMA overlay, unbonded PCC overlay, and for concrete pavement restoration. For the calibration test sections, an assessment was made based on the overall condition of the existing rigid pavement using the guidelines presented in the MEPDG Manual of Practice (AASHTO, 2008).

The modulus of elasticity for the existing PCC slab was estimated based on the existing pavement condition as per the following recommendations from AASHTO (2008):

- Existing pavement condition defined as *Good/Adequate* – Modulus within a typical range of 3 to 4 x 10⁶ psi with a mean modulus of 3.5 x 10⁶ psi
- Existing pavement condition defined as *Marginal* – Modulus within a typical range of 1 to 3 x 10⁶ psi with a mean modulus of 2.0 x 10⁶ psi
- Existing pavement condition defined as *Poor/Inadequate* – Modulus within a typical range of 0.3 to 1 x 10⁶ psi with a mean modulus of 0.65 x 10⁶ psi

7.2.3 Other PCC Layer Inputs

The following is a listing of other rigid pavement inputs and the values assumed for the calibration sections.

- Slab/Base friction factor: The number of months when the PCC slab and base are in full friction was assumed based on the type of material/layer below the PCC slab, as follows:
 - Aggregate base: Full friction for entire design life
 - Asphalt treated base: Full friction for entire design life
 - Cement treated base: Full friction for 10 years
- Permanent curl/warp effective temperature: The permanent curl/warp effective temperature difference defines the temperature difference between top and bottom of the PCC slab at the time of construction. The global default value is -10°F, and was used for all calibration sections.
- Zero stress temperature: Zero stress temperature occurs after placement concrete has cured and hardened sufficiently that the temperature begins to drop, resulting in tensile stress. It can be input directly or the default value in the MEPDG software can calculate the values from the monthly ambient temperature and cement content.

7.3 CEMENT TREATED BASE MIXTURES

The compressive strength (modulus of rupture), elastic modulus, and density are required inputs to the MEPDG for any cementitious or pozzolonic stabilized material. The agency specific calibration factors are determined based on the quality of the CTB material. These values need to be updated after the in place material properties have been determined and established for the LTPP and non-LTPP roadway segments. The LTPP database for test

sections with cementitious layers did not contain material properties for these test sections so the backcalculated elastic modulus values were used for the calibration process.

7.4 UNBOUND AGGREGATE BASE AND SOIL LAYERS/MATERIALS

Volumetric, engineering, and thermal properties are required for all unbound layers including the subgrade (see Appendix A). Most of the unbound layer inputs were extracted from the LTPP database, MDOT sponsored projects, and/or construction records, so input levels 1 and 2 were used for local calibration. The sources of data were presented in Table 3.

Gradation, Atterberg limits, optimum water content, maximum dry density, and resilient modulus test results are included in the LTPP database. All of these properties are also included in the MDOT construction materials database, except for resilient modulus. The following summarizes the input values selected or assumed for the unbound layers and subgrade. For all other properties (including the thermal properties), the global default values (input level 3) were assumed for the unbound layers (see Appendix A).

7.4.1 General Physical and Volumetric Properties

The average gradation, Atterberg limits, water content, and dry density stored in the LTPP database were the input values used for each layer of each calibration site. For the non-LTPP sites, the values recorded in the MDOT construction materials database were used. The local or global default values were used in absence of the physical and volumetric property.

Figure 10 shows a comparison between the optimum water content and maximum dry unit weight for all unbound layers extracted for the Mississippi LTPP sites. The water content and dry density reported for the resilient modulus tests for all unbound layers were entered as input level 1 for the calibration process. Figure 11 shows a comparison between the optimum and in place water contents during the LTPP field investigations. For most layers, the in place water content is higher than the optimum water content at the time of deflection testing. The field investigation for the non-LTPP sites has yet to be completed. Once the field investigations are completed the moisture-density data will be added to Figures 10 and 11.

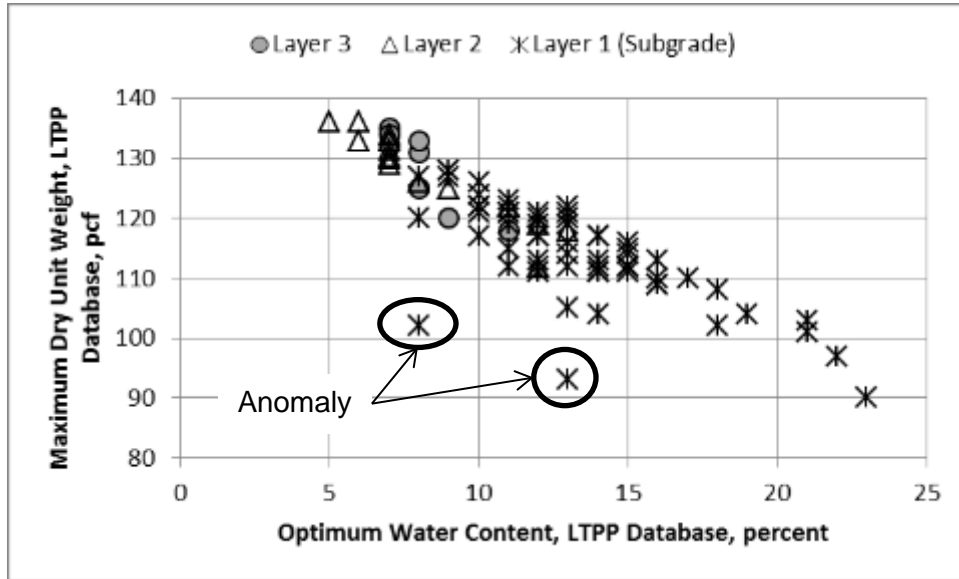


Figure 10—Relationship between Optimum Water Content and Maximum Dry Unit Weight for all Unbound Materials and Soils for the Mississippi LTPP Sites

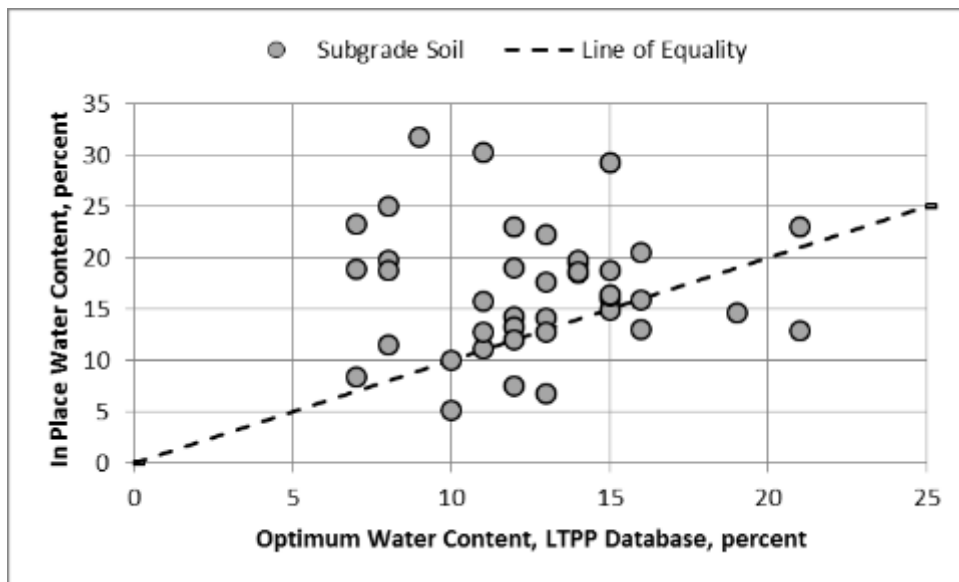


Figure 11—Optimum Water Content and In Place Water Contents for the LTPP Sites

7.4.2 Resilient Modulus

Two approaches were used to determine the resilient modulus at the time of construction: (1) laboratory derived resilient moduli, and (2) field derived elastic moduli. The field derived or backcalculated modulus values are the preferred input, because this value represents the composite value of the soil strata rather than a localized test specimen. In addition, MDOT's standard practice has been to use backcalculated elastic moduli as part of their

rehabilitation design process. It is recommended the use of backcalculated elastic moduli be continued because the majority of MEPDG use will be for pavement rehabilitation.

No deflection basin data, however, were available for the non-LTPP sites. For consistency, one approach was used for the preliminary local calibration process – the laboratory derived values, because only the default resilient moduli and volumetric properties were available for the soils and aggregate base layers of the non-LTPP sites. After the field investigations have been completed, it is suggested that the field-derived layer moduli be used in the final calibration. The following summarizes the laboratory and field-derived moduli for all unbound layers.

7.4.2.1 Laboratory-Derived Resilient Modulus

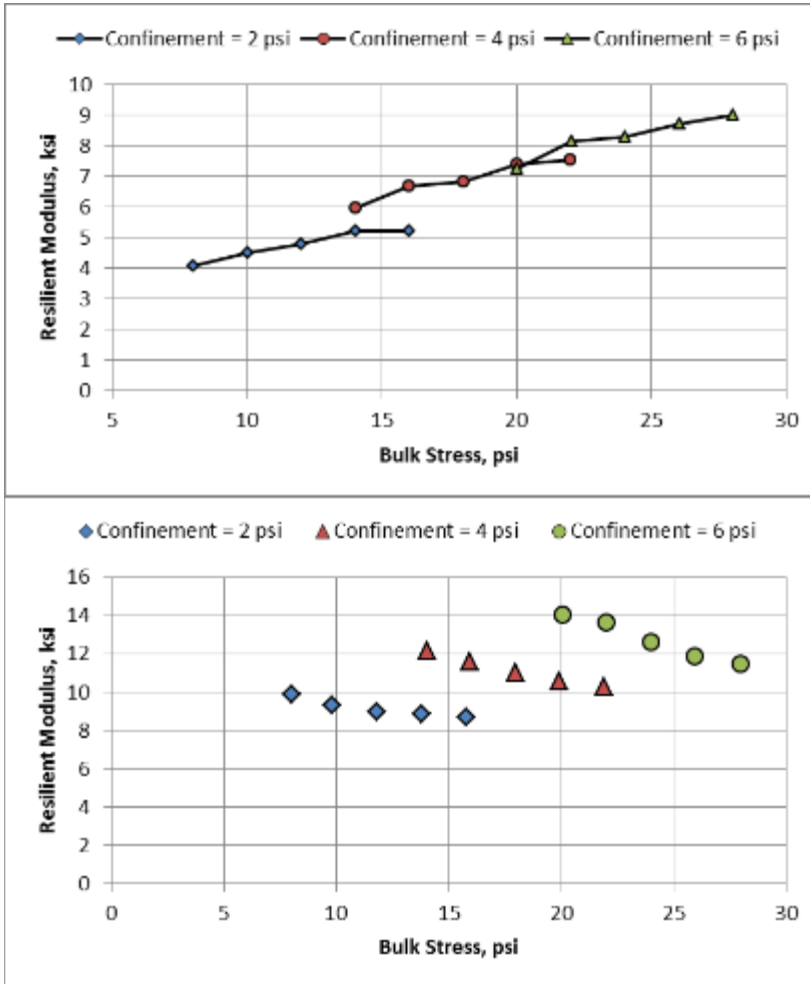
Repeated load resilient modulus lab test results are included in the LTPP database for most unbound layers. Figures 12 and 13 include examples from the resilient modulus tests of the soils and coarse-grained base materials of selected LTPP sites, respectively. Laboratory resilient modulus tests were performed at the optimum moisture content and maximum dry unit weight for some of the sites, while the in place water content and density were also used within the LTPP program.

Burns Cooley Dennis Consulting Engineers conducted repeated load resilient modulus tests on typical aggregate base materials used in Mississippi and on the more common soils encountered in Mississippi. For new alignments or new designs, Table 21 provides the overall mean value and the range of values for different soils and unbound base materials that were used in the preliminary calibration refinement for Mississippi. These local default moduli were derived from repeated load resilient modulus tests and are representative of the soils and base materials from the LTPP sites located in Mississippi.

7.4.2.2 Field-Derived Resilient Modulus

For rehabilitation/reconstruction designs, the resilient modulus of each unbound layer and embankment can be backcalculated from deflection basin data or estimated from DCP and other physical properties of the soil. If the resilient modulus values are determined by backcalculating elastic layer modulus values from deflection basin tests, those values can be used directly or adjusted to laboratory equivalent values. Table 22 lists the adjustment ratios or C-factors that should be applied to the unbound layers for use in design, if laboratory-derived resilient moduli are used.

For the preliminary local calibration process, deflection basins were only available for the LTPP test sections. Deflection basins are to be measured on all of the non-LTPP test sections as part of the field investigation. For these sites, the optimum water content and maximum dry density and laboratory-derived default resilient moduli were used for each soil type. As such, laboratory equivalent resilient moduli were used for the preliminary local calibration process. After the field investigation has been completed, however, the backcalculated moduli from the LTPP and non-LTPP sites should be used for the final calibration. The remainder of this section discusses determination of the field-derived or elastic and laboratory-derived resilient moduli for the unbound layers.



Subgrade soil resilient modulus test results; Section 28-0501.

Subgrade soil resilient modulus test results; Section 28-0805.

Figure 12—Resilient Modulus Test Results for Different Subgrade Soils

Multiple backcalculation programs provide the elastic layer modulus typically used for pavement evaluation and rehabilitation design. ASTM D 5858, *Standard Guide for Calculating In Situ Equivalent Elastic Moduli of Pavement Materials Using Layered Elastic Theory* is a procedure for analyzing deflection basin test results to determine layer elastic moduli (i.e., Young’s modulus).

The absolute error or Root Mean Squared (RMS) error is the value that is used to judge the reasonableness of the backcalculated modulus values. The absolute error term is the absolute difference between the measured and computed deflection basins expressed as a percent error or difference per sensor; the RMS error term represents the goodness-of-fit between the measured and computed deflection basins. The RMS and absolute error terms needs to be as small as possible. An RMSE value in excess of 3 percent generally implies that the layer modulus values calculated from the deflection basins are inaccurate or questionable. RMSE values less than 3 percent were used in selecting the layer moduli for the preliminary local calibration process.

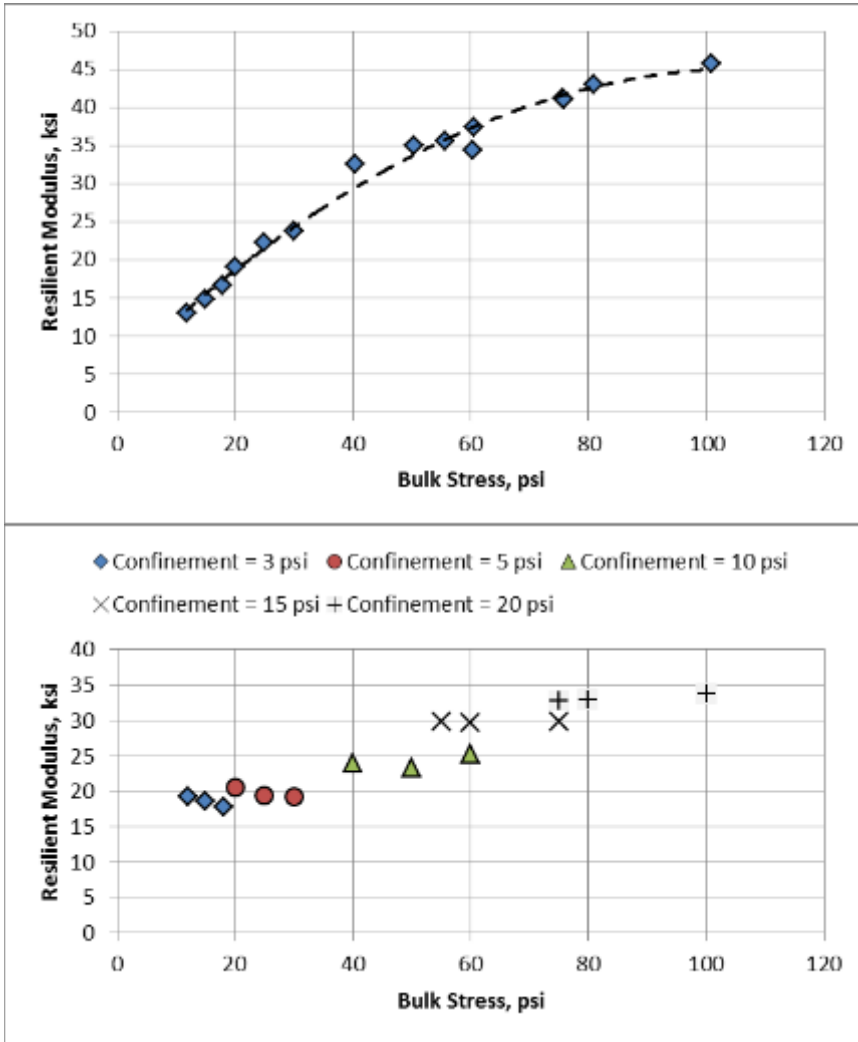


Figure 13—Resilient Modulus Test Results for Different Aggregate Bases

The point in time chosen for the backcalculation was selected to represent the time at which the soils and materials were sampled. This time was selected so the laboratory measured resilient modulus at an equivalent stress state below the pavement surface was determined under the same conditions during which the deflection basins were measured with the FWD. Figure 14 is an example illustrating backcalculated elastic moduli are a function of the in place water content. Deriving both moduli at the same time or subsurface condition, permits the AASHTO C-factor to be determined and compared to the values recommended for use in the MEPDG Manual of Practice. The procedure summarized by Von Quintus and Killingsworth (1997) was used to estimate the in place laboratory-derived resilient modulus for each site and unbound layer.

Table 21—Resilient Modulus Values Derived for Selected Base Materials and Subgrade Soils Typical for Mississippi

Type of Material or Soil		Typical Mean Resilient Modulus, ksi	Typical Range of Resilient Modulus, ksi
Aggregate Base & Subbase Layers	Crushed Stone; Limestone	30	25 to 40
	Crushed Stone; Other	28	20 to 35
	Crushed Gravel	25	20 to 30
	Coarse-Grained Soil-Aggregate Subbase*	20	10 to 30
Subgrade Soil/Foundation	Poorly Graded Gravel	20	12 to 30
	Clayey or Silty Gravel	17	11 to 25
	Silty or Clayey Sand	15	10 to 20
	Poorly Graded Sand*	12	6 to 15
	Gravelly Lean Clay*	15	6 to 25
	Sandy or Silty Lean Clay with Gravel*	12	6 to 25
	High Plasticity Clays	8	5 to 15

*Designates those material and soil types with highly variable resilient modulus values; it is suggested that these values be determined more precisely with a field and/or laboratory test program (Level 2 inputs are recommended).

Table 22—C-Factors Recommended for Use in Mississippi to Convert Backcalculated Layer Modulus Values to Laboratory Equivalent Modulus Values

Layer & Material Type	Layer Description	C-Factor, (M _R /E)	
		FHWA Pamphlet	Mississippi Sites
Aggregate Base Layers	Granular base under a Portland Cement Concrete (PCC) surface	1.32	---
	Granular base under a CAM layer, semi-rigid pavement	---	0.75
	Granular base above a stabilized material (a Sandwich Section)	1.43	---
	Granular base under an HMA surface or base	0.62	0.60
Subgrade Soil/Foundation	Soil under a CAM layer, no granular base	---	1.00
	Soil under a semi-rigid pavement with a granular base/subbase	---	0.50
	Soil Under a Stabilized Subgrade	0.75	---
	Soil under a full-depth HMA pavement	0.52	---
	Soil under flexible pavement with a granular base/subbase	0.35	0.50
Cement Aggregate Base Layer	Cement stabilized or treated aggregate layers	---	1.50
HMA Mixtures	HMA surface and base layers, 41 °F	1.00	0.9
	HMA surface and base layers, 77 °F	0.36	0.6
	HMA surface and base layers, 104 °F	0.25	0.5

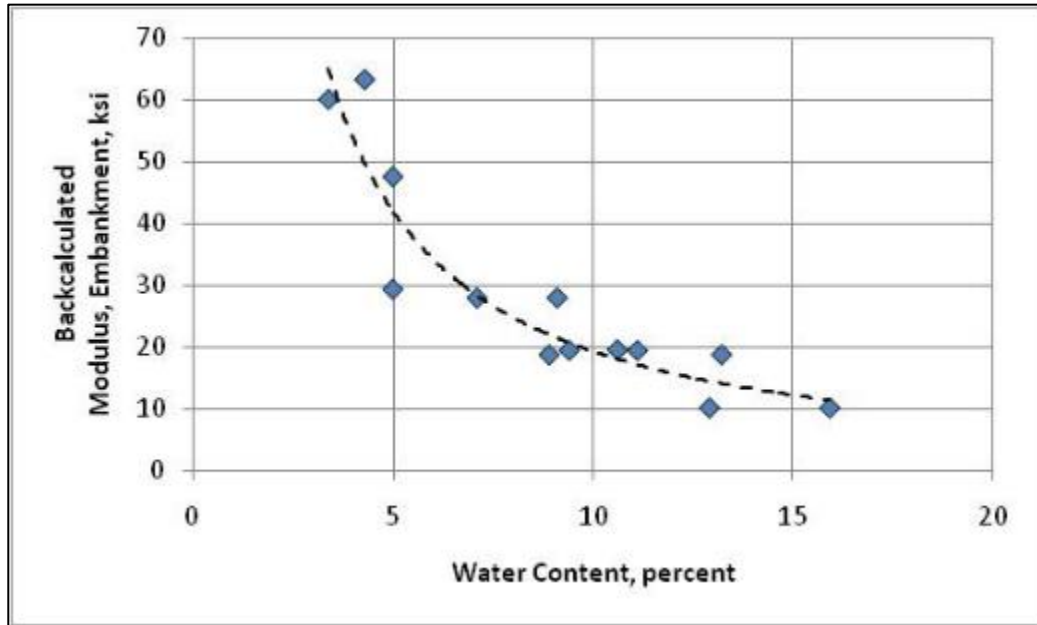


Figure 14—Backcalculated Elastic Modulus as a Function of In Place Water Content

For rigid pavements, the laboratory resilient modulus of the subgrade soil is used to determine a k-value for each month which is used to calculate the stresses and deflections used to compute damage (for JPCP). However, LTPP does not always provide the required subgrade laboratory-derived resilient modulus at optimum moisture content. Thus, FWD deflection data from the LTPP database were used to backcalculate the in place subgrade resilient modulus and k-value, as appropriate.

Resilient modulus values can also be estimated from Dynamic Cone Penetrometer (DCP) tests and physical properties of the material/soil (*Amini, 2003; George, 2000 and 2004*). MDOT has used the Dynamic Cone Penetrometer (DCP) for pavement evaluations and in estimating the resilient modulus of the unbound materials and soils. Equation 47 can be used to calculate the resilient modulus from the penetration rate measured with the DCP.

$$M_R = 17.6 \left(\frac{292}{(DPI)^{1.12}} \right)^{0.64} (C_{DCP}) \quad (47)$$

Where:

- M_R = Resilient modulus of unbound material, MP_a .
- DPI = Penetration rate or index, mm/blow.
- C_{DCP} = Adjustment factor for converting the elastic modulus from DCP tests to a laboratory-derived resilient modulus.

Although the resilient modulus can be estimated from DCP tests, the value needs to be adjusted to laboratory conditions. Table 23 provides the adjustment factors recommended for use in estimating resilient modulus from the DCP test results or penetration rate. It should be noted and understood Pavement ME Design does not adjust the resilient modulus

values calculated from the DCP and the values in Table 23 have not been field-verified for MDOT.

Table 23—DCP Adjustment Factors Recommended for Use in Mississippi to Convert an Elastic Modulus from DCP Tests to a Laboratory Equivalent Resilient Modulus

Material/Soil Type		Condition	Adjustment Factor, C_{DCP}
Fine-Grained; Low Plasticity Soil	Clay-Silt	Above Optimum Water Content	1.90
	Soil-Sand Mix	At or Below Optimum Water Content	1.05
	Soil-Aggregate Mix with Large Aggregate	At or Below Optimum Water Content	0.60
Coarse-Grained Material	Soil-Aggregate Mix	At or Below Optimum Water Content	0.60
	Crushed Aggregate	At or Below Optimum Water Content	1.04

Figures 15 and 16 include a graphical comparison of the laboratory-derived resilient moduli and backcalculated or field-derived elastic moduli. As shown, there is a lot of variability between the laboratory and in place moduli. Table 22 summarized the average C-factors for the different types of structures, in comparison to the values recommended in the MEPDG Manual of Practice. Table 22 and Figures 15 and 16 should get updated with the data from the field investigation of the non-LTPP sites.

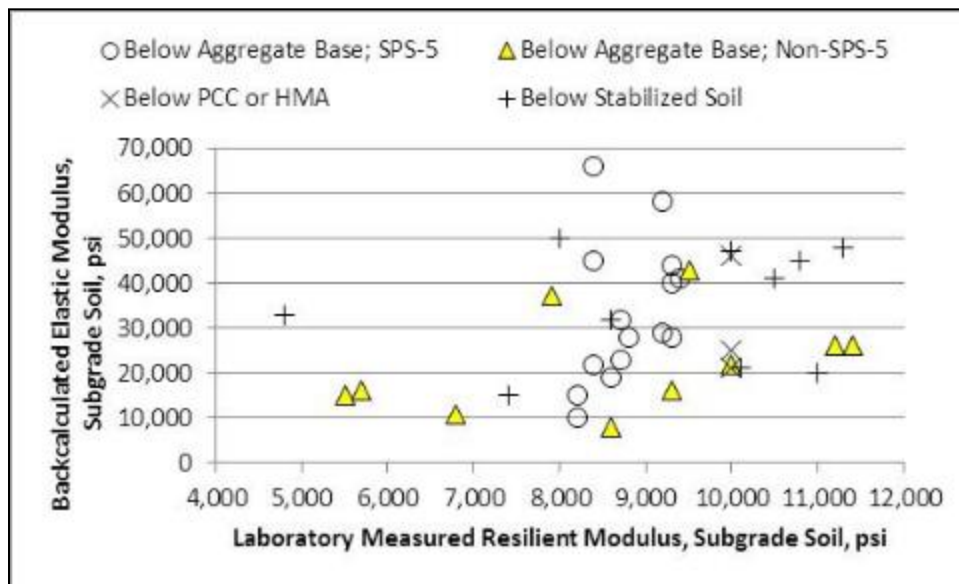


Figure 15—Laboratory-Derived Resilient Modulus Values Compared to the Field-Derived Backcalculated Elastic Modulus Values for the Subgrade Soils – Mississippi LTPP Test Sections

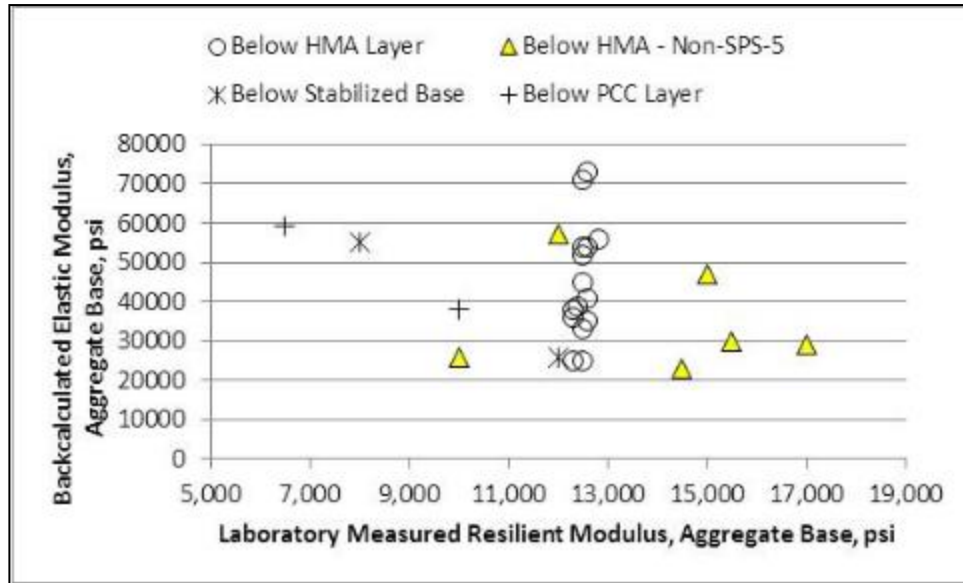


Figure 16—Laboratory-Derived Resilient Modulus Values Compared to the Field-Derived Backcalculated Elastic Modulus Values for the Aggregate Bases – Mississippi LTPP Test Sections

7.4.2.3 Layer Modulus Ratio Limiting Criterion

The resilient modulus of aggregate or granular base/subbase is dependent on the resilient modulus of the supporting layers. As a rule of thumb, the resilient modulus entered into AASHTOWare Pavement ME Design for a granular base layer should be less than three times the resilient modulus of the supporting layer to avoid decompaction of that layer. Figure 17 shows the maximum resilient modulus that can be sustained of an unbound base layer placed above the subgrade or another unbound granular layer. The limiting layer modulus is dependent on the type and thickness of the base layer, as well as on the resilient modulus of the supporting layer.

Figure 17 was used to limit the resilient modulus of the unbound aggregate base layer for the calibration sites to ensure the aggregate base resilient modulus is in agreement with the above rule of thumb. This layer modulus ratio was applied to the laboratory-derived resilient modulus during construction. It should be noted and understood that the MEPDG software will increase and decrease the resilient modulus over time to account for changes in the predicted water content of all unbound layers.

7.4.2.4 Determination of Unbound Layer Elastic Modulus at Time of Construction

This section discusses determination of the elastic moduli at the time of construction for the MEPDG software for the calibration process, and is grouped into two parts. The first part assumes laboratory-derived moduli are to be used in the local calibration process, while the second part assumes that field-derived moduli will be used. In either case, the procedures require that the backcalculated elastic moduli determined at some point in time will need to be adjusted back to the moduli at the time of construction.

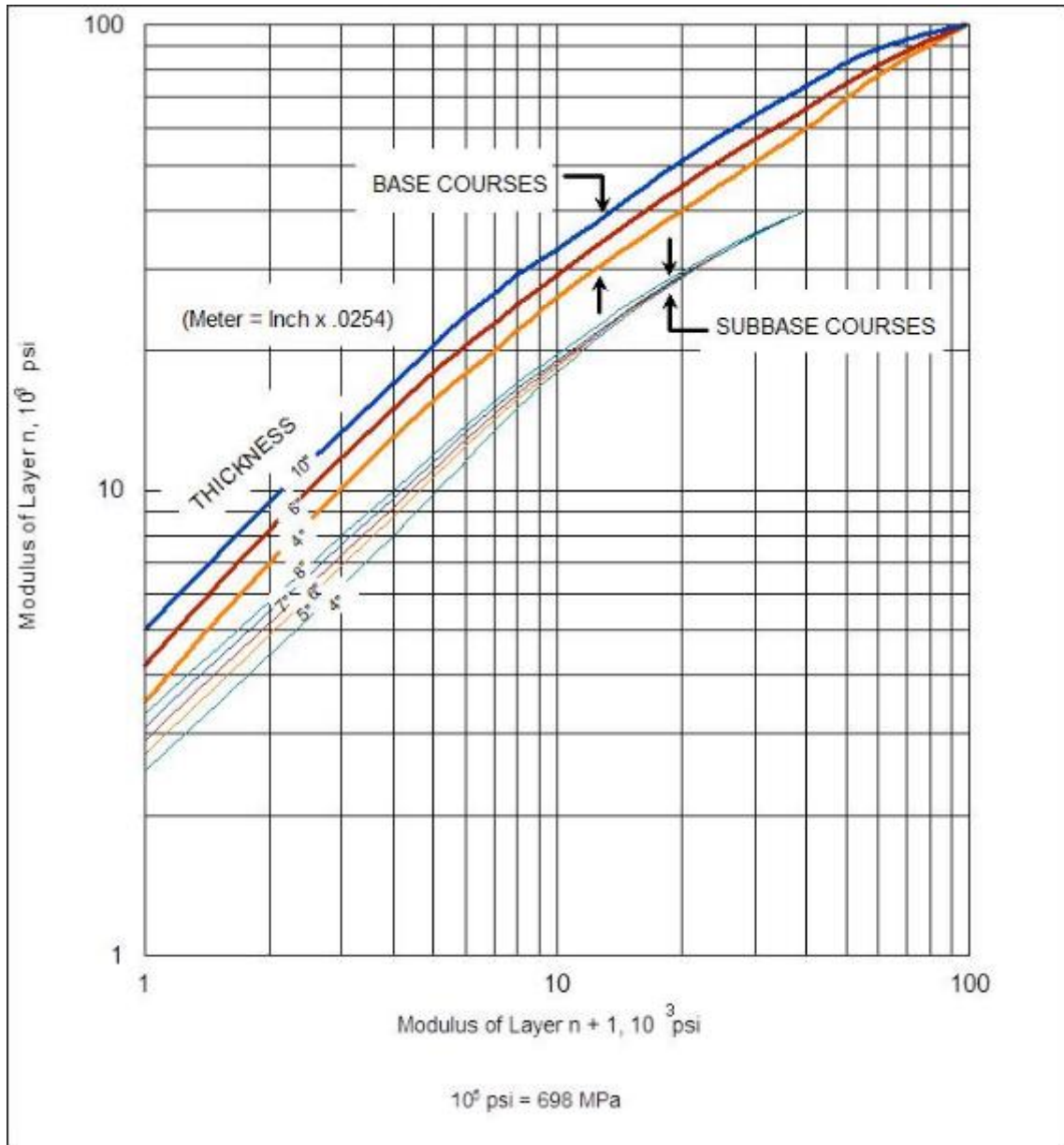


Figure 17—Limiting Layer Modulus Ratio or Criterion of Unbound Aggregate Base Layers (Barker and Brabston, 1975)

Use of Laboratory-Derived Values for Local Calibration

The following is the step by step process for estimating laboratory-derived resilient moduli of unbound layers that are entered into the MEPDG software for the local calibration process.

1. Deflection basin data are measured with the FWD along each roadway segment or test section that will be used in the local calibration process. Cores are taken to measure and confirm the layer thicknesses and material types from the as-built construction records. Material is recovered to determine the in place water content of the unbound layers.
2. MDOT calculates the elastic layer modulus from the deflection basins for the unbound layers of the pavement structure. The calculated elastic layer moduli from each deflection basin are determined, as well as the mean value, standard deviation and coefficient of variation at a particular site. The variability in the backcalculated elastic moduli is evaluated to determine if there are anomalies located along the test section.
3. The backcalculated moduli are adjusted to equivalent laboratory measured values using the C-factors recommended for use in Mississippi (see Table 22) by the following equation:

$$M_R(Lab) = E_{BC} * C$$

4. The laboratory-derived resilient modulus, maximum dry density, and optimum water content are determined for each unbound layer and site at construction. These values are estimated from the MDOT's material library and the default values included in the MEPDG to determine an equivalent resilient modulus value for the site considering the stress sensitivity of the material or soil.
5. The average field adjusted layer modulus value and in place water content are compared to the laboratory-derived values at construction to determine the magnitude of the difference. Figure 14 was an example from a project illustrating the backcalculated elastic modulus values are a function of the in place water content. Depending on the differences in the water content and moduli, trial runs are made with the MEPDG. Figures 18 and 19 show examples of the resilient modulus computed with the MEPDG over time using different starting volumetric properties and resilient modulus values. Similar figures for each calibration site are used to estimate the starting resilient modulus value at the time of construction.
6. The initial or starting resilient modulus is varied until the value calculated by the MEPDG matches the field-adjusted value backcalculated from the deflection basins at the same age or time. This is the value used in the local calibration process. Figures 20 and 21 are examples illustrating this process to determine the laboratory-derived resilient moduli for each unbound layer at construction that are used in the local calibration process.

Although this seems like a complicated and lengthy process, after a couple of sites, the starting laboratory-derived resilient modulus can be estimated with just one or two trial runs.

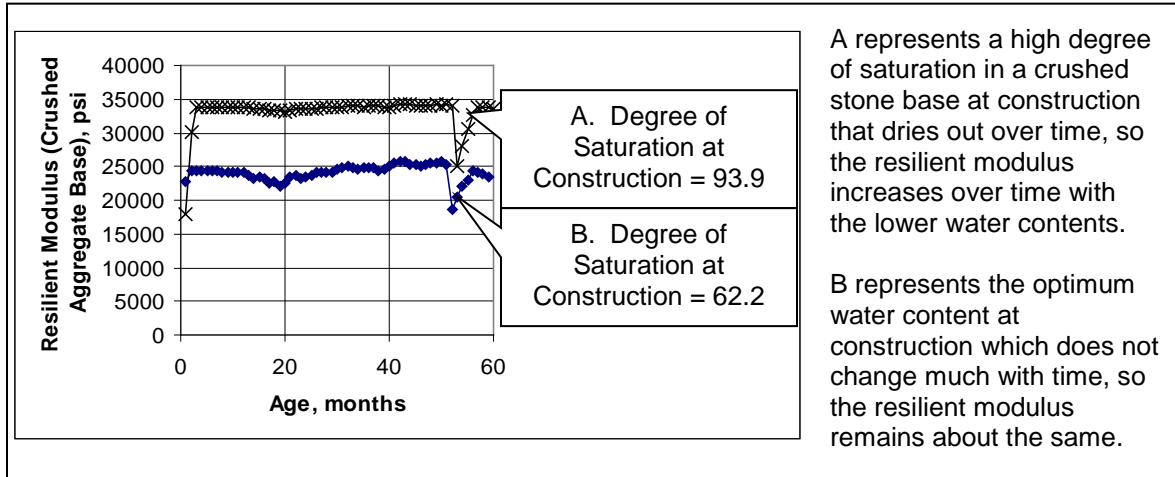


Figure 18—Resilient Modulus over Time for Different Moisture Contents; Example 1

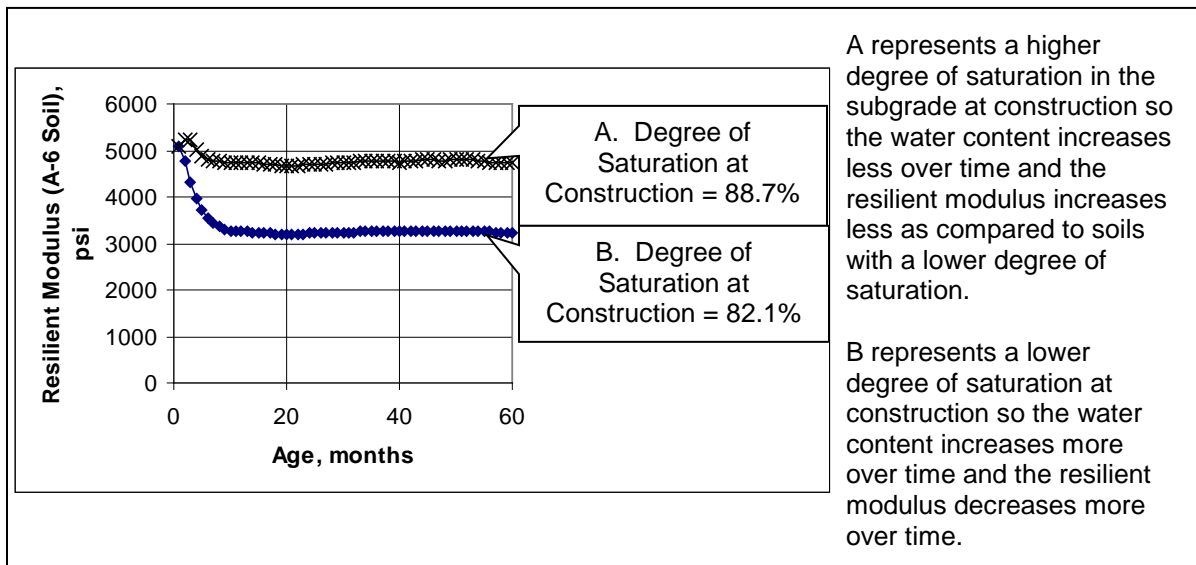
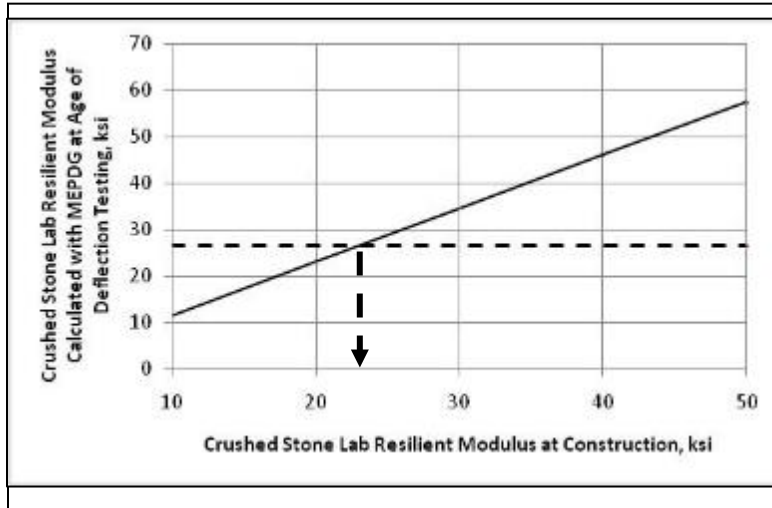


Figure 19—Resilient Modulus over Time for Different Moisture Contents; Example 2

Use of Field Derived or Backcalculated Values for Local Calibration

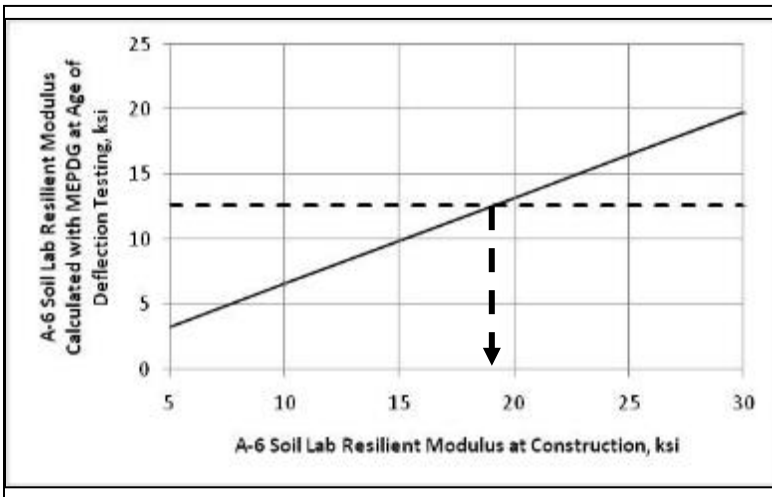
The following is the step by step process for determining the field-derived elastic moduli that are entered into the software for the unbound layers during the local calibration process.

1. The same as Step #1 for “Use of the Laboratory-Derived Values.”
2. The same as Step #2 for “Use of the Laboratory-Derived Values.” The backcalculated values are used as provided by MDOT and not adjusted to laboratory equivalent conditions.
3. The same as Step #4 for “Use of the Laboratory-Derived Values.”



The backcalculated elastic modulus adjusted to laboratory conditions in this example is 26.5 ksi. Thus, the laboratory-derived resilient modulus of the crushed stone at construction needs to be about 22 ksi so that the field adjusted elastic modulus matches the resilient modulus calculated by the MEPDG at the same age or time of the deflection basin testing.

Figure 20—Sample Graph Illustrating the Method to Determine the Resilient Modulus at Construction; Sample 1



The backcalculated elastic modulus adjusted to laboratory conditions in this example is 12.6 ksi. Thus, the laboratory-derived resilient modulus of the A-6 embankment soil at construction needs to be about 19 ksi so that the field adjusted elastic modulus matches the resilient modulus calculated by the MEPDG at the same age or time of the deflection basin testing.

Figure 21—Sample Graph Illustrating the Method to Determine the Resilient Modulus at Construction; Sample 2

4. The laboratory-derived values at construction are adjusted to field-derived, backcalculated values by using the C-Factor values (see Table 22) by the following equation:

$$E_{BC} = \frac{M_R(Lab)}{C}$$

5. The average field-derived or backcalculated elastic layer modulus value and in place water content are compared to the laboratory-derived values at construction to determine the magnitude of the difference. Depending on the differences in the water content and modulus values, trial runs are made with the MEPDG with varying field-derived elastic modulus values at construction. Results from the trial runs will be

similar to Figures 18 and 19, which are used to estimate the field-derived elastic modulus at the time of construction for each roadway segment or test section.

6. The initial or starting elastic modulus is varied until the value calculated by the MEPDG matches the field-derived or backcalculated value from the deflection basins at the same age or time. This is the value used in the local calibration process. Figures 22 and 23 are examples illustrating this process to determine the field-derived, backcalculated elastic moduli for each unbound layer at construction that are used in the local calibration process.

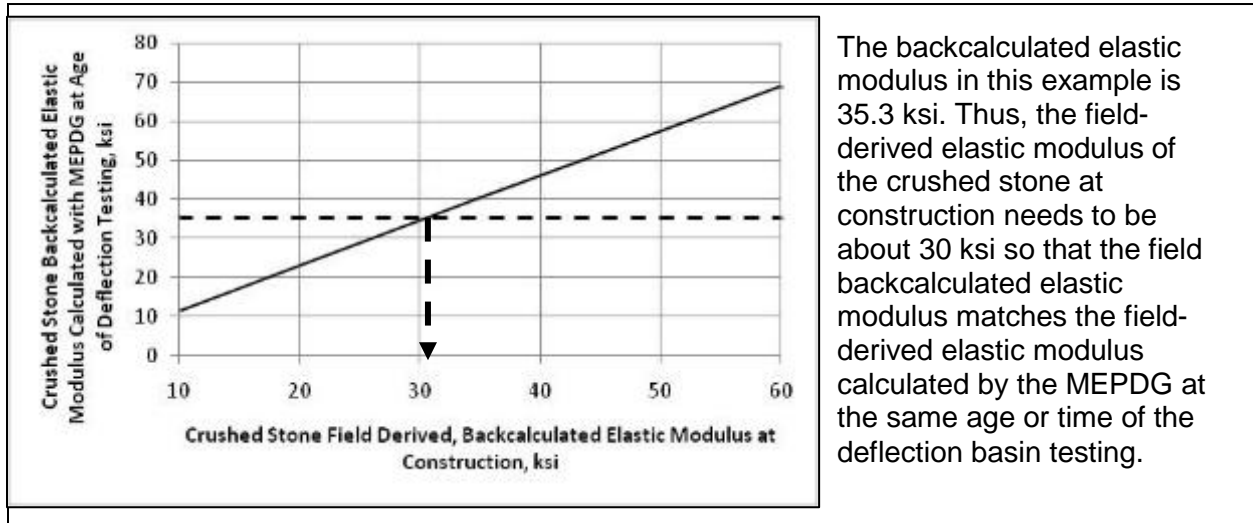


Figure 22—Sample Graph Illustrating the Method to Determine the Resilient Modulus at Construction; Sample 1 for Backcalculated Modulus

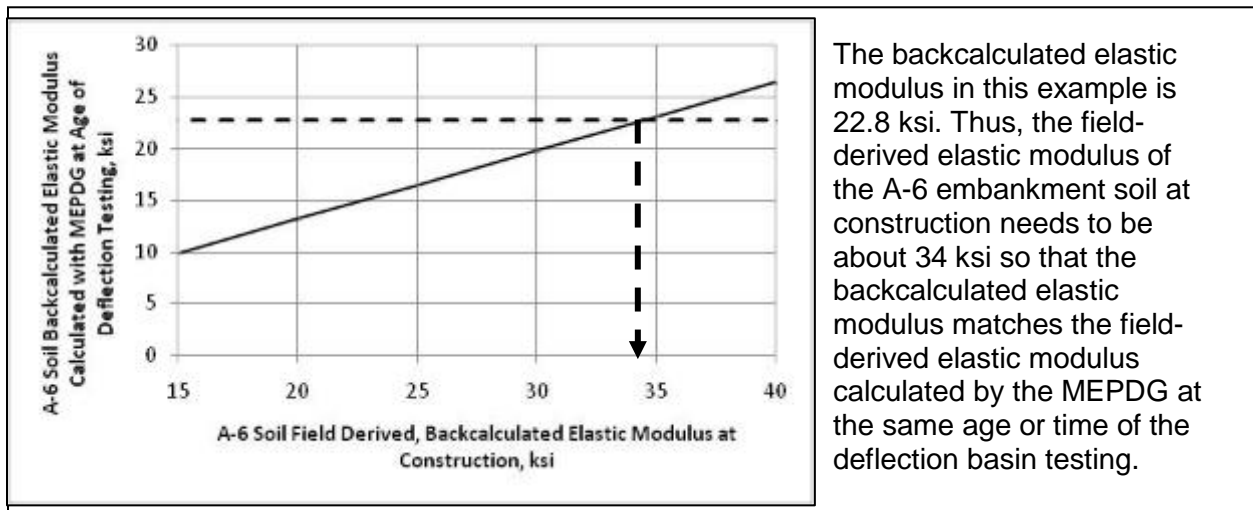


Figure 23—Sample Graph Illustrating the Method to Determine the Resilient Modulus at Construction; Sample 2 for Backcalculated Modulus

7.4.3 Poisson's Ratio

Poisson's ratio is another input parameter needed for the unbound materials and soils. Table 24 lists the values that were used during the local calibration refinement effort and are recommended for use in design.

Table 24—Poisson's Ratio Suggested for Use for Unbound Layers

Type of Soil	Poisson's Ratio
Low plasticity to high plasticity fine-grained soils with moisture contents higher than the optimum value.	0.45
Low plasticity to high plasticity fine-grained soils with moisture contents below the plastic limit.	0.35
Fine-grained soil or coarse-grained soil with more than 35 percent fines or material passing the #200 sieve.	0.35
Soil-Aggregate base materials which are predominately coarse-grained.	0.35
Crushed gravel or crushed stone base materials used as a base or subbase layer.	0.30

7.4.4 Hydraulic Properties

The other input parameters for the unbound layers are more difficult to measure and were not readily available for use in the local calibration refinement effort. For these inputs, the global default values recommended for use in the MEPDG were used to predict the distresses. Therefore, the MEPDG default values also are recommended for use in Mississippi for the following properties.

- Soil saturated hydraulic conductivity.
- Soil-water characteristics curves.

7.5 STABILIZED SUBGRADE FOR STRUCTURAL LAYERS

Stabilized subgrade soils are assumed to be the same as for the unbound materials and soils, with the exception that the resilient modulus is recommended to be constant throughout the design period—a representative layer. Thus, the other material properties needed for stabilized subgrade soils are the same as for unbound aggregate base or subbase layer and embankment or subgrade soils. When an aggregate base is placed above the stabilized subgrade, the following resilient moduli are recommended for use.

Type of Stabilized Subgrade	Recommended Resilient Modulus, psi	Recommended Poisson's Ratio
Soil Cement and Cement Stabilized Soils	100,000	0.20
Lime-Fly Ash Stabilized Soils	50,000	0.30
Lime Stabilized Soils	3 times the resilient modulus of the soil at optimum water content and maximum dry unit weight.	0.35

For a full-depth flexible pavement when the HMA mixture is placed directly over the stabilized subgrade soil, this is considered a semi-rigid pavement. As noted in previous chapters, semi-rigid pavements were not calibrated during the original global calibration studies, and were not calibrated during the MDOT local calibration study.

CHAPTER 8—VERIFICATION AND CALIBRATION OF FLEXIBLE PAVEMENT TRANSFER FUNCTIONS

This chapter describes the work to verify and calibrate, if needed, the MEPDG global flexible pavement distress and smoothness models for Mississippi. The decision to perform local calibration was based on whether the global model exhibited a reasonable goodness of fit (between measured and predicted outputs) and whether distresses/IRI were predicted without significant bias. Reasonable goodness of fit was based on R^2 and SEE, while the presence or absence of bias was based on the hypothesis test described in Chapter 3. The general criteria used to determine global model adequacy for Mississippi conditions were presented in Tables 5 and 6. This chapter explains the local calibration of the global calibration coefficients.

Both the LTPP and non-LTPP roadway segments were used in the verification and local calibration process. Field investigations have yet to be completed on the non-LTPP sections. They are planned for Phase 3 of the implementation study (see Chapter 1, Section 1.2 – Phased Implementation Approach). Field investigations are very important to reduce the standard error of the transfer functions. Thus, the local calibration coefficients are considered preliminary values derived from Phase 2.

8.1 FATIGUE ALLIGATOR CRACKING; BOTTOM-UP CRACKING

8.1.1 Verification of Calibration Coefficients

Verification of the MEPDG global alligator cracking models for Mississippi conditions consisted of the running the MEPDG with the global coefficients for all selected projects and evaluating goodness of fit and bias. Figure 24 shows a plot of measured versus predicted alligator cracking for all Mississippi HMA sections. Measured and MEPDG-predicted alligator cracking data were evaluated to determine model goodness of fit and bias in predicted alligator cracking. The results are presented in Table 25 and show the following:

- Goodness of fit was generally poor, with an $R^2 < 30$ percent, which implies a weak relationship between the MEPDG global model alligator cracking predictions and field-measured/observed cracking. The standard error of the estimate is very large, about 3 times the values reported in the 2008 Manual of Practice (see Table 25).
- Both the paired t-test and predicted versus measured cracking slope p-value indicated the presence of bias in predicted alligator cracking (p-value < 0.05).
- The plot presented in Figure 24 shows that the data points significantly deviate from the line of equality, another indication of bias and that there are confounding factors not considered in predicting the observed alligator area cracking.

In summary, the MEPDG alligator cracking global calibration coefficients did not adequately predict alligator cracking for Mississippi conditions. Local calibration of the MEPDG global alligator cracking transfer function for Mississippi was needed. The sampling matrix (refer to Table 7 in Chapter 3) was used to evaluate the results from the verification runs in terms of the primary factors of the experimental plan. In addition, the results should be re-evaluated after the field investigations have been completed for the non-LTPP segments. As an example this will include a comparison of HMA overlays and new construction, neat mixtures

and modified asphalt mixtures, stabilized and non-stabilized subgrades, and conventional and deep-strength pavement structures.

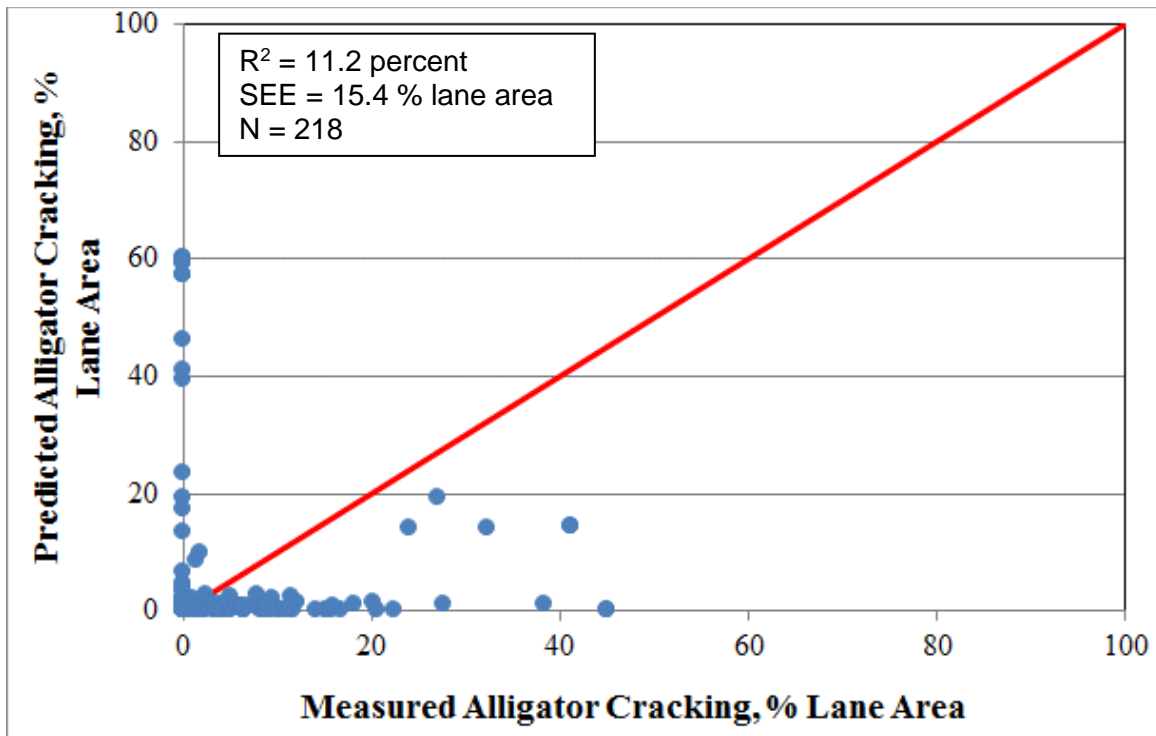


Figure 24. Verification of the HMA alligator cracking and fatigue damage models with MEPDG global coefficients, using Mississippi projects.

Table 25—Results of Statistical Goodness of Fit and Bias Evaluation of the MEPDG Alligator Cracking Global Model for Mississippi Conditions

Statistical Analysis Type			
Goodness of Fit		Bias	
R^2 , %	SEE	p-value (paired t-test)	p-value (slope)
11.2	15.4% lane area	0.0354	< 0.0001

8.1.2 Local Calibration of Alligator Cracking Transfer Function

8.1.2.1 Description of Local Calibration Procedure

Local calibration of the MEPDG alligator cracking model was done simultaneously for both new HMA and HMA-overlaid existing HMA pavement and the MEPDG HMA fatigue, alligator cracking, and reflection cracking models. Calibration consisted of the following steps:

1. Determine the cause of poor goodness of fit and bias produced by the global models, discussed in the previous section of this report.

2. Adjust the MEPDG HMA fatigue and alligator cracking model calibration coefficients as needed based on information derived from step 1 to improve goodness of fit and reduce or eliminate bias. This step was done using data from only the new HMA pavement projects.
3. After determining the local calibration coefficients in step 2, perform a second round of calibration coefficient adjustments using all projects (new HMA and HMA-overlaid HMA projects) for only the reflection cracking model. In other words, the local calibration coefficients for the fatigue cracking and alligator cracking models were fixed while the local calibration coefficients of the reflection cracking model were adjusted as needed to improve overall goodness of fit and reduce bias.
4. Details of specific HMA fatigue cracking, alligator cracking, and reflection cracking models coefficients adjusted are presented below (see Chapter 2 and Table 26).
 - a. HMA fatigue model (allowable number of axle load applications, N equation):
 - i. Global calibration coefficients (k_f1 , k_f2 , k_f3).
 - ii. Local calibration coefficients (β_{f1} , β_{f2} , β_{f3}).
 - b. Alligator cracking model.
 - i. Local/Global calibration coefficients ($C1$, $C2$, $C3$).
 - c. Reflected alligator cracking model.
 - i. Global calibration coefficients (c , d).
5. Perform a final round of calibration coefficient adjustments, if needed, using all the local calibration estimates obtained in steps 2 through 4 as seed values. Adjustments to the calibration coefficients determined in steps 2 through 4 were constrained to ensure reasonableness of the final set of model coefficients.

The backcalculated layer modulus values were used to compute the in place damage index in accordance with the MEPDG procedure. These in place damage indices were compared to the observed or measured area of cracking. Figure 25 shows the comparison between the in place damage and area of cracking. As shown, the higher the in place damage (from the deflection basin testing of the LTPP test sections) the greater the area of cracking. This finding was considered a significant improvement to the predicted cracking, as related to the global coefficients.

This relationship can be used to determine or estimate the $C1$ and $C2$ coefficients (refer to Table 26). The values for $C1$ and $C2$ can be used to evaluate the appropriateness of the fatigue damage relationship. Results from this analysis suggest that the fatigue damage coefficients are reasonable and do not need to be changed. Most of the HMA mixtures included in the LTPP test sections, however, are similar, so the result is not surprising.

Table 26—Description of HMA Fatigue Damage, HMA Alligator Cracking, and Reflection “Alligator” Cracking Models

Model Type	Model Description*
HMA fatigue damage	$N_{f-HMA} = k_{f1}(C)(C_H)\beta_{f1}(\epsilon_t)^{k_{f2}\beta_{f2}}(E_{HMA})^{k_{f3}\beta_{f3}}$
HMA alligator cracking	$FC_{Bottom} = \left(\frac{1}{60}\right) \left(\frac{C_4}{1 + e^{(C_1 C_1^* + C_2 C_2^* \text{Log}(DI_{Bottom}))}} \right)$
HMA reflection “alligator” cracking	$RC = \frac{100}{1 + e^{ac+bd}}$

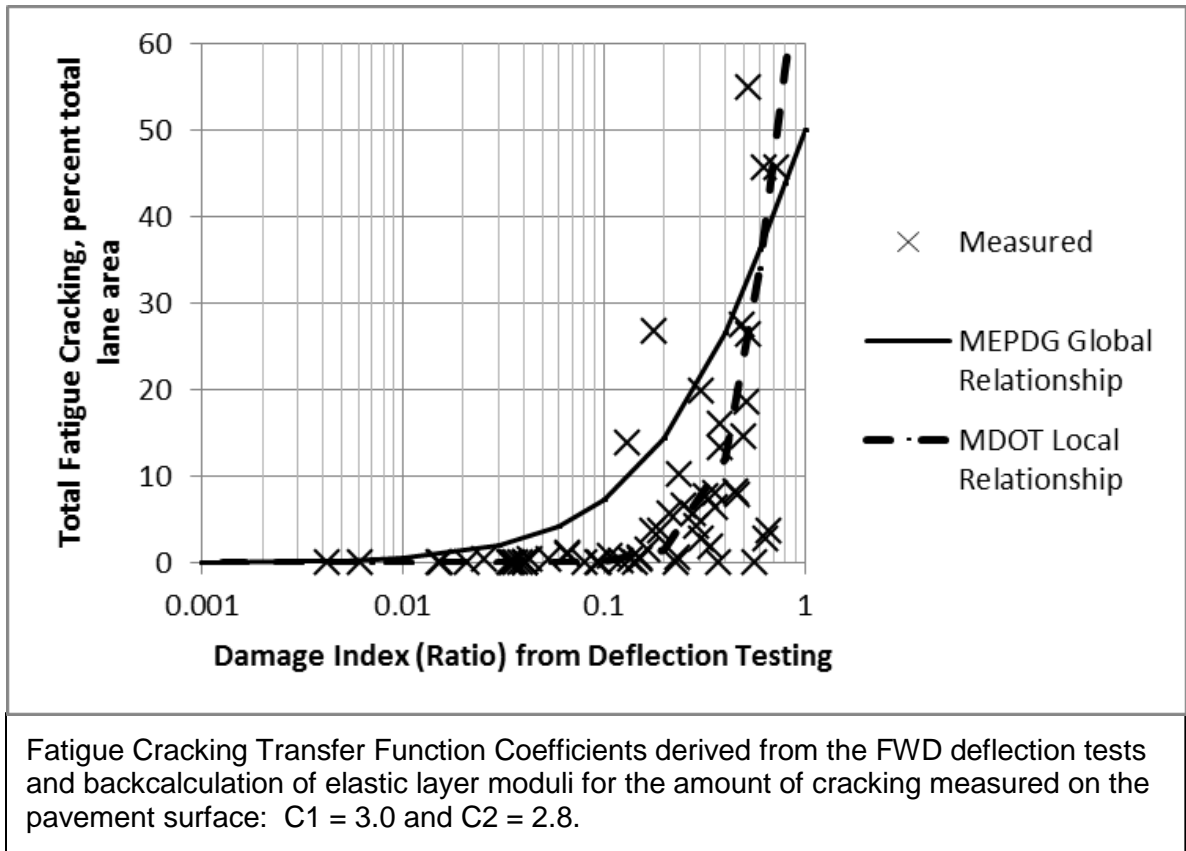


Figure 25—MDOT Local Calibration Coefficients for the Bottom-Up Fatigue Cracking Transfer Function

8.1.2.2 Summary of Alligator Cracking Model Local Calibration Results

The next step was to investigate the possible causes of poor goodness of fit and bias, and no obvious reasons were found (such as erroneous inputs). Thus, local calibration proceeded as previously described. Calibration of the MEPDG global models using MDOT input data was done using nonlinear model optimization tools available in the SAS statistical software. Adjusted HMA fatigue damage and alligator cracking global model coefficients are presented in Table 27 and shows that three of the nine global coefficients were adjusted.

As described earlier, the next step was to calibrate to local conditions the reflection “alligator” cracking model. The results are presented in Table 28. The goodness of fit and bias statistics are presented in Table 29 and show that inclusion of the HMA reflection “alligator” cracking model did not introduce significant bias. Thus, the goodness of fit and bias statistics presented in Table 29 show an adequate goodness of fit for all three HMA alligator cracking sub-models (see equations 9, 14, and 25 in Chapter 2) with no significant bias.

Figure 26 presents a plot of HMA fatigue damage using MDOT local calibration coefficients versus field-measured alligator cracking and Figure 27 shows measured versus predicted alligator cracking. Figure 28 shows the progression of reflection cracking with HMA overlay

age for different HMA overlay thicknesses. Figures 29 through 32 illustrate the MDOT local model prediction of alligator cracking for new HMA pavement and HMA-overlaid HMA pavement.

Table 27—Summary of MEPDG Global and MDOT Local Calibration Coefficients for HMA Alligator Cracking and HMA Fatigue Damage Models

Model Type	Model Coefficients (See Table 4)	Global Model Values	MDOT Local Model Values
HMA fatigue damage	K1	0.007566	0.007566
	K2	3.9492	3.9492
	K3	1.281	1.281
	BF1	1	2.01
	BF2	1	1
	BF3	1	1
HMA alligator cracking	C1Bottom	1	3.0
	C2Bottom	1	2.8
	C3Bottom	6000	6000

Table 28—Local Calibration Coefficients for HMA Overlay Reflection Cracking Model Developed using New HMA and HMA Overlaid HMA Pavement Projects

Model Coefficients (See Table 24)	Global Model Values	MDOT Local Model Values
C	1	0.8
D	1	1

Table 29—Results of Statistical Bias Evaluation of MEPDG Reflection “Alligator” Cracking Local Model for Mississippi Conditions

Statistical Analysis Type					
Goodness of Fit			Bias		
R ² , %	SEE	N	p-value (paired t-test)	p-value (Slope)	N
39.3	4.4 % lane area	218	0.9926	0.2084	218

Local calibration of the HMA fatigue, alligator cracking, and reflection “alligator” cracking models produced MDOT-specific models that predict alligator cracking distress with adequate accuracy and minimal bias. Goodness of fit characterized using R² increased from 11.2 for the global models to 39.3 percent, while SEE decreased from 15.4 to 4.4 percent total lane area. The new model coefficients will increase the accuracy of alligator cracking predictions while minimizing bias. Use of the MDOT model coefficients will produce more accurate and less costly new and overlaid HMA pavement designs at the desired design reliability because of the lower SEE.

It is expected that the R² will be significantly increased after the final calibration using the results from the field investigations under Phase 3. Appendix H summarizes the process to be used for determining the mixture specific fatigue damage relationships for the final

calibration. Use of the procedure summarized in Appendix H may explain some of the variation between fatigue damage and alligator cracking shown in Figures 26 and 27.

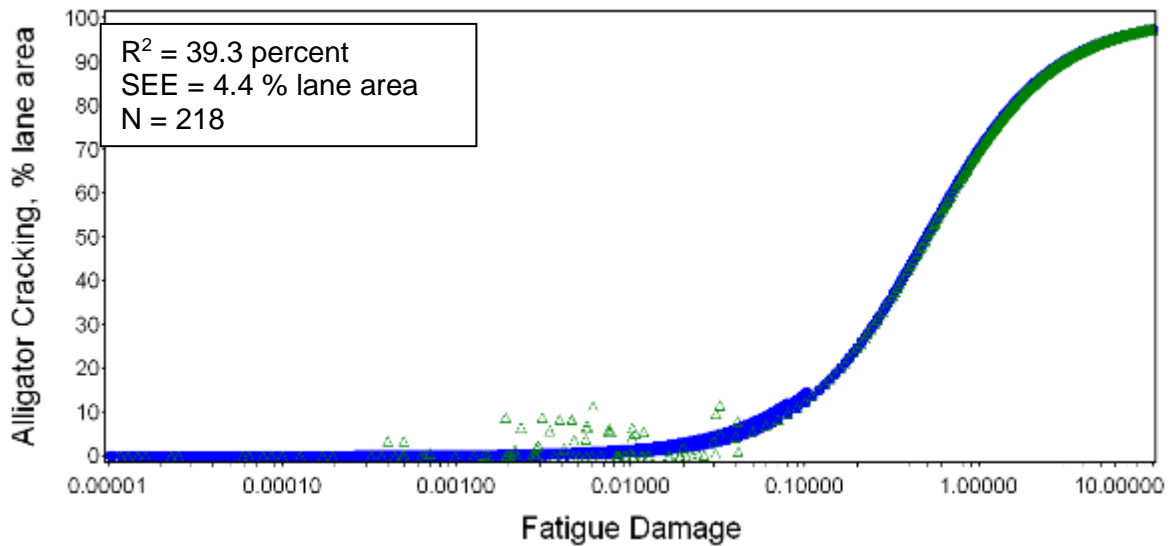


Figure 26. Plot showing measured HMA alligator cracking versus computed fatigue damage developed using MEPDG models with MDOT local coefficients.

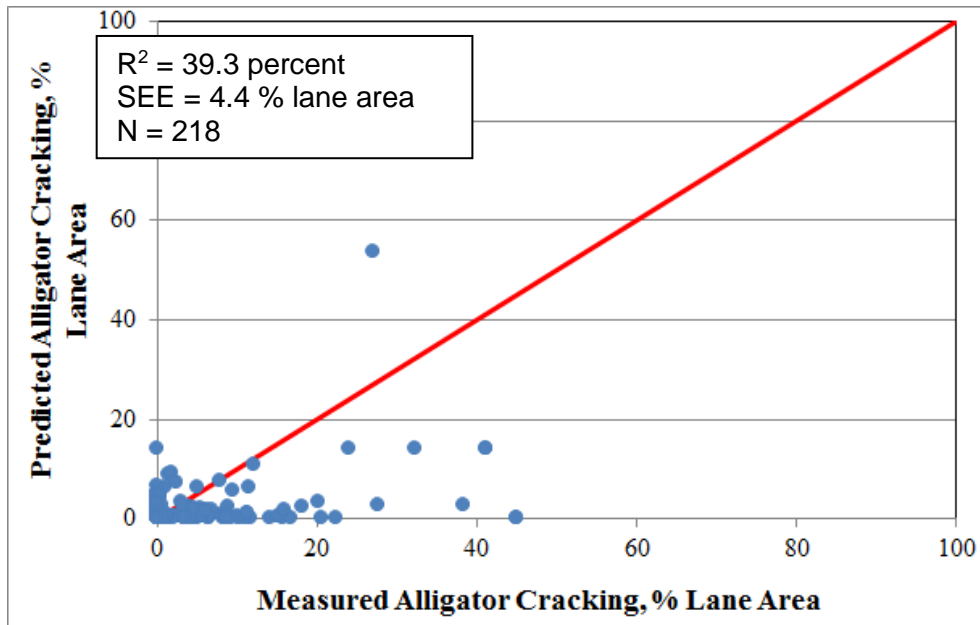


Figure 27. Plot showing measured HMA alligator cracking versus predicted HMA alligator cracking using MEPDG models with MDOT local coefficients.

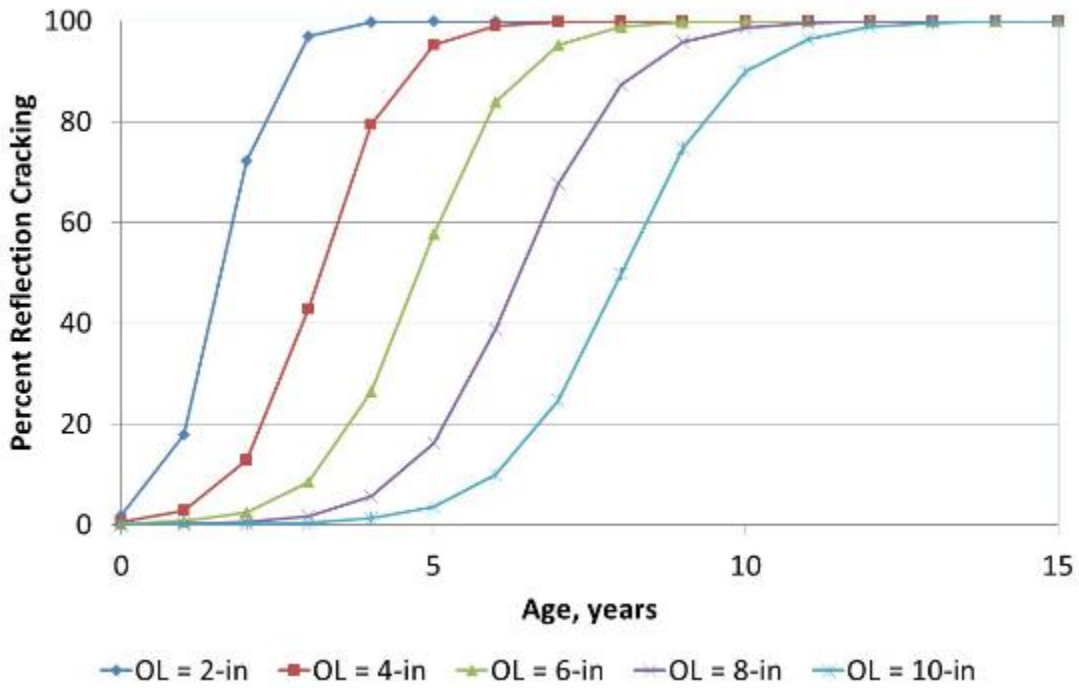


Figure 28. Plot showing progression of reflection cracking with HMA overlay age for different HMA overlay thicknesses.

PTYPE=New SHRPID=4784

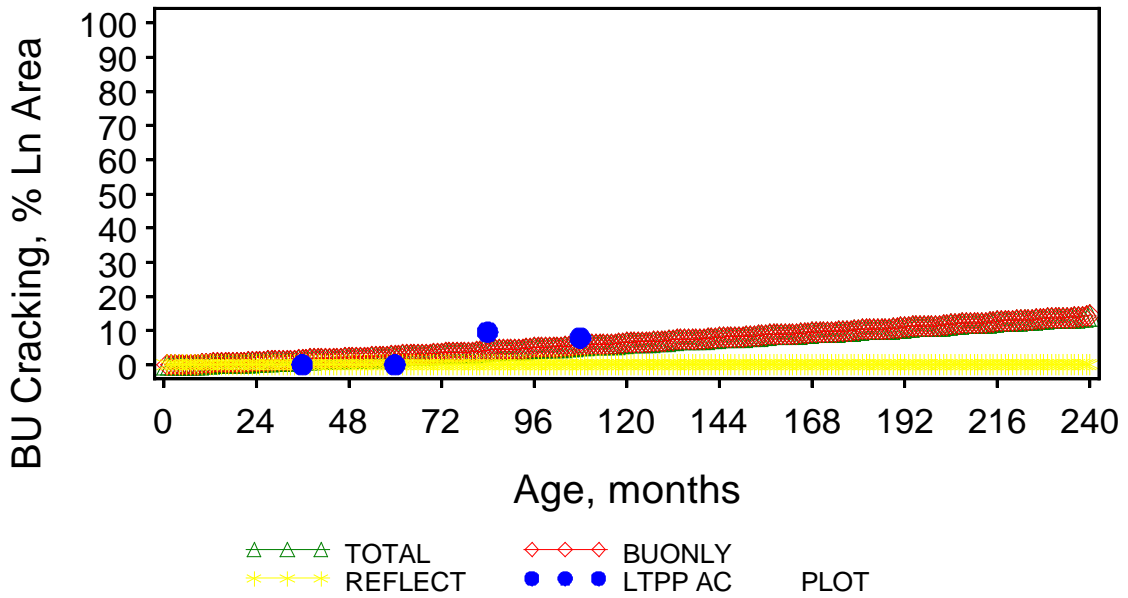


Figure 29. Plot of predicted alligator cracking versus age for MDOT pavement management system project 4784 (new HMA pavement).

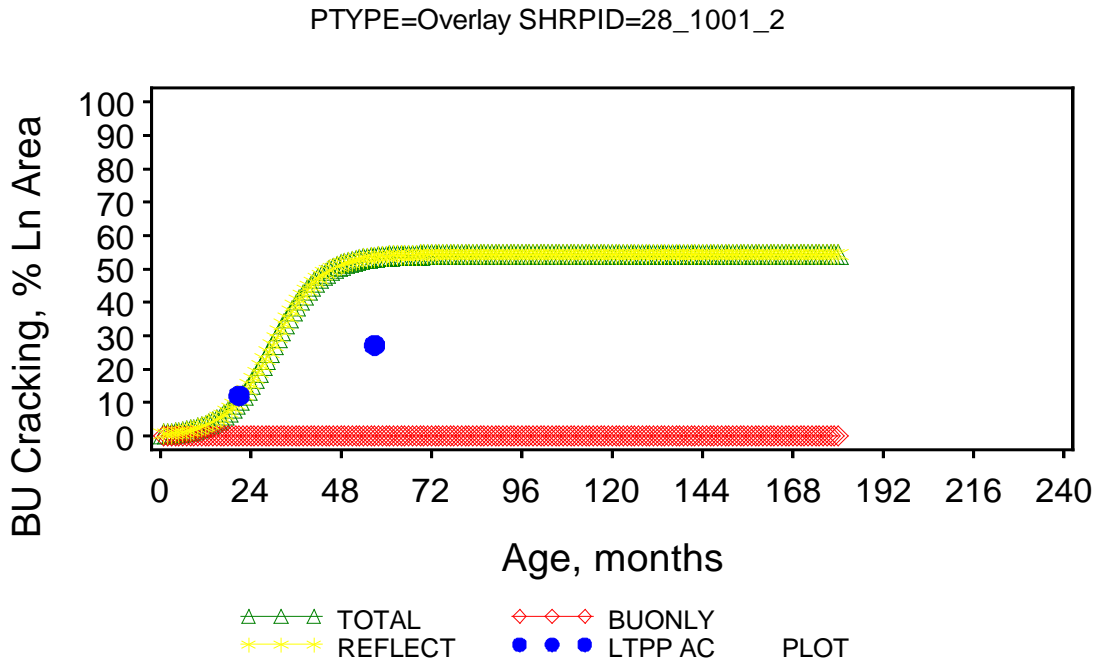


Figure 30. Plot of predicted alligator cracking versus age for LTPP project 1001 (HMA overlaid HMA pavement).

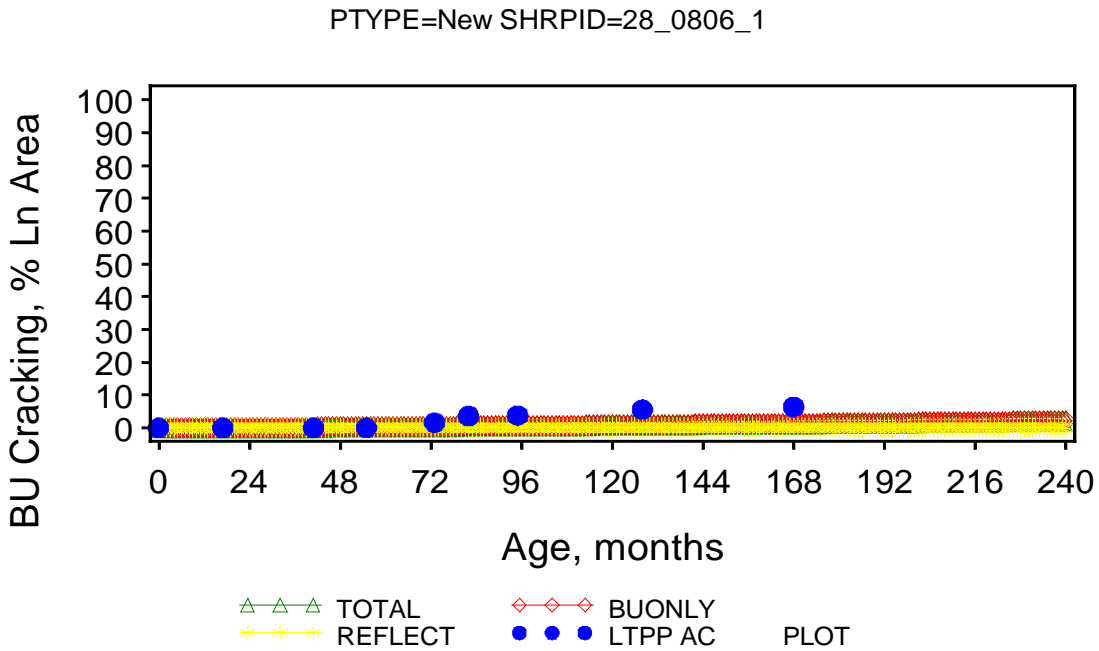


Figure 31. Plot of predicted alligator cracking versus age for LTPP project 0806 (new HMA pavement).

PTYPE=Overlay SHRPID=28_0903_2

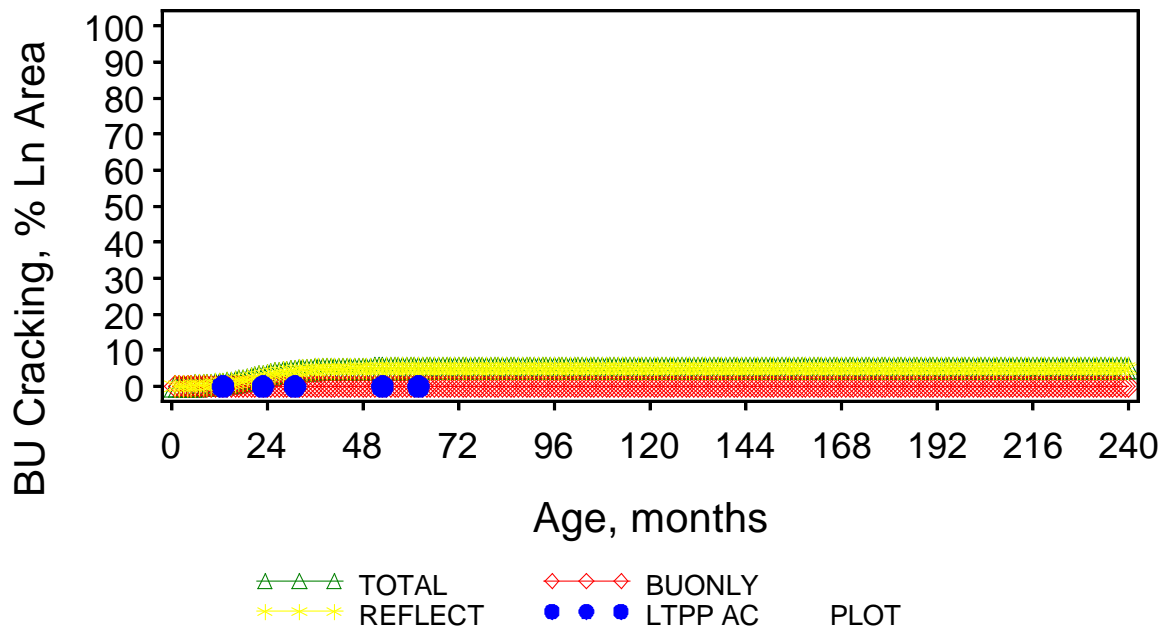


Figure 32. Plot of predicted alligator cracking versus age for LTPP project 0903 (HMA overlaid HMA pavement).

8.2 TOTAL RUTTING

8.2.1 Verification of the Global Calibration Coefficients

The MEPDG predicts HMA pavement total rutting using separate sub-models for the HMA layers, unbound aggregate base, and subgrade soil. The same three sub-models are utilized for HMA-overlaid HMA pavement, with modifications as needed to reflect the existing pavement material properties and permanent strain (existing rutting) present in all three layers.

Verification of the MEPDG global total rutting model consisted of the following steps:

1. Run the three MEPDG rutting sub-models using global coefficients for all new HMA pavement and HMA-overlaid HMA pavement projects to obtain estimates of total rutting.
2. Perform statistical analysis to determine goodness of fit with field-measured total rutting and bias in estimated total rutting.
3. Evaluate goodness of fit and bias statistics and determine any need for local calibration to Mississippi conditions.

Figure 33 shows a plot of the MEPDG global model predicted rutting versus field-measured rutting for all Mississippi new HMA pavement and HMA-overlaid HMA pavement projects. Goodness of fit and bias statistics computed from the data are presented in Table 30.

The information presented in Table 30 shows a poor to fair goodness of fit when compared to the global model statistics and significant bias in predicted total rutting estimates. The MEPDG rutting global model coefficients were, therefore, deemed inadequate for Mississippi site features and conditions, and local calibration of this model was required. The sampling matrix (see Table 9 in Chapter 3) should be used to evaluate the model coefficients after the field investigations to determine any difference in results between the HMA overlays and new construction, as well as between the semi-rigid pavements and conventional and deep strength structures.

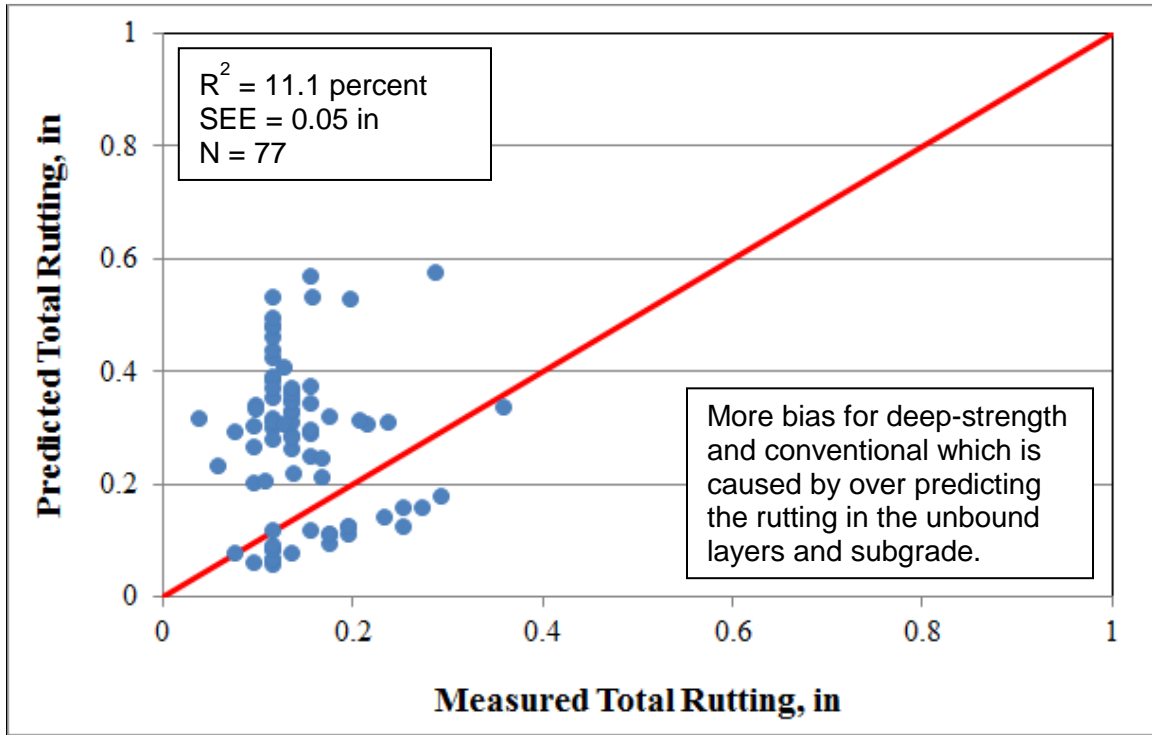


Figure 33. Plot showing MEPDG global model predicted rutting versus measured rutting (HMA, unbound aggregate base, and subgrade).

Table 30—Results of Statistical Evaluation of MEPDG Total Rutting Global Sub-Models for Mississippi Conditions

Statistical Analysis Type					
Goodness of Fit			Bias		
R ² , %	SEE	N	p-value (paired t-test)	p-value (Slope)	N
11.1	0.05in	77	< 0.0001	< 0.0001	77

8.2.2 Mississippi Local Calibration Coefficients

8.2.2.1 Description of Local Calibration Procedure

Local calibration of the three rutting sub-models consisted of the following steps:

1. Determine the cause of poor to fair goodness of fit and bias produced by the global models discussed in the previous section.
2. Adjust sub-model calibration coefficients as needed based on information derived from step 1 to improve goodness of fit and reduce or eliminate bias. Specifically, the following model coefficients can be adjusted:
 - a. HMA rutting:
 - i. Global calibration coefficients (k_{1r} , k_{2r} , k_{3r}).
 - ii. Local calibration coefficients (β_{1r} , β_{2r} , β_{3r}).
 - b. Granular base rutting model.
 - i. Global calibration coefficients (k_{s1}).
 - ii. Local calibration coefficients (β_{s1}).
 - c. Subgrade rutting model.
 - i. Global calibration coefficients (k_{s1}).
 - ii. Local calibration coefficients (β_{s1}).

Local calibration was done simultaneously for new HMA pavements and HMA-overlaid HMA pavements. The three rutting sub-models are presented in Table 31, while a detailed description of each is provided in Chapter 2.

8.2.2.2 Summary of Total Rutting Model Local Calibration Results

Possible causes of the poor goodness of fit and bias were investigated, but no obvious explanations for the poor goodness of fit (such as erroneous inputs) were found. Thus, local calibration proceeded as previously described.

Calibration of the MEPDG global models using MDOT input data was done using nonlinear model optimization tools available in the SAS statistical software. Adjusted HMA rutting, unbound aggregate base rutting, and subgrade rutting global model coefficients obtained from step 2 are presented in Table 32 and show that three of the ten global coefficients were adjusted. The goodness of fit and bias statistics is presented in Table 33. The test results indicate an adequate goodness of fit with minimal bias that was insignificant at a 5 percent significance level for the locally calibrated total rutting sub-models. A plot of field-measured versus MDOT-calibrated total rutting is presented in Figure 34.

The information presented Table 33 also shows no appreciable change in the goodness of fit between the global and MDOT model coefficients (i.e., R^2 changed from 11.1 to 25.4 and SEE changed from 0.05 to 0.057 inches) with local calibration. Both the global and locally calibrated models goodness of fit was characterized as fair. The slight increase in SEE was attributed to high variability exhibited in field measurements of pavement rutting that contributes to lowering R^2 and increasing SEE.

The results presented Table 33 also show that the significant bias produced by the global models in Mississippi had been eliminated through local calibration. This improvement increases overall rutting prediction accuracy and reliability of pavement designs. Thus, new

HMA pavement and HMA-overlaid HMA pavement designs in Mississippi will be more accurate at the selected level of design reliability with the application of the locally calibrated total rutting model coefficients.

Figures 35 through 39 present plots of measured and predicted rutting for several projects in Mississippi. The plots show reasonable predictions of rutting using the locally calibrated model coefficients.

Table 31—Description of Total Rutting Prediction Sub-Models

Model Type	Model Description*
HMA	$\Delta_{p(HMA)} = \varepsilon_{p(HMA)} h_{HMA} = \beta_{1r} k_z \varepsilon_{r(HMA)} 10^{k_{1r}} n^{k_{2r} \beta_{2r}} T^{k_{3r} \beta_{3r}}$
Unbound aggregate base	$\Delta_{p(soil)} = \beta_{s1} k_{s1} \varepsilon_v h_{soil} \left(\frac{\varepsilon_o}{\varepsilon_r} \right) e^{-\left(\frac{\rho}{n} \right)^\beta}$
Subgrade soils	$\Delta_{p(soil)} = \beta_{s1} k_{s1} \varepsilon_v h_{soil} \left(\frac{\varepsilon_o}{\varepsilon_r} \right) e^{-\left(\frac{\rho}{n} \right)^\beta}$

Table 32—Local Calibration Coefficients for HMA, Unbound Base, and Subgrade Soil Rutting Sub-Models

Model	Model Coefficients	Global Model Values	MDOT Local Model Values
HMA rutting submodel	Kr1	-3.35412	-3.35412
	Kr2	1.5606	1.5606
	Kr3	0.4791	0.4791
	β_{r1}	1	1.6
	β_{r2}	1	1
	β_{r3}	1	1
Granular base rutting submodel	ks1	2.03	2.03
	β_{s1}	1	0.65
Subbase rutting submodel	ks1	1.35	1.35
	β_{s1}	1	0.05

Table 33—Results of Statistical Evaluation of MEPDG Total Rutting using Local Rutting Sub-Models for Mississippi Conditions

Statistical Analysis Type					
Goodness of Fit			Bias		
R ² , %	SEE	N	p-value (paired t-test)	p-value (Slope)	N
25.4	0.057 in	77	0.1666	0.8299	77

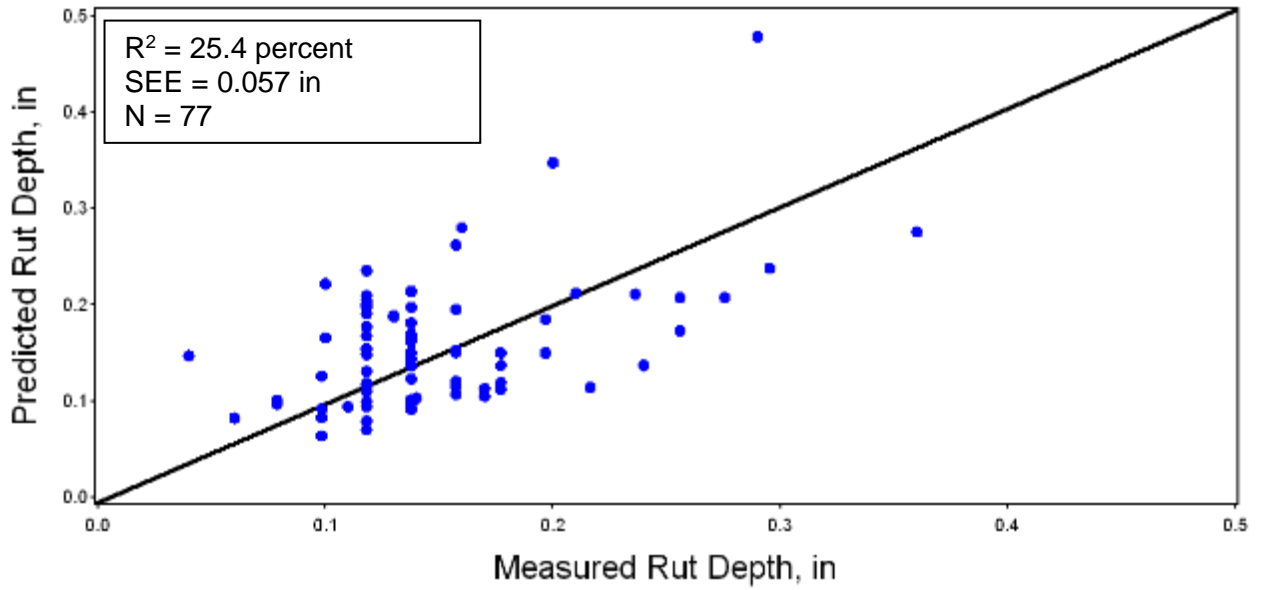


Figure 34. Plot showing predicted using MEPDG sub-models with MDOT local coefficients versus field-measured total rutting.

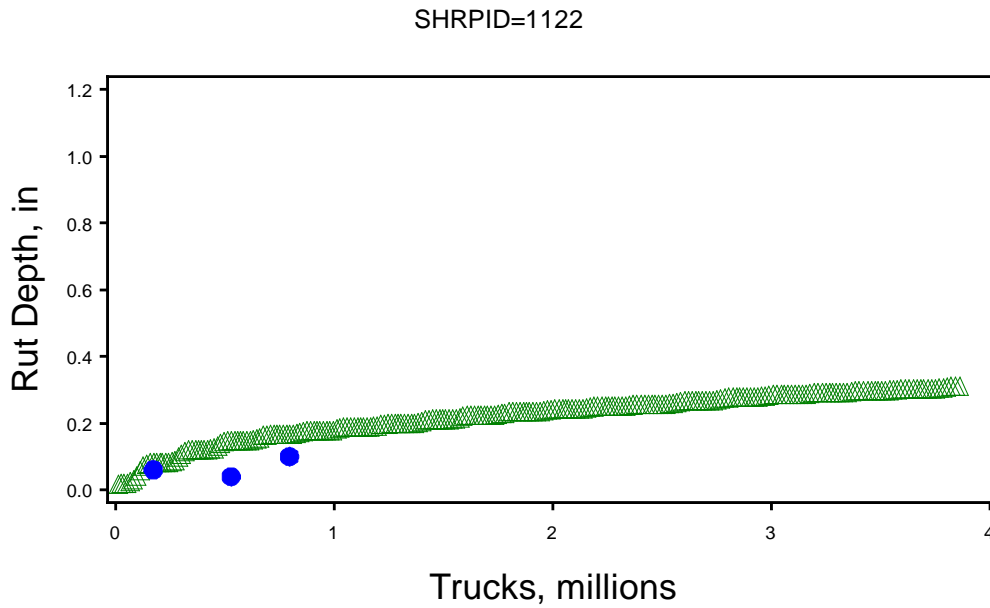


Figure 35. Plot showing predicted rutting versus truck traffic for MDOT pavement management system project 1122 (New HMA pavement).

SHRPID=28_0959_2

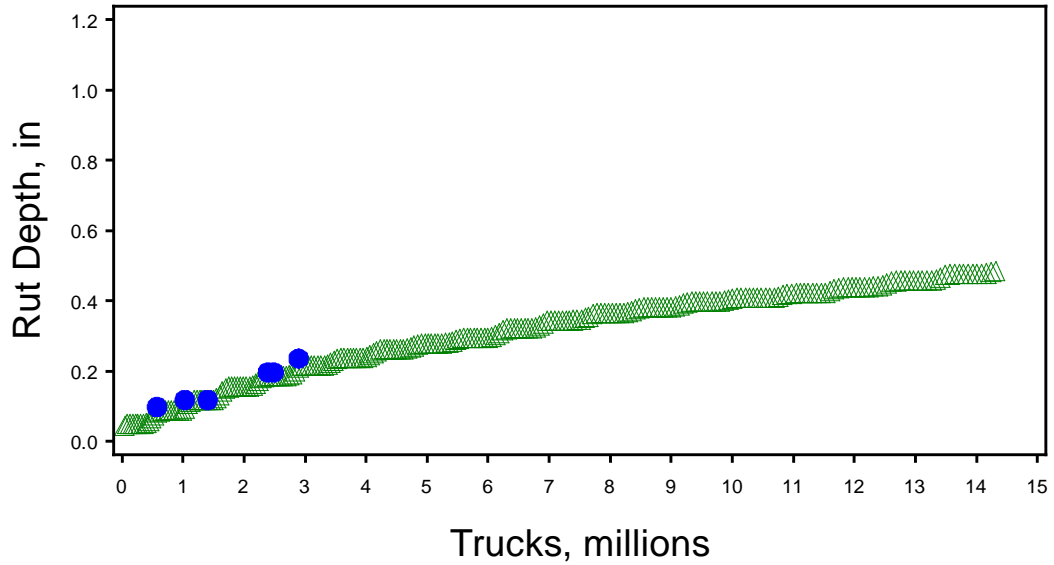


Figure 36. Plot showing predicted rutting versus truck traffic for LTPP project 0959 (HMA overlaid HMA pavement).

SHRPID=28_0806_1

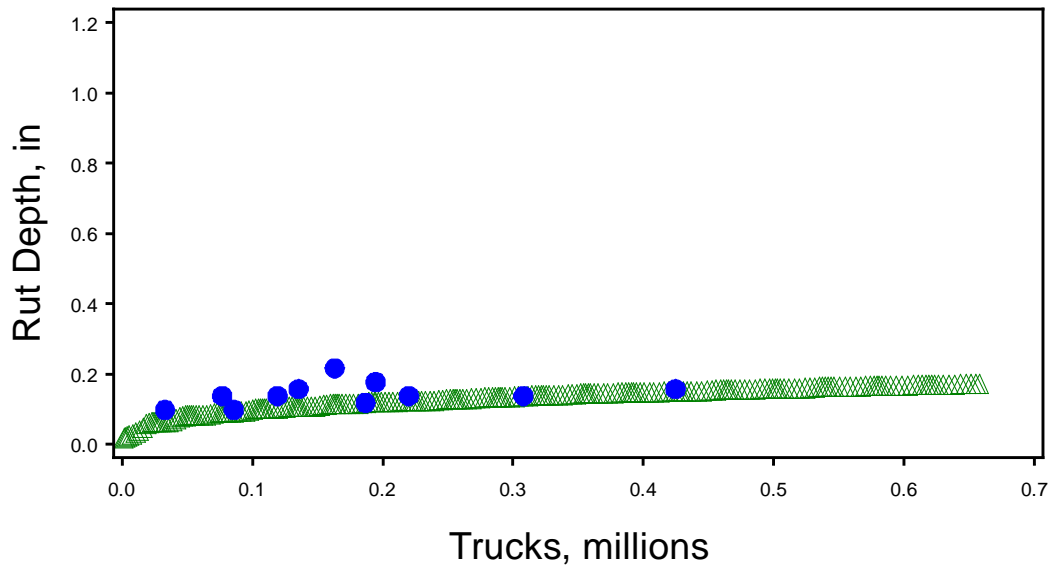


Figure 37. Plot showing predicted rutting versus truck traffic for LTPP project 0806 (New HMA pavement).

SHRPID=28_1802_1

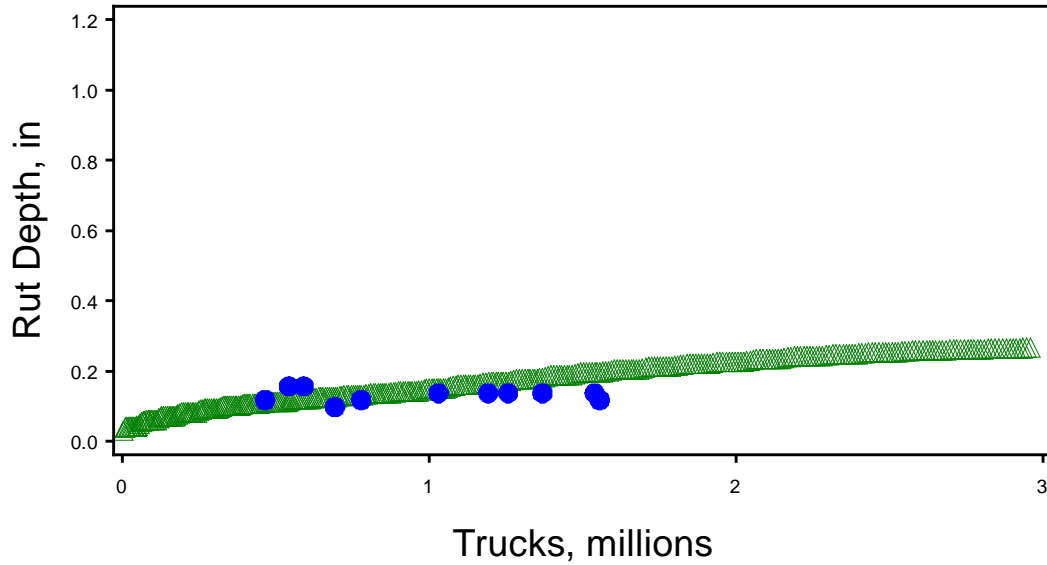


Figure 38. Plot showing predicted rutting versus truck traffic for LTPP project 1802 (New HMA pavement).

SHRPID=5500

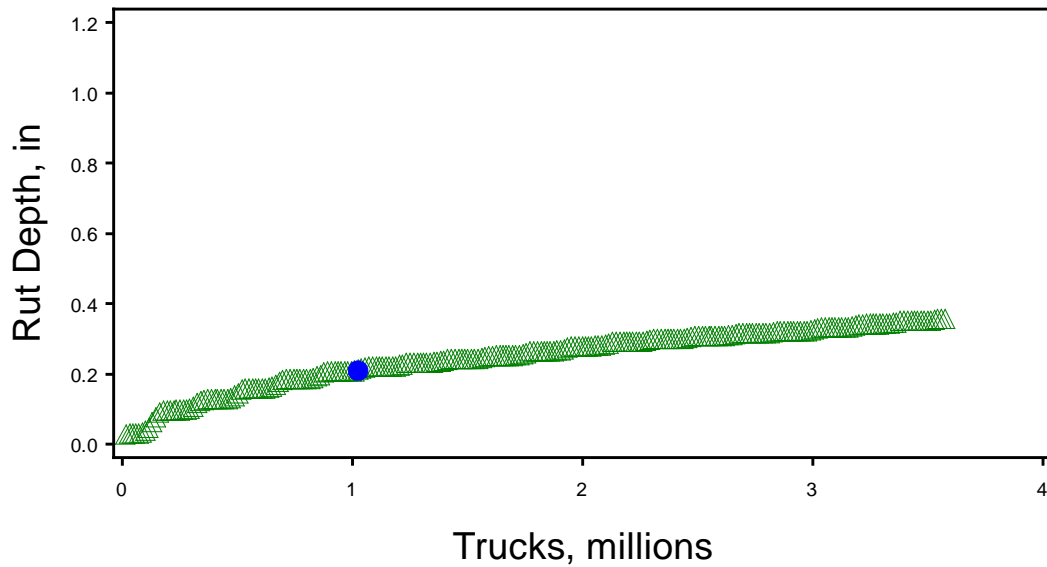


Figure 39. Plot showing predicted rutting versus truck traffic for MDOT pavement management system project 1122 (New HMA pavement).

8.3 TRANSVERSE THERMAL CRACKING

8.3.1 Verification of the Global Calibration Coefficients

The HMA pavement transverse cracking model and transfer function in the MEPDG are based on low temperature contraction of asphalt binders that lead to tensile stresses and the formation of transverse cracks. The MEPDG HMA transverse cracking transfer function was included in Chapter 2 (see equation 20).

Mississippi is not subjected to the low temperature events that result in low temperature cracking. Transverse cracking, however, was exhibited on many LTPP and non-LTPP new flexible pavement sections. As an example, the roadway segments located in Yazoo and Covington Counties had transverse cracks spaced at approximately 50 to 200-ft intervals. Figure 40 shows two LTPP examples with one in the non-freeze Yazoo area and the other in the non-freeze Covington area that have developed extensive transverse cracking over 15 to 25 years. These sections exhibit a total of about 3,500 ft./mi. which corresponds to a crack spacing of about 20 ft. This is a lot of transverse cracks which causes roughness or an increase in IRI as the transverse cracks deteriorate over time.

Sections in colder areas of the state also exhibited transverse cracks with a similar spacing. Thus, the transverse cracking in Mississippi is caused by more than low temperature events for the traditional low temperature transverse cracking mechanism. This observation or finding has also been made as part of Arizona's and Georgia's local calibration studies (*Darter, et al, 2014; Von Quintus, et al, 2014*). These transverse cracks exhibited along new flexible pavement test sections in warm areas caused speculation that significant shrinkage of the HMA mixture, possibly from binder absorbing into the aggregate, is another mechanism. The MEPDG does not consider this type of mechanism, so it under predicts transverse cracking in non-freeze areas in Mississippi.

8.3.2 Local Calibration Coefficient

The MEPDG software will not predict any transverse cracks in Mississippi using the default mixture properties. So the debate is whether to include or ignore transverse cracking in the analysis. In the interim, it was decided to include transverse cracks in the analysis which is consistent with how other agencies approached this issue. Thus, the transverse cracking transfer function was calibrated under this study, but the calibration process was restricted to just eliminating the bias.

The thermal cracking local calibration coefficient for input level 3 (see equation 22 in Chapter 2) of 25 was derived from the roadway segments to eliminate the bias of the transfer function. The standard error of the estimate is large because it is hypothesized that a different mechanism is the cause for these transverse cracks. As a result, a reliability level of 50 percent should be used in evaluating the design strategy. Transverse cracking should be observed and perhaps the PG grade of the binder and other HMA mix properties modified to minimize the potential development of transverse cracking. More importantly, additional research is needed to provide much stronger verification of the HMA transverse cracking model in Mississippi.

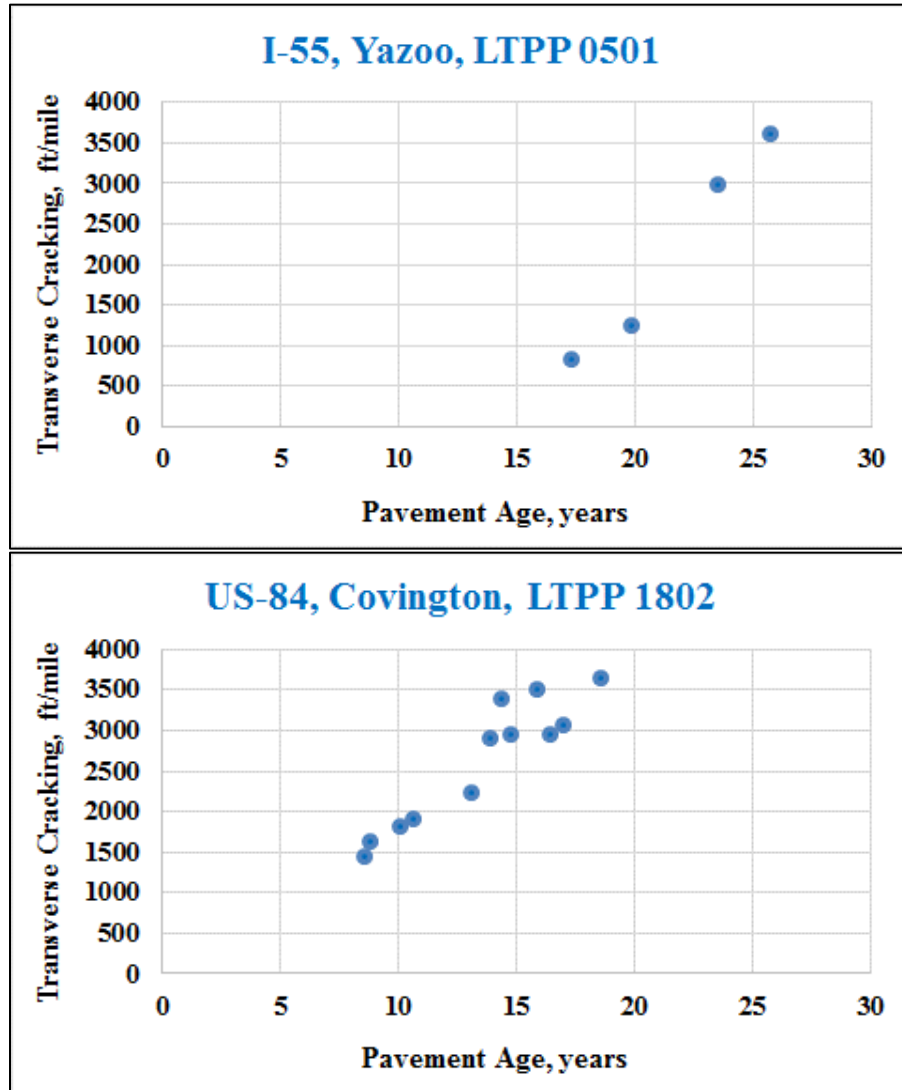


Figure 40. Plots of Transverse Cracking versus Age in Non-Freeze Areas of Yazoo and Covington, MS

8.4 SMOOTHNESS

8.4.1 Global MEPDG HMA Smoothness Model Verification

Verification of the IRI regression equation for Mississippi site features and conditions consisted of running the MEPDG with the global coefficients for all projects and evaluating goodness of fit and bias. Figure 41 shows a plot of predicted versus measured IRI for all relevant pavement projects. Goodness of fit statistics and bias statistics are shown in Table 34.

The goodness of fit statistics are poor, and the hypothesis test results indicate the global regression equation predictions are biased (the model under predicts IRI for rougher pavements or higher IRI values). Thus, local calibration of the regression equation was required.

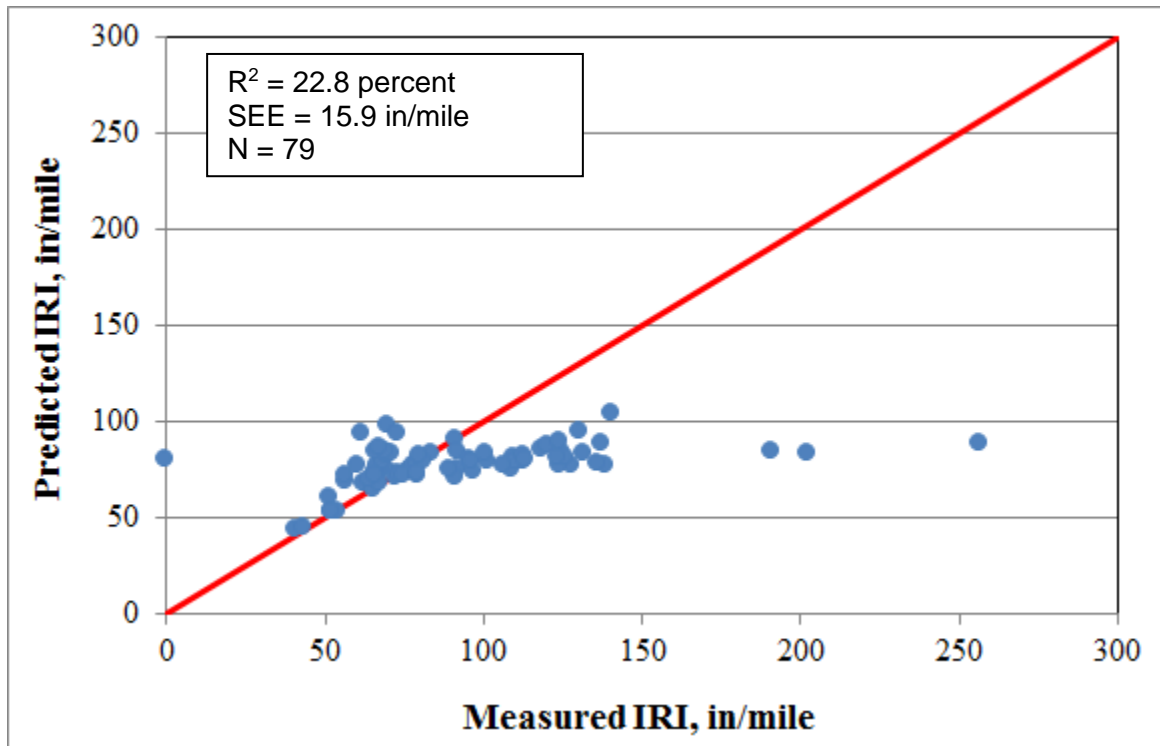


Figure 41. Predicted versus Measured IRI using Global MEPDG HMA IRI Regression Equation Coefficients

Table 34. Results of Statistical Evaluation of MEPDG HMA IRI Global Regression Equation for Mississippi Conditions

Statistical Analysis Type					
Goodness of Fit			Bias		
R ² , %	SEE, in/mi	N	p-value (paired t-test)	p-value (Slope)	N
22.8	15.9 in/mi	79	0.0013	< 0.0001	79

8.4.2 Local Calibration of the MEPDG HMA Smoothness Model for Mississippi

8.4.2.1 Description of Local Calibration Procedure

Local calibration of the MEPDG HMA IRI model for Mississippi consisted of the following steps:

1. Determine the cause of poor to fair goodness of fit and bias produced by the global models.
2. Adjust the global model calibration coefficients as needed based on information derived from step 1 to improve goodness of fit and reduce or eliminate bias. This involved adjusting the MEPDG HMA IRI model global calibration coefficients (C1 through C4 in equations 28 and 30) using nonlinear optimization algorithms in SAS to produce a new set of local calibration coefficients that maximizes goodness of fit and significantly reduces or eliminates bias.
3. Perform statistical analysis (using SAS) to characterize goodness of fit and bias for the new local coefficients.
4. Evaluate goodness of fit and bias and summarize outcome.
5. Repeat steps 2 to 4 as needed until goodness of fit and bias are acceptable.

8.4.2.2 Summary of HMA Smoothness Model Local Calibration Results

The local calibration coefficients for the HMA smoothness regression equation for Mississippi are presented in Table 35. Goodness of fit and bias statistics for the locally calibrated HMA smoothness model are presented in Table 36. A plot of measured and predicted IRI for new HMA pavements and HMA-overlaid existing HMA pavements is presented in Figure 42.

The information presented in Table 36 indicates a large improvement in the goodness of fit between the global HMA smoothness model and the Mississippi locally calibrated HMA smoothness model (i.e., R^2 after calibration was 60.5 percent, compared to a pre-calibration value of 22.8 percent). SEE marginally decreased from 15.9 to 15.5 in/mile, which was considered fair. Hypothesis testing to determine the presence or absence of significant bias indicated that the locally calibrated model predictions were unbiased at a 5 percent significance level. Thus, the significant bias present in the global model IRI predictions for Mississippi was eliminated.

Table 35. Local Calibration Coefficients for HMA Smoothness (IRI) Regression Equation

Model Coefficients	Global Model Values	MDOT Local Model Values
C1 (for rutting)	40	15
C2 (for alligator cracking)	0.4	0.1
C3 (for transverse cracking)	0.008	0.001
C4 (for site factor)	0.015	0.062

Table 36. Results of Statistical Evaluation of MEPDG HMA IRI Local Regression Equation Coefficients for Mississippi Conditions

Statistical Analysis Type					
Goodness of Fit			Bias		
R ² , %	SEE, in/mi	N	p-value (paired t-test)	p-value (Slope)	N
60.6	15.5	79	0.2593	0.1159	79

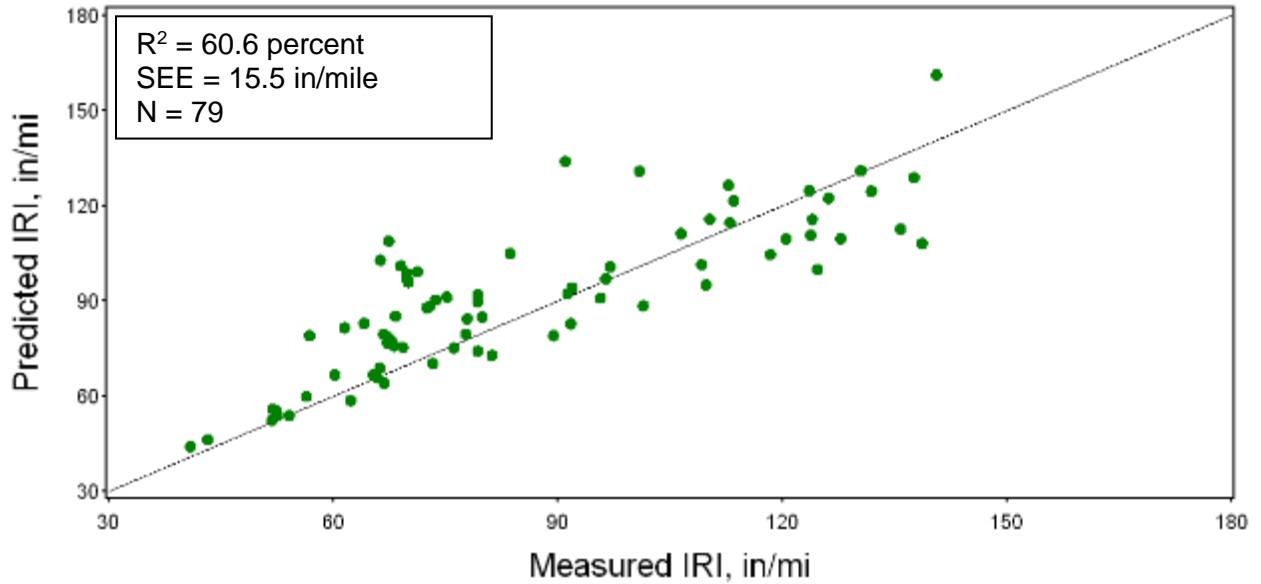


Figure 42. Plot of Measured and Predicted IRI for New HMA and HMA-Overlaid HMA Pavements Developed using the Locally Calibrated MDOT HMA IRI Regression Equation

Figures 43 through 45 illustrate the model IRI prediction for typical HMA pavements. The impact of local calibration is most significant in removing the large under-prediction bias shown in Figure 41. HMA pavement designs based in part on HMA pavement IRI in Mississippi will be more accurate at the selected level of design reliability.

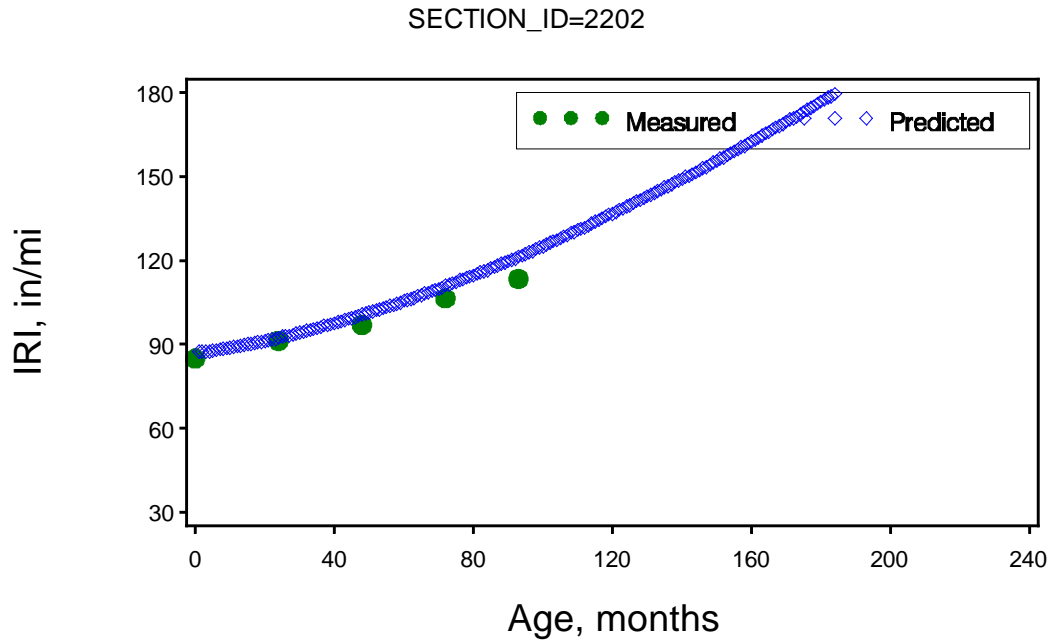


Figure 43. Plot Showing Measured and Predicted IRI versus Time for MDOT Section 28-2202

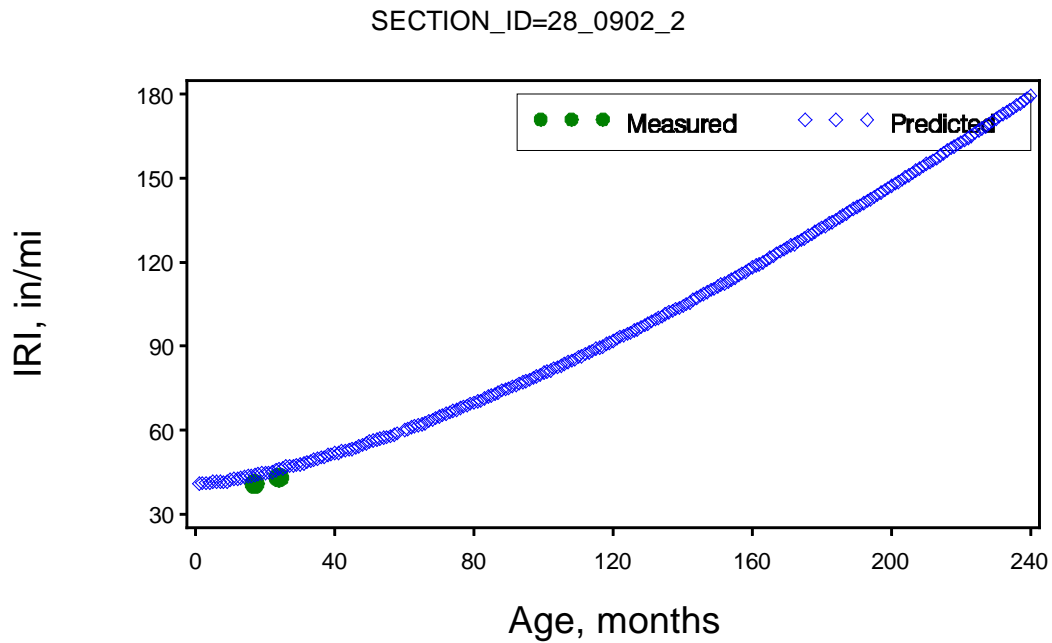


Figure 44. Plot Showing Measured and Predicted IRI versus Time for MDOT LTPP Test Section 28-0902

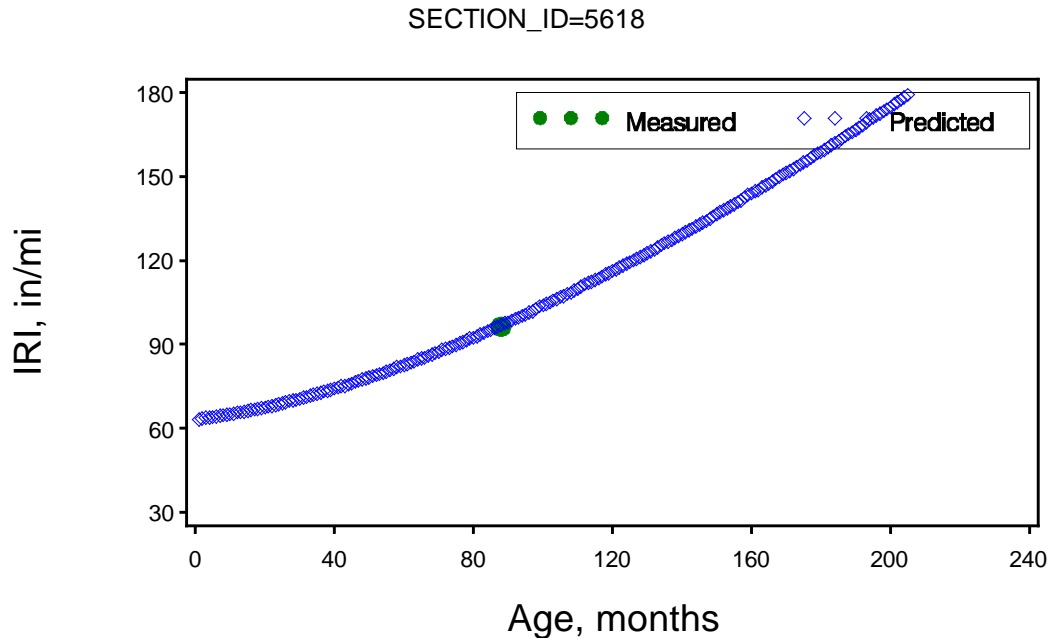


Figure 45. Plot Showing Measured and Predicted IRI versus Time for MDOT LTPP Section 28-5618

8.5 ESTIMATING DESIGN RELIABILITY FOR NEW HMA AND HMA OVERLAY PAVEMENT DISTRESS MODELS

The MEPDG estimates pavement design reliability using estimates of distress and IRI standard deviation for any given level of predicted distress or IRI. Thus, for each HMA pavement distress model, there was a need to develop a relationship between the predicted distress and standard error. Predicted distress standard error equations were developed as follows:

1. Divided predicted distress into 3 or more intervals.
2. For each interval, determine mean predicted distress and standard error (i.e., standard variation of predicted – measured distress for all the predicted distress that falls within the given interval).
3. Develop a nonlinear model to fit mean predicted distress and standard error for each interval.

The resulting standard error of the estimated distress models developed using the local model coefficients calibrated to MDOT conditions for the HMA distress models are presented below:

$$SEE(GATOR) = 1.13 + \frac{13}{1 + e^{(1.4893 - 0.4958 * \log_{10}(DAM + 0.0001))}} \quad (48)$$

$$SEE(ACRUT) = 0.4139 * ACRUT^{0.8} + 0.001 \quad (49)$$

$$SEE(BASERUT) = 0.1309 * BASERUT^{0.5711} + 0.001 \quad (50)$$

$$SEE(SUBRUT) = 0.01 * SUBRUT^{0.4012} + 0.001 \quad (51)$$

Where:

SEE(GATOR)	=	alligator cracking standard deviation, percent lane area
SEE(ACRUT)	=	HMA layer rutting standard deviation, in
SEE(BASERUT)	=	base layer rutting standard deviation, in
SEE(SUBRUT)	=	subgrade layer rutting standard deviation, in
DAM	=	alligator cracking fatigue “bottom-up” damage
ACRUT	=	predicted HMA layer rutting, in
BASERUT	=	predicted base layer rutting, in
SUBRUT	=	predicted subgrade layer rutting, in

The smoothness (IRI) standard error is estimated internally by the MEPDG.

CHAPTER 9—VERIFICATION AND CALIBRATION OF RIGID PAVEMENT TRANSFER FUNCTIONS

This chapter describes work done to verify and calibrate, if needed, the MEPDG global rigid pavement distress and smoothness models for Mississippi. As noted in Chapter 2, some new LTPP JPCP projects from adjacent states were included in the MDOT calibration study to increase the number of sites used in the calibration process. These LTPP sites were selected based on similar design features used and site conditions found in Mississippi.

The criteria for performing local calibration were based on whether the given global model exhibited a reasonable goodness of fit (between measured and predicted outputs) and whether distresses/IRI were predicted without significant bias. Reasonable goodness of fit was determined using R^2 and SEE, while the presence or absence of bias was determined based on the hypothesis test described in Chapter 3. The general criteria used to determine global model adequacy for Mississippi conditions were provided in Tables 5 and 6.

Three rigid pavement models were evaluated as part of the MEPDG implementation in Mississippi and included: JPCP transverse cracking, JPCP transverse faulting, and new JPCP smoothness or IRI. Detailed descriptions of these models are presented in Chapter 2.

Verification of the MEPDG “global” calibration coefficients of the rigid pavement transfer functions for Mississippi conditions consisted of running the *M-E Pavement* for the LTPP test sections and evaluating goodness of fit and bias. The global model coefficients utilized were those developed under the recently completed NCHRP project 20-07 to reflect corrections made to the global concrete CTE values that were used in NCHRP project 1-37A (Sachs, 2014). The corrected CTE values used in the NCHRP project 20-07 were used in evaluating and judging the accuracy of the transfer functions for the Mississippi LTPP rigid test sections.

Table 10 in Chapter 3 grouped the LTPP and non-LTPP rigid pavement test sections by structural features. Most of the sites are JPCP but nine are CRCP. Different design criteria through the transfer functions are used to design JPCP and CRCP and must be considered as two separate groups in evaluating or judging the applicability of the global calibration coefficients to Mississippi conditions. Nine CRCP sections are too few to complete a local calibration of the global transfer functions.

Although IRI is the common design criteria between JPCP and CRCP, two different regression equations are used to predict IRI over time because of the different distresses. This chapter of the report compares the predicted distress and smoothness to the measured values for the JPCP sections for revising the global calibration coefficients, if needed.

9.1 JPCP TRANSVERSE, MID-SLAB CRACKING

9.1.1 Global MEPDG Transverse Cracking Model Verification

Verification of the MEPDG global JPCP transverse cracking model for Mississippi conditions began by running the MEPDG analysis for all JPCP projects. For this analysis, the NCHRP

Project 20-07/(288) JPCP MEPDG global model coefficients were applied, since these coefficients are compatible with MDOT and LTPP revised PCC CTE data used in transverse cracking predictions. Figure 46 shows a plot of cumulative fatigue damage versus transverse cracking for all MDOT JPCP sections. Measured and MEPDG-predicted transverse cracking data were evaluated to determine model goodness of fit and bias in predicted transverse cracking. The results are presented in Table 37 and show the following:

- Goodness of fit was very good, with an $R^2 > 90$ percent, which implies a strong relationship between the MEPDG global model transverse cracking predictions and field-measured/observed cracking.
- However, both the paired t-test and predicted versus measured cracking slope p-value indicated the presence of bias in predicted transverse cracking (p-value < 0.05).

It was concluded that the MEPDG global transverse cracking model did not adequately predict transverse cracking for Mississippi conditions. Local calibration of the MEPDG global transverse cracking model for Mississippi was completed.

9.1.2 Local Calibration of the MEPDG Transverse Cracking Model for Mississippi

9.1.2.1 Description of Local Calibration Procedure

The local calibration process involved two basic steps: (1) investigating the causes of poor goodness of fit and bias of the MEPDG globally calibrated models; and (2) modifying the local calibration coefficients of the transverse fatigue cracking models as needed based on information derived from step 1 to improve goodness of fit and reduce or eliminate bias. Two key models are involved with the calibration of transverse “slab” cracking. Equation 31 in Chapter 2 estimates the fatigue life (N) of PCC when subjected to repeated stress for a given flexural strength. Calibration factors $C1$ and $C2$ can be modified but since the calibration process is based on substantial field data these factors remained unchanged.

The coefficients of the S-shaped curve for the relationship between measured cracking and accumulated fatigue damage (DI_F) at top and bottom of the JPCP slabs were adjusted. Parameters $C4$ and $C5$ in equation 32 (see Chapter 2) were adjusted to remove bias and improve goodness of fit with field data.

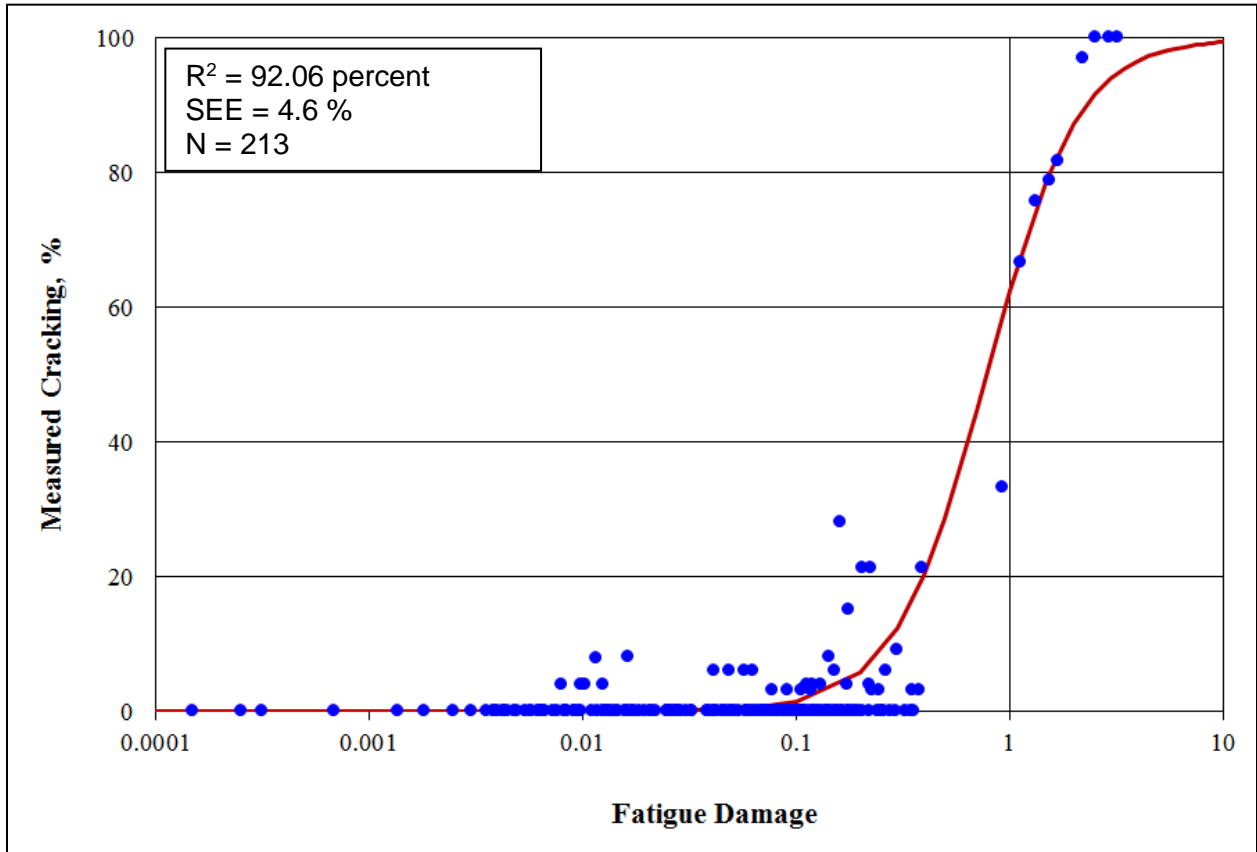


Figure 46. Verification of the JPCP transverse cracking and fatigue damage models with MEPDG global coefficients, using Mississippi JPCP projects.

Table 37. Results of statistical goodness of fit and bias evaluation of the MEPDG transverse cracking global model for Mississippi conditions.

Statistical Analysis Type			
Goodness of Fit		Bias	
R ² , %	SEE	p-value (paired t-test)	p-value (slope)
92.06	4.6%	0.0192	< 0.0001

9.1.2.2 Summary of Transverse Cracking Model Local Calibration Results

Possible causes of poor goodness of fit and bias were investigated, but no obvious explanations were found (such as erroneous inputs). Thus, local calibration proceeded as previously described. Calibration of the MEPDG global models using MDOT input data was done using nonlinear model optimization tools available in the SAS statistical software. JPCP fatigue damage and transverse cracking model coefficients are presented in Table 38. Two of the four global coefficients were adjusted to MDOT local conditions.

The goodness of fit and bias statistics presented in Table 39 show an adequate goodness of fit for the JPCP transverse cracking model with no significant bias. Figure 47 presents a plot of JPCP fatigue damage versus field-measured and MDOT local transverse cracking model predicted cracking. Local calibration of the JPCP transverse cracking model produced

MDOT-specific model that predict transverse cracking distress with adequate accuracy and minimal bias. Goodness of fit characterized using R^2 slightly increased from 92.06 for the global models to 93.1 percent, while SEE slightly decreased from 4.6 to 4.51 percent.

The new model will increase the accuracy of transverse cracking predictions while minimizing bias and will produce for MDOT more accurate new JPCP designs at the desired design reliability. Figures 48 through 50 illustrate the transverse fatigue cracking model for selected projects.

Table 38. Summary of MEPDG global and MDOT local calibration coefficients for JPCP transverse cracking and JPCP fatigue damage models.

Model Type	Model Coefficients (See Equation 1 & 2)	Global Model Values	MDOT Local Model Values
JPCP fatigue damage	C1	2	2
	C2	1.22	1.22
JPCP transverse cracking	C4	0.6	0.5
	C5	-1.98	-2.35

Table 39. Results of statistical bias evaluation of MEPDG JPCP transverse cracking local model for Mississippi conditions.

Statistical Analysis Type					
Goodness of Fit			Bias		
R^2 , %	SEE	N	p-value (paired t-test)	p-value (Slope)	N
93.1	4.51%	213	0.1259	0.4445	213

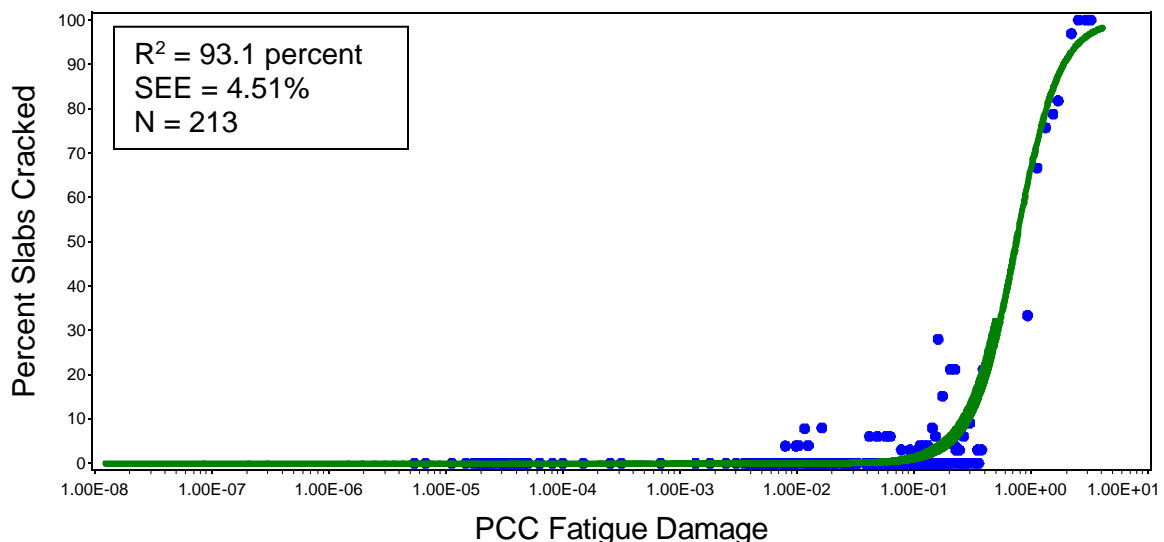


Figure 47. Plot showing predicted JPCP transverse cracking versus computed fatigue damage developed using MEPDG models with MDOT local coefficients.

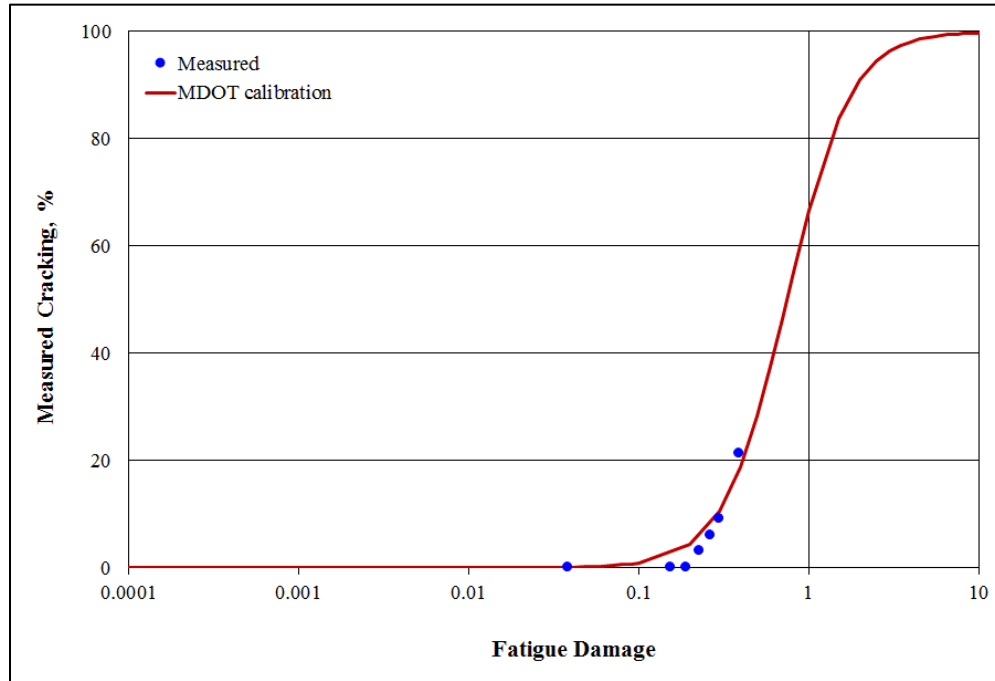


Figure 48. Plot of predicted and measured transverse cracking versus fatigue damage for LTPP 5_0213.

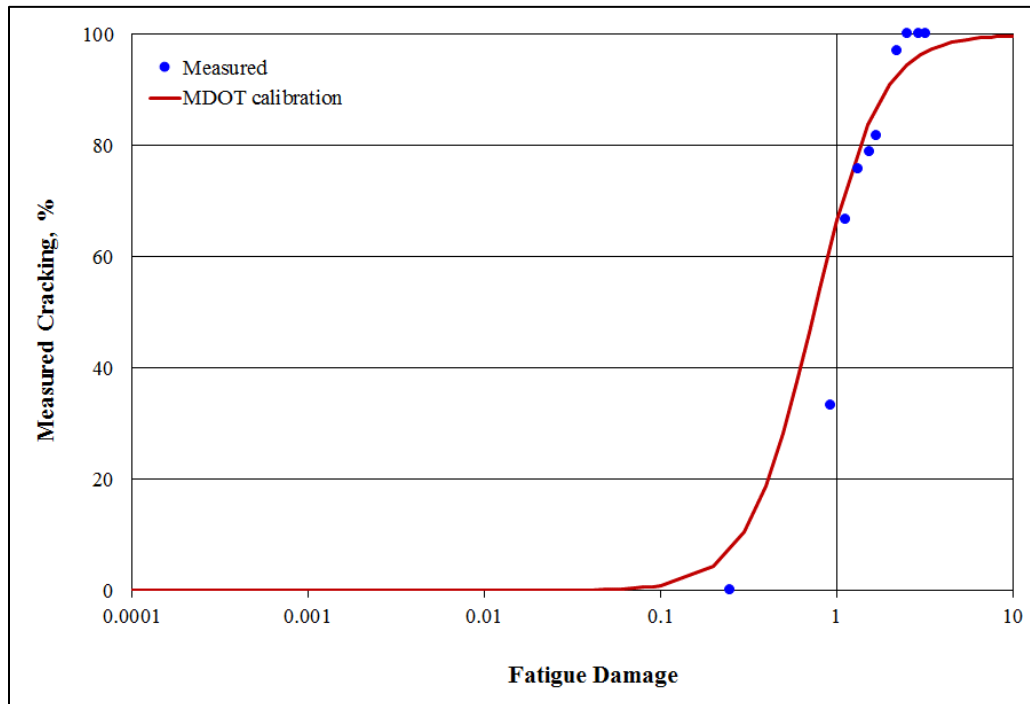


Figure 49. Plot of predicted and measured transverse cracking versus fatigue damage for LTPP 5_0217.

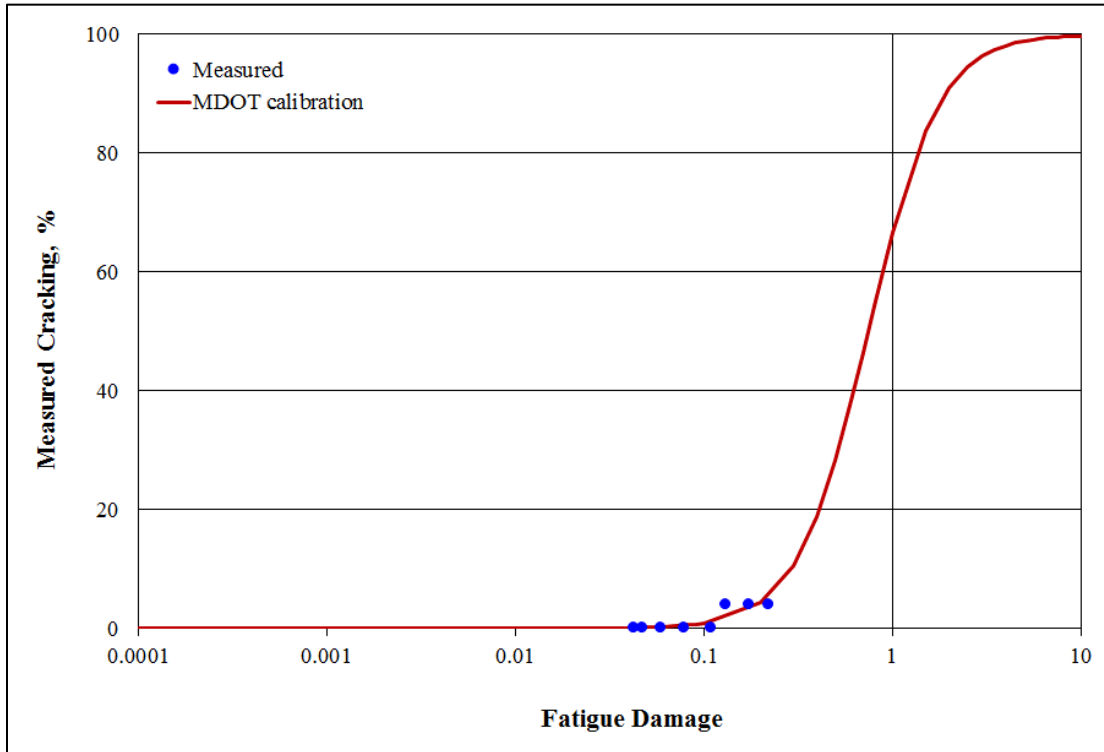


Figure 50. Plot of predicted and measured transverse cracking versus fatigue damage for LTPP 13_3020.

9.2 JPCP TRANSVERSE JOINT FAULTING

9.2.1 Global MEPDG JPCP Transverse Joint Faulting Model Verification

The JPCP faulting prediction models and coefficients were defined in Chapter 2 (see equations 33 through 36). The local calibration process for these prediction models involved the same process and steps previously discussed for transverse, mid-slab cracking.

Figure 51 presents a histogram of all measured (including time series) transverse joint faulting for the LTPP projects included in the analysis. The information provided in the figure shows a limited distribution of measured transverse joint faulting data, with most of the measured faulting being zero. Because the measured transverse joint faulting was mostly zero, commonly applied statistical procedures could not be used to evaluate goodness of fit and bias. Thus, non-statistical methods were applied to verify the suitability of the MEPDG global transverse joint faulting model for local Mississippi conditions.

Verification of the MEPDG global JPCP transverse joint faulting model for Mississippi conditions consisted of the running the MEPDG analysis with the global transverse joint faulting model for all selected projects. For this analysis, the NCHRP Project 20-07(288) JPCP MEPDG global model coefficients were applied. The outcome from these analyses is presented in the following sections.

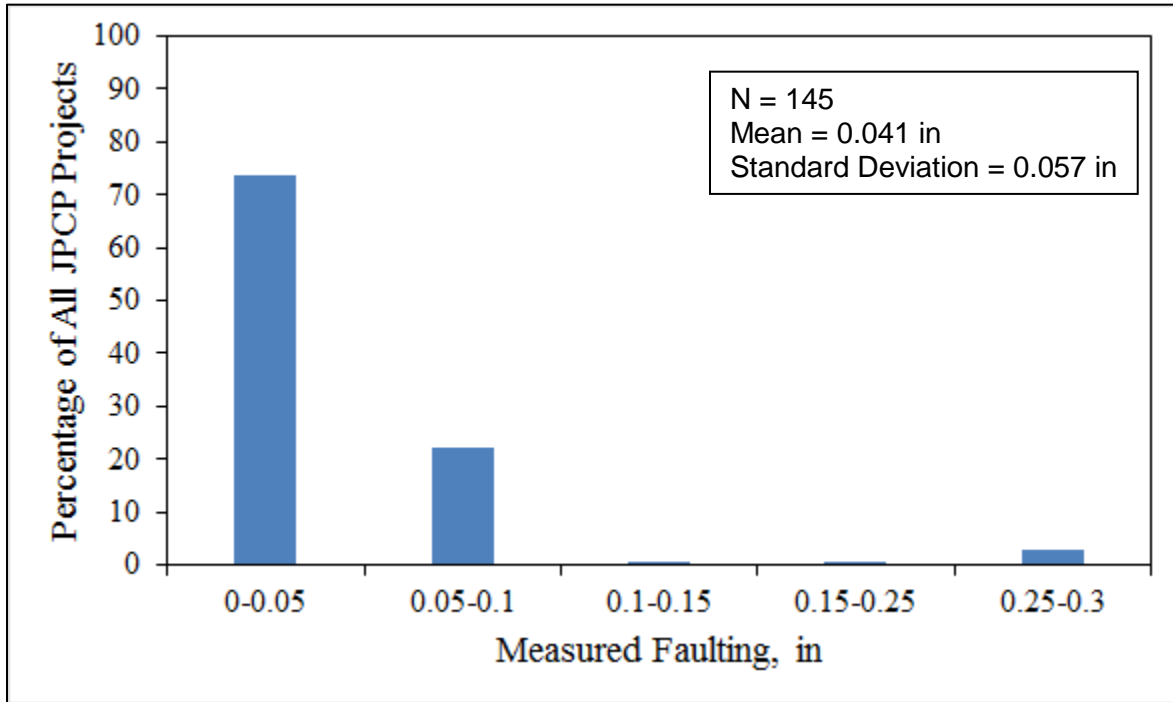


Figure 51. Histogram showing distribution of measured JPCP transverse joint faulting for LTPP projects included in the analysis.

9.2.2 Summary of JPCP Transverse Faulting Verification Results

9.2.2.1 Comparison of Measured and Predicted Transverse Faulting Groupings

For this comparison, transverse faulting was categorized into six groups, as shown in Table 40. The goal was to determine how often measured and predicted transverse faulting fell in the same grouping. The range of each group was determined based on the distribution of the data available and using engineering judgment.

Table 40. Comparison of measured and predicted transverse joint faulting (percentage of all measurements).

Measured Mean Joint Faulting, inch	MEPDG Predicted Mean Joint Faulting, inch				
	<0.05	0.05-0.1	0.1-0.15	0.15-0.25	>0.25
<0.05	93	13	1	0	0
0.05-0.1	24	5	3	0	0
0.1-0.15	0	0	1	0	0
0.15-0.25	0	0	1	0	0
>0.25	0	0	0	4	0

Total data points = 145

A review of the information presented in Table 40 showed the following:

- Approximately 64 percent of all data points (93 of 145) fell within the same measured and predicted transverse joint faulting grouping (< 0.05 in faulting).
- Approximately 17 percent of the data points (24 of 145) fell within an adjacent grouping (i.e., measured grouping 0.05 to 0.1 against predicted grouping <0.05).
- Nine percent of the data points (13 of 145) fell within an adjacent grouping (i.e., measured grouping < 0.05 against predicted grouping 0.05 to 0.1).
- Four percent of the data points (5 of 145) fell within the same measured and predicted transverse joint faulting grouping (0.05 to 0.1).
- Three percent of the data points (4 of 145) fell within an adjacent grouping (i.e., measured grouping >0.25 against predicted grouping 0.15 to 0.25).
- For the remaining three percent of the data points (3 of 145) fell within an adjacent grouping (i.e., measured grouping 0.05 to 0.1 against predicted grouping 0.1 to 0.15).

The results show that a significant majority of predicted transverse joint faulting fell within the same grouping (over 90 percent), indicating that the global model predicted transverse joint faulting accurately with little bias.

9.2.2.2 Local Calibration of Mississippi Transverse Joint Faulting Model

The non-statistical procedures applied to determine goodness of fit and bias indicated that the MEPDG global transverse joint faulting model predicted transverse joint faulting reasonably well, with no significant bias in Mississippi. Thus, there was no need for local calibration of the global transverse joint faulting model at this stage. JPCP transverse joint faulting global model coefficients are presented in Table 41.

The transfer function or model, however, should be re-evaluated in the future to determine how well it predicts significant levels of faulting (non-zero values). This can be done through continuous monitoring of the selected JPCP projects used in this analysis. Figure 52 presents a plot of JPCP transverse joint faulting versus field-measured joint faulting. Figures 53 through 56 illustrate the transverse joint faulting predictions using the global MEPDG model for selected projects.

Table 41. Summary of MEPDG global coefficients for JPCP transverse joint faulting model.

Model Type	Model Coefficients	MDOT Local Calibration
JPCP transverse joint faulting	C1	0.5104
	C2	0.00838
	C3	0.00147
	C4	0.008345
	C5	5999
	C6	0.8404
	C7	5.9293
	C8	400

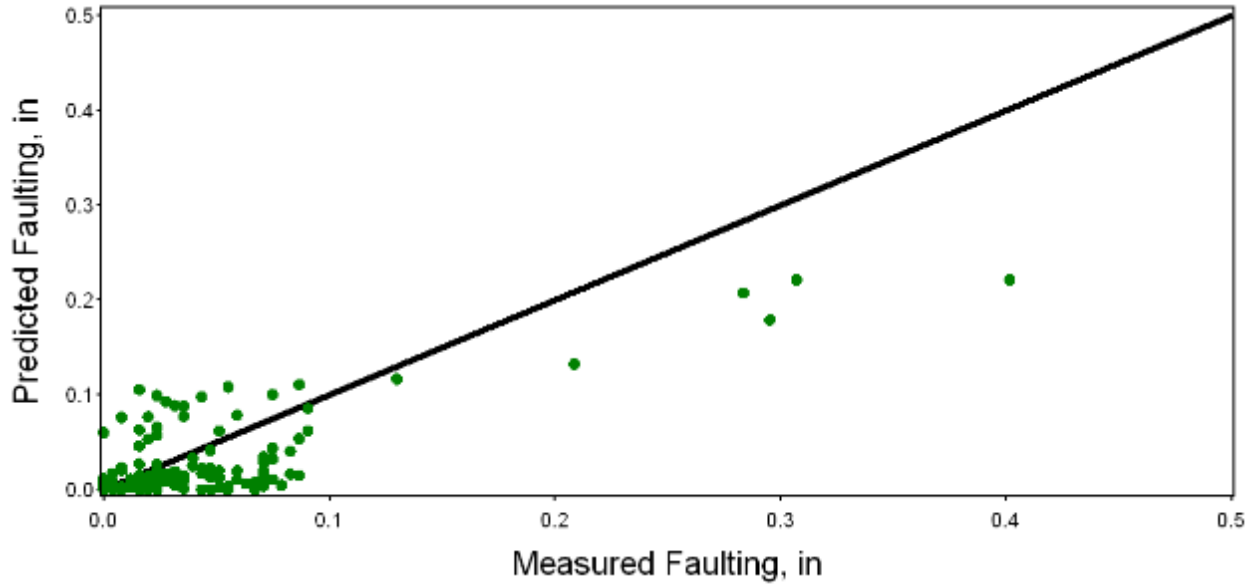


Figure 52. Plot showing predicted JPCP transverse joint faulting using MEPDG models with global coefficients versus measured joint faulting.

SHRPID=13_3016_1

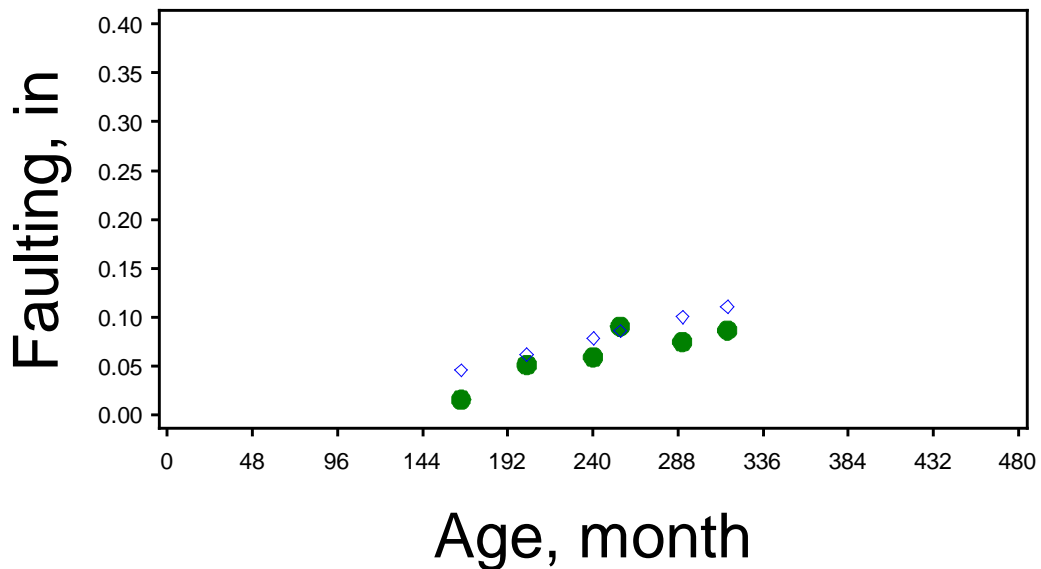


Figure 53. Predicted (using global calibration factors) and measured transverse joint faulting for LTPP 13_3016.

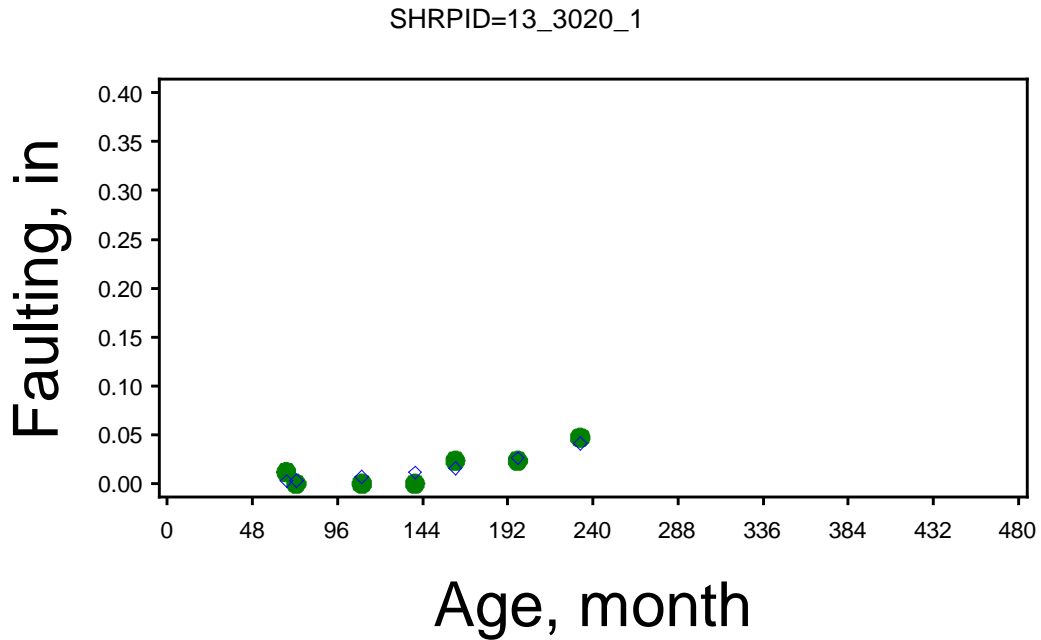


Figure 54. Predicted (using global calibration factors) and measured transverse joint faulting for LTPP 13_3020.

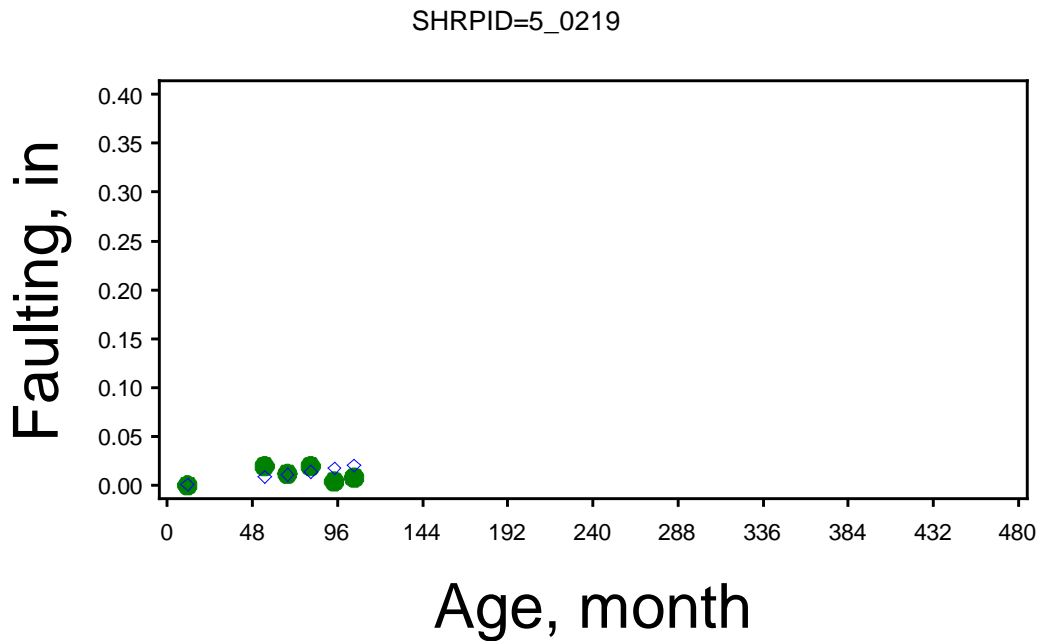


Figure 55. Predicted (using global calibration factors) and measured transverse joint faulting for LTPP 5_0219.

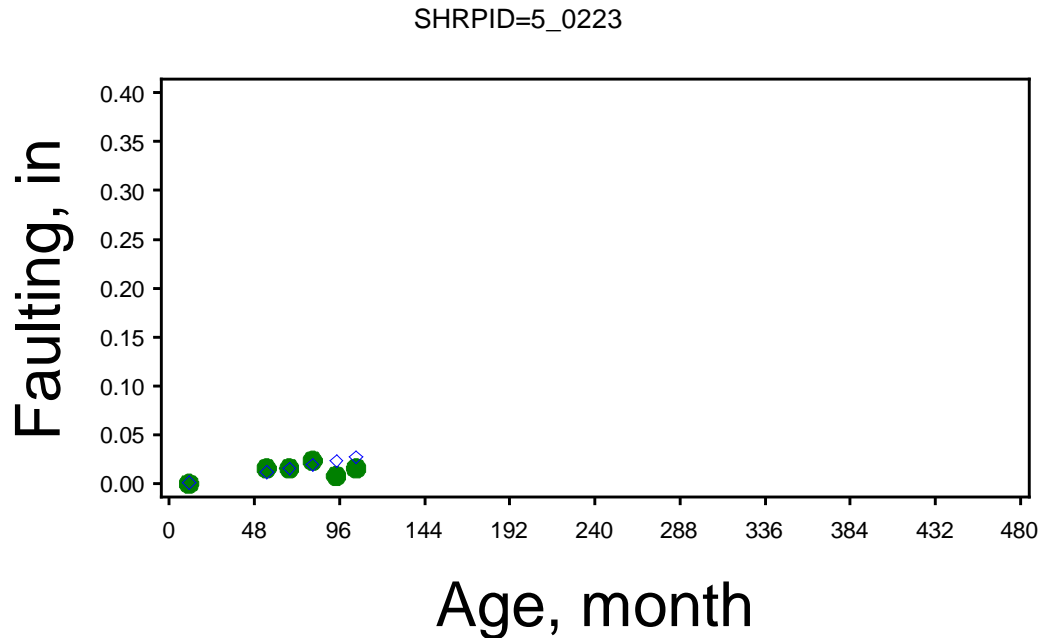


Figure 56. Predicted (using global calibration factors) and measured transverse joint faulting for LTPP 5_0223.

9.3 JPCP SMOOTHNESS

9.3.1 Global MEPDG JPCP Smoothness Model Verification

Verification of the MEPDG global JPCP IRI model for Mississippi conditions consisted of running the MEPDG analysis for all selected projects and evaluating goodness of fit and bias. A plot of predicted versus measured IRI using the selected Mississippi projects is shown in Figure 57, and full details of the outcome of statistical analysis for the goodness of fit and bias are presented in Table 42. These results indicate that goodness of fit was good but the model predictions were biased and thus local calibration with MDOT data is required.

9.3.2 Local Calibration of Mississippi JPCP IRI Model

Local calibration included two steps: (1) investigating the causes of poor goodness of fit and bias of the MEPDG nationally calibrated models and (2) modifying the local calibration coefficients of the JPCP IRI sub models as needed based on information derived from (1) to improve goodness of fit and reduce or eliminate bias. Specifically, the coefficients of the distress inputs and site factor (SF) were modified as needed to improve the predicted JPCP IRI.

There were no obvious causes for poor goodness of fit and bias in the global model. MDOT specific model coefficients were determined through optimization using SAS statistical software for the JPCP IRI model (the inputs and coefficients were defined in Chapter 2).

These results indicate that goodness of fit was very good, and predicted IRI exhibited no significant bias. Model coefficients and the statistics resulting from the local calibration process are presented in Table 43 and 44, respectively.

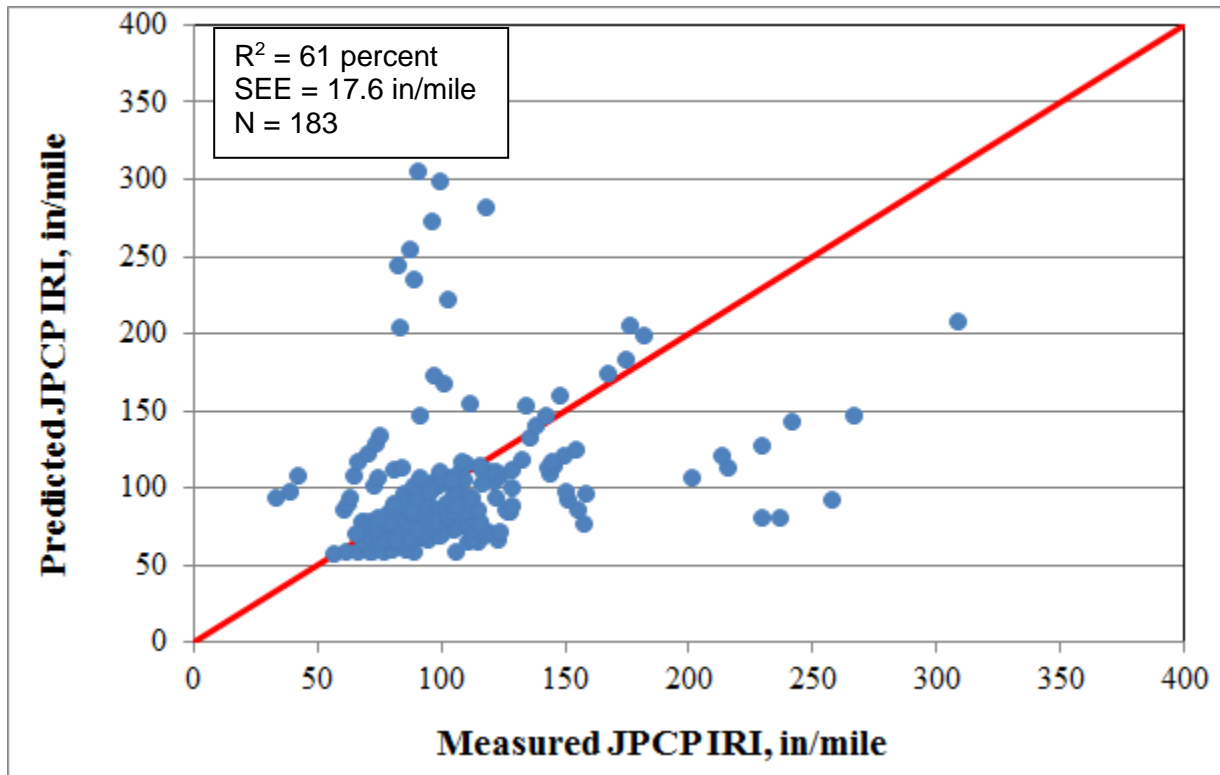


Figure 57. Predicted JPCP IRI versus measured Mississippi JPCP with global calibration coefficients.

Table 42. Goodness of fit and bias test statistics for JPCP IRI global model.

Analysis Type	Diagnostic Statistics	Results
Goodness of Fit	R^2	61 percent
	SEE	17.6 in/mi
	N	183
Bias	H_0 : Slope = 1.0	p-value < 0.0001
	H_0 : Predicted - measured IRI = 0 (paired t-test)	p-value = 0.0115

Table 43. Summary of MEPDG global and Mississippi local calibration coefficients for JPCP IRI model.

Model Type	Model Coefficients (See Equation 7)	Global Model Values	MDOT Local Model Values
JPCP IRI	J1 (CRK)	0.8203	0.8200
	J2 (SPALL)	0.4417	0.4420
	J3 (FLT)	1.4929	1.6500
	J4 (SF)	25.24	25.20

Table 44. Results of statistical bias evaluation of MEPDG JPCP IRI local model for Mississippi conditions.

Statistical Analysis Type					
Goodness of Fit			Bias		
R ² , %	SEE	N	p-value (paired t-test)	p-value (Slope)	N
82.9	15.6 in/mile	183	0.2901	0.1261	183

Figure 58 presents a plot of JPCP IRI using MDOT local calibration coefficients versus field-measured IRI. Figures 59 through 61 illustrate the global JPCP IRI model prediction for various Mississippi JPCP projects over time. The predictions show a good fit of predicted and measured IRI. JPCP designs based in part on IRI in Mississippi using the MDOT model coefficients will be more accurate and less costly at the selected level of design reliability because of the lower SEE.

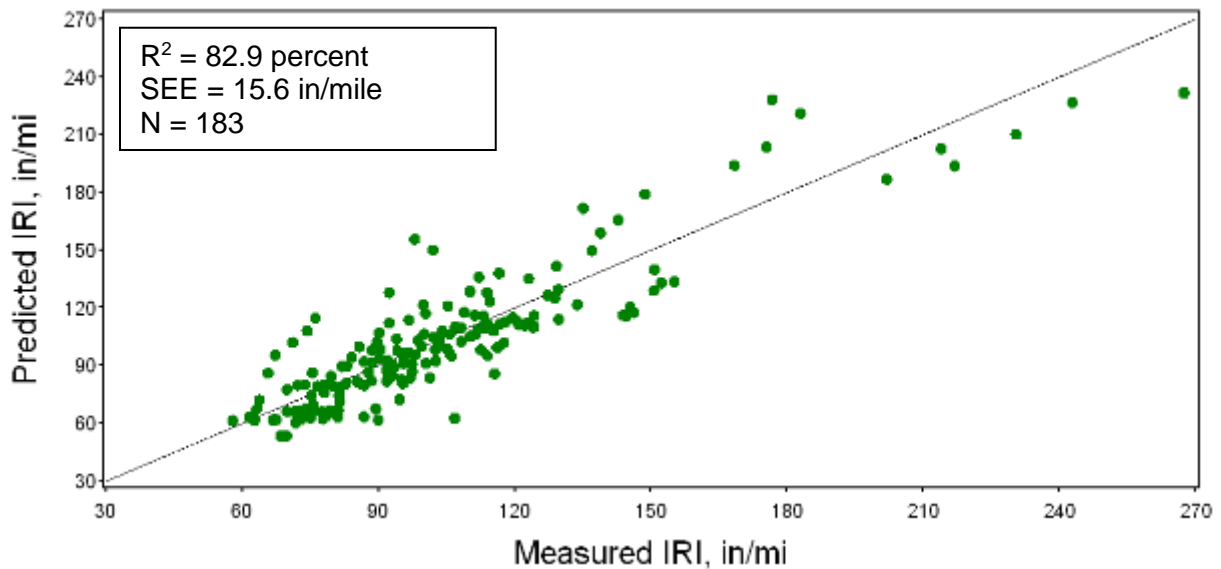


Figure 58. Plot showing predicted JPCP IRI using MEPDG models with MDOT local coefficients versus measured IRI.

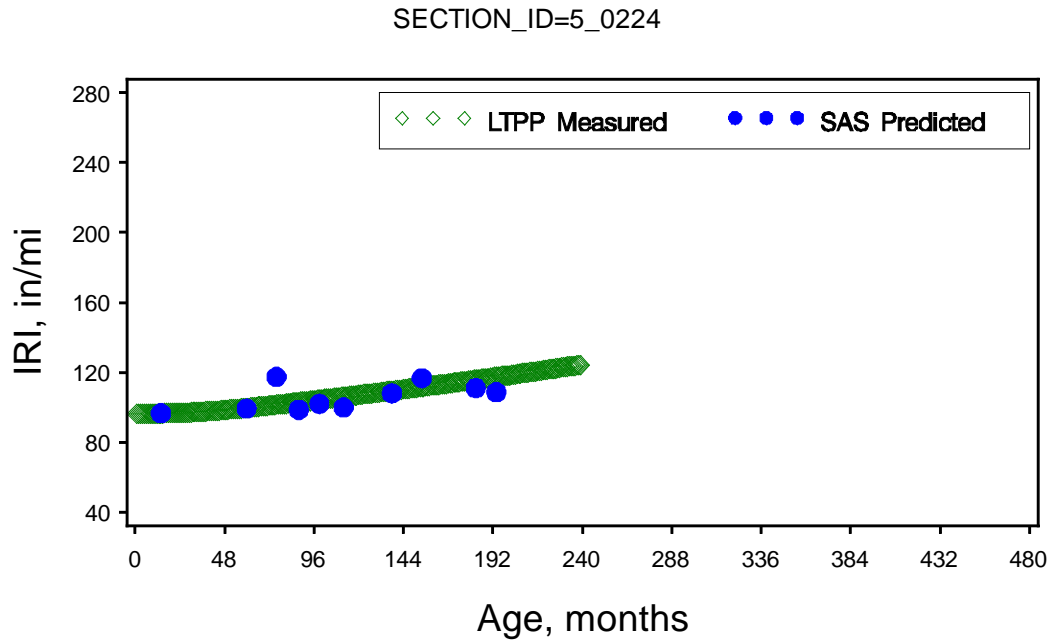


Figure 59. Predicted and measured JPCP IRI for Mississippi LTPP section 5_0224 over time.

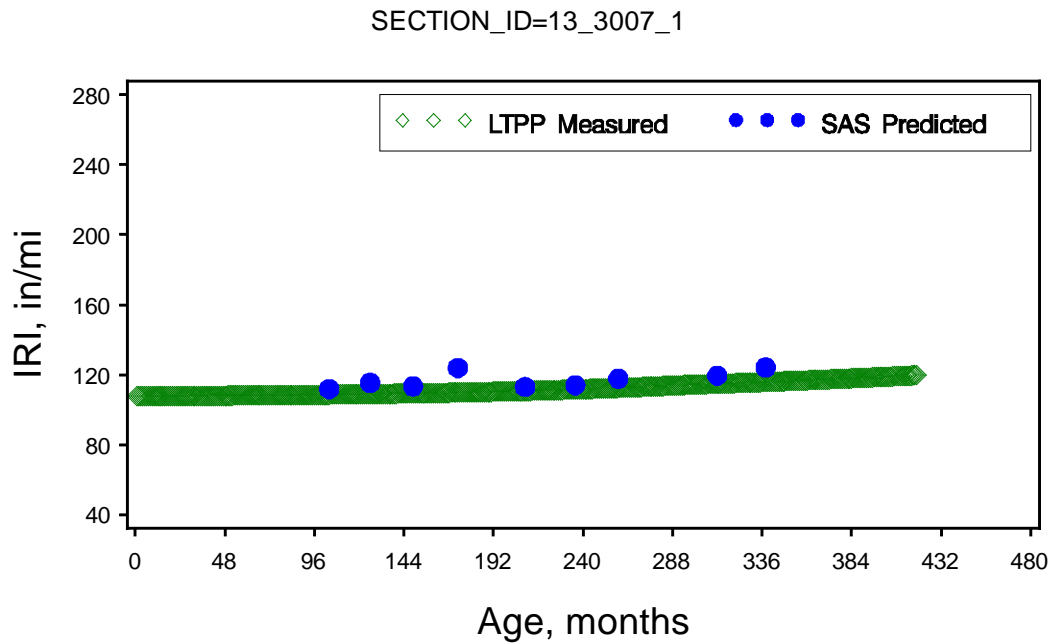


Figure 60. Predicted and measured JPCP IRI for Mississippi LTPP section 13_3007 over time.

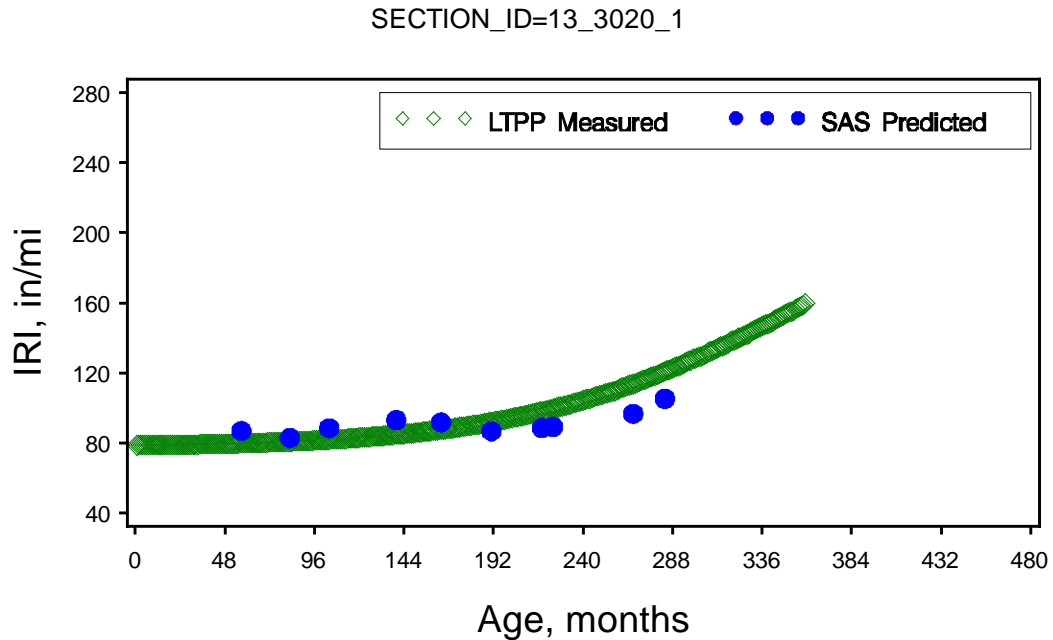


Figure 61. Predicted and measured JPCP IRI for Mississippi LTPP section 13_3020 over time.

9.4 ESTIMATING DESIGN RELIABILITY FOR NEW JPCP DISTRESS MODELS

The MEPDG estimates pavement design reliability using estimates of distress and IRI standard deviation for any given level of predicted distress or IRI. Thus, for each JPCP distress model or transfer function, there was a need to develop a relationship between predicted distress and the predictions standard error. Predicted distress standard error prediction equations were developed as follows:

1. Divided predicted distress into 3 or more intervals.
2. For each interval, determine mean predicted distress and standard error (i.e., standard variation of predicted – measured distress for all the predicted distress that fall within the given interval).
3. Develop a nonlinear model to fit mean predicted distress and standard error for each interval.

The resulting standard error of the estimated distress models developed using the locally calibrated MDOT JPCP distress models are presented below:

$$\text{Stdev}(\text{CRK}) = 0.5 + (34.5861 * \text{PCRK})^{0.2985} \quad (52)$$

$$\text{Stdev}(\text{FLT}) = 0.0831 * (\text{PFLT})^{0.3426} + 0.00521 \quad (53)$$

Where:

Stdev(CRK)	=	transverse fatigue crack standard deviation, percent slabs
PCRK	=	predicted transverse fatigue cracking, percent slabs
Stdev(FLT)	=	faulting standard deviation, in
PFLT	=	predicted joint faulting

Smoothness IRI standard error is estimated internally by the MEPDG. It is important to note that the JPCP standard error of the faulting model was adopted from NCHRP 20-07(288).

CHAPTER 10—SUMMARY AND RECOMMENDATIONS

Chapter 10 summarizes the conclusions and recommendations from the preliminary local calibration process. Both LTPP and non-LTPP test sections were used to estimate the precision and bias of the MEPDG flexible and rigid pavement transfer functions for predicting the performance indicators (distress and roughness) of MDOT's pavements. The resulting calibration coefficients of the distress prediction models, or transfer functions, listed in Chapters 8 and 9 can be used to optimize new pavement and rehabilitation design strategies, and used in forecasting of maintenance, repair, rehabilitation, and reconstruction costs.

It is important to understand, however, that the local calibration coefficients of the transfer functions and smoothness regression equations documented in Chapters 8 and 9 are considered preliminary at this point in time in MDOT's MEPDG implementation process for various reasons. Thus, some important recommendations are noted below prior to summarizing the findings and recommendations from this preliminary local calibration effort.

1. The Phase 3 field investigation of MDOT's phased implementation process should be executed to expand the performance data set for local calibration, and provide more data to supplement the MDOT materials library that has already been established.
2. MDOT is strongly encouraged to re-visit and re-evaluate the local calibration coefficients of the transfer functions and models for all pavement types after the field investigation planned for Phase 3 has been completed.
3. It is also highly recommended that MDOT continue to monitor the calibration sections and establish new ones as new design features, strategies, and materials are adopted for use by MDOT. MDOT should realize local calibration is not a one-time effort. The local calibration coefficients should be periodically verified and confirmed as more data becomes available and the calibration sites are expanded.
4. MDOT is also encouraged to host periodic training courses or workshops on the use of the MEPDG, especially as newer versions of the software are released by AASHTO.

10.1 FINDINGS: ACCURACY AND PRECISION OF TRANSFER FUNCTIONS

- The number of MDOT LTPP and non-LTPP sites and level of distress were adequate for the preliminary calibration process from a statistical perspective, except for rigid pavements. The 2010 AASHTO MEPDG Local Calibration Guide includes a general recommendation for at least 21 flexible and the same for semi-rigid and rigid pavement projects. The following summarizes some of the findings relative to the number of sites for the local calibration effort.
 - A sufficient number of test sections are available to derive the preliminary calibration coefficients of the fatigue cracking, rut depth, and transverse cracking transfer functions, and IRI regression equation for new flexible pavements and HMA overlays. However, the field investigation for the non-LTPP sites needs to be completed to confirm and verify the inputs derived from as-built construction files and records that were used in the preliminary local calibration process.

- There are an insufficient number of MDOT LTPP semi-rigid pavement sections and many of these pavements exhibited little fatigue cracking. In addition, the semi-rigid pavement fatigue cracking transfer function was not calibrated under NCHRP project 1-37A. Thus, the field investigation of the non-LTPP semi-rigid pavement sections needs to be completed so a sufficient number of semi-rigid pavement sites are available to generate reliable local calibration coefficients.
- There were too few new LTPP JPCP rigid pavements for calibration, so LTPP test sections in adjacent states were added to the calibration sampling matrix. With these sites in adjacent states, the number of new JPCP sections is considered minimal but sufficient for the calibration process.
- The number of JPCP overlays and new CRCP sections are inadequate to have confidence in or develop reliable local calibration coefficients. The LTPP sites can only be used to confirm the reasonableness of the global calibration coefficients.
- Relative to the flexible pavement transverse thermal cracking transfer function, the dispersion between the predicted and measured transverse cracks is large. The reason for the large dispersion is believed to be the mechanism for the measured transverse cracks is a combination of lower temperatures and shrinkage. A local calibration coefficient of 25 was derived to eliminate or remove the bias. This local calibration coefficient is similar to what other agencies in a southern climate have reported.
- The MDOT calibration values presented in Chapters 8 and 9 do not include any effect or impact from the use of pavement preservation. The reason for this exclusion is that few of the LTPP sections included the strategic use of pavement preservations strategies to preserve the surface condition of the pavement structure.
- Five TTC groups were found to be applicable to MDOT's roadways. These five groups were specific to different functional roadway classifications in Mississippi, and included: TTC-3, TTC-7, TTC-6, TTC-12, and TTC-15 (see Table 11 in Chapter 4). In addition, the monthly and hourly distribution factors that were found to be dependent on each of the TTC groups from a separate study were used in the calibration process.
- The expanded historical climate database developed on a county-wide basis was found to have a significant impact on some of the distresses. Thus, the expanded historical climate database was used in the calibration process.
- The coefficients of the fatigue cracking transfer function were determined through the use of backcalculated elastic layer moduli of the HMA layers and the amount of fatigue cracking measured on the calibration sections. Use of the calibration coefficients defined through the in place damage index significantly improved the goodness of fit and reduce the bias in relation to use of the global calibration coefficients (see Figure 9 in Chapter 7 and Figure 25 in Chapter 8).

- The following summarizes the findings from the preliminary local calibration effort for the flexible pavements and HMA overlays.
 - Fatigue alligator cracking calibration coefficients: The global calibration coefficients resulted in biased predictions. Three of the coefficients were revised to improve the goodness of fit and to eliminate the bias (see Table 27 in Chapter 8). It is expected that the results from the field investigations will further improve on the goodness of fit.
 - Total rutting: The global calibration coefficients for all three transfer functions or material models resulted in significant biased predictions. One of the HMA calibration coefficients was revised, and both of the calibration coefficients for the subgrade soil and granular base transfer function were revised. These revisions improved the goodness of fit and eliminated the bias (see Table 32 in Chapter 8). It is expected that the results from the field investigations will provide rutting data such that one or two of the other HMA calibration coefficients will be changed but should result in a significant improvement to the goodness of fit.
 - Transverse cracking: The global calibration coefficient for input level 3 resulted in a significant bias. The local calibration coefficient (a value of 25) was derived to remove the bias and was found to be similar to what other agencies in a southern climate have reported.
 - IRI or smoothness: The global calibration coefficients resulted in biased predictions. All four of the calibration coefficients were revised to improve on the goodness of fit and eliminate the bias (see Table 35 in Chapter 8).
- The following summarizes the findings from the preliminary local calibration effort for the JPCP sections.
 - Mid-slab cracking: The global calibration coefficients resulted in biased predictions of transverse cracking. Only one of the four calibration coefficients was revised to improve on the goodness of fit and to eliminate the bias (see Table 38 in Chapter 9).
 - Transverse joint faulting: The global calibration coefficients resulted in unbiased predictions of joint faulting. However, most of the faulting measurements were very low. Only a few of the sections exhibited any appreciable faulting.
 - IRI or smoothness: The global calibration coefficients resulted in biased predictions. One of the four calibration coefficients were slightly revised to improve on the goodness of fit and to eliminate the bias (see Table 43 in Chapter 9).

10.2 RECOMMENDATIONS: MISSISSIPPI'S TRANSFER FUNCTIONS CALIBRATION COEFFICIENTS

Four important recommendations were provided at the beginning of this chapter. Those recommendations are important, but are not repeated within this section. The following summarizes some of the other recommendations from the preliminary local calibration study.

- Relative to the flexible pavement transverse thermal cracking transfer function, the dispersion between the predicted and measured transverse cracks is large. The reason for the large dispersion is believed to be the mechanism for the measured transverse cracks is a combination of lower temperatures and shrinkage. The shrinkage mechanism is not considered or included in the *Pavement ME* software. Thus, 50 percent reliability should be used to evaluate a design strategy.

Multiple agencies in the southern part of the U.S. have also found the existing model to be inadequate resulting in a high standard error. As such, AASHTO and FHWA are evaluating the current transverse cracking prediction model and transfer function embedded in the MEPDG procedure. MDOT should re-evaluate and calibrate the transverse cracking transfer function after AASHTO revises the current transverse cracking model and transfer function, if action is taken to enhance the transverse cracking mechanism.

- Fatigue cracking calibration coefficients were investigated for semi-rigid pavements but are not recommended for use in design at this time. The amount of cracking exhibited on these sections was below the design criterion. It is recommended that additional semi-rigid pavements with higher amounts of cracking be included in the calibration database. Higher amounts of cracking will occur with time on the current calibration sites, so continued monitoring is recommended until the sections are taken out of service. When MDOT uses the *Pavement ME* software to evaluate a semi-rigid pavement structure, a 50 percent reliability level should be used in predicting the area of fatigue cracking for semi-rigid pavements because the standard error has yet to be defined at the global and local levels.
- The MEPDG Manual of Practice recommends that the top-down or longitudinal cracking transfer function not be used to make design decisions. An NCHRP project is currently underway to evaluate and recommend, if necessary, a different top-down cracking model and/or transfer function. Thus, the current transfer function was excluded from the MDOT local calibration study. If AASHTO decides to include a different top-down cracking prediction model in the *Pavement ME* software, MDOT should derive the local calibration coefficients for use in Mississippi.

MDOT, however, should revisit use of the top-down cracking transfer function after the field investigations of the non-LTPP sites has been completed. If the procedure to segregate top-down from bottom-up cracking is found to be reliable, the same field investigation to identify crack propagation used for the non-LTPP field investigation should be performed on the LTPP sites.

REFERENCES

- American Association of State Highway and Transportation Officials, AASHTO Interim Guide for Design of Pavement Structures, Washington, DC, 1972.
- American Association of State Highway and Transportation Officials, AASHTO Guide for Design of Pavement Structures, Washington, DC, 1993.
- American Association of State Highway and Transportation Officials, Mechanistic-Empirical Pavement Design Guide—A Manual of Practice, Publication Code: MEPDG-1, ISBN: 978-1-56051-423-7, AASHTO, Washington, DC, 2008.
- American Association of State Highway and Transportation Officials, Local Calibration of the Mechanistic-Empirical Pavement Design Guide, Publication Code: MEPDG-1, ISBN: 978-1-56051-423-7, AASHTO, Washington, DC, 2010.
- Amini, Farshad, *Potential Applications of the Static and Dynamic Cone Penetrometers in MDOT Pavement Design and Construction*, Report Number FHWA/MS-DOT-RD-03-162, Federal Highway Administration, Mississippi DOT, Research Division, Jackson, MS, September 2003.
- Applied Research Associates, Inc, *Guide for Mechanistic-Empirical Design of New and Rehabilitated Pavement Structures: Part 1-Introduction and Part 2-Design Inputs*, Final Report, NCHRP Project 1-37A, National Cooperative Highway Research Program, Transportation Research Board, National Research Council, Washington, DC, 2004a.
- Applied Research Associates, *Guide for Mechanistic-Empirical Design of New and Rehabilitated Pavement Structures: Part 3-Design Analysis and Part 4-Low Volume Roads*, Final Report, NCHRP Project 1-37A, National Cooperative Highway Research Program, Transportation Research Board, National Research Council, Washington, DC, 2004b.
- Applied Research Associates, Inc, *Guide for Mechanistic-Empirical Design of New and Rehabilitated Pavement Structures: Appendices A to C*, Final Report, NCHRP Project 1-37A, National Cooperative Highway Research Program, Transportation Research Board, National Research Council, Washington, DC, 2004c.
- Applied Research Associates, Inc, *Guide for Mechanistic-Empirical Design of New and Rehabilitated Pavement Structures: Appendix D – User's Guide*, Final Report, NCHRP Project 1-37A, National Cooperative Highway Research Program, Transportation Research Board, National Research Council, Washington, DC, 2004d.
- AASHTO T 336, Standard Test Method for the Coefficient of Thermal Expansion of Hydraulic Cement Concrete, American Association of State Highway and Transportation Officials, Washington, DC, July 2009.
- Barker, W. R. and W. N. Brabston, *Development of a Structural Design Procedure for Flexible Airport Pavements*, FAA Report No. FAA-RD-74-199, Federal Aviation

Administration. U.S. Army Engineer Waterways Experiment Station, Federal Aviation Administration, September 1975.

Buchanan, Shane, *Traffic Load Spectra Development for the 2002 Design Guide*, Report Number FHWA/MS-DOT-RD-04-165, Mississippi Department of Transportation, Research Division, Jackson, Mississippi, July 2004.

Darter, Michael I., Jagannath Mallela, Leslie Titus-Glover, Biplab Bhattacharya, and Harold L. Von Quintus, *Calibration and Implementation of the AASHTO Mechanistic-Empirical Pavement Design Guide in Arizona*, Report Number FHWA-AZ-14-606, Project Number SPR 606, Arizona Department of Transportation, Phoenix, Arizona, September 2014

Federal Highway Administration, *Distress Identification Manual for the Long-Term Pavement Performance Program*, Publication Number FHWA-RD-03-031, McLean, VA, 1993.

George, K.P. and Waheed Uddin, *Subgrade Characterization for Highway Pavement Design*, Report Number FHWA/MS-DOT-RD-00-131, Federal Highway Administration, Mississippi DOT, Research Division, Jackson, MS, December 2000.

George, K.P., *Resilient Modulus Prediction Employing Soil Index Properties*, Report Number FHWA/MS-DOT-RD-04-172, Federal Highway Administration, Mississippi DOT, Research Division, Jackson, MS, August 2004.

Mallela, J., Titus-Glover, L., Sadasivam, S., Bhattacharya, B.B., Darter, M.I., Von Quintus, H., *Implementation of the AASHTO Mechanistic-Empirical Pavement Design Guide for Colorado*, Final Report CDOT-2013-4, Colorado Department of Transportation, Denver, Colorado, 2013.

National Cooperative Highway Research Program, *Changes to the Mechanistic-Empirical Pavement Design Guide Software Through Version 0.900*, NCHRP Research Results Digest 308, NCHRP Project 1-40D, Transportation Research Board, National Research Council, Washington, DC, 2006.

Puppala, Anand J., *Estimating Stiffness of Subgrade and Unbound Materials for Pavement Design – A Synthesis of Highway Practice*, NCHRP Synthesis 382, National Cooperative Highway Research Program, Transportation Research Board, Washington, DC, 2008.

Rao, Chetana, *Guidelines for PCC Inputs to AASHTOWare Pavement ME*, Report Number FHWA/MS-DOT-RD-14-260, Federal Highway Administration, Mississippi DOT, Research Division, Jackson, MS, December 2014.
<http://mdot.ms.gov/documents/research/Reports/Interim%20and%20Final%20Reports/State%20Study%20260%20-%20Guidelines%20for%20PCC%20Inputs%20to%20AASHTOWare%20Pavement%20ME.pdf>

Sachs, S., J. Vandenbossche, M. Snyder, *Developing Recalibrated Concrete Pavement Performance Models for the Mechanistic-Empirical Pavement Design Guide*, NCHRP Project 20-07, Task 327, Transportation Research Board, 2014.

- Truax, Dennis D., Michael Heitzman, and Eugene S. Takle, *Development of Climate Data Input Files for the Mechanistic-Empirical Pavement Design Guide (MEPDG)*, Report Number FHWA/MS-DOT-RD-11-232, Federal Highway Administration, Mississippi DOT, Research Division, Jackson, MS, June 2011.
- Varner, Robert L., *Laboratory Data to Determine Impact of Coarse Aggregate Type and Cementitious Materials on Design Thickness of PCC Pavements*, Report Number FHWA/MS-DOT-RD-15-101000, Federal Highway Administration, Mississippi DOT, Research Division, Jackson, MS, December 2016.
<http://mdot.ms.gov/documents/research/Reports/Interim%20and%20Final%20Reports/State%20Study%20177%20-%20Laboratory%20Data%20to%20Determine%20Impact%20of%20Coarse%20Aggregate%20Type%20and%20Cementitious%20Materials%20on%20Design%20of%20PCC%20Pavements.pdf>
- Von Quintus, H.L. and J.S. Moulthrop, *Performance Prediction Models: Volume I Executive Research Summary*, Publication Number FHWA/MT-07-008/8158-1, Montana Department of Transportation, Research Programs, Helena, MT, 2007a.
- Von Quintus, H.L. and J.S. Moulthrop, *Performance Prediction Models: Volume II Reference Manual*, Publication Number FHWA/MT-07-008/8158-2, Montana Department of Transportation, Research Programs, Helena, MT, 2007b.
- Von Quintus, H.L. and Rohan Perera, *Extending the Life of Asphalt Pavements*, Report #RC-1551, Michigan Department of Transportation, Office of Research and Best Practices, Lansing, Michigan; May 2011.
- Von Quintus, H.L., J. Mallela, R. Bonaquist, C.W. Schwartz, R.L. Carvalho, *Calibration of Rutting Models for Structural and Mix Design*, NCHRP Report No. 719, National Cooperative Highway Research Program, Transportation Research Board, Washington, DC, 2012. http://onlinepubs.trb.org/onlinepubs/nchrp/nchrp_rpt_719.pdf
- Von Quintus, H.L., M.I. Darter, B. Bhattacharya, and L. Titus-Glover, *Implementation and Calibration of the MEPDG in Georgia*, Report Number FHWA/GA-014-11-17, Georgia Department of Transportation, Federal Highway Administration, Atlanta, Georgia, June 2014.
- White, Thomas D., Joshua C. Littlefield, Jamie Pittman, Robert C. Plummer, Jonathan R. Easterling, and James R. Owens, *Hot Mix Asphalt (HMA) Characterization for the 2002 AASHTO Design Guide*, Report Number FHWA/MS-DOT-RD-07-166, Federal Highway Administration, Mississippi DOT, Research Division, Jackson, MS, December 2007.

APPENDIX A—INPUT CHECKLIST FOR MISSISSIPPI

Appendix A includes two worksheets or checklists that include the inputs within each major input category for flexible and rigid pavements. The worksheets identify the default values that were used in Mississippi's local calibration discussed in Chapters 8 and 9 and are the same input checklists included in Mississippi's Input Design Manual.

CHECK LIST OF INPUTS FOR NEW AND REHABILITATED FLEXIBLE PAVEMENT

Input Parameter		MDOT Input Value	Comment
General Information	Design Type		Project specific.
	Pavement Type		
	Design Life, years		Project specific service life.
	Base/Subgrade Construction Date		From construction file database.
	Pavement Construction Date		
	Traffic Opening Date		
Performance Criteria	Initial IRI, in./mi.		Backcast value.
	Terminal IRI, in./mi.		NA for local calibration.
	Top-Down Fatigue Cracking, ft./mi.	(5,000)**	Not used.
	Bottom-Up Fatigue Cracking, %		Not applicable for local calibration.
	Transverse (Thermal) Cracks, ft./mi.		
	Total & HMA/AC Rut Depth (Permanent Deformation), inches		
	Total Cracking (Overlays), %		
	Reliability Level, percent		
Traffic; Volume	Monthly Adjustment Factors		Default from WIM data.
	Number of Axles per Truck Type		
	Hourly Distribution Factors		Not used.
	Normalized Vehicle Class Distribution		Project specific.
	Growth Rate & Function		
Traffic, Site Features	Two-Way Average Annual Daily Truck Traffic		Project specific.
	Number of Lanes in Design Direction		
	Percent Trucks in Design Direction (DDF)		Mississippi default value.
	Percent of Trucks in Design Lane (LDF)		
	Operational Speed		Project specific.
	Traffic Capacity Cap	(Not Enforced)*	Not used

* - Default values were used in Mississippi's local calibration.

General Traffic, Axle Configuration	Avg. Axle Width		(8.5)*	Global default values were used.	
	Dual Tire Spacing		(12)*		
	Dual Tire Pressure		(120)*		
	Tandem Axle Spacing		(51.6)*		
	Tridem Axle Spacing		(49.2)*		
	Quad Axle Spacing		(49.2)*		
Traffic; Lateral Wander	Mean Wheel Location		(18)**	Not used.	
	Wander, Standard Deviation		(10)*	Global default value.	
	Design Lane Width		(12)**	Not used.	
Traffic, Wheelbase	Average Spacing			Not used	
	Percent Trucks				
Traffic; Axle Loads	Single Axles			Project specific and defined from MS-ATLAS.	
	Tandem Axles				
	Tridem Axles				
	Quad Axles				
Climate	Location:	Longitude		Location is project specific using expanded County weather station data.	
		Latitude			
		Elevation, ft.			
	Depth to Water Table, ft.			Groundwater software tool used.	
Climate Station			County station.		
HMA/AC Design Features	Multi-Layer Rutting Parameters			Not used	
	Shortwave Absorptivity		(0.85)*	Global default value.	
	Endurance Limit			Not used	
	Layer Interface		(1)*	Global default value.	
	Rehabilitation	Milled Thickness			Project specific.
		Condition or cracking of pavement			Project specific; input level 1 or 2.
Rutting in existing layers		(Layer Percentages)*	Mississippi default values.		

New HMA/AC Layers	Thickness, inches	Surface Layer		Project specific; construction database.
		Binder Layer		
		Base Layer		
	Unit Weight, pcf	Surface Layer		Project specific; construction database.
		Binder Layer		
		Base Layer		
	Effective Asphalt Content by Volume, %	Surface Layer		Calculated based on construction database.
		Binder Layer		
		Base Layer		
	Air Voids, %	Surface Layer		Construction database.
		Binder Layer		
		Base Layer		
	Poisson's Ratio	All Layers	(Regression Equation)*	Use global default values
	Dynamic Modulus	Surface Layer		Input level 1 from HMA mixture library or input level 3 from construction database.
		Binder Layer		
		Base Layer		
	Gradation	Surface Layer		
		Binder Layer		
		Base Layer		
	Estar Predictive Model	All Layers	(Viscosity Model)*	Global default equation
Reference Temp., °F	All Layers	(70)*	Global default value	
Asphalt Binder Grade	Surface Layer		Construction database.	
	Binder Layer			
	Base Layer			
Tensile Strength, psi	Surface	(Calculated)*	Global default value	
	Binder & Base	(Calculated)*		
Creep Compliance	Surface	(Calculated)*	Global default value	
	Binder & Base	(Calculated)*		
Thermal Conductivity		(0.67)*	Global default value	
Heat Capacity		(0.23)*		
Thermal Contraction		(Calculated)*		
Existing HMA/AC Layer(s)	Same inputs as for new HMA/AC layers, except for modulus or condition of existing layer.		Project specific.	
	Number of existing HMA/AC layers		Project specific.	

	Thickness after milling	Upper		Project specific.
		Lower		
	Existing HMA – Backcalculated Modulus			Only LTPP sites; with FWD deflection basins.

Asphalt Stabilized or Treated Base	The inputs for an asphalt stabilized or treated base layer are the same as for an HMA/AC layer		See HMA/AC layer inputs.
Cement Stabilized or Treated Base Layer	Thickness, inches		Project specific.
	Unit Weight, pcf	(150)*	Mississippi input level 3.
	Poisson's Ratio	(0.20)*	
	Minimum Elastic Modulus, psi		Mississippi input level 3 or construction database.
	Modulus of Rupture, psi		
	Elastic/Resilient Modulus, psi		
	Thermal Conductivity	(1.25)*	Global default values.
Heat Capacity	(0.28)*		
Unbound Granular Aggregate Base (GAB) Layer	Thickness, inches		Project specific.
	Poisson's Ratio		Global default values.
	Coefficient of Lateral Earth Pressure	(0.50)**	Not used.
	Classification		MDOT materials library.
	Resilient Modulus		
	Is Layer Compacted?	Yes	Box checked when compacted.
	Specific Gravity	(2.7)*	Global default values.
	Saturated Hydraulic Conductivity	(5.054e-02)*	
	Soil-Water Characteristic Curve	Calculated	Mississippi's default values for a Crushed Stone
	Water Content; Optimum	(7.4)*	
	Dry Unit Weight; Modified Proctor	(127.2)*	
	Gradation		
	Plasticity Index	(1)*	
Liquid Limit	(6)*		
Stabilized Subgrade Layer; Soil Cement and Lime Stabilized Soil	Thickness, inches		Project specific.
	Poisson's Ratio		Global default values.
	Coefficient of Lateral Earth Pressure	(0.50)*	Not used
	Resilient Modulus		Annual representative modulus value.
	AASHTO Soil Classification	(A-1-b)*	Project specific from construction database.
	Specific Gravity	(2.7)*	Global default values for an A-1-b soil
	Saturated Hydraulic Conductivity	(1.803e-03)*	
	Soil-Water Characteristic Curve	Calculated	
	Water Content; Optimum	(9.3)*	
	Dry Unit Weight; Modified Proctor	(124.0)*	
	Gradation		
	Plasticity Index	(1)*	
Liquid Limit	(6)*		

Subgrade (embankment and natural soil layers)	Thickness, inches (if applicable)		Project specific.
	Poisson's Ratio		Global default value.
	Resilient Modulus		Input level 3 or 2.
	Coefficient of Lateral Pressure	(0.50)*	Not used.
	Is Layer Compacted?		Box checked for upper subgrade layer, if used.
	Specific Gravity	(2.7)*	Global default values.
	Saturated Hydraulic Conductivity	(5.051e-02)	
	Soil-Water Characteristic Curve	Calculated	
	Water Content		Mississippi's local materials library.
	Dry Unit Weight		
	Gradation		
	Plasticity Index		
Liquid Limit			
Bedrock	Resilient Modulus, psi	(1,000 ksi)*	Global default values; used only when subgrade thickness is less than 100 inches.
	Poisson's Ratio	(0.2)*	
	Unit Weight, pcf	(140)*	
Local Calibration Factors	Alligator Cracking; Bottom-Up Cracking		Defined in Chapter 8.
	HMA Rutting (Permanent Deformation)		
	Rutting; Coarse-Grained Soil		
	Rutting; Fine-Grained Soil		
	HMA IRI Regression Equation		
	Reflection Cracking		

CHECK LIST OF INPUTS FOR NEW AND REHABILITATED RIGID PAVEMENT

Input Parameter		MDOT Input Value	Comment
General Information	Design Type	New Pavement or Overlay	Project specific.
	Pavement Type	Rigid Pavement	
	Design Life, years		Project specific service life.
	Base/Subgrade Construction Date		From construction file database.
	Pavement Construction Date		
	Traffic Opening Date		
Performance Criteria	Initial IRI, in./mi.		Backcast value.
	Terminal IRI, in./mi.		NA for local calibration.
	Mid-Slab Cracking, %		
	Faulting, inches		
	Reliability Level, percent		
Traffic; Volume	Monthly Adjustment Factors		MDOT default values
	Number of Axles per Truck Type		
	Hourly Distribution Factors		
	Normalized Vehicle Class Distribution		Project specific.
	Growth Rate & Function		
Traffic, Site Features	Two-Way Average Annual Daily Truck Traffic		Project specific.
	Number of Lanes in Design Direction		
	Percent Trucks in Design Direction (DDF)		MDOT default value.
	Percent of Trucks in Design Lane (LDF)		
	Operational Speed		Project specific.
	Traffic Capacity Cap	(Not Enforced)*	Not used
General Traffic, Axle Configuration	Avg. Axle Width	(8.5)*	Global default values.
	Dual Tire Spacing	(12)*	
	Dual Tire Pressure	(120)*	
	Tandem Axle Spacing	(51.6)*	
	Tridem Axle Spacing	(49.2)*	
	Quad Axle Spacing	(49.2)*	
Traffic; Lateral Wander	Mean Wheel Location	(18)**	Project specific.
	Wander, Standard Deviation	(10)*	Global default value.
	Design Lane Width	(12)**	Project specific.

Traffic, Wheelbase	Average Spacing		MDOT default values.
	Percent Trucks		
Traffic; Axle Loads	Single Axles		MDOT project specific values from MS- ATLAS.
	Tandem Axles		
	Tridem Axles		
	Quad Axles		
Climate	Location:	Longitude	Location specific for County expanded weather station.
		Latitude	
		Elevation, ft.	
	Depth to Water Table, ft.		Groundwater software tool used.
Climate Station		County specific.	
JPCP Design Properties	Shortwave Absorptivity		(0.85)* Global default value.
	PCC Joint Spacing, ft.		Project specific.
	Sealant Type		
	Dowelled Joints		
	Widened Slabs		
	Tied Shoulders		Global default values.
	Erodibility Index		
	PCC Base Contact Friction		Global default value.
Permanent Curl/Warp Effective Temperature Difference			
Foundation	Modulus of Subgrade Reaction		(Calculated)* MDOT default value.
PCC Layer	Thickness, inches		Project specific.
	Unit Weight, pcf		Construction database.
	Poisson's Ratio		Global default value.
	Coefficient of Thermal Contraction		MDOT default value.
	Thermal Conductivity		(0.67)* Global default values.
	Heat Capacity		(0.23)*
	Cement Type		Project specific from construction database.
	Cementitious Material Content		
	Water to cement ratio		
	Aggregate Type		Global default values.
	PCC Zero-stress temperature		
	Ultimate shrinkage		
	Reversible shrinkage		
	Time to develop 50% ultimate shrinkage, days		
	Curing Method		Project specific.
PCC Strength and Modulus		Backcast from LTPP data or MDOT construction database.	

Existing JPCP Rehabilitation	Same inputs as for new JPCP except for modulus or condition of existing layer.		Project specific; see PCC Layer
	Slabs cracked or replaced before restoration		Project specific.
	Slabs repaired or replaced after restoration		
Asphalt Stabilized or Treated Base	The inputs for an asphalt stabilized or treated base layer are the same as for an HMA/AC layer		Project specific; see HMA/AC layer inputs.
Cement Stabilized or Treated Base Layer	Thickness, inches		Project specific.
	Unit Weight, pcf	(150)*	MDOT construction database.
	Poisson's Ratio	(0.20)*	Global default values.
	Minimum Elastic Modulus, psi		
	Modulus of Rupture, psi		MDOT construction database.
	Elastic/Resilient Modulus, psi		
	Thermal Conductivity	(1.25)*	Global default values.
	Heat Capacity	(0.28)*	
Unbound Granular Aggregate Base (GAB) Layer	Thickness, inches		Project specific.
	Poisson's Ratio		Global default value.
	Coefficient of Lateral Earth Pressure	(0.50)**	Not used.
	Classification		MDOT materials library.
	Resilient Modulus		
	Is Layer Compacted?		Box checked for compacted layer.
	Specific Gravity	(2.7)*	Global default values for a Crushed Stone
	Saturated Hydraulic Conductivity	(5.054e-02)*	
	Soil-Water Characteristic Curve	Calculated	
	Water Content; Optimum	(7.4)*	MDOT materials library.
	Dry Unit Weight; Modified Proctor	(127.2)*	
	Gradation		
	Plasticity Index	(1)*	
Liquid Limit	(6)*		

Stabilized Subgrade Layer; Soil Cement and Lime Stabilized Soil	Thickness, inches		Project specific.
	Poisson's Ratio	(0.30)*	Global default value.
	Coefficient of Lateral Earth Pressure	(0.50)*	Not used
	Resilient Modulus		MDOT soil representative modulus value.
	AASHTO Soil Classification	(A-1-b)*	Project specific.
	Specific Gravity	(2.7)*	Global default value.
	Saturated Hydraulic Conductivity	(1.803e-03)*	
	Soil-Water Characteristic Curve	Calculated	
	Water Content; Optimum	(9.3)*	MDOT materials library.
	Dry Unit Weight; Modified Proctor	(124.0)*	
	Gradation		
	Plasticity Index	(1)*	
Liquid Limit	(6)*		
Subgrade (embankment and natural soil layers)	Thickness, inches (if applicable)		Project specific.
	Poisson's Ratio		Global default value.
	Resilient Modulus		MDOT input level 2.
	Coefficient of Lateral Pressure	(0.50)*	Not used.
	Is Layer Compacted?		Box checked for compacted layer, if used.
	Specific Gravity	(2.7)*	Global default values.
	Saturated Hydraulic Conductivity	(5.051e-02)	
	Soil-Water Characteristic Curve	Calculated	
	Water Content		MDOT materials library.
	Dry Unit Weight		
	Gradation		
	Plasticity Index		
Liquid Limit			
Bedrock	Resilient Modulus, psi	(1,000 ksi)*	Global default values; used when subgrade thickness is less than 100 inches.
	Poisson's Ratio	(0.20)*	
	Unit Weight, pcf	(140)*	
Local Calibration Factors	Mid-Slab Cracking, %		See Chapter 9.
	Joint Faulting, inches		
	IRI, in./mi.		

APPENDIX B—MATERIAL SAMPLING AND TESTING PLANS FOR NON-LTPP PROJECTS USED FOR LOCAL CALIBRATION

B.1 INTRODUCTION

B.1.1 Purpose of Document

The purpose of this document (appendix) is to provide the sampling and testing recommendations to determine the layer properties of non-LTPP roadway projects being used for the local calibration of the MEPDG transfer functions. This material sampling and testing plan is applicable to new construction (original construction) and rehabilitated roadway segments.

B.1.2 Background

The LTPP test sections located in Mississippi represent the “best” candidates for the local calibration of the distress transfer functions in the DARWin-ME software package. The number of test sections, however, was found to be insufficient to cover the range of materials, pavement structures, and other design features commonly used by the Mississippi DOT.

Non-LTPP roadway segments were designated for use to supplement the LTPP test sections in calibrating DARWin-ME to Mississippi materials, conditions, and operational policies. Both new and rehabilitated roadway projects were identified for the local calibration experimental fractional factorial and sampling plan (see Chapter 3). It was envisioned that all of the layer inputs needed for DARWin-ME would be extracted from construction files and as-built construction plans.

For new pavement construction or newer projects, the accuracy of the as-built plans and construction files were believed to be sufficient. Thus, the Mississippi DOT began the task of extracting the required input data from construction files. The accuracy of the as-built plans and construction files, for the rehabilitated or older projects (existing pavement layers prior to overlay placement), however, were questioned. More importantly, many of the plans and files for the rehabilitated roadway segments were unavailable because of their age.

Falling weight deflectometer (FWD) deflection basins were initially planned for the rehabilitated projects, but not for new construction projects. The use of deflection basin measurements is discussed in more detail in a latter part of this document (appendix). Accurate layer thickness is important for back-calculation of layer modulus values. As such, MDOT decided to determine or confirm the layer properties and thickness through a limited sampling and testing program. This field investigation should improve on the accuracy of the input parameters; specifically for the rehabilitated non-LTPP roadway segments.

The construction files and as-built plans for the high priority projects were reviewed and all available data were extracted and included in the local calibration database. Some critical data elements were unavailable from the construction files. As a result of missing data believed to be critical to the local calibration process, the deflection basin testing program

was expanded to include this family of pavements. The initial materials sampling and testing plan submitted in 2010 was expanded to include new construction high priority sites.

A complete list of projects included in the field and laboratory testing plan are provided in a standalone excel file that was submitted to MDOT in November 2011. This file includes individual tables for:

- New HMA construction projects
- HMA rehabilitation projects, and
- Jointed plain concrete pavement (JPCP) projects

Each table contains the following information for each layer of the pavement structure:

- Test section number
- Location details
- Layers and materials information available and list of additional material properties needed. (Note that no materials information is available for rehabilitation and JPCP projects)
- Level of distress expected during a subsequent visual distress survey based on 2006 condition reported in MDOT pavement management database.

B.2 NEW CONSTRUCTION NON-LTPP PROJECTS WITH CRITICAL DATA MISSING

Table B.1 is a listing of the non-LTPP new construction flexible pavement projects with critical or basic data missing for the local calibration process. For example, many of the high priority roadway segments or projects were found to have no information on the soil or subgrade type and no information on the base and/or subbase layers. These roadway segments should be tested in the same manner as for the rehabilitation segments.

Table B.2 is a listing of the non-LTPP rigid pavement projects in Mississippi for which no data are available. These projects were selected for inclusion into the rigid pavement distress model calibrations. No construction and materials data were available for these projects. It was decided by MDOT to use LTPP sections from Mississippi and neighboring States to develop local calibration models for rigid pavement distresses. If MDOT decides to collect field data and subsequently perform laboratory tests for rigid pavement sections, the projects listed in Table B.2 should be considered for testing.

Table B.3 is a listing of the non-LTPP HMA rehabilitation projects in Mississippi for which no data are available. If MDOT decides to collect field data and subsequently perform laboratory tests for rigid pavement sections, the projects listed in Table B.3 should be considered for testing.

Table B.1—Non-LTPP Flexible Pavement New Construction, High Priority Projects

1122	4602	4889	5310	5627
1123	4669	4894	5318	5628
2202	4742	4902	5446	5688
2580	4776	4933	5500	5828
3144	4782	5105	5506	5849
3163	4784	5210	5511	6015
3204	4816	5230	5526	
4527	4834	5244	5554	
4580	4864	5249	5616	
4588	4865	5280	5618	

Table B.2—Non-LTPP Rigid Pavement Construction, High Priority Projects

987	2797
989	2798
991	2838
1682	5380

Table B.3—Non-LTPP Rehabilitated Flexible Pavement, High Priority Projects

222	1708	2108	2836	3699
1125	1797	2358	2851	3868
1351	1799	2824	3038	
1463	1822	2830	3512	
1703	1823	2833	3686	

B.3 REQUIREMENTS FOR THE SAMPLING AND TESTING PLAN

The following provides a listing of the factors or items used to establish the sampling and testing plan for these rehabilitated and new construction non-LTPP flexible pavement roadway projects included in the local calibration process.

1. The input levels used for the rehabilitated roadway segments should be the same as for the new construction roadway segments. Using input levels 1 or 2 material properties for the rehabilitated roadway projects and input level 3 for new construction projects may result in a bias of the transfer functions between new construction and rehabilitation. Most of the material properties for the LTPP test sections are input level 1 or 2. A concerted effort was made to determine input levels 1 or 2 for the non-LTPP test sections.
2. The layer properties measured for the rehabilitated segments need to be consistent with the input requirements for the MEPDG. Air voids of HMA, density and water content of unbound layers should represent the condition of the layer at overlay placement or construction.

3. The number of samples taken from the roadway segments should be similar to that used for the LTPP test sections for specific input properties – depending on the data elements that are missing or unavailable from construction records. The number of sample locations and type of sample is covered under a latter section of this appendix.

B.4 PRIORITIZATION OF ROADWAY SEGMENTS INCLUDED IN THE FIELD MATERIAL SAMPLING AND TESTING PLAN

The following lists and itemizes the field work for determining the inputs to the MEPDG that are proposed for use in the initial local calibration process.

1. The rehabilitated Non-LTPP flexible pavement roadway segments have the highest priority because of the amount of missing data from the construction files. The sampling and testing plan should be executed for those Non-LTPP roadway segments without pavement construction information and data for all structural layers. If sufficient data is recovered from the construction files and as-built plans, however, the amount of field work for those segments can be significantly reduced and the funds diverted to other field work.
2. Deflection basin testing is routinely used by MDOT. Deflection basins were measured with the FWD on all of the LTPP test sections and are being measured on all of the rehabilitated non-LTPP test sections. The Department plans to continue to use FWD deflection basins as a part of their pavement design and evaluation process. Thus, deflection basins should be measured on the Non-LTPP new construction flexible pavement roadway segments with critical or basic data missing. This is considered the second high priority field test.
3. The third priority of expending MDOT funds is to recover materials and soils from some of the Non-LTPP new construction roadway segments. Those that should be included are the roadway sections with stabilized base layers using Portland cement, fly ash, and/or lime. This additional work can be used to confirm the current condition of those in place stabilized layers and subgrade soils. Cores of the stabilized layers and undisturbed soil samples should be taken as noted in the sampling plan. Deflection basin testing should be performed on each of these non-LTPP new construction sections. The semi-rigid pavements were never calibrated under the NCHRP 1-37A or NCHRP 1-40D studies. It is anticipated that more accurate layer properties will be needed in accordance with the MEPDG distress prediction methodology.
4. The fourth priority of expending MDOT funds is to complete the deflection basin testing on the remaining flexible pavement new construction projects so the layer modulus values used in the local calibration process were determined from the same type and set of data – backcalculated layer modulus values from deflection basins.
5. The next priority for expending MDOT funds it to complete deflection basin testing for the rigid pavement sections so that layer modulus data can be obtained for local calibration of rigid pavement models. These sections will be added to the set of LTPP sections from Mississippi and neighboring States for the local calibration process.

6. If funds still remain, a forensic investigation should be conducted on those roadway segments and LTPP test sections with anomalous performance characteristics. The test sections with anomalous performance will not be identified until the initial calibration process has been completed. Those non-LTPP test sections with anomalous performance characteristics are listed in Chapters 8, 9, and 10. MDOT should decide whether to initiate a forensic investigation for those non-LTPP test sections to ensure that funds are spent effectively.

B.5 MATERIAL AND LAYER PROPERTIES FOR PAVEMENT ME DESIGN

Table B.4 is a summary of the layer properties needed for local calibration. If data elements are unavailable through as-built plans and construction files, these properties should be determined through a limited sampling and testing program. The remainder of this section discusses the layer properties in terms of the local calibration process.

B.5.1 HMA Inputs—Overlays and Existing Layers Prior to Overlay

HMA material inputs required for the MEPDG can be grouped into five categories, which are listed and briefly discussed below in terms of the testing plan.

1. **Mixture Mechanistic Properties, Load Related Transfer Functions:** These properties include the dynamic modulus, permanent deformation coefficients, and fatigue strength parameters. None of these properties were measured on the LTPP and non-LTPP new construction projects. Dynamic modulus tests were performed on some of the common HMA mixtures specified by MDOT. Results from these tests were used to build the initial HMA mixture property library. Dynamic modulus tests are not included in the field and laboratory testing plan for the non-LTPP test sections.
2. **Thermal Properties, Non-Load Related Transfer Functions:** These properties include the indirect tensile strength and creep compliance, coefficient of thermal contraction, asphalt thermal conductivity, asphalt heat capacity, and surface shortwave absorptivity. None of these properties were measured on the Mississippi LTPP and non-LTPP new construction projects. Input level 3 or default values will be used for the local calibration process. Thermal properties of the HMA are not included in the field and laboratory testing plan for the non-LTPP test sections.
3. **Mixture Volumetric Properties:** In place air voids (bulk and maximum specific gravities of the HMA mixture) at the time of HMA mixture placement, asphalt content, and density. The mixture volumetric properties will be extracted from the construction files, if available. For those projects where construction data are unavailable, cores will be taken for measuring the gradation and asphalt content for each structural HMA layer. The bulk and maximum specific gravities are included in the HMA mixture testing plan to estimate the effective asphalt content by volume.

It should be noted the air voids calculated from the bulk and maximum specific gravities needs to be determined at the time of placement. All of the new and rehabilitated projects have been in place for many years, so the air void level will need to be back-casted to time of placement. The back-casting procedure was

illustrated in Figure 6, Chapter 6. The back-casting procedure will result in an undefined error, so it is considered appropriate or cost effective to determine default values for different mixtures and use the default air void level for the local calibration process.

Table B.4—Properties for Local Calibration of the Pavement ME Design Software

Layer/Material Property		Source of Input Value	Include in Sampling & Testing Program
HMA	Layer Thickness	As-Built Plans	Yes
	Dynamic Modulus	Default Value or Materials Library	No
	Bulk Specific Gravity	Construction Files	Yes
	Maximum Specific Gravity	Construction Files	Yes
	Asphalt Content	Construction Files or Mix Design Records	Yes
	Asphalt Specific Gravity		No
	Asphalt P-G Designation		No
	Aggregate Gradation		Yes
Combined Aggregate Specific Gravity	Yes		
PCC	Layer thickness	Not in plans – Use values from field sampling and FWD testing	Yes
	Modulus		Yes
	Compressive strength	Not in plans; test field core; CTE may be estimated from aggregate type.	Yes
	Coefficient of thermal expansion (CTE)		Yes
Asphalt Stabilized Layer	Asphalt or Emulsion; Plant or Cold In Place Recycled layer	See HMA	---
Portland cement, Fly-Ash, and/or Lime Stabilized Layer	Layer Thickness	As-Built Plans	Yes
	Density	Construction Files	Yes
	Elastic Modulus	Construction Files or Mix Design Records	Yes
	Compressive Strength		Yes
Unbound Aggregate	Layer Thickness	As-Built Plans	Yes
	Resilient Modulus	Default Value or Materials Library	No
	Gradation	Construction Files	Yes
	Density	Construction Files	No
	Water Content	Construction Files	Yes
	Classification	As-Built Plans or Construction Files	Yes
Subgrade or Embankment	Same as for Unbound Aggregate Layers		---

4. **Aggregate Properties:** Gradation and specific gravity of the aggregate blend. The gradation and combined specific gravity of the aggregate blend will be extracted from the construction files, if available. For those projects where construction data are unavailable, larger diameter cores should be taken for measuring these properties for each structural layer.
5. **Asphalt Properties:** Specific gravity and performance grade (PG) designation of the asphalt included in the existing HMA layers, as well as for the HMA overlay. The viscosity of the recovered asphalt can be measured to estimate the grade of the asphalt at the time of construction. The specific gravity and viscosity of the recovered asphalt are needed, but it is recommended that this input parameter be estimated from historical data on similar asphalts typically specific by MDOT. Using the historical data means that extracting the asphalt from the recovered cores is not needed.

B.5.2 Stabilized Layer Inputs—Overlays and Existing Layers Prior to Overlay

Layers or materials stabilized with an emulsion or asphalt (plant or cold in place recycled layer) should be treated as an HMA layer in terms of layer properties.

The properties of the layers stabilized with Portland cement, fly ash, and/or lime include: elastic modulus, compressive strength, and density. If these properties are unavailable from construction records, these tests should be performed on test specimens recovered from the pavement. Indirect test strengths can be measured if test specimens of sufficient height are not recovered. If no test specimens can be recovered from the stabilized layer (material disintegrates during the coring process), the layer should be treated as a lime-treated or unbound material. The default values for these layers are defined in Chapter 7.

B.5.3 Unbound Aggregate Layers and Subgrade Material Property Inputs, Prior to Overlay Placement

Unbound layer material inputs required for the MEPDG are listed and briefly discussed below in terms of the testing plan.

1. **Resilient Modulus:** Repeated load resilient modulus tests on the unbound pavement layers of the non-LTPP roadway segments for new construction are not being performed. Repeated load resilient modulus tests were performed on some of the common soils and unbound aggregate materials used in Mississippi. These tests were used to build the soil library. Default values were used in the local calibration process. Resilient modulus testing should be continued to expand the materials library over time. However, repeated load resilient modulus tests of any unbound aggregate layer, embankment, or subgrade are not included in the field and laboratory testing plan. The resilient or elastic modulus values used in the local calibration will be backcalculated from the FWD deflection basin data.

Deflection basins were measured on all of the LTPP test sections to estimate the in place modulus values for all pavement structural layers. Resilient modulus of all unbound layers for the rehabilitated roadways segments should also represent the

- default values or values estimated from deflection basin or DCP values (refer to item 2 below).
2. **Dynamic Cone Penetrometer (DCP) Tests:** DCP tests were not performed on any of the LTPP projects and non-LTPP roadway segments for new pavement construction. MDOT does use the DCP to estimate the in place stiffness of unbound pavement layers and the subgrade and plans to continue its use. Limited DCP testing is suggested for use in back-calculation of layer modulus values from the FWD deflection basin testing and to confirm layer thickness. The added effort to conduct DCP tests after cores are taken for layer thickness confirmation is minimal and believed to be cost effective. The DCP tests can be used for expanding the library of material properties for the unbound layers and soils.
 3. **Gradation:** The gradation of the unbound layers and soils is used in classifying the material and to estimate the movement of water into the upper pavement and subgrade layers. Gradations of the unbound layers were measured on most of the LTPP test sections and are available for the non-LTPP new construction projects. Resilient modulus of the unbound layers is the key structural input. The gradation of the unbound layers is used to estimate the change in moisture content over time, which has an impact on the resilient modulus of the layer.
 4. **Atterberg Limits:** The plasticity index and liquid limit of the unbound layers are available for most all of the LTPP and non-LTPP new construction segments. These properties should be determined on samples recovered from the rehabilitated pavement structures for classification and determining the default values of other inputs.
 5. **Optimum Water Content and Maximum Dry Density:** These two properties should represent in place values at the time of construction. Trenches are needed to recover sufficient material for measuring these properties. Trenches are time consuming and require much more time during the material sampling process and are difficult to repair. Thus, the maximum dry density and optimum water content were based on the default values estimated from classification properties. The in place water content can be measured from auger samples for the lower unbound layers to compare the computed water content from the MEPDG to the value measured at one point in time—assuming that the wet coring process does not infiltrate the lower unbound layers.

B.5.4 PCC Inputs—Overlays and Surface Layers with PCC

PCC material inputs required for the MEPDG can be grouped into four categories, which are listed and briefly discussed below in terms of the testing plan.

1. **Layer Thickness:** This category mainly includes the thickness and density of the layer. This can be determined by measuring the depth of the core and performing a simple density test.
2. **Thermal Properties:** These properties include the PCC coefficient of thermal expansion (CTE), the thermal conductivity, and the heat capacity. The CTE is a critical input for performance prediction and may be measured directly in the

laboratory. The other two inputs are non-critical and the default values for PCC materials (as was used in the original calibration of the MEPDG) will be used for the sections included in the local calibration. In the event the CTE cannot be measured in the laboratory, knowledge about the aggregate source or aggregate type from the local area can be used to estimate the CTE.

3. **Mix Properties:** These properties include details about the mix proportions and materials used in the mix design. Typically, the cement type, the cement content in the mix, and the aggregate type are required. Additionally, the curing method used during the construction is also input. These inputs are used to estimate various other PCC material properties such as shrinkage, and zero-stress temperature for the specific month of construction. These data can be best recovered from MDOT's construction and materials data records. In the event these data will not become available, these data will be assumed for calibration. Global default values will be used.
4. **Strength Properties:** The strength properties required for jointed concrete pavement sections include flexural strength and elastic modulus. Standard correlations exist to estimate flexural strength and elastic modulus based on compressive strength, which may be utilized. Alternatively, the elastic modulus test may be performed on the core samples prior to the compressive strength test, because the elastic modulus test is a nondestructive test. In summary, the PCC tests may be prioritized in the following manner:
 - i. PCC thickness and compressive strength
 - ii. PCC CTE
 - iii. PCC elastic modulus

The CTE and elastic modulus can be performed on the same core sample prior to the compressive strength cylinder break.

B.6 SAMPLING AND FIELD TESTING PLAN FOR THE HMA, UNBOUND AGGREGATE LAYERS, EMBANKMENTS, SUBGRADES, AND PCC LAYERS

Attachment B.1 provides an HMA, unbound, and PCC pavement layer sampling and field testing plan for estimating the layer properties for the rehabilitated pavement structures included in the local calibration process. Table B.5 summarizes the materials sampling plan for the non-LTPP rehabilitated and new construction projects.

B.7 LABORATORY TESTING PLAN FOR THE HMA, UNBOUND AGGREGATE LAYERS, EMBANKMENTS, SUBGRADE, AND PCC LAYERS

The following provides the recommended testing plan for HMA, unbound, and PCC pavement layers to estimate the layer properties for the rehabilitated pavement structures included in the local calibration process, which is summarized in Attachment B.1. Table B.6 summarizes the materials testing plan for the non-LTPP rehabilitated and new construction projects.

Table B.5—Materials Sampling Plan for the Non-LTPP Projects

1	FWD Deflection Basin Tests		Used to back-calculate in place elastic layer modulus values.
NOTE:			<i>The FWD deflection basins should be measured prior to the sampling program. The deflection basins should be used on site to select the area for recovering the samples, and to ensure that the section is relatively uniform – no abrupt change in deflections along the sections or systematic increase or decrease in deflections.</i>
2	HMA Cores	6-inch diameter	Used for determining the bulk and maximum specific gravity of the HMA layer.
		8-inch diameter	Used for determining the asphalt content, aggregate gradation, and aggregate blend specific gravity.
3	DCP Tests	6-inch diameter cores	Conduct DCP test after 6-inch core recovered from pavement. Used to estimate the stiffness with depth below the HMA, CTB or stabilized layers.
4	Auger Samples	8-inch diameter cores	Recover samples to determine visual classification, gradation, water content, atterberg limits of in place material after 8-inch core recovered from pavement.
NOTE:			<i>NOTE: Ensure water infiltration from wet coring process is minimized into the lower unbound layers. Water content of layer immediately below layer cored should be eliminated.</i>
5	Shelby Tube Samples	8-inch diameter cores	Recover undisturbed samples using one to two Shelby tubes after recovering the 8-inch diameter core and taking an auger sample of any unbound aggregate base layer. Density, water content, atterberg limits, gradation, and visual classification. If undisturbed sampling is not possible, auger samples should be taken of the subgrade/embankment soils.
6	PCC Cores	6-inch diameter	Used to determine CTE, elastic modulus, and compressive strength. Note that CTE is a non-destructive test and the samples may be reused for the elastic modulus test. The compressive strength test shall be performed prior to the elastic modulus test to estimate the load level for the elastic modulus test.

B.8 SUGGESTED STEPS FOR PLANNING THE FIELD INVESTIGATIONS

The following summarizes the recommended steps in planning and preparing for the field sampling program. Table B.7 can be used as a general guide on assessing or interpretation of the results from the sampling plan.

1. From the as-built plans and construction records, record the pavement structure (thickness and material types for each layer). Also record the properties of each layer that are needed as inputs to the MEPDG (refer to section 4 of this document). Prepare a summary of pavement structure and expected condition of each roadway segment included in the materials sampling plan. This summary will assist the field personnel to know what should be expected during the recovery of the materials.
2. Select a representative section of 500 to 1000 ft. along the project considering safety of all field personnel. Safety considerations should always take precedent over collecting data. The section should exhibit similar distresses along the project, as close as possible.
3. Conduct a condition survey along the designated section in accordance with the FHWA Distress Identification Manual.

Table B.6—Materials Testing Plan for the Non-LTPP Projects

NOTES:				<i>If material properties for the HMA overlay layers are available from construction files, it is not necessary to conduct testing on the HMA overlay layers.</i>
1	HMA Cores	6-inch diameter	4 per layer	Bulk specific gravity of HMA layers exceeding 1.5 inches in thickness.
2			2 per layer	Maximum specific gravity of HMA layers exceeding 1.5 inches in thickness.
3			2 per layer	Asphalt content of HMA layers exceeding 1.5 inches in thickness.
NOTES for 6-inch Diameter HMA Core Tests:				2. <i>Bulk specific gravity is measured prior to measuring the maximum specific gravity.</i>
4	Stabilized	6-inch diameter	3 per layer	Density
5	Base			Elastic Modulus
6	Cores			Indirect Tensile Strength or Compressive Strength
NOTES for Stabilized Layer Tests:				3. <i>If cores cannot be extracted from the pavement of the stabilized layer, recover sufficient pieces of the layer to complete a visual examination of the layer and make notes on the material type.</i>
7	HMA Cores	8-inch diameter	2 per layer	Asphalt content and gradation of the recovered aggregate blend from each layer with sufficient thickness; at least 1.5 inches.
8			2 per layer	
9			2 per layer	
NOTES for 8-inch Diameter HMA Core Tests:				4. <i>Depending on the layer thickness, it maybe necessary to combine the aggregate from multiple locations for measuring the gradation of the HMA mixture.</i>
10	Shelby or	3 per layer		Water content of each layer and top of subgrade.
11	Auger	3 per layer		Density (Undisturbed samples only)
12	Samples	3 per layer		Atterberg Limits of each layer and top of subgrade.
13		3 per layer		Gradation of each layer and top of subgrade. The gradation samples can be combined into one test specimen for an individual layer.
14	PCC Cores	6-inch diameter	6 cores per layer	CTE for 3 cores (nondestructive test)
15				Elastic modulus testing for 3 cores (nondestructive test)
16				Compressive test for 3 cores (destructive test)
NOTES for PCC Tests:				1. <i>Perform the compressive strength test first.</i> 2. <i>Next, perform the CTE test and reuse cores after CTE testing for Young's modulus testing.</i>

4. Measure deflection basins using the FWD. The Mississippi standard test protocol can be used to measure the deflection basins. Suggestions for these include:
 - a. Selected representation segments along the project; primarily where the distress survey was conducted. The length of the segments should be 500 to 1,000 feet in length.
 - b. Measure deflection basins at a frequency of 100 to 200 feet. A minimum of 5 stations should be recorded.
 - c. Three load levels should be used to determine if the layer stiffness is varying with load.
 - d. Record the surface and air temperatures.

5. Conduct a visual inspection and take notes on the condition of the areas adjacent to the roadway.
6. Take photographs of the surface and other features that may be having an effect on the performance of the section and/or project – drainage condition, shoulders, etc.
7. Execute the materials sampling plan.
8. Execute the materials testing plan.

Table B.7—Checklist of Factors for Overall Pavement Condition Assessment and Problem Definition

Facet	Factors	Description	
Structural Adequacy	Existing Distress	1. Little or no load/fatigue-related distress 2. Moderate load/fatigue-related distress (possible deficiency in load-carrying capacity) 3. Major load/fatigue-related distress (obvious deficiency in current load-carrying capacity) 4. Load-carrying capacity deficiency: (yes or no)	
	Nondestructive testing (FWD deflection testing)	1. High deflections or weak layers: (yes or no) 2. Are backcalculated layer moduli reasonable? 3. Are joint load transfer efficiencies reasonable?	
	Nondestructive testing (GPR testing)	1. Determine layer thickness 2. Are voids located beneath PCC pavements?	
	Nondestructive testing (profile testing)	Determine joint/crack faulting	
	Destructive testing	1. Are core strengths & condition reasonable? 2. Are the layer thicknesses adequate?	
	Previous maintenance performed	Minor <input type="checkbox"/> Normal <input type="checkbox"/> Major <input type="checkbox"/>	
	Has lack of maintenance contributed to structural deterioration?	Yes ___ No ___ Describe _____	
Functional Adequacy	Smoothness:	Measurement _____ Very Good <input type="checkbox"/> Good <input type="checkbox"/> Fair <input type="checkbox"/> Poor <input type="checkbox"/> Very Poor <input type="checkbox"/>	
	Cause of smoothness deficiency:	Foundation movement Localized distress or deterioration Other _____	
	Noise	Measurement _____ Satisfactory <input type="checkbox"/> Questionable <input type="checkbox"/> Unsatisfactory <input type="checkbox"/>	
	Friction resistance	Measurement _____ Satisfactory <input type="checkbox"/> Questionable <input type="checkbox"/> Unsatisfactory <input type="checkbox"/>	
	Subsurface Drainage	Climate (moisture and temperature region)	Moisture throughout the year: <ul style="list-style-type: none"> • Seasonal moisture or high water table • Very little moisture • Deep frost penetration • Freeze-thaw cycles • No frost problems
		Presence of moisture-accelerated distress	Yes <input type="checkbox"/> Possible <input type="checkbox"/> No <input type="checkbox"/>
Subsurface drainage facilities		Satisfactory <input type="checkbox"/> Marginal <input type="checkbox"/> Unsatisfactory <input type="checkbox"/>	
Surface drainage facilities		Satisfactory <input type="checkbox"/> Marginal <input type="checkbox"/> Unsatisfactory <input type="checkbox"/>	
Has lack of maintenance contributed to deterioration of drainage facilities?		Yes <input type="checkbox"/> No <input type="checkbox"/> Describe: _____	

Table B.7 continued on the next page.

Table B.7—Checklist of Factors for Overall Pavement Condition Assessment and Problem Definition

Facet	Factors	Description		
Materials Durability	Presence of durability-related distress (surface layer)	1. Little to not durability-related distress. 2. Moderate durability-related distress 3. Major durability-related distress		
	Base erosion or stripping	1. Little or no base erosion or stripping 2. Moderate base erosion or stripping 3. Major base erosion or stripping		
	Nondestructive testing (GPR testing)	Determine areas with material deterioration/moisture damage (stripping)		
Shoulder Adequacy	Surface condition	1. Little or not load-associated/joint distress 2. Moderate load-associated/joint distress 3. Major load-associated/joint distress 4. Structural load-carrying capacity deficiency: (yes or no)		
	Localized deteriorated areas	Yes	No	Location:
Condition- Performance Variability	Does the project section include significant deterioration of the following: • Bridge approaches • Intersections • Lane to lane • Cuts and fills	Yes		No
	Is there a systematic variation in pavement condition along project (localized variation)?	Yes		No
	Systematic lane to lane variation in pavement condition	Yes		No
Miscellaneous	PCC joint damage: • Is there adequate load transfer (transverse joints)? • Is there adequate load transfer (centerline joint)? • Is there excessive centerline joint width? • Is there adequate load transfer (lane-shoulder)? • Is there joint seal damage? • Is there excessive joint spalling (transverse)? • Is there excessive joint spalling (longitudinal)? • Has there been any blowups?	Yes		No
Constraints	Are detours available for rehabilitation construction?	Yes		No
	Should construction be accomplished under traffic	Yes		No
	Can construction be done during off-peak hours	Yes		No
	Bridge clearance problems?	Yes		No
	Lateral obstruction problems	Yes		No
	Utility problems/issues	Yes		No
	Other constraint problems	Yes		No

Table B.8 provides a summary of the standard test procedures that are recommended for determining the various material properties required for the local calibration process. The test protocols are listed by material type. In keeping with the MEPDG Manual of Practice, the standard AASHTO test protocols are provided. When necessary (or if an AASHTO test procedure is not available) an equivalent ASTM test protocol is identified.

Table B.8—Summary of Standard Test Procedures to be used for the Laboratory and Field Tests

Layer type (new and rehabilitation)	Measured Property	Standard AASHTO Test Protocol
All	FWD backcalculated layer modulus	AASHTO T 256 and ASTM D 5858
HMA layer	Unit weight	AASHTO T 166
	Effective asphalt content by volume	AASHTO T-308
	Gradation	AASHTO T 27 (cores or blocks)
	Max. theoretical specific gravity	Max. theoretical specific gravity
	Air voids (If MDOT chooses to perform this test)	AASHTO T 209 (cores)
	Asphalt recovery (If MDOT chooses to perform this test)	AASHTO T 164/T 170/T 319 (cores)
PCC layer	Unit weight	AASHTO T 121
	Compressive strength	AASHTO T 22
	CTE	AASHTO T 336
	Young's modulus	ASTM C 469 (AASHTO Test procedure unavailable)
Unbound layers	DCP (field testing)	
	Moisture content and density (from Shelby tube samples)	AASHTO T 265
	Gradation	AASHTO T 88
	Atterberg limits	AASHTO T 89 and T 90
Stabilized layers (if samples can be recovered)	Density	Measure weight of core recovered and determine density
	Unconfined compressive strength	AASHTO T22
	Elastic Modulus	No testing required. Estimate using levels 2 and 3. Will use modulus from FWD.

ATTACHMENT B.1

MATERIALS SAMPLING & FIELD TESTING PLAN FOR NEW CONSTRUCTION & OVERLAY PROJECTS – NON-LTPP SECTIONS

Test Section Identification: _____
 Highway/Route Number: _____
 Number of Sample Lots: _____

Pavement Cross Section (Planning Pavement Sampling Operation):

Layer & Material Type		Layer Thickness, inches	
		Plan	Field
1			
2			
3			
4			
5			

Material Sampling/Laboratory Testing Plan Summary (Layer thickness should be measured for each layer in the pavement structure during the sampling operation):

Material/Layer Type	Material Properties				
Bound or Stabilized Layers					
HMA	Bulk & Maximum Specific Gravities	Asphalt Content	Gradation	Combined Aggregate Specific Gravity	
PCC	CTE	Modulus	Compressive strength		
Lime, LFA, or Cement Stabilized Base	Density	Elastic Modulus	Strength	Visual Examination of Material	
Unbound Materials and Layers					
Aggregate Base or Subbase – 1	Water Content	Density	Atterberg Limits	Gradation	DCP
Aggregate Base or Subbase – 2	Water Content	Density	Atterberg Limits	Gradation	DCP
Embankment or Subgrade	Water Content	Density	Atterberg Limits	Gradation	DCP

General Instructions and Guidelines for Sampling and Material Recovery for Laboratory Testing and Materials Characterization:

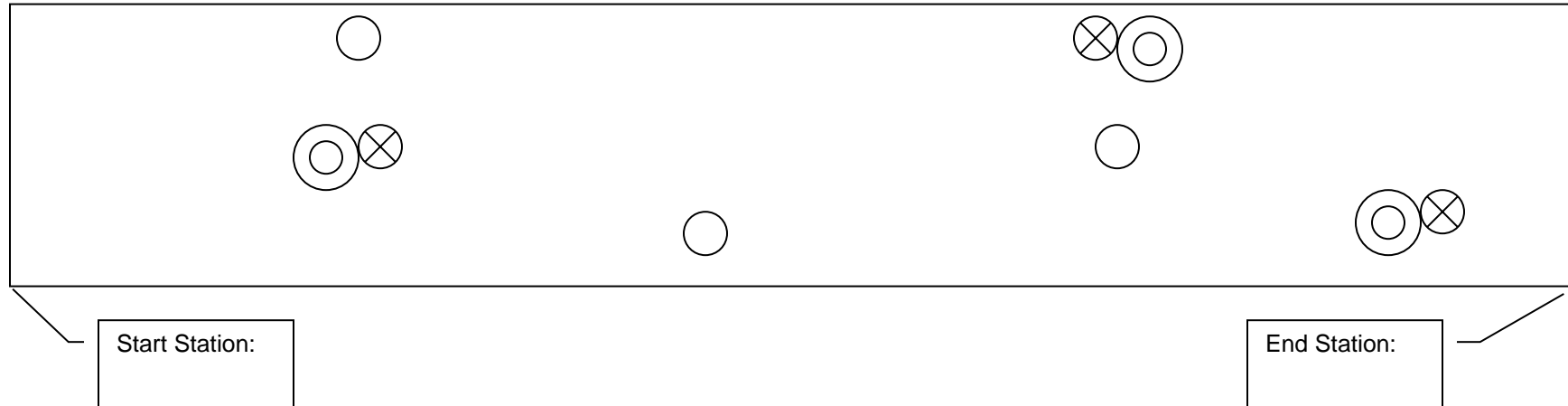
1. Location of all 6-inch diameter cores should be outside the wheel path area.
2. The sampling and materials recovery process should NOT be performed when there is a possibility that the unbound layers could be frozen beneath the pavement surface.
3. Prior to or after marking the cores on the pavement surface, the visual distress survey maps should be confirmed. Identify on the maps any discrepancies that are found.
4. Deflection basins should be measured with the Falling Weight Deflectometer prior to the coring program or certainly within the same season or moisture condition that the moisture content samples and cores were taken.
5. Do not locate any core across cracks or areas with raveling and other surface defects. Additional cores should be used to confirm the direction of cracking (top-down versus bottom-up cracking). Two cores should be taken in or adjacent to the wheel path to determine the direction of crack propagation. If the cores reveal different locations of crack initiation, additional cores should be taken. This is a decision of the field personnel. Photographs of all cores should be taken.
6. Locate cores outside the wheel path areas, if possible. All cores taken should be at least 6-inches in diameter. Some of the cores need to be 8-inches in diameter. The attached field sampling plans show the general location of the 6 and 8-inch diameter cores. It is suggested that two coring rigs be on site to reduce the amount of time needed to take the cores. If only one coring rig is available, then one size core can be used. 8-inch diameter cores were noted to ensure that sufficient materials can be recovered from the unbound layers for some of the laboratory tests.
7. A dry coring process is preferred, but cores can be taken using a wet coring process. If a wet coring process is used, any excess or free water should be removed from the bottom of the holes immediately after the cores have been extracted from the pavement for the locations where the dynamic cone penetrometer tests are to be performed and where auger samples are to be taken for measuring the moisture content of the unbound materials.
8. If cores are damaged during recovery, take an additional core in an adjacent area. Damaged is defined as cores that are found to have cracks beneath the surface, disintegrate during the wet coring operation, because of stripping beneath the surface, and crack or break when trying to extract them from the pavement. If layers become unbonded or delaminated during the coring operations or during the extraction process, another core does NOT need to be taken.
9. Dynamic cone penetrometer (DCP) tests should be made at the locations designated. If a wet coring process is used to recover the cores, any free water should be removed from the hole immediately after the core has been extracted and prior to performing the DCP test.
10. Auger samples of the unbound layers (aggregate base materials and soils samples 12 inches within the top of the embankment or foundation) should be taken at the locations designated. These auger samples should be placed in containers or heavy duty plastic bags to prevent changes in moisture content.
11. After samples are taken, measure the thickness of the unbound pavement layers.
12. Two Shelby tubes should be taken in the embankment and subgrade soils below the stabilized or unbound aggregate base layers to recover "undisturbed" soil samples for measuring in place densities and moisture contents. If the soils are non-cohesive

- and undisturbed samples is not possible, auger samples should be recovered for classification and moisture content tests.
13. All samples should be marked with the sampling number identification scheme for future reference and proper identification during laboratory tests.




Only two sampling locations are needed for the confirmation of layer material type and thickness and in place material condition. These two locations are the same as used within SHRP for confirming the LTPP test sections prior to the extensive or more detailed sampling program for measuring multiple properties and field testing.

NOTE: In preparing the materials sampling and field testing plan, one section per roadway segment was assumed. If there are significant changes in the distress magnitudes between the limits established for the section, however, multiple sections should be identified and materials/cores recovered from each section, or the field personnel identify and notate the type of distress associated with the section of pavement sampled. This decision should be made by the field engineer.

Sample Lot – 1; Number of Cores = 9.



LEGEND:

-  Location of 6-inch diameter cores and Dynamic Cone Penetrometer Tests
-  Location of 8-inch diameter cores; including auger samples and/or one or two undisturbed Shelby Tube samples for water content and other tests of the unbound materials and soils.
-  Locations of 6-inch diameter cores for air void determination (bulk and maximum specific gravity tests)

The above cores can be relocated depending on the distresses found along the test section. If multiple sections are required, treat the sections as two different sections.

APPENDIX C—MS-ATLAS: TRUCK TRAFFIC ANALYSIS TOOL

The Planning Division at MDOT is the primary user of MS-ATLAS and is tasked with providing traffic data for MDOT's pavement design projects. These data are used for both new and rehabilitation designs. The program works off a standalone computer and uses/saves data stored in a Microsoft Access Database file on the standalone computer and is not on a server. With the current set up, the program is not accessible to multiple users. Additionally, there are certain limitations with data integration across other databases in the Department. The MS-ATLAS tool has a Geographic Information System (GIS) database and the State GIS information is managed in an ORACLE Spatial database by a different Division within MDOT. The MS-ATLAS database is not set up for concurrency with MDOT's GIS database.

The analysis performed by MS-ATLAS and its features are relatively limited in light of the following:

- Growing traffic characterization needs in support of pavement design.
- Special loading analysis necessary to support new legislature policies on truck overloads in Mississippi and to analyze their effects on pavement performance.
- Updates to the data collection hardware and procedures.
- Software used in the development of DARWin-ME necessitating MS-ATLAS output files in an .xml format.

Finally, the current MS-ATLAS software format is incompatible with the next generation of Windows platform. It will be necessary to perform the required traffic analysis using a tool compatible with DARWin-ME and the next generation of Windows.

Until the adoption of the MEPDG procedure, traffic inputs were fairly minimal for pavement design. Traffic inputs included traffic volume in equivalent single axle loads (ESALs), percent trucks and truck loading factors. The MEPDG, on the other hand, uses the standard FHWA vehicle classifications in determining the traffic inputs to the program. Specifically, it needs the normalized truck volume and axle load distributions for vehicle classes 4 to 13.

The traffic analysis tool MS-ATLAS was designed and developed to read data collected by weigh-in-motion (WIM) sites to develop the normalized axle load spectra required for the MEPDG damage analysis and performance predictions. The current version of MS-ATLAS includes four modules.

1. ATR Data Processing – This module imports automated traffic recorder (ATR) data in ASCII format and performs traffic volume calculations necessary to determine the average annual daily truck traffic. This data is stored in the MS Access database. The raw data can be read by FHWA's Traffic Monitoring Guide (TMG) data formats for automated vehicle classifiers and weigh-in-motion (WIM) sensors from the 2nd and 3rd versions of TMG. The 3rd version of TMG used by MDOT uses the W-Card and C-Card. The data formats for the 2nd version, 7-card and 4-card, are not used by MDOT and this feature is unnecessary for MS-ATLAS today.
2. Traffic Data Analysis – This module analyzes ATR data to produce MEPDG required data tables such as the normalized vehicle class distribution, normalized axle load

- spectra by class, axle per class coefficients, truck volume and growth, monthly truck volume adjustment factors, hourly truck distribution. It also calculates the total ESALs loading for the analysis period. This module contains the analysis essential to develop inputs for MEPDG based procedures. Data tables generated are charted as per requirements envisioned at the time of MS-ATLAS development.
3. Traffic Library Exploration – This module allows users to explore traffic data library either through user-set filters or through a GIS enabled map. The GIS mapping is basic and the information is plotted on a line map of the State.
 4. Generate MEPDG Inputs – This module generates traffic input files for MEPDG. The user is required to select either an ATR site or use regional defaults. The formats of the files generated are compatible with MEPDG Software Versions. However, an additional xml conversion will be necessary to import the files into DARWin-ME tool.

The MS-ATLAS tool was also written on a VBNET platform, which is incompatible with future Windows platforms. The analysis capabilities of MS-ATLAS need to be transferred over to a more current programming environment. Several discussions were held with MDOT to identify the traffic analysis needs and any related upgrades to the MS-ATLAS tool. The following requirements were identified through detailed discussions with MDOT Research and Planning Divisions:

- The MS-ATLAS software will take roadway data captured by ATR sites and apply it as input to the AASHTOWare DARWinME software using lessons learned in the production of the MEPDG software and earlier software prototypes.
- The MS-ATLAS software will accept the input of the new format files from ATR machines throughout the state of Mississippi. This will be the W-Card and C-Card formats compatible with Version 3 and higher of TMG ATR data formats.
- The ATR data input to MS-ATLAS will be stored in a Microsoft Access relational database. This database will reside on a central server identified by MDOT and the program will allow for the repositioning of this database from within the software. This will enable multiple users to access the database and be aware of updates made to the software.
- MS-ATLAS will produce spectra of traffic based on the ATR data and user inputs.
- The output from the MS-ATLAS program will be in a format that can be directly imported into the AASHTOWare DARWinME software. When an output is created for the DARWinME program, a short report of input selections in producing the output will be included.
- ATR sites in Mississippi will be displayed on a Google Map display to show their location and their proximity to nearby roads and county markers. The ATR site information will come from the ORACLE Spatial Database at MDOT. The MS-ATLAS software will not allow the addition of ATR sites. That will be done through the existing ORACLE Spatial Database. The reference to the ORACLE Spatial

Database will allow for the changing of the location of this database within the MDOT network.

- The MS-ATLAS software will analyze the traffic data entered to produce spectra required by the DARWinME program such as normalized axle load spectra by class, axle per class coefficients, truck volume, estimated growth in truck traffic, monthly truck volume adjustment coefficients, hourly truck volume distribution, and estimated ESALs.
- The MS-ATLAS software will include options to analyze specific special loading cases and have the capability to show comparisons of default cases and special loading cases through the charting tools.
- The software created will reflect the current state of the software art, and be compatible in techniques and useful software life with the DARWinME software.

[This page intentionally left blank.]

APPENDIX D—NORMALIZED AXLE LOAD DISTRIBUTION FACTORS OR AXLE LOAD SPECTRA

Appendix D includes the normalized axle load distribution factors that were determined from the Mississippi State University study on truck traffic data collected on Mississippi roadways (*Buchanan, 2004*). Tables D.1 to D.3 provide the axle load distribution factors for TTC group 3, Tables 26 to 28 for TTC Group 6, Tables D.4 to D.6 for TTC group 7, Tables D.7 to D.9 for TTC group 12, and Tables D.10 to D.12 for TTC group 15.

Table D.1—Normalized Single Axle Load Spectra for TTC Group 3

Axle Load	Vehicle/Truck Class Number										
	lbs.	4	5	6	7	8	9	10	11	12	13
4	1,000	0.00	0.00	0.00	0.00	0.05	0.00	0.00	0.00	0.00	0.00
9	2,000	0.00	0.00	0.07	0.00	0.18	0.00	0.00	0.00	0.00	0.00
13	3,000	0.28	5.40	1.01	3.89	7.39	0.35	0.00	0.04	0.00	55.64
18	4,000	1.06	9.42	0.47	0.56	2.88	0.61	0.00	0.53	0.58	6.88
22	5,000	1.11	24.48	1.07	4.33	8.31	1.14	0.63	2.52	3.29	0.00
27	6,000	1.56	12.74	2.99	2.22	6.81	1.75	0.84	4.86	7.16	0.00
31	7,000	3.86	10.32	6.29	9.330	8.83	3.84	4.00	6.31	10.74	4.79
36	8,000	6.93	9.33	11.76	10.910	11.77	8.22	11.59	8.01	11.97	1.67
40	9,000	11.08	7.82	18.52	15.37	13.27	13.87	19.09	10.49	15.21	15.02
44	10,000	14.42	6.09	20.12	7.94	11.57	18.15	25.33	12.18	15.56	1.70
49	11,000	17.83	4.51	17.23	19.89	8.44	19.37	22.04	11.18	11.85	7.57
53	12,000	13.60	3.06	10.32	4.07	5.62	14.83	11.24	9.31	9.80	2.30
58	13,000	11.16	2.06	5.74	2.96	3.95	7.30	4.35	7.93	5.71	0.99
62	14,000	8.73	1.45	2.53	1.11	2.95	3.18	0.71	6.88	3.70	0.33
67	15,000	4.12	1.12	0.81	1.85	2.32	1.75	0.18	5.69	2.26	1.04
71	16,000	2.41	0.87	0.44	5.00	1.79	1.33	0.00	4.66	1.51	0.00
76	17,000	1.12	0.46	0.33	1.39	1.45	1.22	0.00	3.43	0.37	0.00
80	18,000	0.43	0.33	0.11	1.39	0.98	1.07	0.00	2.50	0.19	0.00
85	19,000	0.15	0.21	0.09	5.00	0.63	0.81	0.00	1.72	0.05	2.08
89	20,000	0.09	0.14	0.10	0.00	0.37	0.54	0.00	0.94	0.05	0.00
93	21,000	0.02	0.07	0.00	0.00	0.23	0.31	0.00	0.40	0.00	0.00
98	22,000	0.02	0.04	0.00	1.39	0.09	0.17	0.00	0.25	0.00	0.00
102	23,000	0.02	0.02	0.00	0.00	0.09	0.09	0.00	0.11	0.00	0.00
107	24,000	0.00	0.02	0.00	0.00	0.01	0.05	0.00	0.04	0.00	0.00
111	25,000	0.00	0.01	0.00	0.00	0.00	0.01	0.00	0.01	0.00	0.00
116	26,000	0.00	0.01	0.00	0.00	0.00	0.01	0.00	0.01	0.00	0.00
120	27,000	0.00	0.01	0.00	1.39	0.00	0.00	0.00	0.00	0.00	0.00
125	28,000	0.00	0.00	0.00	0.00	0.00	0.00	0.00	0.00	0.00	0.00
129	29,000	0.00	0.00	0.00	0.00	0.00	0.00	0.00	0.00	0.00	0.00
133	30,000	0.00	0.00	0.00	0.00	0.00	0.00	0.00	0.00	0.00	0.00
138	31,000	0.00	0.00	0.00	0.00	0.00	0.00	0.00	0.00	0.00	0.00
142	32,000	0.00	0.00	0.00	0.00	0.00	0.00	0.00	0.00	0.00	0.00
147	33,000	0.00	0.00	0.00	0.00	0.00	0.00	0.00	0.00	0.00	0.00
151	34,000	0.00	0.00	0.00	0.00	0.00	0.00	0.00	0.00	0.00	0.00
156	35,000	0.00	0.00	0.00	0.00	0.00	0.00	0.00	0.00	0.00	0.00
160	36,000	0.00	0.00	0.00	0.00	0.00	0.00	0.00	0.00	0.00	0.00
165	37,000	0.00	0.01	0.00	0.00	0.00	0.00	0.00	0.00	0.00	0.00
169	38,000	0.00	0.00	0.00	0.00	0.00	0.00	0.00	0.00	0.00	0.00
173	39,000	0.00	0.00	0.00	0.00	0.00	0.00	0.00	0.00	0.00	0.00
178	40,000	0.00	0.00	0.00	0.00	0.00	0.00	0.00	0.00	0.00	0.00

Table D.2—Normalized Tandem Axle Load Spectra for TTC Group 3

Axle Load	Vehicle/Truck Class Number										
	lbs.	4	5	6	7	8	9	10	11	12	13
9	2,000	0.00	0.00	0.00	0.00	0.00	0.00	0.00	0.00	0.00	0.00
18	4,000	0.00	0.00	0.00	0.00	0.00	0.00	0.00	0.00	0.00	0.00
27	6,000	0.00	0.00	2.95	19.56	8.81	0.60	0.00	0.00	0.00	2.38
36	8,000	0.13	84.63	15.27	8.07	7.88	3.48	0.71	0.00	0.00	0.00
44	10,000	0.26	8.70	27.21	19.04	14.65	6.65	1.55	0.00	0.48	0.00
53	12,000	0.18	2.22	12.50	12.89	17.83	7.75	0.71	15.56	4.92	2.38
62	14,000	0.54	2.22	7.01	1.84	15.92	7.57	36.05	15.56	14.93	2.38
71	16,000	3.05	2.22	9.29	1.50	11.76	6.45	16.05	15.56	18.33	35.71
80	18,000	6.58	0.00	6.49	8.64	7.00	5.66	7.71	21.11	26.90	2.38
89	20,000	11.84	0.00	4.05	6.36	4.52	5.28	29.38	21.11	20.75	2.38
98	22,000	19.16	0.00	2.92	0.56	3.69	5.27	4.50	11.11	13.21	2.38
107	24,000	26.19	0.00	2.34	2.49	2.57	5.53	1.67	0.00	0.24	0.00
116	26,000	17.33	0.00	2.26	4.22	1.15	5.99	1.67	0.00	0.24	19.05
125	28,000	8.19	0.00	2.71	0.00	0.99	6.55	0.00	0.00	0.00	2.38
133	30,000	3.71	0.00	1.53	0.00	0.91	7.12	0.00	0.00	0.00	2.38
142	32,000	1.70	0.00	1.27	0.00	0.82	7.68	0.00	0.00	0.00	2.38
151	34,000	0.61	0.00	1.00	3.70	0.59	7.26	0.00	0.00	0.00	10.71
160	36,000	0.24	0.00	0.42	0.00	0.37	4.95	0.00	0.00	0.00	10.71
169	38,000	0.18	0.00	0.22	11.11	0.25	2.77	0.00	0.00	0.00	2.38
178	40,000	0.05	0.00	0.14	0.00	0.15	1.56	0.00	0.00	0.00	0.00
187	42,000	0.05	0.00	0.11	0.00	0.07	0.89	0.00	0.00	0.00	0.00
196	44,000	0.00	0.00	0.11	0.00	0.04	0.47	0.00	0.00	0.00	0.00
205	46,000	0.00	0.00	0.09	0.00	0.02	0.26	0.00	0.00	0.00	0.00
214	48,000	0.00	0.00	0.04	0.00	0.01	0.13	0.00	0.00	0.00	0.00
222	50,000	0.00	0.00	0.04	0.00	0.00	0.06	0.00	0.00	0.00	0.00
231	52,000	0.00	0.00	0.04	0.00	0.00	0.04	0.00	0.00	0.00	0.00
240	54,000	0.00	0.00	0.00	0.00	0.00	0.01	0.00	0.00	0.00	0.00
249	56,000	0.00	0.00	0.00	0.00	0.00	0.00	0.00	0.00	0.00	0.00
258	58,000	0.00	0.00	0.00	0.00	0.00	0.00	0.00	0.00	0.00	0.00
267	60,000	0.00	0.00	0.00	0.00	0.00	0.00	0.00	0.00	0.00	0.00
276	62,000	0.00	0.00	0.00	0.00	0.00	0.00	0.00	0.00	0.00	0.00
285	64,000	0.00	0.00	0.00	0.00	0.00	0.00	0.00	0.00	0.00	0.00
294	66,000	0.00	0.00	0.00	0.00	0.00	0.00	0.00	0.00	0.00	0.00
302	68,000	0.00	0.00	0.00	0.00	0.00	0.00	0.00	0.00	0.00	0.00
311	70,000	0.00	0.00	0.00	0.00	0.00	0.00	0.00	0.00	0.00	0.00
320	72,000	0.00	0.00	0.00	0.00	0.00	0.00	0.00	0.00	0.00	0.00
329	74,000	0.00	0.00	0.00	0.00	0.00	0.00	0.00	0.00	0.00	0.00
338	76,000	0.00	0.00	0.00	0.00	0.00	0.00	0.00	0.00	0.00	0.00
347	78,000	0.00	0.00	0.00	0.00	0.00	0.00	0.00	0.00	0.00	0.00
356	80,000	0.00	0.00	0.00	0.00	0.00	0.00	0.00	0.00	0.00	0.00

Table D.3—Normalized Tridem Axle Load Spectra for TTC Group 3

Axle Load		Vehicle/Truck Class Number										
		4	5	6	7	8	9	10	11	12	13	
kN	lbs.											
13	3,000	0.00	0.00	0.00	0.00	0.00	0.00	0.00	0.00	0.00	0.00	0.00
27	6,000	0.00	0.00	0.00	0.00	5.56	0.00	0.00	0.00	0.00	0.00	0.00
40	9,000	0.00	0.00	0.00	0.00	0.00	0.00	0.00	33.33	0.00	0.00	0.00
53	12,000	0.00	0.00	0.00	25.83	50.93	87.50	61.67	11.11	27.5	33.33	0.00
67	15,000	0.00	0.00	0.00	19.38	2.78	0.00	28.33	0.00	6.25	11.11	0.00
80	18,000	0.00	0.00	0.00	6.25	0.00	0.00	10.00	11.11	18.13	0.00	0.00
93	21,000	0.00	0.00	0.00	9.38	0.00	0.00	0.00	11.11	15.63	0.00	0.00
107	24,000	0.00	0.00	0.00	0.00	5.56	0.00	0.00	0.00	15.00	0.00	0.00
120	27,000	0.00	0.00	0.00	4.17	0.00	0.00	0.00	0.00	0.00	0.00	0.00
133	30,000	0.00	0.00	0.00	8.33	0.00	0.00	0.00	0.00	0.00	0.00	0.00
147	33,000	0.00	0.00	0.00	5.63	5.56	0.00	0.00	0.00	0.00	0.00	0.00
160	36,000	0.00	0.00	0.00	5.00	3.70	0.00	0.00	16.67	6.25	16.67	0.00
173	39,000	0.00	0.00	0.00	2.50	5.56	0.00	0.00	0.00	2.50	16.67	0.00
187	42,000	0.00	0.00	0.00	0.00	0.00	0.00	0.00	0.00	0.00	0.00	0.00
200	45,000	0.00	0.00	0.00	3.75	3.70	0.00	0.00	0.00	0.00	0.00	0.00
214	48,000	0.00	0.00	0.00	0.00	5.56	12.50	0.00	0.00	0.00	0.00	0.00
227	51,000	0.00	0.00	0.00	0.00	0.00	0.00	0.00	0.00	0.00	0.00	0.00
240	54,000	0.00	0.00	0.00	4.17	0.00	0.00	0.00	0.00	0.00	0.00	0.00
254	57,000	0.00	0.00	0.00	0.00	0.00	0.00	0.00	0.00	6.25	0.00	0.00
267	60,000	0.00	0.00	0.00	3.13	0.00	0.00	0.00	0.00	0.00	11.11	0.00
280	63,000	0.00	0.00	0.00	0.00	0.00	0.00	0.00	0.00	0.00	11.11	0.00
294	66,000	0.00	0.00	0.00	2.50	0.00	0.00	0.00	0.00	2.50	0.00	0.00
307	69,000	0.00	0.00	0.00	0.00	0.00	0.00	0.00	0.00	0.00	0.00	0.00
320	72,000	0.00	0.00	0.00	0.00	0.00	0.00	0.00	16.67	0.00	0.00	0.00
334	75,000	0.00	0.00	0.00	0.00	0.00	0.00	0.00	0.00	0.00	0.00	0.00
347	78,000	0.00	0.00	0.00	0.00	0.00	0.00	0.00	0.00	0.00	0.00	0.00
360	81,000	0.00	0.00	0.00	0.00	11.11	0.00	0.00	0.00	0.00	0.00	0.00
374	84,000	0.00	0.00	0.00	0.00	0.00	0.00	0.00	0.00	0.00	0.00	0.00
387	87,000	0.00	0.00	0.00	0.00	0.00	0.00	0.00	0.00	0.00	0.00	0.00
400	90,000	0.00	0.00	0.00	0.00	0.00	0.00	0.00	0.00	0.00	0.00	0.00
414	93,000	0.00	0.00	0.00	0.00	0.00	0.00	0.00	0.00	0.00	0.00	0.00
427	96,000	0.00	0.00	0.00	0.00	0.00	0.00	0.00	0.00	0.00	0.00	0.00
440	99,000	0.00	0.00	0.00	0.00	0.00	0.00	0.00	0.00	0.00	0.00	0.00
454	102,000	0.00	0.00	0.00	0.00	0.00	0.00	0.00	0.00	0.00	0.00	0.00
467	105,000	0.00	0.00	0.00	0.00	0.00	0.00	0.00	0.00	0.00	0.00	0.00
480	108,000	0.00	0.00	0.00	0.00	0.00	0.00	0.00	0.00	0.00	0.00	0.00
494	111,000	0.00	0.00	0.00	0.00	0.00	0.00	0.00	0.00	0.00	0.00	0.00
507	114,000	0.00	0.00	0.00	0.00	0.00	0.00	0.00	0.00	0.00	0.00	0.00
520	117,000	0.00	0.00	0.00	0.00	0.00	0.00	0.00	0.00	0.00	0.00	0.00
534	120,000	0.00	0.00	0.00	0.00	0.00	0.00	0.00	0.00	0.00	0.00	0.00

Table D.4—Normalized Single Axle Load Spectra for TTC Group 6

Axle Load		Vehicle/Truck Class Number										
		4	5	6	7	8	9	10	11	12	13	
kN	lbs.											
4	1,000	0.00	0.00	0.00	0.00	0.00	0.00	0.00	0.00	0.00	0.00	0.00
9	2,000	0.00	0.00	0.00	0.00	0.00	0.00	0.00	0.00	0.00	0.00	0.00
13	3,000	11.69	6.70	0.00	12.50	1.25	0.00	0.00	0.00	3.57	35.83	
18	4,000	27.92	6.93	0.00	0.00	0.00	0.00	0.00	1.92	0.00	0.00	
22	5,000	44.15	33.78	0.00	20.83	9.83	0.85	0.00	5.79	6.25	5.00	
27	6,000	16.23	13.02	6.25	20.83	11.08	1.65	0.00	7.72	10.27	5.00	
31	7,000	0.00	9.11	9.82	0.00	13.66	5.31	0.00	7.72	13.39	5.00	
36	8,000	0.00	7.24	17.11	0.00	14.75	9.04	0.00	7.72	13.39	5.00	
40	9,000	0.00	5.91	20.24	25.00	14.75	14.45	0.00	7.72	12.95	8.33	
44	10,000	0.00	4.53	17.11	0.00	12.11	16.83	0.00	7.72	9.82	13.33	
49	11,000	0.00	3.20	13.99	8.33	7.19	15.61	0.00	7.72	17.41	0.00	
53	12,000	0.00	2.65	7.74	0.00	6.00	12.74	0.00	7.72	6.70	10.00	
58	13,000	0.00	1.56	7.74	0.00	4.92	9.75	0.00	7.72	6.25	0.00	
62	14,000	0.00	1.33	0.00	0.00	2.28	6.76	0.00	7.72	0.00	0.00	
67	15,000	0.00	1.33	0.00	12.50	1.09	3.72	0.00	7.72	0.00	12.50	
71	16,000	0.00	1.33	0.00	0.00	0.00	1.80	0.00	7.72	0.00	0.00	
76	17,000	0.00	0.55	0.00	0.00	1.09	1.17	0.00	3.71	0.00	0.00	
80	18,000	0.00	0.60	0.00	0.00	0.00	0.31	0.00	3.71	0.00	0.00	
85	19,000	0.00	0.00	0.00	0.00	0.00	0.00	0.00	0.00	0.00	0.00	
89	20,000	0.00	0.24	0.00	0.00	0.00	0.00	0.00	0.00	0.00	0.00	
93	21,000	0.00	0.00	0.00	0.00	0.00	0.00	0.00	0.00	0.00	0.00	
98	22,000	0.00	0.00	0.00	0.00	0.00	0.00	0.00	0.00	0.00	0.00	
102	23,000	0.00	0.00	0.00	0.00	0.00	0.00	0.00	0.00	0.00	0.00	
107	24,000	0.00	0.00	0.00	0.00	0.00	0.00	0.00	0.00	0.00	0.00	
111	25,000	0.00	0.00	0.00	0.00	0.00	0.00	0.00	0.00	0.00	0.00	
116	26,000	0.00	0.00	0.00	0.00	0.00	0.00	0.00	0.00	0.00	0.00	
120	27,000	0.00	0.00	0.00	0.00	0.00	0.00	0.00	0.00	0.00	0.00	
125	28,000	0.00	0.00	0.00	0.00	0.00	0.00	0.00	0.00	0.00	0.00	
129	29,000	0.00	0.00	0.00	0.00	0.00	0.00	0.00	0.00	0.00	0.00	
133	30,000	0.00	0.00	0.00	0.00	0.00	0.00	0.00	0.00	0.00	0.00	
138	31,000	0.00	0.00	0.00	0.00	0.00	0.00	0.00	0.00	0.00	0.00	
142	32,000	0.00	0.00	0.00	0.00	0.00	0.00	0.00	0.00	0.00	0.00	
147	33,000	0.00	0.00	0.00	0.00	0.00	0.00	0.00	0.00	0.00	0.00	
151	34,000	0.00	0.00	0.00	0.00	0.00	0.00	0.00	0.00	0.00	0.00	
156	35,000	0.00	0.00	0.00	0.00	0.00	0.00	0.00	0.00	0.00	0.00	
160	36,000	0.00	0.00	0.00	0.00	0.00	0.00	0.00	0.00	0.00	0.00	
165	37,000	0.00	0.00	0.00	0.00	0.00	0.00	0.00	0.00	0.00	0.00	
169	38,000	0.00	0.00	0.00	0.00	0.00	0.00	0.00	0.00	0.00	0.00	
173	39,000	0.00	0.00	0.00	0.00	0.00	0.00	0.00	0.00	0.00	0.00	
178	40,000	0.00	0.00	0.00	0.00	0.00	0.00	0.00	0.00	0.00	0.00	

Table D.5—Normalized Tandem Axle Load Spectra for TTC Group 6

Axle Load		Vehicle/Truck Class Number										
		4	5	6	7	8	9	10	11	12	13	
kN	lbs.											
9	2,000	0.00	0.00	0.00	0.00	0.00	0.00	0.00	0.00	0.00	0.00	0.00
18	4,000	0.00	0.00	0.00	0.00	0.00	0.00	0.00	0.00	0.00	0.00	0.00
27	6,000	0.00	0.00	0.00	0.00	0.00	2.02	0.00	0.00	0.00	0.00	0.00
36	8,000	0.00	100.0	33.33	50.00	0.00	5.90	0.00	0.00	0.00	0.00	0.00
44	10,000	0.00	0.00	33.33	50.00	0.00	9.40	0.00	0.00	33.33	0.00	0.00
53	12,000	0.00	0.00	33.34	0.00	0.00	9.86	0.00	0.00	0.00	0.00	0.00
62	14,000	0.00	0.00	0.00	0.00	0.00	8.83	0.00	0.00	50.00	16.67	0.00
71	16,000	0.00	0.00	0.00	0.00	0.00	6.74	100.0	0.00	0.00	0.00	0.00
80	18,000	0.00	0.00	0.00	0.00	0.00	4.28	0.00	0.00	0.00	0.00	0.00
89	20,000	0.00	0.00	0.00	0.00	0.00	3.57	0.00	0.00	0.00	0.00	16.66
98	22,000	0.00	0.00	0.00	0.00	0.00	2.85	0.00	0.00	16.67	0.00	0.00
107	24,000	0.00	0.00	0.00	0.00	0.00	2.78	0.00	0.00	0.00	0.00	0.00
116	26,000	0.00	0.00	0.00	0.00	0.00	2.78	0.00	0.00	0.00	0.00	0.00
125	28,000	0.00	0.00	0.00	0.00	0.00	3.81	0.00	0.00	0.00	0.00	0.00
133	30,000	0.00	0.00	0.00	0.00	0.00	4.55	0.00	0.00	0.00	0.00	50.00
142	32,000	0.00	0.00	0.00	0.00	0.00	4.55	0.00	0.00	0.00	0.00	0.00
151	34,000	0.00	0.00	0.00	0.00	0.00	4.62	0.00	0.00	0.00	0.00	0.00
160	36,000	0.00	0.00	0.00	0.00	0.00	4.30	0.00	0.00	0.00	0.00	0.00
169	38,000	0.00	0.00	0.00	0.00	0.00	3.95	0.00	0.00	0.00	0.00	16.67
178	40,000	0.00	0.00	0.00	0.00	0.00	4.01	0.00	0.00	0.00	0.00	0.00
187	42,000	0.00	0.00	0.00	0.00	0.00	2.92	0.00	0.00	0.00	0.00	0.00
196	44,000	0.00	0.00	0.00	0.00	0.00	2.58	0.00	0.00	0.00	0.00	0.00
205	46,000	0.00	0.00	0.00	0.00	0.00	2.22	0.00	0.00	0.00	0.00	0.00
214	48,000	0.00	0.00	0.00	0.00	0.00	1.16	0.00	0.00	0.00	0.00	0.00
222	50,000	0.00	0.00	0.00	0.00	0.00	1.16	0.00	0.00	0.00	0.00	0.00
231	52,000	0.00	0.00	0.00	0.00	0.00	0.76	0.00	0.00	0.00	0.00	0.00
240	54,000	0.00	0.00	0.00	0.00	0.00	0.40	0.00	0.00	0.00	0.00	0.00
249	56,000	0.00	0.00	0.00	0.00	0.00	0.00	0.00	0.00	0.00	0.00	0.00
258	58,000	0.00	0.00	0.00	0.00	0.00	0.00	0.00	0.00	0.00	0.00	0.00
267	60,000	0.00	0.00	0.00	0.00	0.00	0.00	0.00	0.00	0.00	0.00	0.00
276	62,000	0.00	0.00	0.00	0.00	0.00	0.00	0.00	0.00	0.00	0.00	0.00
285	64,000	0.00	0.00	0.00	0.00	0.00	0.00	0.00	0.00	0.00	0.00	0.00
294	66,000	0.00	0.00	0.00	0.00	0.00	0.00	0.00	0.00	0.00	0.00	0.00
302	68,000	0.00	0.00	0.00	0.00	0.00	0.00	0.00	0.00	0.00	0.00	0.00
311	70,000	0.00	0.00	0.00	0.00	0.00	0.00	0.00	0.00	0.00	0.00	0.00
320	72,000	0.00	0.00	0.00	0.00	0.00	0.00	0.00	0.00	0.00	0.00	0.00
329	74,000	0.00	0.00	0.00	0.00	0.00	0.00	0.00	0.00	0.00	0.00	0.00
338	76,000	0.00	0.00	0.00	0.00	0.00	0.00	0.00	0.00	0.00	0.00	0.00
347	78,000	0.00	0.00	0.00	0.00	0.00	0.00	0.00	0.00	0.00	0.00	0.00
356	80,000	0.00	0.00	0.00	0.00	0.00	0.00	0.00	0.00	0.00	0.00	0.00

Table D.6—Normalized Tridem Axle Load Spectra for TTC Group 6

Axle Load		Vehicle/Truck Class Number										
		4	5	6	7	8	9	10	11	12	13	
kN	lbs.											
13	3,000	0.00	0.00	0.00	0.00	0.00	0.00	0.00	0.00	0.00	0.00	0.00
27	6,000	0.00	0.00	0.00	0.00	0.00	0.00	0.00	0.00	0.00	0.00	0.00
40	9,000	0.00	0.00	0.00	0.00	0.00	0.00	0.00	0.00	0.00	0.00	0.00
53	12,000	0.00	0.00	0.00	33.33	50.00	0.00	0.00	0.00	0.00	0.00	0.00
67	15,000	0.00	0.00	0.00	0.00	0.00	0.00	0.00	0.00	0.00	0.00	0.00
80	18,000	0.00	0.00	0.00	0.00	50.00	0.00	0.00	0.00	50.00	33.33	0.00
93	21,000	0.00	0.00	0.00	0.00	0.00	66.67	0.00	0.00	0.00	0.00	0.00
107	24,000	0.00	0.00	0.00	0.00	0.00	0.00	0.00	0.00	50.00	0.00	0.00
120	27,000	0.00	0.00	0.00	0.00	0.00	0.00	0.00	0.00	0.00	0.00	0.00
133	30,000	0.00	0.00	0.00	33.34	0.00	0.00	0.00	0.00	0.00	0.00	0.00
147	33,000	0.00	0.00	0.00	0.00	0.00	0.00	0.00	0.00	0.00	0.00	0.00
160	36,000	0.00	0.00	0.00	0.00	0.00	0.00	0.00	0.00	0.00	0.00	0.00
173	39,000	0.00	0.00	0.00	0.00	0.00	0.00	0.00	0.00	0.00	0.00	0.00
187	42,000	0.00	0.00	0.00	0.00	0.00	0.00	0.00	0.00	0.00	0.00	0.00
200	45,000	0.00	0.00	0.00	0.00	0.00	0.00	0.00	0.00	0.00	0.00	33.34
214	48,000	0.00	0.00	0.00	0.00	0.00	0.00	0.00	0.00	0.00	0.00	0.00
227	51,000	0.00	0.00	0.00	0.00	0.00	0.00	0.00	0.00	0.00	0.00	0.00
240	54,000	0.00	0.00	0.00	0.00	0.00	0.00	0.00	0.00	0.00	0.00	0.00
254	57,000	0.00	0.00	0.00	33.33	0.00	0.00	0.00	0.00	0.00	0.00	0.00
267	60,000	0.00	0.00	0.00	0.00	0.00	0.00	0.00	0.00	0.00	0.00	33.33
280	63,000	0.00	0.00	0.00	0.00	0.00	0.00	0.00	0.00	0.00	0.00	0.00
294	66,000	0.00	0.00	0.00	0.00	0.00	0.00	0.00	0.00	0.00	0.00	0.00
307	69,000	0.00	0.00	0.00	0.00	0.00	0.00	33.33	0.00	0.00	0.00	0.00
320	72,000	0.00	0.00	0.00	0.00	0.00	0.00	0.00	0.00	0.00	0.00	0.00
334	75,000	0.00	0.00	0.00	0.00	0.00	0.00	0.00	0.00	0.00	0.00	0.00
347	78,000	0.00	0.00	0.00	0.00	0.00	0.00	0.00	0.00	0.00	0.00	0.00
360	81,000	0.00	0.00	0.00	0.00	0.00	0.00	0.00	0.00	0.00	0.00	0.00
374	84,000	0.00	0.00	0.00	0.00	0.00	0.00	0.00	0.00	0.00	0.00	0.00
387	87,000	0.00	0.00	0.00	0.00	0.00	0.00	0.00	0.00	0.00	0.00	0.00
400	90,000	0.00	0.00	0.00	0.00	0.00	0.00	0.00	0.00	0.00	0.00	0.00
414	93,000	0.00	0.00	0.00	0.00	0.00	0.00	0.00	0.00	0.00	0.00	0.00
427	96,000	0.00	0.00	0.00	0.00	0.00	0.00	0.00	0.00	0.00	0.00	0.00
440	99,000	0.00	0.00	0.00	0.00	0.00	0.00	0.00	0.00	0.00	0.00	0.00
454	102,000	0.00	0.00	0.00	0.00	0.00	0.00	0.00	0.00	0.00	0.00	0.00
467	105,000	0.00	0.00	0.00	0.00	0.00	0.00	0.00	0.00	0.00	0.00	0.00
480	108,000	0.00	0.00	0.00	0.00	0.00	0.00	0.00	0.00	0.00	0.00	0.00
494	111,000	0.00	0.00	0.00	0.00	0.00	0.00	0.00	0.00	0.00	0.00	0.00
507	114,000	0.00	0.00	0.00	0.00	0.00	0.00	0.00	0.00	0.00	0.00	0.00
520	117,000	0.00	0.00	0.00	0.00	0.00	0.00	0.00	0.00	0.00	0.00	0.00
534	120,000	0.00	0.00	0.00	0.00	0.00	0.00	0.00	0.00	0.00	0.00	0.00

Table D.7—Normalized Single Axle Load Spectra for TTC Group 7

Axle Load		Vehicle/Truck Class Number										
		kN	lbs.	4	5	6	7	8	9	10	11	12
4	1,000	0.00	0.00	0.00	0.00	0.00	0.00	0.00	0.00	0.00	0.00	0.00
9	2,000	0.00	0.00	0.00	0.00	0.00	0.00	0.00	0.00	0.00	0.00	0.00
13	3,000	0.00	9.00	0.00	0.00	3.49	0.98	6.22	0.71	1.19	34.30	
18	4,000	0.00	9.97	0.00	0.00	1.92	1.21	3.48	5.38	3.38	4.41	
22	5,000	67.11	31.52	0.76	9.17	11.24	2.69	5.53	14.51	8.37	6.19	
27	6,000	2.00	15.16	4.10	4.43	10.93	4.63	13.72	14.32	14.63	3.11	
31	7,000	2.89	9.54	7.89	5.40	13.28	7.90	18.03	12.75	16.22	2.34	
36	8,000	7.70	6.96	18.77	14.03	13.60	11.71	18.20	8.39	6.79	4.41	
40	9,000	4.44	5.31	12.59	11.07	12.13	14.70	8.34	7.15	9.50	8.48	
44	10,000	2.44	3.75	20.37	22.34	9.61	15.16	8.34	9.27	11.44	15.71	
49	11,000	5.70	2.69	12.47	4.05	7.73	13.36	8.34	6.28	10.88	3.90	
53	12,000	1.56	1.90	9.81	10.22	5.39	10.44	3.34	5.11	5.21	4.71	
58	13,000	5.26	1.37	5.71	0.82	4.12	6.93	3.34	5.51	2.49	7.05	
62	14,000	0.44	0.95	3.65	0.00	3.07	4.00	1.95	2.77	1.16	0.00	
67	15,000	0.44	0.74	2.26	5.33	1.82	2.14	0.60	1.50	3.31	0.00	
71	16,000	0.00	0.41	1.05	2.00	0.95	1.36	0.60	1.41	1.95	0.83	
76	17,000	0.00	0.27	0.44	0.00	0.48	0.94	0.00	1.26	0.00	2.17	
80	18,000	0.00	0.22	0.06	0.00	0.19	0.67	0.00	1.73	0.00	2.38	
85	19,000	0.00	0.11	0.06	1.43	0.04	0.48	0.00	0.63	1.34	0.00	
89	20,000	0.00	0.11	0.00	5.71	0.01	0.31	0.00	1.29	1.21	0.00	
93	21,000	0.00	0.00	0.00	0.00	0.00	0.23	0.00	0.00	0.00	0.00	
98	22,000	0.00	0.00	0.00	0.00	0.00	0.08	0.00	0.03	0.00	0.00	
102	23,000	0.00	0.01	0.00	0.00	0.00	0.02	0.00	0.00	0.75	0.00	
107	24,000	0.00	0.00	0.00	4.00	0.00	0.02	0.00	0.00	0.00	0.00	
111	25,000	0.00	0.00	0.00	0.00	0.00	0.02	0.00	0.00	0.00	0.00	
116	26,000	0.00	0.00	0.00	0.00	0.00	0.00	0.00	0.00	0.18	0.00	
120	27,000	0.00	0.00	0.00	0.00	0.00	0.00	0.00	0.00	0.00	0.00	
125	28,000	0.00	0.00	0.00	0.00	0.00	0.00	0.00	0.00	0.00	0.00	
129	29,000	0.00	0.00	0.00	0.00	0.00	0.00	0.00	0.00	0.00	0.00	
133	30,000	0.00	0.00	0.00	0.00	0.00	0.00	0.00	0.00	0.00	0.00	
138	31,000	0.00	0.00	0.00	0.00	0.00	0.00	0.00	0.00	0.00	0.00	
142	32,000	0.00	0.00	0.00	0.00	0.00	0.00	0.00	0.00	0.00	0.00	
147	33,000	0.00	0.00	0.00	0.00	0.00	0.00	0.00	0.00	0.00	0.00	
151	34,000	0.00	0.00	0.00	0.00	0.00	0.00	0.00	0.00	0.00	0.00	
156	35,000	0.00	0.00	0.00	0.00	0.00	0.00	0.00	0.00	0.00	0.00	
160	36,000	0.00	0.00	0.00	0.00	0.00	0.00	0.00	0.00	0.00	0.00	
165	37,000	0.00	0.00	0.00	0.00	0.00	0.00	0.00	0.00	0.00	0.00	
169	38,000	0.00	0.00	0.00	0.00	0.00	0.00	0.00	0.00	0.00	0.00	
173	39,000	0.00	0.00	0.00	0.00	0.00	0.00	0.00	0.00	0.00	0.00	
178	40,000	0.00	0.00	0.00	0.00	0.00	0.00	0.00	0.00	0.00	0.00	

Table D.8—Normalized Tandem Axle Load Spectra for TTC Group 7

Axle Load		Vehicle/Truck Class Number										
		4	5	6	7	8	9	10	11	12	13	
kN	lbs.											
9	2,000	0.00	0.00	0.00	0.00	0.00	0.00	0.00	0.00	0.00	0.00	0.00
18	4,000	0.00	0.00	0.00	0.00	0.00	0.00	0.00	0.00	0.00	0.00	0.00
27	6,000	0.00	0.00	0.00	0.00	55.15	2.68	0.00	0.00	0.00	0.00	0.00
36	8,000	0.00	75.00	1.17	11.11	9.74	6.09	1.79	12.50	0.00	0.00	0.00
44	10,000	0.00	25.00	17.54	11.11	12.07	8.62	3.87	16.67	25.00	5.00	5.00
53	12,000	0.00	0.00	26.25	0.00	11.39	9.09	1.79	0.00	29.17	6.25	6.25
62	14,000	0.00	0.00	12.50	0.00	6.62	8.03	8.04	12.50	12.50	0.00	0.00
71	16,000	0.00	0.00	9.17	16.67	3.18	6.45	58.04	0.00	12.50	5.00	5.00
80	18,000	0.00	0.00	4.56	33.33	1.50	5.08	8.04	0.00	12.50	12.50	12.50
89	20,000	100.0	0.00	3.35	0.00	0.35	4.38	3.87	0.00	0.00	0.00	5.00
98	22,000	0.00	0.00	6.17	0.00	0.00	4.38	6.25	0.00	0.00	0.00	2.50
107	24,000	0.00	0.00	5.49	11.11	0.00	4.78	4.17	0.00	0.00	0.00	11.25
116	26,000	0.00	0.00	4.54	0.00	0.00	5.08	4.17	0.00	0.00	0.00	25.00
125	28,000	0.00	0.00	3.35	0.00	0.00	5.15	0.00	0.00	8.33	0.00	0.00
133	30,000	0.00	0.00	3.35	0.00	0.00	5.13	0.00	12.50	0.00	12.50	12.50
142	32,000	0.00	0.00	1.28	0.00	0.00	4.74	0.00	0.00	0.00	0.00	0.00
151	34,000	0.00	0.00	1.28	0.00	0.00	4.38	0.00	33.33	0.00	0.00	0.00
160	36,000	0.00	0.00	0.00	0.00	0.00	3.75	0.00	0.00	0.00	0.00	0.00
169	38,000	0.00	0.00	0.00	16.67	0.00	3.25	0.00	12.50	0.00	0.00	0.00
178	40,000	0.00	0.00	0.00	0.00	0.00	2.55	0.00	0.00	0.00	0.00	0.00
187	42,000	0.00	0.00	0.00	0.00	0.00	2.00	0.00	0.00	0.00	0.00	0.00
196	44,000	0.00	0.00	0.00	0.00	0.00	1.64	0.00	0.00	0.00	0.00	0.00
205	46,000	0.00	0.00	0.00	0.00	0.00	1.04	0.00	0.00	0.00	0.00	6.25
214	48,000	0.00	0.00	0.00	0.00	0.00	0.55	0.00	0.00	0.00	0.00	0.00
222	50,000	0.00	0.00	0.00	0.00	0.00	0.40	0.00	0.00	0.00	0.00	0.00
231	52,000	0.00	0.00	0.00	0.00	0.00	0.33	0.00	0.00	0.00	0.00	0.00
240	54,000	0.00	0.00	0.00	0.00	0.00	0.16	0.00	0.00	0.00	0.00	2.50
249	56,000	0.00	0.00	0.00	0.00	0.00	0.10	0.00	0.00	0.00	0.00	0.00
258	58,000	0.00	0.00	0.00	0.00	0.00	0.05	0.00	0.00	0.00	0.00	6.25
267	60,000	0.00	0.00	0.00	0.00	0.00	0.05	0.00	0.00	0.00	0.00	0.00
276	62,000	0.00	0.00	0.00	0.00	0.00	0.05	0.00	0.00	0.00	0.00	0.00
285	64,000	0.00	0.00	0.00	0.00	0.00	0.02	0.00	0.00	0.00	0.00	0.00
294	66,000	0.00	0.00	0.00	0.00	0.00	0.00	0.00	0.00	0.00	0.00	0.00
302	68,000	0.00	0.00	0.00	0.00	0.00	0.00	0.00	0.00	0.00	0.00	0.00
311	70,000	0.00	0.00	0.00	0.00	0.00	0.00	0.00	0.00	0.00	0.00	0.00
320	72,000	0.00	0.00	0.00	0.00	0.00	0.00	0.00	0.00	0.00	0.00	0.00
329	74,000	0.00	0.00	0.00	0.00	0.00	0.00	0.00	0.00	0.00	0.00	0.00
338	76,000	0.00	0.00	0.00	0.00	0.00	0.00	0.00	0.00	0.00	0.00	0.00
347	78,000	0.00	0.00	0.00	0.00	0.00	0.00	0.00	0.00	0.00	0.00	0.00
356	80,000	0.00	0.00	0.00	0.00	0.00	0.00	0.00	0.00	0.00	0.00	0.00

Table D.9—Normalized Tridem Axle Load Spectra for TTC Group 7

Axle Load		Vehicle/Truck Class Number										
		4	5	6	7	8	9	10	11	12	13	
kN	lbs.											
13	3,000	0.00	0.00	0.00	0.00	0.00	0.00	0.00	0.00	0.00	0.00	0.00
27	6,000	0.00	0.00	0.00	0.00	0.00	0.00	0.00	0.00	0.00	0.00	0.00
40	9,000	0.00	0.00	0.00	0.00	0.00	0.00	0.00	0.00	0.00	0.00	0.00
53	12,000	0.00	0.00	0.00	25.00	66.67	33.33	66.67	0.00	58.33	25.00	
67	15,000	0.00	0.00	0.00	0.00	0.00	16.67	33.33	0.00	0.00	0.00	
80	18,000	0.00	0.00	0.00	0.00	0.00	16.67	0.00	0.00	16.67	20.83	
93	21,000	0.00	0.00	0.00	0.00	0.00	0.00	0.00	25.00	25.00	0.00	
107	24,000	0.00	0.00	0.00	0.00	0.00	0.00	0.00	0.00	0.00	0.00	
120	27,000	0.00	0.00	0.00	3.13	0.00	0.00	0.00	0.00	0.00	0.00	
133	30,000	0.00	0.00	0.00	6.25	0.00	0.00	0.00	0.00	0.00	8.33	
147	33,000	0.00	0.00	0.00	0.00	33.33	0.00	0.00	12.50	0.00	0.00	
160	36,000	0.00	0.00	0.00	9.38	0.00	0.00	0.00	0.00	0.00	8.33	
173	39,000	0.00	0.00	0.00	18.75	0.00	0.00	0.00	0.00	0.00	0.00	
187	42,000	0.00	0.00	0.00	12.50	0.00	0.00	0.00	0.00	0.00	0.00	
200	45,000	0.00	0.00	0.00	10.42	0.00	33.33	0.00	0.00	0.00	0.00	
214	48,000	0.00	0.00	0.00	6.25	0.00	0.00	0.00	12.50	0.00	12.50	
227	51,000	0.00	0.00	0.00	2.08	0.00	0.00	0.00	0.00	0.00	0.00	
240	54,000	0.00	0.00	0.00	6.25	0.00	0.00	0.00	0.00	0.00	0.00	
254	57,000	0.00	0.00	0.00	0.00	0.00	0.00	0.00	50.00	0.00	12.50	
267	60,000	0.00	0.00	0.00	0.00	0.00	0.00	0.00	0.00	0.00	0.00	
280	63,000	0.00	0.00	0.00	0.00	0.00	0.00	0.00	0.00	0.00	0.00	
294	66,000	0.00	0.00	0.00	0.00	0.00	0.00	0.00	0.00	0.00	0.00	
307	69,000	0.00	0.00	0.00	0.00	0.00	0.00	0.00	0.00	0.00	0.00	
320	72,000	0.00	0.00	0.00	0.00	0.00	0.00	0.00	0.00	0.00	0.00	
334	75,000	0.00	0.00	0.00	0.00	0.00	0.00	0.00	0.00	0.00	0.00	
347	78,000	0.00	0.00	0.00	0.00	0.00	0.00	0.00	0.00	0.00	12.50	
360	81,000	0.00	0.00	0.00	0.00	0.00	0.00	0.00	0.00	0.00	0.00	
374	84,000	0.00	0.00	0.00	0.00	0.00	0.00	0.00	0.00	0.00	0.00	
387	87,000	0.00	0.00	0.00	0.00	0.00	0.00	0.00	0.00	0.00	0.00	
400	90,000	0.00	0.00	0.00	0.00	0.00	0.00	0.00	0.00	0.00	0.00	
414	93,000	0.00	0.00	0.00	0.00	0.00	0.00	0.00	0.00	0.00	0.00	
427	96,000	0.00	0.00	0.00	0.00	0.00	0.00	0.00	0.00	0.00	0.00	
440	99,000	0.00	0.00	0.00	0.00	0.00	0.00	0.00	0.00	0.00	0.00	
454	102,000	0.00	0.00	0.00	0.00	0.00	0.00	0.00	0.00	0.00	0.00	
467	105,000	0.00	0.00	0.00	0.00	0.00	0.00	0.00	0.00	0.00	0.00	
480	108,000	0.00	0.00	0.00	0.00	0.00	0.00	0.00	0.00	0.00	0.00	
494	111,000	0.00	0.00	0.00	0.00	0.00	0.00	0.00	0.00	0.00	0.00	
507	114,000	0.00	0.00	0.00	0.00	0.00	0.00	0.00	0.00	0.00	0.00	
520	117,000	0.00	0.00	0.00	0.00	0.00	0.00	0.00	0.00	0.00	0.00	
534	120,000	0.00	0.00	0.00	0.00	0.00	0.00	0.00	0.00	0.00	0.00	

Table D.10—Normalized Single Axle Load Spectra for TTC Group 12

Axle Load		Vehicle/Truck Class Number										
		kN	lbs.	4	5	6	7	8	9	10	11	12
4	1,000	0.00	0.00	0.00	0.00	0.00	0.00	0.00	0.00	0.00	0.00	0.00
9	2,000	0.00	0.00	0.00	0.00	0.00	0.00	0.00	0.00	0.00	0.00	0.00
13	3,000	35.23	10.46	0.00	0.00	6.23	0.46	0.00	0.00	0.00	0.00	19.18
18	4,000	13.18	12.57	0.00	0.00	1.43	0.51	0.00	0.00	4.17	2.86	
22	5,000	44.47	42.55	0.00	0.72	19.20	1.43	0.00	0.00	6.25	6.86	
27	6,000	6.59	13.16	2.38	9.90	12.78	3.39	0.00	6.68	8.33	12.86	
31	7,000	0.53	6.39	9.52	1.42	12.78	8.52	0.00	5.87	6.53	15.19	
36	8,000	0.00	4.09	15.48	18.47	12.78	14.54	75.00	6.21	10.69	15.00	
40	9,000	0.00	2.57	16.67	8.57	12.78	17.38	25.00	13.49	5.44	10.19	
44	10,000	0.00	2.00	26.67	15.71	12.78	17.13	0.00	12.52	12.38	7.86	
49	11,000	0.00	1.32	17.14	17.62	6.23	15.23	0.00	13.96	7.92	0.00	
53	12,000	0.00	1.22	6.43	3.47	3.02	10.20	0.00	8.25	2.38	0.00	
58	13,000	0.00	1.10	2.86	2.04	0.00	6.07	0.00	11.11	8.61	0.00	
62	14,000	0.00	1.06	2.86	7.65	0.00	3.29	0.00	14.30	8.21	10.00	
67	15,000	0.00	0.74	0.00	9.66	0.00	1.34	0.00	2.86	3.77	0.00	
71	16,000	0.00	0.72	0.00	0.00	0.00	0.51	0.00	0.00	5.16	0.00	
76	17,000	0.00	0.03	0.00	0.00	0.00	0.00	0.00	0.00	2.38	0.00	
80	18,000	0.00	0.00	0.00	4.76	0.00	0.00	0.00	2.38	0.00	0.00	
85	19,000	0.00	0.03	0.00	0.00	0.00	0.00	0.00	0.00	5.00	0.00	
89	20,000	0.00	0.00	0.00	0.00	0.00	0.00	0.00	2.38	0.00	0.00	
93	21,000	0.00	0.00	0.00	0.00	0.00	0.00	0.00	0.00	0.00	0.00	
98	22,000	0.00	0.00	0.00	0.00	0.00	0.00	0.00	0.00	2.78	0.00	
102	23,000	0.00	0.00	0.00	0.00	0.00	0.00	0.00	0.00	0.00	0.00	
107	24,000	0.00	0.00	0.00	0.00	0.00	0.00	0.00	0.00	0.00	0.00	
111	25,000	0.00	0.00	0.00	0.00	0.00	0.00	0.00	0.00	0.00	0.00	
116	26,000	0.00	0.00	0.00	0.00	0.00	0.00	0.00	0.00	0.00	0.00	
120	27,000	0.00	0.00	0.00	0.00	0.00	0.00	0.00	0.00	0.00	0.00	
125	28,000	0.00	0.00	0.00	0.00	0.00	0.00	0.00	0.00	0.00	0.00	
129	29,000	0.00	0.00	0.00	0.00	0.00	0.00	0.00	0.00	0.00	0.00	
133	30,000	0.00	0.00	0.00	0.00	0.00	0.00	0.00	0.00	0.00	0.00	
138	31,000	0.00	0.00	0.00	0.00	0.00	0.00	0.00	0.00	0.00	0.00	
142	32,000	0.00	0.00	0.00	0.00	0.00	0.00	0.00	0.00	0.00	0.00	
147	33,000	0.00	0.00	0.00	0.00	0.00	0.00	0.00	0.00	0.00	0.00	
151	34,000	0.00	0.00	0.00	0.00	0.00	0.00	0.00	0.00	0.00	0.00	
156	35,000	0.00	0.00	0.00	0.00	0.00	0.00	0.00	0.00	0.00	0.00	
160	36,000	0.00	0.00	0.00	0.00	0.00	0.00	0.00	0.00	0.00	0.00	
165	37,000	0.00	0.00	0.00	0.00	0.00	0.00	0.00	0.00	0.00	0.00	
169	38,000	0.00	0.00	0.00	0.00	0.00	0.00	0.00	0.00	0.00	0.00	
173	39,000	0.00	0.00	0.00	0.00	0.00	0.00	0.00	0.00	0.00	0.00	
178	40,000	0.00	0.00	0.00	0.00	0.00	0.00	0.00	0.00	0.00	0.00	

Table D.11—Normalized Tandem Axle Load Spectra for TTC Group 12

Axle Load		Vehicle/Truck Class Number										
		4	5	6	7	8	9	10	11	12	13	
kN	lbs.											
9	2,000	0.00	0.00	0.00	0.00	0.00	0.00	0.00	0.00	0.00	0.00	0.00
18	4,000	0.00	0.00	0.00	0.00	0.00	0.00	0.00	0.00	0.00	0.00	0.00
27	6,000	0.00	0.00	0.00	0.00	0.00	2.38	0.00	0.00	0.00	0.00	26.67
36	8,000	0.00	66.67	50.00	0.00	0.00	7.92	0.00	0.00	0.00	0.00	0.00
44	10,000	0.00	33.33	50.00	0.00	0.00	10.03	0.00	0.00	0.00	0.00	0.00
53	12,000	0.00	0.00	0.00	0.00	0.00	11.9	0.00	0.00	0.00	0.00	20.00
62	14,000	0.00	0.00	0.00	0.00	0.00	10.07	0.00	33.33	0.00	40.00	0.00
71	16,000	0.00	0.00	0.00	0.00	0.00	7.22	0.00	0.00	50.00	0.00	0.00
80	18,000	0.00	0.00	0.00	0.00	0.00	4.81	0.00	33.33	0.00	0.00	0.00
89	20,000	0.00	0.00	0.00	100.0	0.00	3.77	0.00	0.00	25.00	0.00	0.00
98	22,000	0.00	0.00	0.00	0.00	0.00	2.85	0.00	0.00	0.00	0.00	6.67
107	24,000	0.00	0.00	0.00	0.00	0.00	2.76	100.0	0.00	0.00	0.00	0.00
116	26,000	0.00	0.00	0.00	0.00	0.00	3.33	0.00	0.00	25.00	0.00	0.00
125	28,000	0.00	0.00	0.00	0.00	0.00	3.33	0.00	0.00	0.00	0.00	0.00
133	30,000	0.00	0.00	0.00	0.00	0.00	3.33	0.00	0.00	0.00	0.00	6.67
142	32,000	0.00	0.00	0.00	0.00	0.00	4.04	0.00	0.00	0.00	0.00	0.00
151	34,000	0.00	0.00	0.00	0.00	0.00	4.04	0.00	0.00	0.00	0.00	0.00
160	36,000	0.00	0.00	0.00	0.00	0.00	3.45	0.00	0.00	0.00	0.00	0.00
169	38,000	0.00	0.00	0.00	0.00	0.00	3.91	0.00	0.00	0.00	0.00	0.00
178	40,000	0.00	0.00	0.00	0.00	0.00	2.83	0.00	0.00	0.00	0.00	0.00
187	42,000	0.00	0.00	0.00	0.00	0.00	1.64	0.00	16.67	0.00	0.00	0.00
196	44,000	0.00	0.00	0.00	0.00	0.00	1.64	0.00	16.67	0.00	0.00	0.00
205	46,000	0.00	0.00	0.00	0.00	0.00	1.64	0.00	0.00	0.00	0.00	0.00
214	48,000	0.00	0.00	0.00	0.00	0.00	1.64	0.00	0.00	0.00	0.00	0.00
222	50,000	0.00	0.00	0.00	0.00	0.00	0.92	0.00	0.00	0.00	0.00	0.00
231	52,000	0.00	0.00	0.00	0.00	0.00	0.46	0.00	0.00	0.00	0.00	0.00
240	54,000	0.00	0.00	0.00	0.00	0.00	0.00	0.00	0.00	0.00	0.00	0.00
249	56,000	0.00	0.00	0.00	0.00	0.00	0.00	0.00	0.00	0.00	0.00	0.00
258	58,000	0.00	0.00	0.00	0.00	0.00	0.00	0.00	0.00	0.00	0.00	0.00
267	60,000	0.00	0.00	0.00	0.00	0.00	0.00	0.00	0.00	0.00	0.00	0.00
276	62,000	0.00	0.00	0.00	0.00	0.00	0.00	0.00	0.00	0.00	0.00	0.00
285	64,000	0.00	0.00	0.00	0.00	0.00	0.00	0.00	0.00	0.00	0.00	0.00
294	66,000	0.00	0.00	0.00	0.00	0.00	0.00	0.00	0.00	0.00	0.00	0.00
302	68,000	0.00	0.00	0.00	0.00	0.00	0.00	0.00	0.00	0.00	0.00	0.00
311	70,000	0.00	0.00	0.00	0.00	0.00	0.00	0.00	0.00	0.00	0.00	0.00
320	72,000	0.00	0.00	0.00	0.00	0.00	0.00	0.00	0.00	0.00	0.00	0.00
329	74,000	0.00	0.00	0.00	0.00	0.00	0.00	0.00	0.00	0.00	0.00	0.00
338	76,000	0.00	0.00	0.00	0.00	0.00	0.00	0.00	0.00	0.00	0.00	0.00
347	78,000	0.00	0.00	0.00	0.00	0.00	0.00	0.00	0.00	0.00	0.00	0.00
356	80,000	0.00	0.00	0.00	0.00	0.00	0.00	0.00	0.00	0.00	0.00	0.00

Table D.12—Normalized Tridem Axle Load Spectra for TTC Group 12

Axle Load		Vehicle/Truck Class Number										
		4	5	6	7	8	9	10	11	12	13	
kN	lbs.											
13	3,000	0.00	0.00	0.00	0.00	0.00	0.00	0.00	0.00	0.00	0.00	0.00
27	6,000	0.00	0.00	0.00	0.00	0.00	0.00	0.00	0.00	0.00	0.00	0.00
40	9,000	0.00	0.00	0.00	0.00	0.00	0.00	0.00	0.00	0.00	0.00	0.00
53	12,000	0.00	0.00	0.00	0.00	16.67	100.0	100.0	0.00	0.00	0.00	28.57
67	15,000	0.00	0.00	0.00	0.00	0.00	0.00	0.00	0.00	0.00	0.00	0.00
80	18,000	0.00	0.00	0.00	50.00	16.67	0.00	0.00	0.00	0.00	0.00	0.00
93	21,000	0.00	0.00	0.00	0.00	0.00	0.00	0.00	0.00	0.00	0.00	14.29
107	24,000	0.00	0.00	0.00	0.00	0.00	0.00	0.00	0.00	0.00	0.00	14.29
120	27,000	0.00	0.00	0.00	50.00	0.00	0.00	0.00	0.00	0.00	0.00	14.29
133	30,000	0.00	0.00	0.00	0.00	0.00	0.00	0.00	0.00	0.00	0.00	0.00
147	33,000	0.00	0.00	0.00	0.00	16.67	0.00	0.00	100.0	100.0	0.00	0.00
160	36,000	0.00	0.00	0.00	0.00	1.29	0.00	0.00	0.00	0.00	0.00	0.00
173	39,000	0.00	0.00	0.00	0.00	1.29	0.00	0.00	0.00	0.00	0.00	0.00
187	42,000	0.00	0.00	0.00	0.00	5.89	0.00	0.00	0.00	0.00	0.00	0.00
200	45,000	0.00	0.00	0.00	0.00	12.55	0.00	0.00	0.00	0.00	0.00	0.00
214	48,000	0.00	0.00	0.00	0.00	7.18	0.00	0.00	0.00	0.00	0.00	14.29
227	51,000	0.00	0.00	0.00	0.00	19.22	0.00	0.00	0.00	0.00	0.00	0.00
240	54,000	0.00	0.00	0.00	0.00	1.29	0.00	0.00	0.00	0.00	0.00	14.29
254	57,000	0.00	0.00	0.00	0.00	1.29	0.00	0.00	0.00	0.00	0.00	0.00
267	60,000	0.00	0.00	0.00	0.00	0.00	0.00	0.00	0.00	0.00	0.00	0.00
280	63,000	0.00	0.00	0.00	0.00	0.00	0.00	0.00	0.00	0.00	0.00	0.00
294	66,000	0.00	0.00	0.00	0.00	0.00	0.00	0.00	0.00	0.00	0.00	0.00
307	69,000	0.00	0.00	0.00	0.00	0.00	0.00	0.00	0.00	0.00	0.00	0.00
320	72,000	0.00	0.00	0.00	0.00	0.00	0.00	0.00	0.00	0.00	0.00	0.00
334	75,000	0.00	0.00	0.00	0.00	0.00	0.00	0.00	0.00	0.00	0.00	0.00
347	78,000	0.00	0.00	0.00	0.00	0.00	0.00	0.00	0.00	0.00	0.00	0.00
360	81,000	0.00	0.00	0.00	0.00	0.00	0.00	0.00	0.00	0.00	0.00	0.00
374	84,000	0.00	0.00	0.00	0.00	0.00	0.00	0.00	0.00	0.00	0.00	0.00
387	87,000	0.00	0.00	0.00	0.00	0.00	0.00	0.00	0.00	0.00	0.00	0.00
400	90,000	0.00	0.00	0.00	0.00	0.00	0.00	0.00	0.00	0.00	0.00	0.00
414	93,000	0.00	0.00	0.00	0.00	0.00	0.00	0.00	0.00	0.00	0.00	0.00
427	96,000	0.00	0.00	0.00	0.00	0.00	0.00	0.00	0.00	0.00	0.00	0.00
440	99,000	0.00	0.00	0.00	0.00	0.00	0.00	0.00	0.00	0.00	0.00	0.00
454	102,000	0.00	0.00	0.00	0.00	0.00	0.00	0.00	0.00	0.00	0.00	0.00
467	105,000	0.00	0.00	0.00	0.00	0.00	0.00	0.00	0.00	0.00	0.00	0.00
480	108,000	0.00	0.00	0.00	0.00	0.00	0.00	0.00	0.00	0.00	0.00	0.00
494	111,000	0.00	0.00	0.00	0.00	0.00	0.00	0.00	0.00	0.00	0.00	0.00
507	114,000	0.00	0.00	0.00	0.00	0.00	0.00	0.00	0.00	0.00	0.00	0.00
520	117,000	0.00	0.00	0.00	0.00	0.00	0.00	0.00	0.00	0.00	0.00	0.00
534	120,000	0.00	0.00	0.00	0.00	0.00	0.00	0.00	0.00	0.00	0.00	0.00

Table D.13—Normalized Single Axle Load Spectra for TTC Group 15

Axle Load		Vehicle/Truck Class Number										
		kN	lbs.	4	5	6	7	8	9	10	11	12
4	1,000	0.00	0.00	0.00	0.00	0.00	0.00	0.00	0.00	0.00	0.00	0.00
9	2,000	0.00	0.00	0.00	0.00	0.00	0.00	0.00	0.00	0.00	0.00	0.00
13	3,000	8.33	27.65	0.00	6.25	35.37	0.00	0.00	23.99	0.32	8.40	
18	4,000	4.17	20.28	0.00	0.00	10.29	0.00	0.00	7.35	1.04	10.49	
22	5,000	0.00	24.32	3.46	0.00	30.78	3.33	9.72	9.27	13.86	4.58	
27	6,000	0.00	11.91	5.42	8.93	12.59	16.67	0.00	9.48	15.32	7.71	
31	7,000	12.50	5.28	4.88	8.63	6.04	26.67	52.08	7.87	2.50	6.25	
36	8,000	16.67	3.41	55.19	14.88	3.91	23.33	11.81	11.11	2.01	10.83	
40	9,000	8.33	2.39	3.83	4.17	0.34	23.33	0.00	6.43	0.32	8.33	
44	10,000	3.13	1.41	4.14	1.43	0.34	6.67	4.17	3.83	17.11	0.00	
49	11,000	3.13	1.57	3.30	4.17	0.34	0.00	5.56	1.79	3.15	4.86	
53	12,000	3.13	0.57	3.61	7.98	0.00	0.00	0.00	6.67	13.47	5.21	
58	13,000	3.13	0.50	10.75	3.81	0.00	0.00	0.00	1.30	0.97	0.00	
62	14,000	10.42	0.25	1.76	3.81	0.00	0.00	0.00	1.16	1.04	0.00	
67	15,000	3.13	0.25	1.38	1.43	0.00	0.00	0.00	1.81	1.04	0.00	
71	16,000	15.63	0.06	0.73	0.00	0.00	0.00	0.00	1.16	0.71	4.17	
76	17,000	0.00	0.06	0.31	0.00	0.00	0.00	0.00	1.16	0.00	16.67	
80	18,000	4.17	0.06	0.31	14.88	0.00	0.00	0.00	1.11	0.00	0.00	
85	19,000	0.00	0.00	0.31	0.00	0.00	0.00	0.00	0.51	0.00	0.00	
89	20,000	0.00	0.00	0.31	0.00	0.00	0.00	0.00	0.65	12.82	0.00	
93	21,000	0.00	0.00	0.00	0.00	0.00	0.00	0.00	0.00	0.00	0.00	
98	22,000	0.00	0.00	0.31	0.00	0.00	0.00	0.00	1.43	14.29	0.00	
102	23,000	0.00	0.00	0.00	9.82	0.00	0.00	0.00	0.51	0.00	0.00	
107	24,000	0.00	0.00	0.00	0.00	0.00	0.00	16.67	0.00	0.00	0.00	
111	25,000	0.00	0.00	0.00	0.00	0.00	0.00	0.00	0.00	0.00	0.00	
116	26,000	0.00	0.00	0.00	6.25	0.00	0.00	0.00	0.00	0.00	0.00	
120	27,000	0.00	0.00	0.00	0.00	0.00	0.00	0.00	0.00	0.00	0.00	
125	28,000	0.00	0.00	0.00	0.00	0.00	0.00	0.00	1.43	0.00	6.25	
129	29,000	0.00	0.00	0.00	0.00	0.00	0.00	0.00	0.00	0.00	0.00	
133	30,000	0.00	0.00	0.00	0.00	0.00	0.00	0.00	0.00	0.00	0.00	
138	31,000	4.17	0.00	0.00	0.00	0.00	0.00	0.00	0.00	0.00	0.00	
142	32,000	0.00	0.00	0.00	3.57	0.00	0.00	0.00	0.00	0.00	0.00	
147	33,000	0.00	0.00	0.00	0.00	0.00	0.00	0.00	0.00	0.00	0.00	
151	34,000	0.00	0.00	0.00	0.00	0.00	0.00	0.00	0.00	0.00	6.25	
156	35,000	0.00	0.00	0.00	0.00	0.00	0.00	0.00	0.00	0.00	0.00	
160	36,000	0.00	0.00	0.00	0.00	0.00	0.00	0.00	0.00	0.00	0.00	
165	37,000	0.00	0.00	0.00	0.00	0.00	0.00	0.00	0.00	0.00	0.00	
169	38,000	0.00	0.00	0.00	0.00	0.00	0.00	0.00	0.00	0.00	0.00	
173	39,000	0.00	0.00	0.00	0.00	0.00	0.00	0.00	0.00	0.00	0.00	
178	40,000	0.00	0.00	0.00	0.00	0.00	0.00	0.00	0.00	0.00	0.00	

Table D.14—Normalized Tandem Axle Load Spectra for TTC Group 15

Axle Load		Vehicle/Truck Class Number										
		4	5	6	7	8	9	10	11	12	13	
kN	lbs.											
9	2,000	0.00	0.00	0.00	0.00	0.00	0.00	0.00	0.00	0.00	0.00	0.00
18	4,000	0.00	0.00	0.00	0.00	0.00	0.00	0.00	0.00	0.00	0.00	0.00
27	6,000	0.00	0.00	0.00	0.00	100.0	2.26	0.00	0.00	0.00	0.00	13.33
36	8,000	0.00	45.83	50.00	0.00	0.00	6.58	50.00	0.00	0.00	0.00	0.00
44	10,000	0.00	54.17	50.00	0.00	0.00	8.86	0.00	0.00	0.00	0.00	0.00
53	12,000	0.00	0.00	0.00	0.00	0.00	10.58	0.00	0.00	8.33	22.50	0.00
62	14,000	0.00	0.00	0.00	0.00	0.00	9.15	0.00	33.33	0.00	20.00	0.00
71	16,000	0.00	0.00	0.00	0.00	0.00	7.25	0.00	0.00	50.00	0.00	0.00
80	18,000	0.00	0.00	0.00	0.00	0.00	5.19	0.00	33.33	0.00	12.50	0.00
89	20,000	0.00	0.00	0.00	100.0	0.00	3.95	0.00	0.00	12.50	0.00	0.00
98	22,000	0.00	0.00	0.00	0.00	0.00	3.35	0.00	0.00	0.00	3.33	0.00
107	24,000	0.00	0.00	0.00	0.00	0.00	3.30	50.00	0.00	0.00	0.00	0.00
116	26,000	0.00	0.00	0.00	0.00	0.00	3.82	0.00	0.00	12.50	0.00	0.00
125	28,000	0.00	0.00	0.00	0.00	0.00	3.71	0.00	0.00	16.67	0.00	0.00
133	30,000	0.00	0.00	0.00	0.00	0.00	3.82	0.00	0.00	0.00	28.33	0.00
142	32,000	0.00	0.00	0.00	0.00	0.00	3.95	0.00	0.00	0.00	0.00	0.00
151	34,000	0.00	0.00	0.00	0.00	0.00	4.08	0.00	0.00	0.00	0.00	0.00
160	36,000	0.00	0.00	0.00	0.00	0.00	3.67	0.00	0.00	0.00	0.00	0.00
169	38,000	0.00	0.00	0.00	0.00	0.00	3.90	0.00	0.00	0.00	0.00	0.00
178	40,000	0.00	0.00	0.00	0.00	0.00	3.12	0.00	0.00	0.00	0.00	0.00
187	42,000	0.00	0.00	0.00	0.00	0.00	2.52	0.00	16.67	0.00	0.00	0.00
196	44,000	0.00	0.00	0.00	0.00	0.00	2.40	0.00	16.67	0.00	0.00	0.00
205	46,000	0.00	0.00	0.00	0.00	0.00	1.80	0.00	0.00	0.00	0.00	0.00
214	48,000	0.00	0.00	0.00	0.00	0.00	1.31	0.00	0.00	0.00	0.00	0.00
222	50,000	0.00	0.00	0.00	0.00	0.00	0.83	0.00	0.00	0.00	0.00	0.00
231	52,000	0.00	0.00	0.00	0.00	0.00	0.48	0.00	0.00	0.00	0.00	0.00
240	54,000	0.00	0.00	0.00	0.00	0.00	0.12	0.00	0.00	0.00	0.00	0.00
249	56,000	0.00	0.00	0.00	0.00	0.00	0.00	0.00	0.00	0.00	0.00	0.00
258	58,000	0.00	0.00	0.00	0.00	0.00	0.00	0.00	0.00	0.00	0.00	0.00
267	60,000	0.00	0.00	0.00	0.00	0.00	0.00	0.00	0.00	0.00	0.00	0.00
276	62,000	0.00	0.00	0.00	0.00	0.00	0.00	0.00	0.00	0.00	0.00	0.00
285	64,000	0.00	0.00	0.00	0.00	0.00	0.00	0.00	0.00	0.00	0.00	0.00
294	66,000	0.00	0.00	0.00	0.00	0.00	0.00	0.00	0.00	0.00	0.00	0.00
302	68,000	0.00	0.00	0.00	0.00	0.00	0.00	0.00	0.00	0.00	0.00	0.00
311	70,000	0.00	0.00	0.00	0.00	0.00	0.00	0.00	0.00	0.00	0.00	0.00
320	72,000	0.00	0.00	0.00	0.00	0.00	0.00	0.00	0.00	0.00	0.00	0.00
329	74,000	0.00	0.00	0.00	0.00	0.00	0.00	0.00	0.00	0.00	0.00	0.00
338	76,000	0.00	0.00	0.00	0.00	0.00	0.00	0.00	0.00	0.00	0.00	0.00
347	78,000	0.00	0.00	0.00	0.00	0.00	0.00	0.00	0.00	0.00	0.00	0.00
356	80,000	0.00	0.00	0.00	0.00	0.00	0.00	0.00	0.00	0.00	0.00	0.00

Table D.15—Normalized Tridem Axle Load Spectra for TTC Group 15

Axle Load		Vehicle/Truck Class Number										
		kN	lbs.	4	5	6	7	8	9	10	11	12
13	3,000	0.00	0.00	0.00	0.00	0.00	0.00	0.00	0.00	0.00	0.00	0.00
27	6,000	0.00	0.00	0.00	0.00	0.00	0.00	0.00	0.00	0.00	0.00	0.00
40	9,000	0.00	0.00	0.00	0.00	0.00	0.00	0.00	0.00	0.00	0.00	0.00
53	12,000	0.00	0.00	0.00	100.0	100.0	0.00	0.00	0.00	0.00	0.00	50.00
67	15,000	0.00	0.00	0.00	0.00	0.00	0.00	66.67	0.00	0.00	0.00	0.00
80	18,000	0.00	0.00	0.00	0.00	0.00	0.00	33.33	0.00	0.00	0.00	0.00
93	21,000	0.00	0.00	0.00	0.00	0.00	0.00	0.00	0.00	0.00	0.00	0.00
107	24,000	0.00	0.00	0.00	0.00	0.00	0.00	0.00	0.00	0.00	0.00	0.00
120	27,000	0.00	0.00	0.00	0.00	0.00	0.00	0.00	0.00	0.00	0.00	0.00
133	30,000	0.00	0.00	0.00	0.00	0.00	0.00	0.00	0.00	0.00	0.00	0.00
147	33,000	0.00	0.00	0.00	0.00	0.00	0.00	0.00	0.00	0.00	0.00	0.00
160	36,000	0.00	0.00	0.00	0.00	0.00	0.00	0.00	0.00	50.00	0.00	0.00
173	39,000	0.00	0.00	0.00	0.00	0.00	0.00	0.00	0.00	0.00	0.00	0.00
187	42,000	0.00	0.00	0.00	0.00	0.00	0.00	0.00	0.00	0.00	0.00	0.00
200	45,000	0.00	0.00	0.00	0.00	0.00	0.00	0.00	0.00	0.00	0.00	0.00
214	48,000	0.00	0.00	0.00	0.00	0.00	0.00	100.0	0.00	0.00	0.00	0.00
227	51,000	0.00	0.00	0.00	0.00	0.00	0.00	0.00	0.00	0.00	0.00	0.00
240	54,000	0.00	0.00	0.00	0.00	0.00	0.00	0.00	0.00	0.00	0.00	0.00
254	57,000	0.00	0.00	0.00	0.00	0.00	0.00	0.00	0.00	0.00	0.00	50.00
267	60,000	0.00	0.00	0.00	0.00	0.00	0.00	0.00	0.00	0.00	0.00	0.00
280	63,000	0.00	0.00	0.00	0.00	0.00	0.00	0.00	0.00	0.00	0.00	0.00
294	66,000	0.00	0.00	0.00	0.00	0.00	0.00	0.00	0.00	0.00	0.00	0.00
307	69,000	0.00	0.00	0.00	0.00	0.00	0.00	0.00	0.00	0.00	0.00	0.00
320	72,000	0.00	0.00	0.00	0.00	0.00	0.00	0.00	0.00	50.00	0.00	0.00
334	75,000	0.00	0.00	0.00	0.00	0.00	0.00	0.00	0.00	0.00	0.00	0.00
347	78,000	0.00	0.00	0.00	0.00	0.00	0.00	0.00	0.00	0.00	0.00	0.00
360	81,000	0.00	0.00	0.00	0.00	0.00	0.00	0.00	0.00	0.00	0.00	0.00
374	84,000	0.00	0.00	0.00	0.00	0.00	0.00	0.00	0.00	0.00	0.00	0.00
387	87,000	0.00	0.00	0.00	0.00	0.00	0.00	0.00	0.00	0.00	0.00	0.00
400	90,000	0.00	0.00	0.00	0.00	0.00	0.00	0.00	0.00	0.00	0.00	0.00
414	93,000	0.00	0.00	0.00	0.00	0.00	0.00	0.00	0.00	0.00	0.00	0.00
427	96,000	0.00	0.00	0.00	0.00	0.00	0.00	0.00	0.00	0.00	0.00	0.00
440	99,000	0.00	0.00	0.00	0.00	0.00	0.00	0.00	0.00	0.00	0.00	0.00
454	102,000	0.00	0.00	0.00	0.00	0.00	0.00	0.00	0.00	0.00	0.00	0.00
467	105,000	0.00	0.00	0.00	0.00	0.00	0.00	0.00	0.00	0.00	0.00	0.00
480	108,000	0.00	0.00	0.00	0.00	0.00	0.00	0.00	0.00	0.00	0.00	0.00
494	111,000	0.00	0.00	0.00	0.00	0.00	0.00	0.00	0.00	0.00	0.00	0.00
507	114,000	0.00	0.00	0.00	0.00	0.00	0.00	0.00	0.00	0.00	0.00	0.00
520	117,000	0.00	0.00	0.00	0.00	0.00	0.00	0.00	0.00	0.00	0.00	0.00
534	120,000	0.00	0.00	0.00	0.00	0.00	0.00	0.00	0.00	0.00	0.00	0.00

APPENDIX E—GROUND WATER DEPTH TOOL

The depth to the water table can be estimated using the tool or software developed under the MEPDG implementation project for MDOT. This tool or software is a separate program from Pavement ME Design and can be used for other applications. This appendix includes a description and discussion of program itself for completeness.

E.1 INTRODUCTION

The depth to ground water table (or often referred to as simply the water table) is an input to the Climate module of the AASHTOWare Pavement ME Design software program. The depth to the water table is used to predict the moisture state of each pavement layer so that time-dependent changes in the material properties can be adequately captured by the MEPDG analysis procedure. The MEPDG uses the Enhanced Integrated Climatic Model (EICM) to estimate the moisture level in all layers of the pavement. Soil at the level of the ground water is considered fully saturated. The EICM analysis uses the depth to water table and other climate variables, material index properties, soil-moisture characteristic parameters, and thicknesses of the layers to predict the moisture profile over all months of the design period. Next, the moisture level in each unbound layer of the pavement structure is used to make monthly adjustments to the modulus values of the given layer. The effect of time-dependent modulus values is reflected in the calculated critical responses in the mechanistic process. In concrete layers, the moisture content in the top 2 inches at the surface is used to determine shrinkage gradients and the resulting stresses at the top of the pavement.

The MDOT uses the GIS-based Ground Water Table (GWT) tool to determine the depth to ground water table at a project site for use in the AASHTOWare Pavement ME Design procedure. The GWT tool allows the user to estimate the elevation of the water table at any given location based on water level measurements in wells and aquifers in the general vicinity. To develop this tool, data from existing wells and aquifers in Mississippi were obtained from a national database maintained by the United States Geological Survey (USGS). The USGS stores historical water level data in its online database, and this information includes the location of the well, well depth, elevation of the surface of the well, depth of water at each measurement time, and date of each measurement. The MDOT GWT tool utilizes the Google Earth plug-in to visualize USGS well data with reference to the project location that can be defined with a latitude-longitude reference or a roadway location reference. The display features allow the use of several Google Earth layers, including the borders and names of places, roads, buildings, and topography.

This appendix provides basic guidance for using the MDOT GWT tool to determine the depth to water table.

E.2 TERMINOLOGIES AND CONCEPTS USED IN THE GWT TOOL

This section of Appendix E provides an explanation of several terminologies used in the GWT tool. It also provides an explanation of certain physical phenomena that impact the ground water level under the surface of the earth, as well as the ground water level measurements recorded in the USGS database.

E.2.1 Water Table

Below a certain depth under the surface of the earth, the ground, if permeable, is saturated with water. The water table is the top of the zone of saturation, where all available spaces are filled with water. As shown in Figure E.1, the voids in the rocks below the water table are considered to be saturated with water. Note that the unsaturated zone above the water table has pockets of air filled with water but can be filled with more moisture. This zone is not totally dry, as shown in the zoomed-in portion of the image at the lower half.

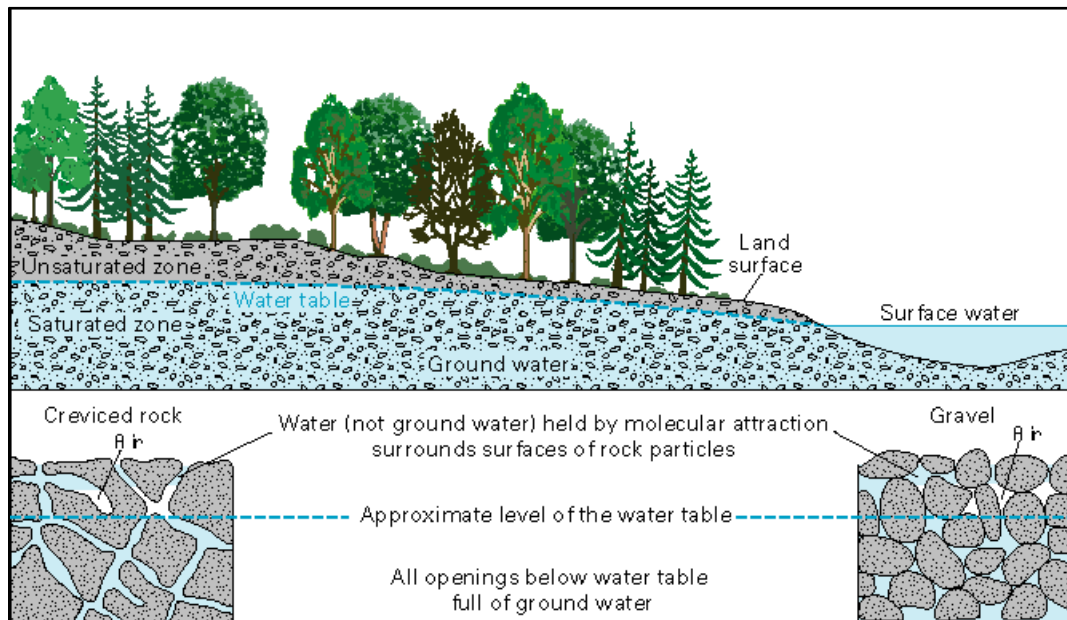


Figure E.1. Ground Water Level (Source: USGS)

E.2.2 Aquifers and Wells

Aquifers are generally the rock or unconsolidated materials from which ground water are extracted. They serve as large store houses of water. Water well is used to extract ground water from the aquifer. A well, if dug deep enough to strike the ground water table, exposes the water from the aquifer underneath, or provides for a means to withdraw water from the aquifer.

E.2.3 Ground Water Table Depth

Water table depth is the depth to the top of the saturated zone, typically measured from the land surface, as shown in Figure E.2. Figure E.2 also shows the well depth, which indicates the depth of the aquifer or the geological formation holding the saturated zone. The USGS database includes the ground water table depth as well as the well depth. In addition, it contains the elevation of the surface of the well with respect to the mean sea level.

In the context of using this tool to determine the depth to water table for a pavement project analysis, because the elevation of the pavement may not exactly coincide with the elevation of the ground surface, the MDOT GWT tool was designed to report the elevation of the water table with respect to the mean sea level. As shown in Figure E.2, the elevation of the

GWT is the difference between the elevation of the ground surface at the well location and the GWT depth.

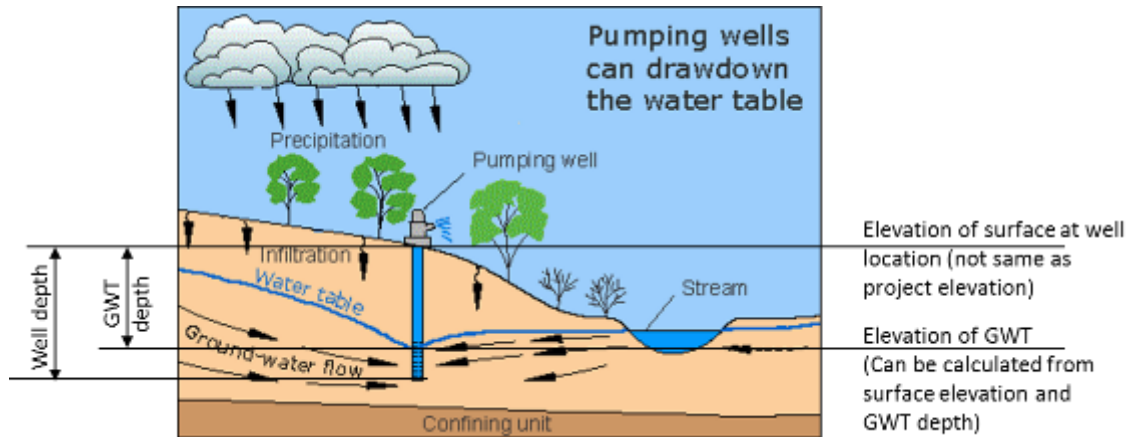


Figure E.2. Definition of Ground Water Table Depth and Results Displayed in the GWT Tool (Original Image Source: USGS, image labeled to explain terminologies)

Therefore, the depth to water table input to the AASHTOWare Pavement ME Design procedure is determined as the difference between the elevation of the project roadway and the elevation of the GWT reported in the GWT tool. The user needs to determine this value for each project depending on the elevation of the roadway being analyzed.

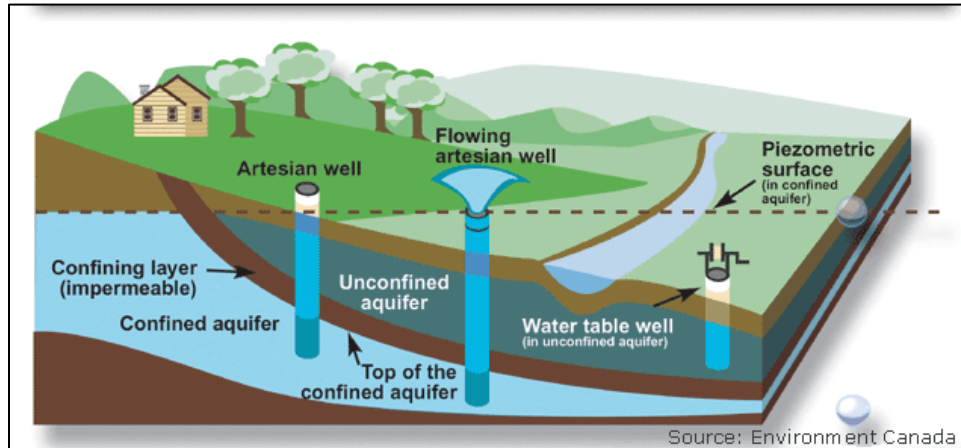
E.2.4 Time Dependent Changes to the Water Table Depth

The water table level changes with time for multiple reasons; mostly, it is influenced by weather cycles or human usage of well water. Natural precipitation is a significant source of water level increase, and excessive pumping of well water can draw down the water level. However, other factors include stream flow, geological changes, and other human-induced changes like an increase in impervious surfaces on the landscape. Further, the geological or hydrologic conditions of the aquifer can impact the extent of and the duration over which the change in water level lasts. The water level can change by a few inches or by hundreds of feet, and the change can be short-lived or last for decades, or even be permanent. In fact, active wells can go dry. Therefore, in the data retrieved from the USGS database to develop the GWT tool, the date of measurement is a key parameter to determine the depth to water table.

E.2.5 Water Level in Wells from Confined Aquifers

Groundwater can sometime be drawn from confined aquifers, in which the water is confined under higher pressures. When a well is drilled in such locations, as a result of the high pressure, water surges up the wells and can rise above the top of the aquifer and may even flow from the well onto the land surface. The apparent high water table is a result of water being tapped from a relatively high pressure zone, rather than from the existence of ground water closer to the surface. These phenomena are most typical when the well strikes an artesian aquifer where a confining layer of less porous rock exists both above and below the porous saturated layer, as shown in Figure E.3. This may also be noticed when the water level is measured from a secondary aquifer, which is usually a deep lying aquifer, well below

a primary aquifer, and with water-filled fractures in rocks under high confining pressures. They are typically over 300 to 500 feet from the surface of the earth. A secondary aquifer is shown in Figure E.4.



Note that the water level in the well to the left is higher than the ground water level

Figure E.3. Artesian Aquifer (Source: Environment Canada)

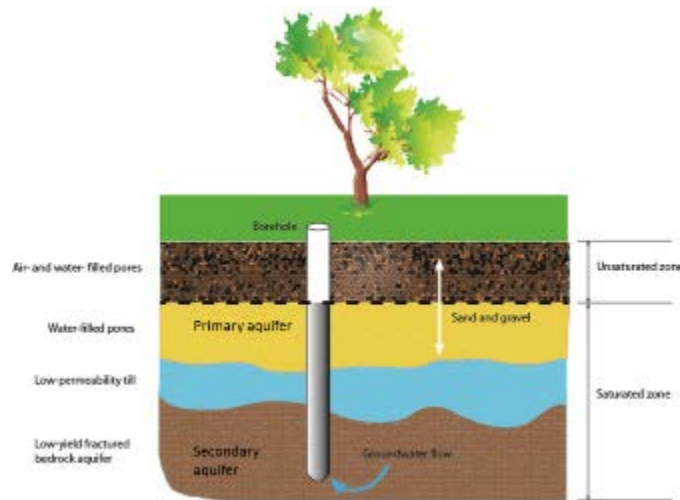


Figure E.4. Secondary Aquifer Source

Water table depth reported from measurements taken from such wells may indicate, incorrectly, a higher elevation for the ground water. These values may also appear as outliers in the GWT tool. The GWT tool therefore provides a filter to exclude such data in determining the elevation of the water table. Further, it alerts the user to data that are outliers.

E.3 DESCRIPTION OF GWT TOOL AND USER INTERFACE

E.3.1 Launching GWT Tool

The GWT tool is a web-based application that runs from the Firefox© internet browser. The following steps are needed to launch the GWT tool application:

1. Open the Firefox browser.
2. From the *File* menu, select *Open File*, as shown in Figure E.5.
3. Browse to the MDOT GWT folder and open the html file “*index*,” as shown in Figure E.6.
4. The tool launches Google Earth and displays the user interface of the MDOT GWT tool, as shown in Figure E.7. The left side of the tool is the *control panel* and forms the user interface for entering appropriate project-related information. The right pane of the screen displays the map. The default setting in the tool opens the topographical map and zooms to a default location in Mississippi. There is also a circular area of interest that is displayed on the screen. The circle represents the region of interest over which wells are located by the tool. The center of the circle, displayed with a pushpin marker, represents the point of interest or the location where the ground water table depth needs to be determined. The user may zoom in or zoom out of a location on the map by using the scroll wheel of the mouse.
5. The next step is to load the database into the tool. Click on the *Browse* button next to the *Load KML file* label on the user interface. Browse to the location of the MDOT GWT folder, and select the *Data* folder. Within this folder, select the “*alldata.kml*” file as shown in Figure E.8. Click *Open*. For the default location displayed in the map, the user should see three light green square markers appear within the circular area. These three markers represent three wells within the area of interest. Note that the wells displayed are limited to the circular region. Wells outside the circular area of interest are not displayed on the map.

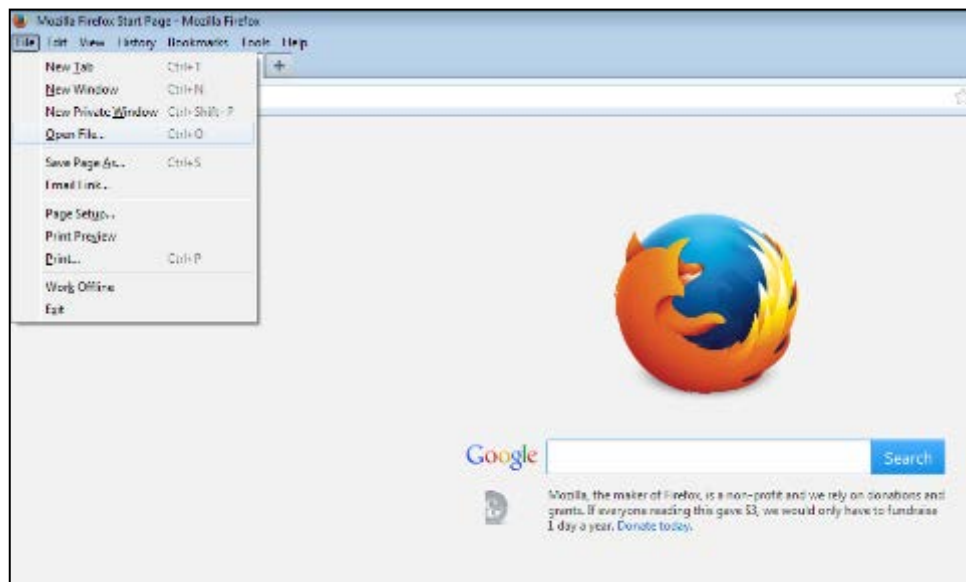


Figure E.5. Opening GWT Tool in Firefox Browser Window

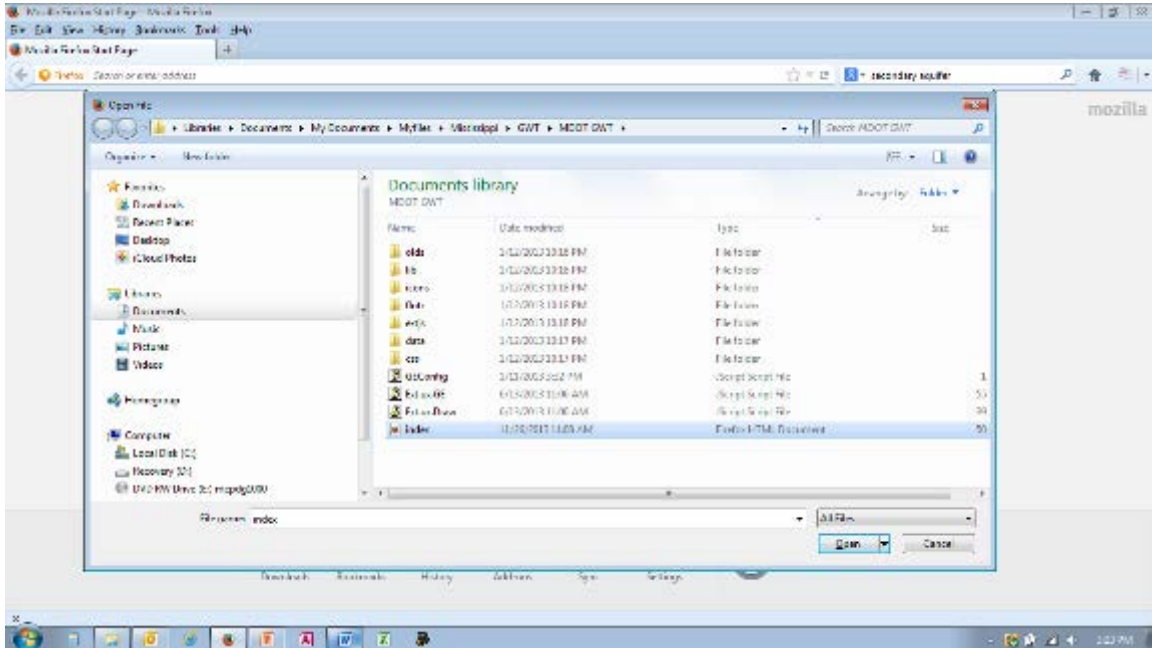


Figure E.6. Selecting the html.file Index to Open the GWT Tool

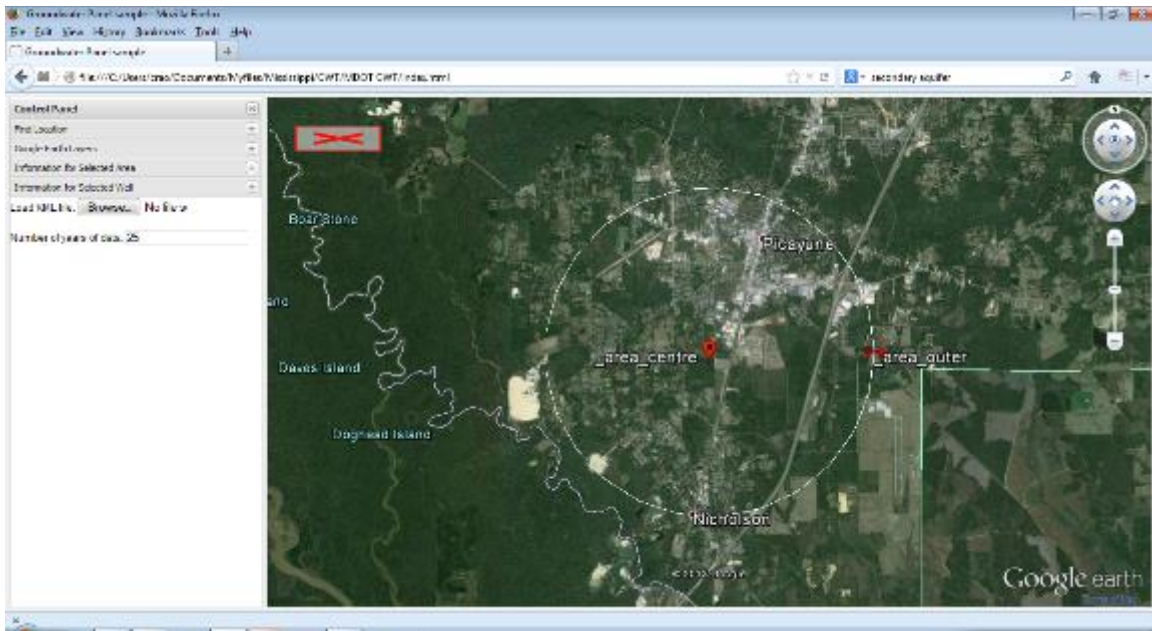


Figure E.7. User Interface after Launching MDOT GWT Tool

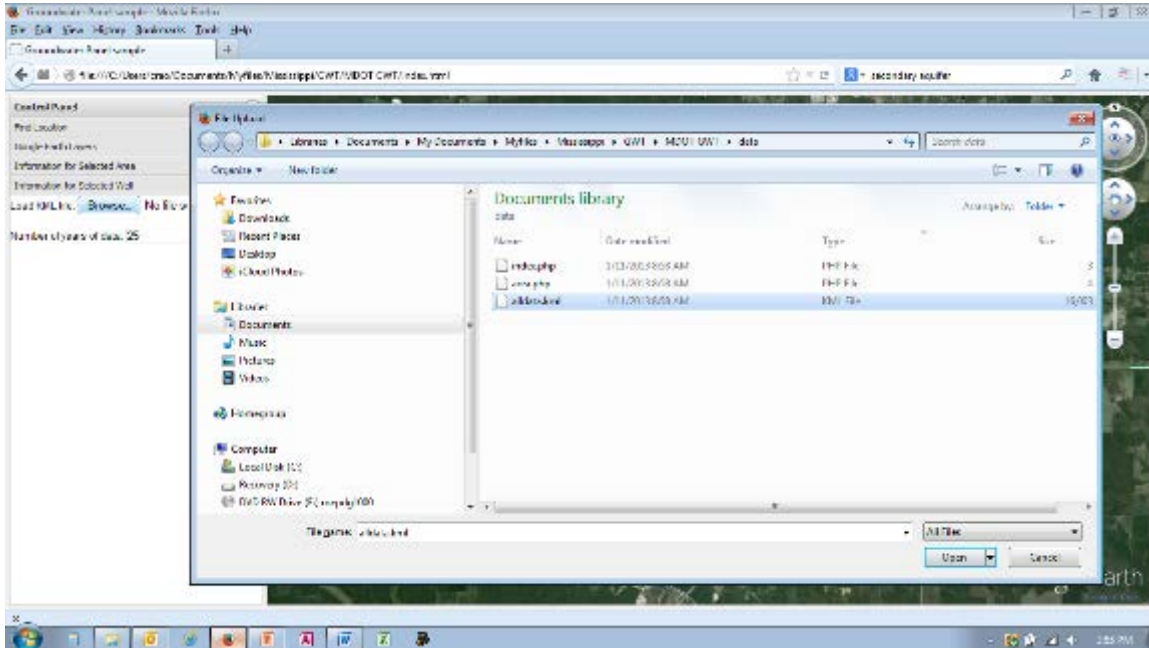


Figure E.8. Loading the Data File to Import the Well Information and Water Table Depth Data

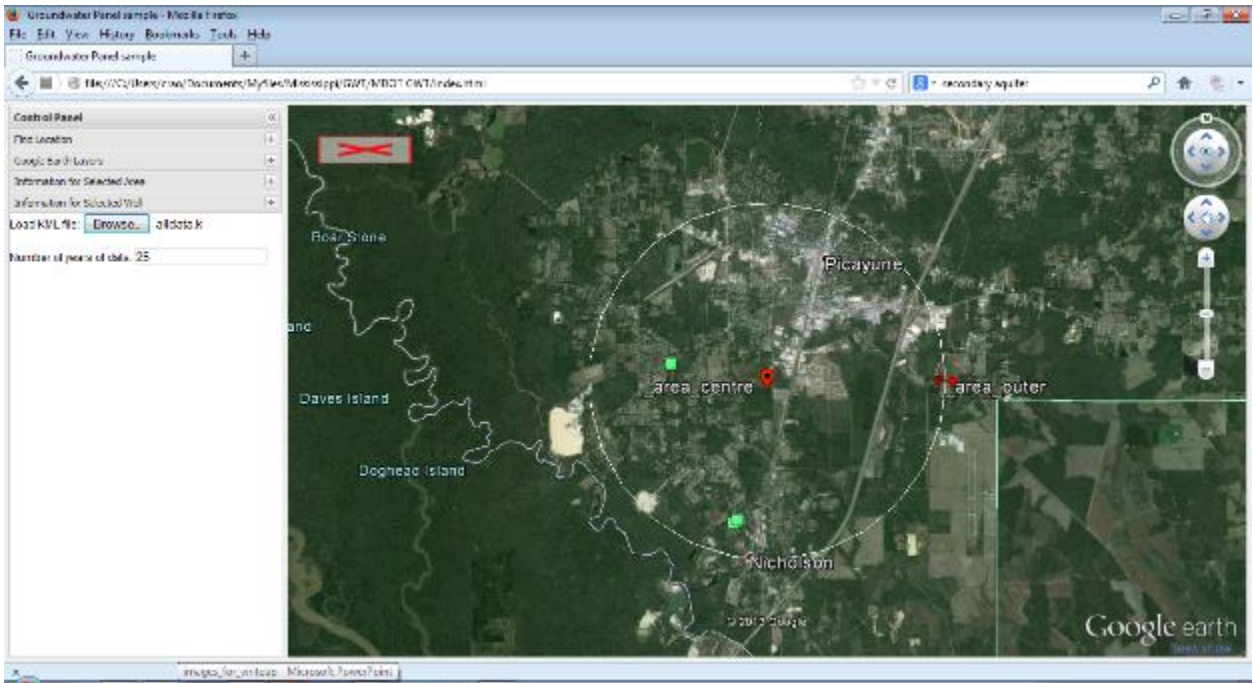


Figure E.9. Wells Displayed as Green Squares in the Region of Interest

E.3.2 User Interface and Definition of Terms

The control panel on the left pane provides the tools for user interaction to determine the depth to the water table. The control consists of four tabs and an additional user-defined filter setting, which provide the user multiple tools to:

- Narrow down to the project location using multiple options.
- Set appropriate filters in the database to determine the water table depth.
- Read the estimated elevation of the ground water table at the project location.
- Display historical measurements of the water table depth at the wells identified in the region of interest.
- Alert the user to potential outliers in the data.

Number of Year of Data: This user-defined input pertains to selecting the subset of historical ground water table depth data to determine the current water table depth in the project site. As discussed earlier, the water table depth may change with time. The USGS database contains data over several decades, with records from as early as 1900. The GWT tool allows the user to select the number of recent years of data to use in determining the depth to water table.

The four tabs on the control panel and their features are discussed in the following subsections.

E.3.3 Find Location

The *Find Location* tab allows the user to enter text to locate a region of interest (see Figure E.10). It is expected that this feature will be used to narrow down (or zoom into) a general area. Note that the GWT tool contains other features to locate a specific roadway using a latitude-longitude reference.

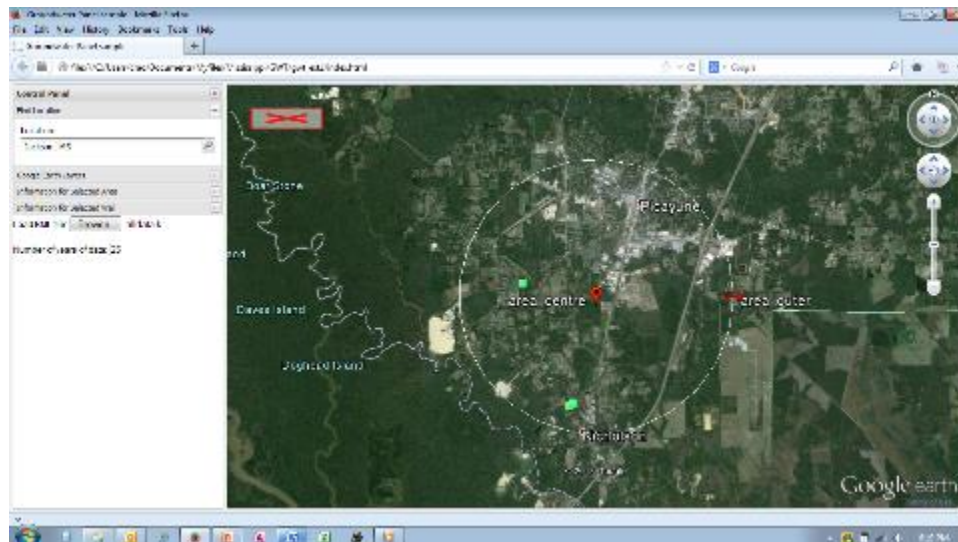


Figure E.10. *Location* Tab to Select a Project Location by Name of Place

E.3.4 Google Earth Layers

The *Google Earth Layers* tab allows the user to select the topographical features that can be displayed. For example, by clicking on the Roads option, the roadways are displayed appropriate for the level of zoom (see Figure E.11).

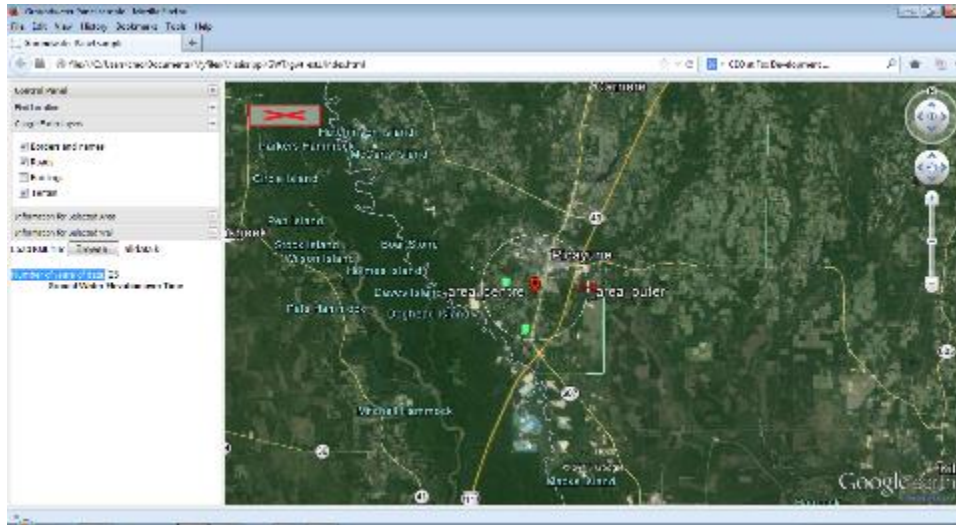


Figure E.11. *Google Earth Layers* Tab to Select the Topographical Features for Display

E.3.5 Information for Selected Area

The *Information for Selected Area* tab shows the information on the ground water for the specific area (see Figure E.12).

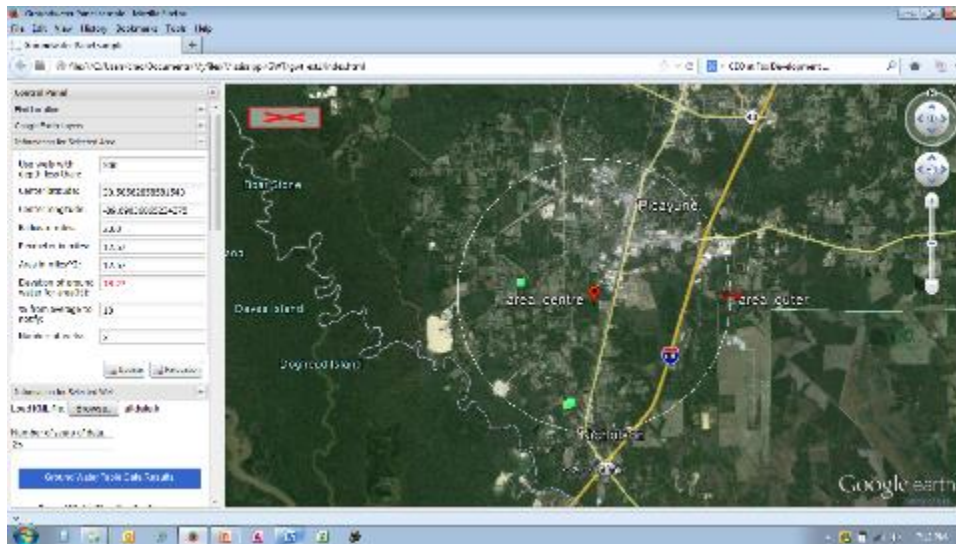


Figure E.12. *Information for Selected Area* Tab

The labels seen on this tab here include:

- Use wells with depth less than: This is a filter to select wells with depths less than a certain value. This filter allows data from wells in secondary aquifers to be eliminated in calculating the average water table depth in the area. This may be user-defined. The recommended default is 300 feet.
- Center latitude: This is the latitude of the project/center the circular area of interest. If the project extends over a significant length, the depth to water table can be determined at various points along the project by changing the latitude-longitude reference. This may be user-defined.
- Center longitude: This is the longitude of the project/center the circular area of interest. If the project extends over a significant length, the depth to water table can be determined at various points along the project by changing the latitude-longitude reference. This may be user-defined.
- Radius in miles: This is the radius of the circular area of interest. The circular area can be expanded or decreased using the two way arrow. As the size of this area of interest is altered the control panel displays the radius of this circular area. The tool does not allow the user to control the size of the circular area of reference by inputting a numeric value for this parameter. The area adjustments can only be made by physically sizing the circular area using a mouse/touchpad.
- Perimeter in miles: This displays the perimeter of the circular area of reference. This parameter is not user-defined. The value of this parameter changes as the size of the circular area of reference is altered.
- Area in miles²: This displays the area of the circular area of reference. This parameter is not user-defined. The value of this parameter changes as the size of the circular area of reference is altered.
- Elevation of ground water for area: This is the result reported by the GWT tool for the selected area. This value is calculated as an average of the water table depths recorded in all the wells within this area of interest based on historical data. The input to the AASHTOWare ME Design procedure is the difference between the elevation of the project and the elevation of ground water for the area.
- Percent from average to notify: This setting allows the program to alert the user if there is a large variability in the data used to calculate the average in the region. It is more or less a tolerance level for the extent by which each recorded water level in the historical data can deviate from the average. This tolerance is intended to capture large outliers in the data, possibly as a result of an artesian well or proximity to a water body, or even topographical changes. This is a user-defined input. The recommended default value is 20 percent.

Figure E.13 shows the alert message for the default location of the software program. The alert appears on the screen when the mouse is clicked anywhere in the circular region of interest. Also, note that when the average does not meet the

tolerance level, the average elevation of the water table is reported in a red font as shown in Figure E.13.

- Number of wells: This displays the number of wells for which water table depth exists in the database. The user does not have an option to enter this number.

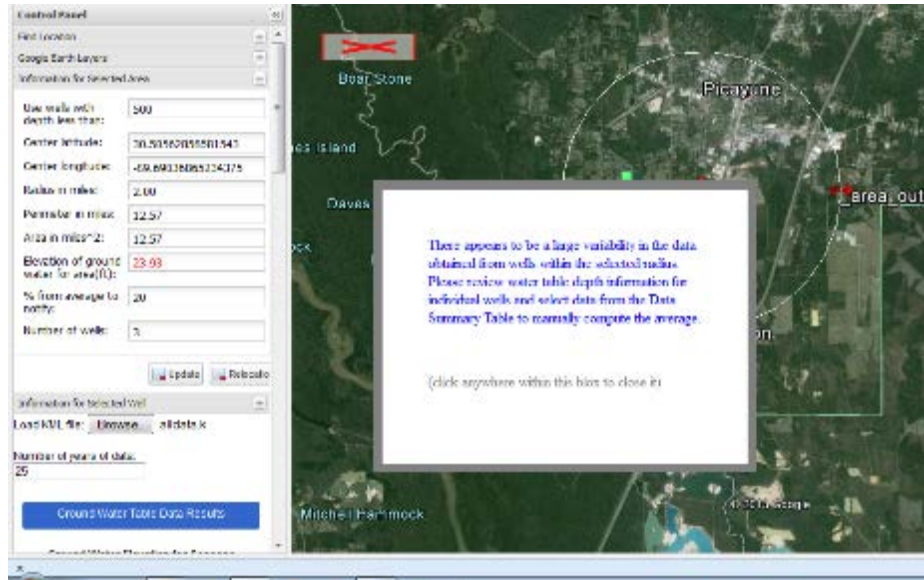


Figure E.13. Warning to Alert the User that the Data used in Computing the Average has a Large Variability or Outliers that are Outside the Set Tolerance Level

The *Information for Selected Area* tab also provides two buttons:

- **Update:** After user-defined inputs are entered or changed on this screen, click on the *Update* button to update the results displayed or the map. The user may enter the latitude-longitude for a project location and click on *Update* for the map as well as the results to reflect the selection of a new location. For example, for latitude and longitude inputs of 32.3 and -90.1, respectively, clicking on the *Update* button shifts the center of the circular area of interest to this location. The screen and results also change, as shown in Figure E.14. Note that the results indicate there are three wells in the 2-mile radius with an average elevation of water table of 148 feet.
- **Relocation:** The *Relocation* button allows the user to manually click on the map to select the point of interest. This may be used when the user has a clear idea of the project location based on references of highway, routes, or intersections of roadways. Once the *Relocation* button is clicked, the program switches the mouse to a “relocation” mode. This implies any click by the mouse on the map places the pushpin center of the circular area at that point. Once the point of interest or the project location is selected, to disable the relocation mode, click on the *Relocation* button again and then click on *Update* to display results.

For example, if the project of interest is on I-55 just east of Jackson, clicking the *Relocation* button and then clicking on the I-55 segment of interest will move the circular area of interest to the location selected on the map. Click the *Relocation*

button to disable this mode. Next, click *Update*. The map and the results are now changed, as shown in Figure E.15, indicating that based on data from three wells, the average elevation of the water table is 154.94 feet. The coordinates of the new location are also displayed on the screen.

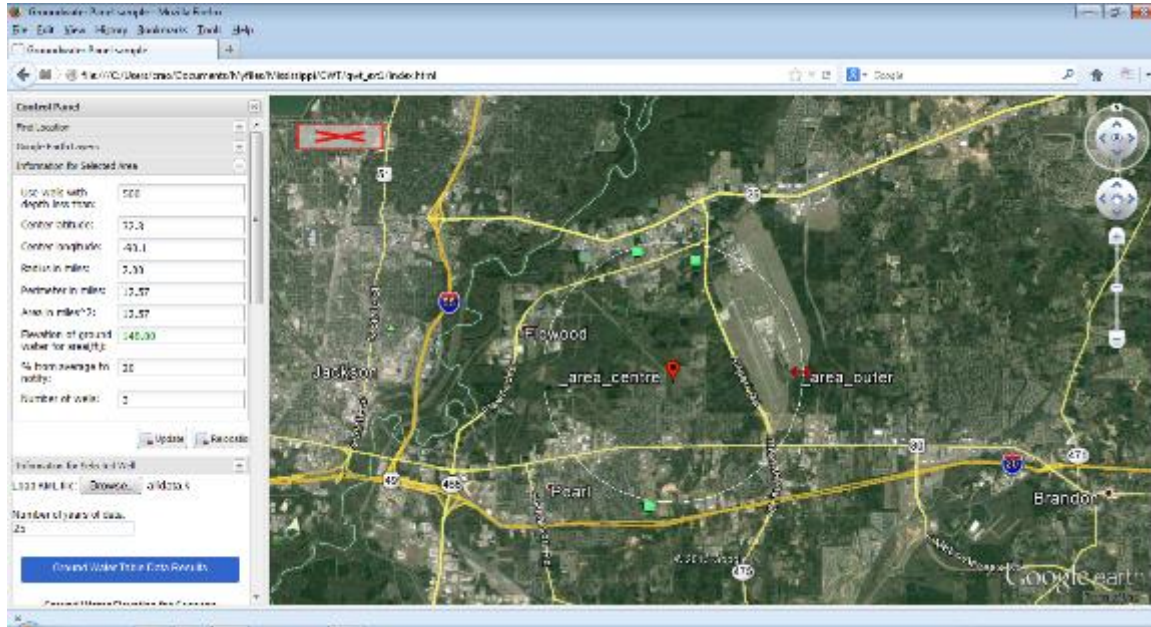


Figure E.14. Update after User-Input Latitude and Longitude Inputs and Results Displayed

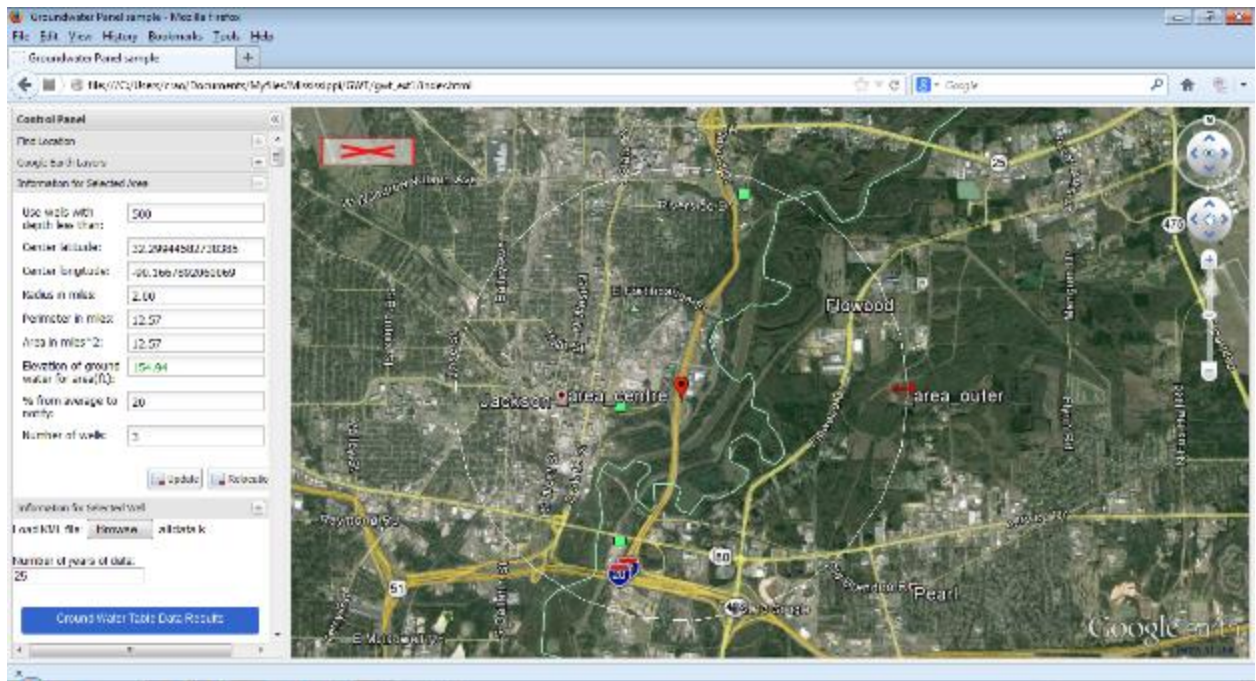


Figure E.15. Relocate Button to Manually Select the Project Location of Interest

As the user scrolls down this tab, under the heading *Ground Water Table Data Results*, the data used to calculate the average elevation of the water table are displayed graphically first and are tabulated in a summary format next. The graphical format shows the charts for the average elevation of the water table by season, then for each season over time, and finally all data over time, as shown in Figure E.16. The results in the figure correspond to the project location on I-55 east of Jackson. The user may infer here that the average water table elevation more or less stays constant over all season, and that over a 25-year period, the water table elevation appears to have reduced (especially in the most recent 7 to 8 years). Below the charts, the GWT tool provides a tabular list of all recorded data used in calculating the average water table elevation.

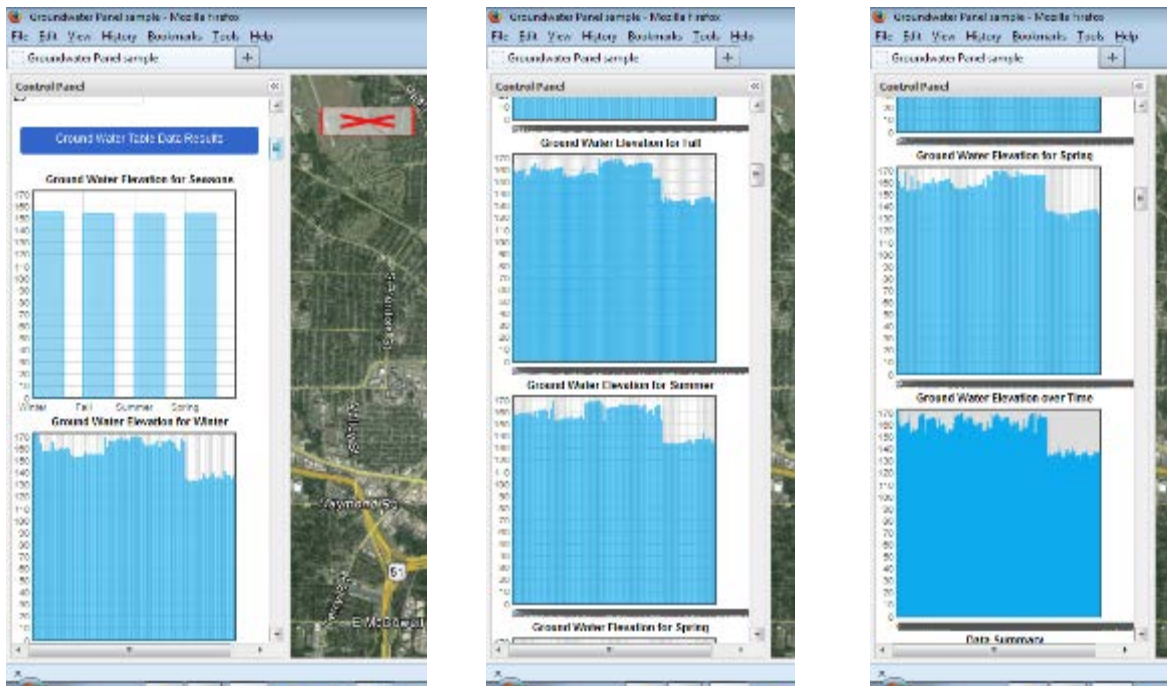


Figure E.16. Graphical Display of Results by Season and over Time

E.3.6 Information for Selected Well

The *Information for Selected Well* tab shows the information for a specific well that can be selected by the user. This selection can be made by a simple click of the mouse on the square marker representing any of the wells displayed on the map. For example, by clicking on the well closest to the I-55 project location, as shown in Figure E.17, the program displays all information relevant to that well, including its USGS ID, the latitude-longitude, the altitude of the well, the well depth, the dates over which water table depth measurements were recorded, and average water table elevation. In addition, all graphical and tabulated data relevant to that well are displayed similar to the information given for the area in Figure E.16.

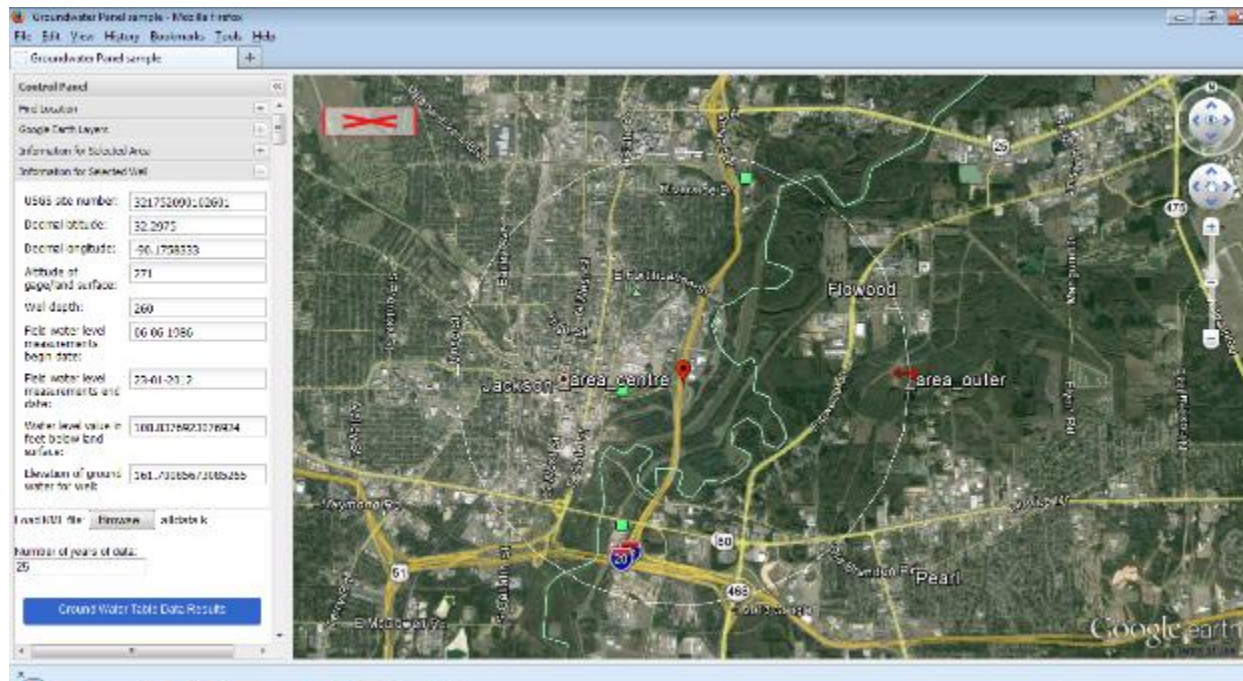


Figure E.17. Data Displayed in the *Information for Selected Well* Tab

E.4 DETERMINATION OF WATER TABLE DEPTH

E.4.1 Setting Filters

The MDOT GWT tool offers the user the options of setting certain filters in the database from which the water table depth is determined for a specific project. The recommendations provided below are based on filters set for the GWT tool in the local calibration of the AASHTOWare Pavement ME Design distress models for Mississippi:

1. *Number of years of data* Variable: As described in the previous section, the GWT tool allows the user to select the number of recent years of data to use in determining the depth to water table. The default value used for the calibration of the MDOT AASHTOWare models was 25 years. It is recommended that the value for the variable *Number of years of data* be set to 25 years for future AASHTOWare Pavement ME Design. This may be changed when special cases are analyzed, or when data anomalies are noticed.
2. *Percent from average to notify* Variable: This variable sets the tolerance level to alert the user if the data deviate from the average water table depth by more than the set value. The default value is 20 percent under the *Information for Selected Area* tab.
3. *Use wells with depth less than* Variable: This variable helps filter out data from wells that might be striking water in secondary aquifers. Set the value to 300 feet under the *Information for Selected Area* tab. If detailed information about wells in a specific location is available, the user may make a more informed judgment for this parameter.

E.4.2 Other Settings

1. *Google Earth Layers*: Under the *Google Earth Layers* tab, select *Borders and Names, Roads, and Terrain* so the user can visualize the project location in relation to these references.
2. *Radius in miles*: This variable is displayed under the *Information for Selected Area* tab. This parameter cannot be user “input,” but it can be set by manually adjusting the size of the circular area of interest using the computer mouse. It is recommended that that the area of interest be limited to a circle of 1-mile radius. If there are no wells, then expand the circle incrementally to 2-mile radius, 5-mile radius, and 10-mile radius. If there are no wells within a 10-mile radius, it is recommended that historical boring logs data be referred prior to using the closest well in the vicinity of the project.

E.4.3 Determining Water Table Depth for Project.

Step 1 – Obtain the elevation of the roadway along the project length. If the elevation of the entire project alignment is not available, the approximate range of the elevations will be useful to determine the range of water table depth that is to be used in the analysis.

Step 2 – Obtain the latitude-longitude of the project. If this is a significantly longer length of the roadway, obtain the coordinates at every mile, if possible, and determine the depth to the water table at all locations. If not, determine the depth to water table at the coordinates corresponding to the start and end of the project. It is recommended that the design developed using the AASHTOWare Pavement ME Design procedure be verified using the smallest and largest values of the depth to water table parameter.

Step 3 – Launch the MDOT GWT tool and load the data file as explained in the section *Launching GWT Tool*.

Step 4 – Locate the project on the Google Earth map. There are two ways to locate the project, as described below in order of preference:

- If the coordinates of the project location are available, enter the latitude and longitude. When this option is used, verify that the location identified by the map is on the specific highway/roadway being designed.
- If the coordinates are not available, zoom in to the project location using the roadway and names of places as a reference. Using the *Relocation* button, identify the location of interest.

Step 5 – Set the radius of the circular area of interest to 1 mile. If there is at least one well displayed on the screen, click *Update* to view the results. If no wells appear on the screen, incrementally increase the radius of the circular area of reference to 2 miles, 5 miles, and 10 miles until at least one well appears within the circular boundary around the project. Click *Update* to view results.

Step 6 – Obtain the elevation of the water table for the region of interest depending on the outcome displayed by the GWT tool in step 5:

- Step 6a: If the *Elevation of ground water for area* parameter displays a number in green, and no alert message appears on the screen, use the value reported. However, view the map and examine if there are any anomalies, like the presence of water bodies that might skew results. The user should also review the water table elevation data tabulated in the results section. If there are anomalies, follow data reduction steps recommended in step 6b.
- Step 6b: If the *Elevation of ground water for area* parameter displays a number in red and an alert pops up, review the data printed in the table. There are multiple ways to estimate a value most representative of the water table elevation at the required location:
 - Identify the well closest to the project site and consider using data only from this well.
 - Identify the well with data that show a large deviation from the average. Manually eliminate the water table elevation data from that well and recomputed the average (calculations may be performed using Microsoft Excel or a calculator).
 - Identify causes for anomalous results (such as presence of a lake or topographic changes) and eliminate data from select wells to recomputed the average manually (calculations may be performed using Microsoft Excel or a calculator).

Step 7 – Determine the *depth to water table* input for the AASHTOWare Pavement ME Design procedure by calculating the difference between the elevation of the project (step 1) and the average elevation of the water table determined in step 6.

APPENDIX F—DYNAMIC MODULUS TEST RESULTS

Appendix F provides a summary or tabular listing of the dynamic modulus values measured on multiple HMA mixtures measured by Mississippi State University. These dynamic modulus values are stored in the HMA materials library. The following lists the test results included in the HMA library.

Nominal Maximum Size of the Mixture	Asphalt Performance Grade Designation	Number of Gyration
9.5 mm	GR 67-22	N50
9.5 mm	GR 67-22	N65
9.5 mm	GR 76-22	N85
9.5 mm	GR- 82-22	N85
12.5 mm	GR 67-22	N50
12.5 mm	GR 67-22	N65
12.5 mm	GR 76-22	N85
12.5 mm	GR- 82-22	N85
19.0 mm	GR 67-22	N50
19.0 mm	GR 67-22	N65
19.0 mm	GR 76-22	N85
19.0 mm	GR- 82-22	N85
9.5L mm	GR 67-22	N50
9.5L mm	GR 67-22	N65
9.5L mm	GR 76-22	N85
9.5L mm	GR- 82-22	N85
12.5L mm	GR 67-22	N50
12.5L mm	GR 67-22	N65
12.5L mm	GR 76-22	N85
12.5L mm	GR- 82-22	N85
19.0L mm	GR 67-22	N50
19.0L mm	GR 67-22	N65
19.0L mm	GR 76-22	N85
19.0L mm	GR- 82-22	N85

9.5mm; GR 67-22, N50						9.5mm; GR67-22, N65							
Temperature, °C	Frequency, Hz	Dynamic Modulus, psi				Average	Temperature, °C	Frequency, Hz	Dynamic Modulus, psi				Average
		A	B	C	Average				A	B	C	Average	
-10	25	2637304	1761973	2387725	2262334	-10	25	1543523	2886312	3499598	2643144		
	10	2529084	1670636	2306228	2168649		10	1521930	2827788	3261238	2536985		
	5	2438805	1614603	2229588	2094332		5	1471132	2768035	3160150	2466439		
	1	2240194	1464418	2037050	1913887		1	1350957	2567141	2856438	2258179		
	0.5	2141993	1396979	1943819	1827597		0.5	1288724	2483762	2738496	2170327		
	0.1	1891148	1241528	1702177	1611618		0.1	1137673	2267806	2419108	1941529		
4	25	1825279	1447866	1741300	1671482	4	25	1031875	2116659	2230451	1792995		
	10	1657567	1279496	1569146	1502070		10	951226	1999431	2027614	1659424		
	5	1546643	1189964	1459427	1398678		5	892869	1908007	1882464	1561113		
	1	1272673	991296	1196245	1153405		1	743658	1588765	1558503	1296975		
	0.5	1152306	907609	1070749	1043555		0.5	671405	1433794	1412410	1172536		
	0.1	876746	705849	788478	790358		0.1	516089	1098421	1083066	899192		
21	25	838131	802233	508602	716322	21	25	936901	989042	1028195	984713		
	10	685207	643618	643095	657307		10	659377	805633	890048	785019		
	5	569005	545852	554946	556601		5	585891	683643	772487	680674		
	1	359648	345229	359410	354762		1	369974	440166	577059	462400		
	0.5	281586	278091	284038	281238		0.5	318656	354118	483087	385287		
	0.1	294560	162568	161735	206288		0.1	202237	209079	284458	231925		
37	25	406667	385005	304619	365431	37	25	481481	432790	444596	452956		
	10	276736	240085	172388	229736		10	330086	304501	299519	311369		
	5	205601	174511	132748	170953		5	250715	229137	219148	233000		
	1	100004	79635	59608	79749		1	120133	111178	119954	117088		
	0.5	76283	64253	46644	62393		0.5	99397	87868	92845	93370		
	0.1	47587	39774	30387	39249		0.1	63760	50518	52840	55706		
54	25	127529	115039	81451	108006	54	25	160658	148774	140766	150066		
	10	62529	54685	45985	54400		10	85083	67955	65257	72765		
	5	34171	28451	23846	28822		5	45176	39615	40587	41793		
	1	20496	16884	13860	17080		1	25827	22392	23920	24047		
	0.5	16903	14273	12407	14528		0.5	21543	19109	20021	20224		
	0.1	13265	11306	10018	11530		0.1	15392	13772	14179	14448		

9.5mm; GR 76-22, N85						9.5mm; GR 82-22, N85							
Temperature, °C	Frequency, Hz	Dynamic Modulus, psi				Average	Temperature, °C	Frequency, Hz	Dynamic Modulus, psi				Average
		A	B	C	Average				A	B	C	Average	
-10	25	2562490	2517532	2277809	2452610	-10	25	2227577	2786160	2557425	2523721		
	10	2450255	2434667	2154857	2346593		10	2132169	2739214	2473986	2448456		
	5	2325048	2362043	2086654	2257915		5	2077387	2682263	2619951	2459867		
	1	2114564	2174021	1911429	2066671		1	1943519	2502746	2430111	2292125		
	0.5	2010162	2077083	1834608	1973951		0.5	1867370	2420640	2343879	2210630		
	0.1	1755920	1842411	1638973	1745768		0.1	1694870	2197363	2122030	2004754		
4	25	1849556	1808765	1750790	1803037	4	25	1837565	2189923	1639089	1888859		
	10	1653907	1637880	1607216	1633001		10	1685473	2053681	1513486	1750880		
	5	1529526	1519171	1480470	1509722		5	1608955	1942469	1455113	1668846		
	1	1243861	1261920	1196758	1234180		1	1384111	1653718	1262143	1433324		
	0.5	1118485	1151467	1070574	1113509		0.5	1276969	1527817	1218627	1341138		
	0.1	841053	891815	793224	842030		0.1	1020243	1232504	978149	1076965		
21	25	898101	965652	860729	908161	21	25	1033867	1261415	1202300	1165861		
	10	715006	791907	677968	728294		10	860755	1041264	908899	936973		
	5	598028	683859	560292	614060		5	752512	920879	816836	830076		
	1	379237	454081	350338	394552		1	548544	654555	604040	602379		
	0.5	316980	376182	285292	326152		0.5	460915	557177	517622	511905		
	0.1	189041	228887	169859	195929		0.1	296189	359382	334573	330048		
37	25	357062	422515	363651	381076	37	25	535338	561451	595448	564079		
	10	233096	261323	215778	236732		10	337322	361987	374845	358051		
	5	155403	180942	145582	160642		5	237729	228624	274345	246899		
	1	84999	109911	85722	93544		1	147469	140589	167713	151924		
	0.5	69762	86665	67085	74504		0.5	119807	123977	133616	125800		
	0.1	45536	54022	41991	47183		0.1	74246	78636	81609	78164		
54	25	149309	151520	135125	145318	54	25	240512	244388	233593	239498		
	10	80532	89632	73398	81187		10	128729	135173	139623	134508		
	5	52359	58551	45616	52175		5	76721	82002	86131	81618		
	1	25385	28476	23048	25636		1	47455	49355	48466	48425		
	0.5	26068	28331	23496	25965		0.5	42395	42508	42414	42439		
	0.1	23216	25131	21571	23306		0.1	31439	30718	31879	31345		

12.5mm; GR 67-22; N50						12.5mm; GR 67-22; N65							
Temperature, °C	Frequency, Hz	Dynamic Modulus, psi				Average	Temperature, °C	Frequency, Hz	Dynamic Modulus, psi				Average
		A	B	C	Average				A	B	C	Average	
-10	25	2379602	2314931	2373096	2355876	-10	25	3247427	2149028	1505146	2300534		
	10	2241301	2078574	2251130	2190335		10	3166864	1833077	1466523	2155488		
	5	2163412	1999872	2171920	2111735		5	3043298	1775758	1396609	2071888		
	1	1965776	1844215	1971356	1927116		1	2770611	1641851	1319360	1910607		
	0.5	1862891	1790750	1873949	1842530		0.5	2642129	1613332	1298847	1851436		
	0.1	1614892	1606184	1644606	1621894		0.1	2337619	1441483	1211746	1663616		
4	25	1640535	1764633	1667952	1691040	4	25	2290449	2005068	1637919	1977812		
	10	1459645	1603536	1533100	1532094		10	2075110	1853955	1398558	1775874		
	5	1342064	1499342	1434886	1425431		5	1891141	1712292	1321432	1641622		
	1	1084823	1243847	1188075	1172248		1	1566685	1393159	1087459	1349101		
	0.5	974641	1129936	1084034	1062870		0.5	1405585	1264181	986939	1218902		
	0.1	731604	863630	837381	810872		0.1	1045908	966753	737393	916685		
21	25	802454	854406	848917	835259	21	25	924062	958967	900396	927808		
	10	649239	700719	681705	677221		10	726008	779180	722415	742534		
	5	543281	596242	581148	573557		5	601355	659542	623638	628178		
	1	332683	377905	361290	357293		1	356703	410999	385535	384412		
	0.5	265950	308893	292751	289198		0.5	280353	324558	308160	304357		
	0.1	150561	181286	171310	167719		0.1	154325	179815	310829	214990		
37	25	360500	342239	382288	361676	37	25	356344	421706	343262	373771		
	10	218835	211691	230715	220413		10	234463	283807	218745	245672		
	5	153883	147280	160651	153938		5	105703	206760	155687	156050		
	1	86479	79502	89160	85047		1	81820	88543	69481	79948		
	0.5	65461	59045	66952	63819		0.5	62565	70260	51038	61287		
	0.1	39035	33897	39007	37313		0.1	38599	42803	36203	39201		
54	25	118155	124739	111783	118226	54	25	124307	170251	91525	128694		
	10	49259	66207	46573	54013		10	60026	87190	51411	66209		
	5	32588	41968	32352	35636		5	32734	46945	25729	35136		
	1	14158	18811	14123	15697		1	19150	24845	14324	19440		
	0.5	11474	15304	11827	12869		0.5	15929	21214	12741	16628		
	0.1	11292	11164	11623	11360		0.1	12475	14552	10428	12485		

12.5mm; GR 76-22, N85						12.5mm; GR 82-22, N85							
Temperature, °C	Frequency, Hz	Dynamic Modulus, psi				Average	Temperature, °C	Frequency, Hz	Dynamic Modulus, psi				Average
		A	B	C	Average				A	B	C	Average	
-10	25	1916321	2363933	1815373	2031876	-10	25	1998082	1946225	2388849	2111052		
	10	1825697	2278821	1712284	1938934		10	1897602	1811269	2291371	2000081		
	5	1760424	2196942	1686797	1881388		5	1829384	1724657	2211781	1921941		
	1	1593116	1993899	1569998	1719004		1	1686771	1590656	2019571	1765666		
	0.5	1527273	1910299	1548915	1662162		0.5	1615243	1491562	1920126	1675644		
	0.1	1357318	1693905	1386734	1479319		0.1	1437344	1247601	1692519	1459155		
4	25	1468264	1755348	1746830	1656814	4	25	1533877	1406782	1798809	1579823		
	10	1333425	1626322	1602475	1520741		10	1397217	1263824	1638799	1433280		
	5	1264889	1527991	1502977	1431952		5	1319014	1222260	1534630	1358635		
	1	1047994	1269123	1237990	1185036		1	1113725	1010152	1256946	1126941		
	0.5	960596	1158141	1125180	1081306		0.5	1018187	921062	1127826	1022358		
	0.1	744559	891989	865247	833932		0.1	792863	695004	842427	776764		
21	25	798185	900130	831887	843401	21	25	836193	769234	831719	812382		
	10	626236	717446	671735	671806		10	656556	583494	643731	627927		
	5	531256	607167	558036	565486		5	548588	483881	531510	521326		
	1	353257	398176	355570	369001		1	365873	299685	336774	334111		
	0.5	288326	320717	287207	298750		0.5	298905	241303	268649	269619		
	0.1	177091	191955	173902	180983		0.1	184148	143764	160777	162896		
37	25	416285	446512	445450	436082	37	25	434637	373802	383936	397458		
	10	272734	323915	316985	304544		10	264720	248682	259086	257496		
	5	213207	232265	241084	228852		5	193818	188798	171106	184574		
	1	87387	117812	117041	107413		1	112087	85999	97803	98630		
	0.5	81114	97679	99067	92620		0.5	90089	73677	79556	81107		
	0.1	61970	60946	62428	61781		0.1	58503	47858	51459	52607		
54	25	166760	180374	172155	173096	54	25	183272	156106	164724	168034		
	10	92444	95023	91523	92997		10	109187	88328	99661	99058		
	5	61934	59054	82646	67878		5	60683	69821	75949	68818		
	1	35183	35266	33625	34691		1	36471	27424	30087	31327		
	0.5	31665	32267	33401	32444		0.5	34296	27809	31747	31284		
	0.1	26668	27091	27863	27207		0.1	27661	24921	27514	26699		

19.0mm; GR 67-22, N50						19.0mm; GR 67-22, N65							
Temperature, °C	Frequency, Hz	Dynamic Modulus, psi				Average	Temperature, °C	Frequency, Hz	Dynamic Modulus, psi				Average
		A	B	C	Average				A	B	C	Average	
-10	25	2857665	2300001	2372923	2510196	-10	25	4076065	2852158	2806858	3245027		
	10	2756453	2194506	2291951	2414303		10	3838666	2668390	2775649	3094235		
	5	2670699	2128283	2227817	2342266		5	3698581	2556100	2688920	2981200		
	1	2450877	1947014	2047968	2148620		1	3332749	2423048	2443047	2732948		
	0.5	2342858	1862697	1964418	2056658		0.5	3191511	2335609	2326718	2617946		
	0.1	2091729	1661567	1781667	1844988		0.1	2801716	2083356	2040350	2308474		
4	25	2145500	1894703	1827294	1955832	4	25	2964887	1651698	2076875	2231153		
	10	1980452	1729922	1698662	1803012		10	2686806	1454781	1917229	2019605		
	5	1862181	1620096	1602469	1694915		5	2484849	1332479	1788990	1868773		
	1	1544974	1354785	1341087	1413615		1	2038890	1101969	1472837	1537899		
	0.5	1398558	1230336	1219497	1282797		0.5	1833471	1036174	1335950	1401865		
	0.1	1075177	945020	940339	986845		0.1	1380117	814918	1034262	1076432		
21	25	1161989	1072178	1088220	1107462	21	25	1211591	1087599	1054452	1117881		
	10	932946	845870	878604	885806		10	969918	856952	858869	895246		
	5	790006	712833	744807	749216		5	811159	713053	731977	752063		
	1	497376	438480	467331	467729		1	496856	428196	456706	460586		
	0.5	390683	353195	373365	372414		0.5	387902	331950	361343	360399		
	0.1	211821	192530	202074	202142		0.1	204676	176771	200983	194144		
37	25	588490	477805	385227	483841	37	25	398138	419825	438648	418870		
	10	363856	291418	227767	294347		10	236491	244259	258544	246431		
	5	266434	213682	159831	213316		5	168047	173407	183312	174922		
	1	137327	114713	87713	113251		1	89906	91318	98201	93142		
	0.5	105653	86969	66834	86485		0.5	63973	67703	72453	68043		
	0.1	52533	45812	40146	46164		0.1	42332	39680	42058	41357		
54	25	136768	123740	126355	128954	54	25	121492	123527	130732	125250		
	10	67212	60436	63010	63553		10	58667	54350	69367	60794		
	5	35480	32201	33072	33584		5	30732	35468	39998	35399		
	1	20670	18157	19568	19465		1	17231	14601	17681	16504		
	0.5	17123	15952	16573	16549		0.5	15386	12521	14997	14301		
	0.1	13605	12649	13454	13236		0.1	13254	11855	13893	13000		

19.0mm; GR 67-22, N85						19.0mm; GR 76-22, N85							
Temperature, °C	Frequency, Hz	Dynamic Modulus, psi				Average	Temperature, °C	Frequency, Hz	Dynamic Modulus, psi				Average
		A	B	C	Average				A	B	C	Average	
-10	25	3233151	2685985	2665207	2861448	-10	25	2803166	2709223	2410840	2641076		
	10	3013983	2608817	2607806	2743535		10	2629214	2471932	2308306	2469817		
	5	2879232	2550388	2593596	2674405		5	2516642	2378741	2236369	2377251		
	1	2652868	2376504	2408930	2479434		1	2277078	2185106	2061066	2174417		
	0.5	2558197	2299821	2355854	2404624		0.5	2167920	2099378	1979640	2082313		
	0.1	2285325	2099579	2144655	2176520		0.1	1901964	1882209	1774125	1852766		
4	25	2506052	2098003	2266147	2290067	4	25	1713852	1919206	1785962	1806340		
	10	2334062	1968691	2077673	2126809		10	1545203	1769787	1170009	1495000		
	5	2187930	1856432	1942243	1995535		5	1415664	1667845	1069101	1384203		
	1	1809201	1549483	1587531	1648738		1	1147892	1415267	928393	1163851		
	0.5	1648846	1422936	1439182	1503655		0.5	1028906	1300164	857129	1062066		
	0.1	1265287	1098566	1078944	1147599		0.1	776699	1021839	682122	826886		
21	25	1318866	1223215	1200183	1247421	21	25	854402	1040939	944889	946743		
	10	1094759	1005992	1019816	1040189		10	654593	843962	763731	754096		
	5	934216	871540	877835	894530		5	550679	728212	657007	645299		
	1	611047	580108	574856	588670		1	370073	501861	449818	440584		
	0.5	490814	470014	461131	473986		0.5	300484	416872	366444	361267		
	0.1	272320	264786	253639	263582		0.1	182256	257432	224028	221239		
37	25	456564	471675	471625	466621	37	25	467158	575992	574427	539192		
	10	309535	316397	290089	305340		10	293170	419586	406998	373251		
	5	213917	217284	206713	212638		5	209822	302540	286658	266340		
	1	90693	104888	110210	101930		1	117893	163501	152939	144778		
	0.5	72991	78699	85477	79056		0.5	94662	137228	127882	119924		
	0.1	49442	51618	47116	49392		0.1	59089	86531	79263	74961		
54	25	160249	151133	151272	154218	54	25	190856	227649	222074	213526		
	10	75754	71303	71996	73017		10	108767	128038	135086	123964		
	5	41552	37917	38341	39270		5	83727	98660	103330	95239		
	1	21472	21167	21449	21363		1	36642	40579	40842	39355		
	0.5	18992	18224	18456	18557		0.5	33630	44532	39926	39363		
	0.1	14985	14190	14214	14463		0.1	27917	35783	32165	31955		

9.5Lmm; G6 7-22, N50						9.5Lmm; G 67-22, N65							
Temperature, °C	Frequency, Hz	Dynamic Modulus, psi				Average	Temperature, °C	Frequency, Hz	Dynamic Modulus, psi				Average
		A	B	C	Average				A	B	C	Average	
-10	25	2264704	2976439	2669092	2636745	-10	25	3210071	2670750	2280123	2720315		
	10	2206261	2905678	2608500	2573480		10	3083510	2568892	2201130	2617844		
	5	2150457	2820387	2524510	2498451		5	2974653	2516115	2137212	2542660		
	1	1993313	2626513	2363402	2327743		1	2772203	2351512	1981420	2368378		
	0.5	1925400	2527621	2275374	2242798		0.5	2658030	2269562	1900742	2276111		
	0.1	1738866	2263323	2043558	2015249		0.1	2375515	2044839	1709065	2043140		
4	25	1830206	2157326	2175660	2054397	4	25	2456121	2153769	1813257	2141049		
	10	1745990	1961356	2007735	1905027		10	2278385	2011372	1674493	1988083		
	5	1682518	1871965	1885043	1813175		5	2135446	1901216	1576889	1871184		
	1	1442826	1580559	1593323	1538903		1	1792805	1597626	1331607	1574013		
	0.5	1334512	1455251	1463422	1417728		0.5	1642342	1465630	1232075	1446682		
	0.1	1041778	1126233	1139344	1102452		0.1	1286223	1146494	979528	1137415		
21	25	1067684	1180861	1122396	1123647	21	25	1219354	1171109	1071487	1153983		
	10	866124	963855	921430	917137		10	1002964	961312	864596	942957		
	5	748466	822830	796375	789223		5	866795	829699	754493	816996		
	1	480772	528853	521154	510260		1	570227	553317	492176	538573		
	0.5	395381	427429	426040	416284		0.5	472665	452227	411268	445387		
	0.1	230498	239798	247525	239273		0.1	271993	262108	240138	258080		
37	25	499381	476248	520533	498721	37	25	563648	566220	555164	561677		
	10	343686	327348	367779	346271		10	381979	363533	391601	379037		
	5	230588	215136	257066	234263		5	267063	294003	247487	269517		
	1	120356	112748	120826	117977		1	136667	129939	124986	130531		
	0.5	94670	88119	98034	93608		0.5	108079	107319	99584	104994		
	0.1	55150	52682	56825	54886		0.1	63159	62866	59493	61839		
54	25	165628	160283	163342	163084	54	25	199675	195865	183287	192942		
	10	85206	87172	85965	86114		10	95208	93696	89628	92844		
	5	68070	48949	68947	61989		5	56986	55809	51114	54636		
	1	32613	31716	31997	32109		1	37032	36635	34018	35895		
	0.5	26795	26271	27945	27004		0.5	33304	33132	31086	32507		
	0.1	24072	23788	23398	23753		0.1	27203	26489	25475	26389		

9.5Lmm; G 76-22, N85						9.5Lmm; G 82-22, N85							
Temperature, °C	Frequency, Hz	Dynamic Modulus, psi				Average	Temperature, °C	Frequency, Hz	Dynamic Modulus, psi				Average
		A	B	C	Average				A	B	C	Average	
-10	25	2606841	3414968	3102703	3041504	-10	25	2181610	1747452	1904197	1944420		
	10	2337526	3255884	3136826	2910079		10	2126893	1678244	1731284	1845474		
	5	2142889	3118185	3043354	2768143		5	1976890	1620987	1797570	1798482		
	1	1968064	2849587	2809694	2542448		1	1802299	1475459	1719071	1665610		
	0.5	1929776	2713896	2703952	2449208		0.5	1716277	1414886	1671791	1600985		
	0.1	1659691	2387175	2402546	2149804		0.1	1483131	1255980	1425821	1388311		
4	25	1847770	2233161	2440582	2173838	4	25	1799183	1455336	1665459	1639993		
	10	1733496	2054855	2166073	1984808		10	1609429	1313549	1537492	1486823		
	5	1623204	1902250	2008605	1844686		5	1509133	1241312	1421222	1390556		
	1	1333675	1555000	1660785	1516487		1	1262440	1018497	1137273	1139403		
	0.5	1210056	1411458	1500641	1374052		0.5	1153917	924603	1045993	1041504		
	0.1	931556	1076480	1145533	1051190		0.1	902120	701584	770856	791520		
21	25	969333	1080345	1136393	1062024	21	25	1079055	823320	908497	936957		
	10	725974	870000	911579	835851		10	865783	664879	673054	734572		
	5	589348	742048	779487	703627		5	753534	566580	556787	625634		
	1	388240	486704	517545	464163		1	511317	373223	386320	423620		
	0.5	357952	400826	426523	395100		0.5	424117	307105	321018	350747		
	0.1	222362	239871	258296	240176		0.1	260514	189682	193468	214555		
37	25	516094	520666	510205	515655	37	25	446876	369934	375334	397381		
	10	378834	372528	319210	356857		10	276176	216900	221117	238064		
	5	273401	229552	230916	244623		5	193985	149010	150506	164500		
	1	142011	141745	142320	142025		1	120702	92399	91719	101607		
	0.5	113345	115169	113286	113933		0.5	97526	74703	73615	81948		
	0.1	74916	74125	72328	73790		0.1	61706	48783	47847	52779		
54	25	204325	215887	210673	210295	54	25	153959	159263	151582	154935		
	10	138902	126111	110109	125040		10	111773	92227	81665	95222		
	5	101834	68352	67108	79098		5	67160	53302	48172	56211		
	1	39313	48060	46478	44617		1	29420	30066	27312	28933		
	0.5	45913	41162	40541	42539		0.5	34704	30027	29501	31411		
	0.1	37503	36330	35227	36353		0.1	28652	25630	25855	26712		

12.5Lmm; G 67-22, N50						12.5Lmm; G 67-22, N65							
Temperature, °C	Frequency, Hz	Dynamic Modulus, psi				Average	Temperature, °C	Frequency, Hz	Dynamic Modulus, psi				Average
		A	B	C	Average				A	B	C	Average	
-10	25	3425536	3111881	3335854	3291090	-10	25	3580866	2930145	3442356	3317789		
	10	3172356	3069974	3256404	3166245		10	3493684	2844022	3346496	3228067		
	5	3063921	3011057	3182311	3085763		5	3413561	2769644	3254954	3146053		
	1	2812228	2823723	2975970	2870640		1	3180548	2576786	3051971	2936435		
	0.5	2750457	2734619	2871921	2785666		0.5	3071841	2489510	2942839	2834730		
	0.1	2424431	2501324	2613694	2513150		0.1	2785392	2268532	2676854	2576923		
4	25	2696047	2335422	2497394	2509621	4	25	2578949	2225593	2499428	2434657		
	10	2563497	2200371	2332580	2365483		10	2412441	2085255	2354930	2284209		
	5	2431127	2079721	2226895	2245914		5	2265461	1957235	2243010	2155235		
	1	2052719	1762739	1899932	1905130		1	1916371	1684075	1917171	1839206		
	0.5	1880056	1621992	1757981	1753343		0.5	1751238	1564956	1775513	1697236		
	0.1	1466377	1274692	1399519	1380196		0.1	1378754	1261497	1424238	1354830		
21	25	1443260	1308484	1435765	1395836	21	25	1295659	1318478	1350097	1321411		
	10	1169791	1085765	1212199	1155918		10	762046	1082319	1119618	987994		
	5	1001027	938326	1056589	998647		5	564553	944105	968843	825834		
	1	666265	635570	726825	676220		1	374729	655540	655022	561763		
	0.5	543710	526843	601680	557411		0.5	322393	539473	538799	466888		
	0.1	315333	314189	362673	330732		0.1	211314	322314	320241	284623		
37	25	661429	639697	670817	657314	37	25	643814	695932	653533	664426		
	10	427954	456679	486244	456959		10	460514	443908	428112	444178		
	5	327611	326858	343403	332624		5	318265	347592	327161	331006		
	1	158346	166384	172059	165596		1	164436	172919	162829	166728		
	0.5	123487	130561	135880	129976		0.5	129021	138124	129801	132315		
	0.1	71210	76017	76907	74711		0.1	71702	78618	75058	75126		
54	25	217726	206902	225341	216656	54	25	197220	232396	215644	215086		
	10	117067	99561	106406	107678		10	95621	112120	106293	104678		
	5	64397	63047	66787	64744		5	61663	70863	83968	72165		
	1	43336	42902	43632	43290		1	40881	45743	36137	40921		
	0.5	37581	37187	37855	37541		0.5	33603	36639	36982	35741		
	0.1	29612	28833	29001	29149		0.1	27350	30793	31090	29744		

12.5Lmm; G 76-22, N85						12.5Lmm; G 82-22, N85							
Temperature, °C	Frequency, Hz	Dynamic Modulus, psi				Average	Temperature, °C	Frequency, Hz	Dynamic Modulus, psi				Average
		A	B	C	Average				A	B	C	Average	
-10	25	3042500	2582971	1774466	2466646	-10	25	2443927	2459005	2501492	2468141		
	10	2900955	2496372	1699831	2365719		10	2333763	2373073	2419322	2375386		
	5	2845888	2416386	1629779	2297351		5	2240015	2317827	2357657	2305166		
	1	2591734	2221343	1520112	2111063		1	2007927	2125058	2175455	2102813		
	0.5	2480450	2127605	1473911	2027322		0.5	1899459	2037616	2086484	2007853		
	0.1	2204172	1899660	1327967	1810600		0.1	1631937	1768878	1830219	1743678		
4	25	2081808	1782107	1565292	1809736	4	25	1669292	1725240	1763587	1719373		
	10	1909067	1714074	1406898	1676680		10	1517296	1559849	1562605	1546583		
	5	1775882	1581737	1330602	1562740		5	1401256	1439073	1413768	1418032		
	1	1482934	1343549	1095657	1307380		1	1104238	1142303	1100115	1115552		
	0.5	1359291	1224512	1035316	1206373		0.5	974388	1010453	962469	982437		
	0.1	1051972	945827	823518	940439		0.1	690079	717862	671222	693054		
21	25	1109585	1009953	1079893	1066477	21	25	755844	791956	721851	756550		
	10	882594	773964	845146	833901		10	556956	597925	525942	560274		
	5	753697	658998	697440	703378		5	451757	493171	427996	457641		
	1	514357	432261	489710	478776		1	270692	302545	261935	278391		
	0.5	426774	351580	405113	394489		0.5	212600	237671	206056	218775		
	0.1	258001	211774	251536	240437		0.1	125462	137765	215437	159555		
37	25	619827	536505	583522	579951	37	25	332064	362438	353437	349313		
	10	436072	367698	415085	406285		10	212403	244876	234996	230758		
	5	298291	255212	301089	284864		5	162225	183118	134494	159946		
	1	162404	138512	163752	154889		1	78325	83096	75150	78857		
	0.5	136478	115723	133523	128575		0.5	65535	71002	65476	67338		
	0.1	84399	73912	83357	80556		0.1	45169	47299	45690	46052		
54	25	228555	217482	237552	227863	54	25	141522	156405	148772	148900		
	10	117400	108741	121023	115721		10	70648	76360	72378	73129		
	5	76396	66888	73355	72213		5	40736	44363	42355	42485		
	1	52145	49150	52141	51146		1	33335	34374	34782	34164		
	0.5	45377	40564	45603	43848		0.5	31267	31470	32738	31825		
	0.1	37621	36011	35111	36248		0.1	27158	26019	28126	27101		

19.0Lmm; G 67-22, N50						19.0Lmm; G 67-22, N65							
Temperature, °C	Frequency, Hz	Dynamic Modulus, psi				Average	Temperature, °C	Frequency, Hz	Dynamic Modulus, psi				Average
		A	B	C	Average				A	B	C	Average	
-10	25	2206421	3511103	3333381	3016968	-10	25	3134571	3175055	2959952	3089859		
	10	1883416	3464295	3210639	2852783		10	3056929	3115594	2868836	3013786		
	5	1718303	3420124	3115310	2751246		5	2978308	3042892	2789158	2936786		
	1	1589194	3227496	2965505	2594065		1	2779774	2843716	2588796	2737429		
	0.5	1580135	3135439	2878556	2531377		0.5	2679848	2750208	2501054	2643703		
	0.1	1479688	2888739	2654944	2341124		0.1	2450874	2519861	2277167	2415967		
4	25	1613364	2499709	2587479	2233517	4	25	2316290	2470794	2213156	2333413		
	10	1427078	2341396	2395730	2054735		10	2167567	2293593	2042508	2167889		
	5	1377716	2211176	2264864	1951252		5	2048476	2169467	1946620	2054854		
	1	1239009	1892377	1949510	1693632		1	1757084	1864235	1649781	1757033		
	0.5	1136807	1755689	1808594	1567030		0.5	1628816	1733926	1539577	1634106		
	0.1	897373	1423722	1474655	1265250		0.1	1323464	1419091	1253923	1332159		
21	25	1086941	1414783	1400354	1300693	21	25	1300624	1572599	1362128	1411784		
	10	880192	1184443	1181695	1082110		10	1103927	1328695	1131755	1188126		
	5	789293	1051780	1047160	962744		5	982622	1166705	1001431	1050253		
	1	553484	738218	737119	676274		1	695467	818843	693997	736102		
	0.5	482707	624430	623896	577011		0.5	592717	679057	582701	618158		
	0.1	298270	390938	394911	361373		0.1	379633	413918	356492	383348		
37	25	722834	780453	802372	768553	37	25	762464	814125	746968	774519		
	10	466849	572847	591358	543685		10	559020	591247	494324	548197		
	5	361379	438572	437558	412503		5	437190	430363	399262	422272		
	1	197230	241304	236984	225172		1	248844	226499	206521	227288		
	0.5	149925	189996	189553	176491		0.5	199848	177028	168028	181635		
	0.1	84073	105249	108037	99120		0.1	113643	97217	95152	102004		
54	25	238340	288418	308298	278352	54	25	302360	289590	253293	281748		
	10	126039	151698	144607	140781		10	173395	166284	125331	155003		
	5	68370	90603	92543	83838		5	119680	87685	83035	96800		
	1	45879	57975	60882	54912		1	61326	53492	51206	55341		
	0.5	39111	49550	52016	46892		0.5	50014	45363	44872	46750		
	0.1	29907	37026	38773	35235		0.1	38843	35854	34069	36256		

19.0Lmm; G 67-22, N85						19.0Lmm; G 76-22, N85							
Temperature, °C	Frequency, Hz	Dynamic Modulus, psi				Average	Temperature, °C	Frequency, Hz	Dynamic Modulus, psi				Average
		A	B	C	Average				A	B	C	Average	
-10	25	3439059	3664403	2879614	3327692	-10	25	2971337	3754954	2955335	3227209		
	10	3384540	3619954	2840667	3281720		10	2920033	3572905	2831693	3108210		
	5	3326361	3526351	2798875	3217196		5	2856994	3453443	2765743	3025393		
	1	3113879	3277093	2671848	3020940		1	2664024	3221678	2594587	2826763		
	0.5	3013342	3151228	2575016	2913195		0.5	2572948	3095566	2506482	2724999		
	0.1	2739194	2858644	2359032	2652290		0.1	2323132	2798367	2247843	2456447		
4	25	2332350	2601093	2264513	2399319	4	25	2060484	2507711	1998470	2188888		
	10	2151498	2424596	2071354	2215816		10	1893987	2313922	1821684	2009864		
	5	2020185	2275967	1939982	2078711		5	1773398	2161773	1721071	1885414		
	1	1725267	1927194	1660544	1771002		1	1487091	1811267	1461951	1586770		
	0.5	1585757	1775719	1546351	1635942		0.5	1354278	1651916	1335886	1447360		
	0.1	1275355	1405221	1271377	1317318		0.1	1065224	1296830	1048031	1136695		
21	25	1197080	1313840	1294657	1268526	21	25	1100648	1205898	1024085	1110210		
	10	828967	1083487	1083910	998788		10	826071	986220	803293	871861		
	5	851439	952173	960216	921276		5	736389	857317	692084	761930		
	1	632980	652127	683126	656078		1	511315	592873	472774	525654		
	0.5	559002	547447	589784	565411		0.5	427207	495000	385649	435952		
	0.1	369664	336760	369293	358572		0.1	262772	308841	236546	269387		
37	25	768146	680897	782560	743868	37	25	518733	579109	501284	533042		
	10	522427	483319	564216	523320		10	331674	370490	305937	336034		
	5	421271	351263	408392	393642		5	218790	255061	194996	222949		
	1	230394	192636	231020	218017		1	139037	161575	123350	141321		
	0.5	180883	151576	194486	175648		0.5	113472	131258	99718	114816		
	0.1	96664	83720	105940	95441		0.1	74353	86347	64287	74995		
54	25	298903	252371	291798	281024	54	25	264562	275047	233662	257757		
	10	150530	129545	146478	142185		10	136493	134808	118076	129793		
	5	82829	74824	104371	87342		5	69105	76280	61442	68943		
	1	46014	42162	49641	45939		1	52904	59083	47031	53006		
	0.5	46719	42197	42620	43845		0.5	47690	54042	42402	48045		
	0.1	34687	32361	31991	33013		0.1	38312	44401	34066	38926		

19.0mm; GR 67-22, N50 3%					
Temperature, °C	Frequency, Hz	Dynamic Modulus, psi			
		A	B	C	Average
-10	25	2523419	2746261	2484936	2584872
	10	2470531	2629027	2283974	2461177
	5	2415275	2545163	2181034	2380491
	1	2215676	2331924	2087787	2211796
	0.5	2147219	2236698	2011592	2131836
	0.1	1941118	2000620	1814572	1918770
4	25	1929937	2055436	1913104	1966159
	10	1771723	1888519	1768571	1809604
	5	1645021	1768217	1645420	1686219
	1	1343722	1470083	1355061	1389622
	0.5	1219775	1347370	1226618	1264588
	0.1	941066	1050128	933642	974945
21	25	925724	1099457	795561	940247
	10	736681	884282	786782	802582
	5	632810	763159	666480	687483
	1	418446	515523	442622	458864
	0.5	343378	424709	355157	374415
	0.1	216793	261320	205475	227862
37	25	386086	475436	374749	412090
	10	264113	327583	225154	272284
	5	179285	224504	154548	186113
	1	101364	116552	87207	101707
	0.5	82062	96703	67372	82046
	0.1	51391	57377	41254	50007
54	25	163115	173525	132277	156306
	10	96894	116211	72219	95108
	5	61340	59274	39804	53473
	1	34104	33179	28860	32048
	0.5	NA	NA	NA	NA
	0.1	NA	NA	NA	NA

APPENDIX G—CALIBRATION OF RUT DEPTH TRANSFER FUNCTION

This appendix covers the use of repeated load triaxial tests with the Asphalt Mixture Performance Tester (AMPT) for evaluating the rutting resistance of dense-graded asphalt concrete mixtures in accordance with the Mechanistic-Empirical Pavement Design Guide (MEPDG) rut depth computational methodology.

G.1 INTRODUCTION

The rutting resistance of dense-graded asphalt concrete mixtures is defined by the use of plastic strain coefficients of the rut depth transfer function included in the MEPDG software referred to as the Kaloush vertical strain rut depth transfer function. The plastic strain coefficients are determined from an analysis of the accumulated plastic strain from the repeated load triaxial test.

The method is used in support of the design and evaluation of dense-graded asphalt concrete mixtures using mixture specific plastic strain coefficients instead of the default coefficients derived from the global calibration of the Kaloush vertical strain rut depth transfer function. The plastic strain coefficients are given and defined in Chapter 2 of the report and in Section 5 of the 2008 MEPDG Manual of Practice.

Repeated load triaxial tests are used to determine values for the plastic strain coefficients to the Kaloush vertical strain rut depth transfer function included in the MEPDG software. The laboratory-derived plastic strain coefficients are adjusted to represent field conditions.

Repeated load testing is suggested for use in calculating the level of rutting of HMA mixtures for rehabilitation and new pavement construction during design and/or to create a materials library on a mixture specific basis. The following bullets summarize the conditions most appropriate for using this test method and rut depth transfer function identified in the above paragraphs.

- Repeated load triaxial tests using the AMPT in support of the Kaloush rut depth transfer function can be used during the mixture design stage and mixture production when the component materials or bulk mixture can be sampled for preparing test specimens in accordance with AASHTO TP 79.
- The height-to-diameter requirement required for the test specimens eliminates the use of cores for HMA lifts less than 4 inches in thickness. The test procedure can be used for lift thicknesses that are greater than 6 inches. For lift thicknesses of 4 to 6 inches, test specimens can be cored laterally along a larger sample extracted from the HMA mat assuming that aggregate alignment has little to no impact on the plastic deformation parameters. That assumption or hypothesis is believed to be false (Von Quintus, et al., 1991). In addition, coring the test specimens laterally from a larger diameter sample is not included within this test method.
- The height-to-diameter requirement in AASHTO TP 79 restricts the use of this procedure to determine the MEPDG inputs for forensic investigations or follow-up studies when there are disputes between the owner and contractor over any

warranty work and actual materials are unavailable to reconstitute the HMA mixture, since most HMA lifts or layers are less than 4 inches in thickness.

- The use of the gyratory compactor is known to result in variable air voids across the radial axis as well as along the vertical axis of the compacted specimen. AASHTO TP 79 requires that the gyratory compacted specimens be cored to test the center part of the specimen. Coring the center portion of the gyratory specimen reduces the air void gradients within the test specimen and is a preferred surface for mounting the LVDTs on the test specimen.

G.2 TEST TEMPERATURE OPTION AND NUMBER OF TEST SPECIMENS

Two test temperature options are available for use, which are applicable to all rut depth transfer functions: Option A – the multiple test temperature option; and Option B – the equivalent test temperature option. The number of test specimens is dependent on whether the multiple temperature or equivalent temperature option is selected.

G.2.1 Option A – Multiple Test Temperatures

The multiple temperature option uses three test temperatures, defined as: (1) 50 percent reliability PG high temperature minus 5°C, (2) 20°C, and (3) the middle temperature between the first two.

For the multiple test temperature option, 2 test specimens at each temperature are required for a total of six test specimens. The multiple test temperature option should be used for pavement structural designs, during the final mixture design stage, and for detailed forensic investigations.

G.2.2 Option B – Equivalent Test Temperatures

The equivalent temperature option uses one test temperature that is defined as the equivalent annual or representative temperature that will result in the same level of rutting at the end of the design period with the rutting predicted using daily temperatures defined for that climate and structure. Determination of the equivalent test temperature is provided in Section 8.2.2.

For the equivalent test temperature option, 3 test specimens are required. The equivalent test temperature option should be used for mixture design verification and acceptance of HMA mixtures during construction.

G.3 TEST SPECIMEN PREPARATION

This section provides guidance on preparing the mixture samples for measuring the plastic strain coefficients. Three types of samples can be used: reconstituted samples, bulk mixture sampled during mixture production, or cores of a sufficient height and diameter. Cores can be tested, but they must satisfy the strict height to diameter ratio requirement specified in AASHTO TP 79. If cores are being tested in accordance with this test method, refer to Section 6.4.5.

The required number of test specimens shall be prepared depending on whether the multiple test temperature or equivalent test temperature option is being used (refer to

Section 5 of this method). All test specimens should be prepared from reconstituted samples of the aggregate and asphalt that are blended and compacted to the volumetric conditions after construction, or bulk mixture sampled during production.

G.3.1 Short Term Aging of the Asphalt Concrete Mixture

The test specimen preparation process for reconstituting the materials includes the short-term aging procedure to simulate asphalt concrete production. Mixture for all specimens should be short-term oven aged for 4 hours at 135°C in accordance with AASHTO R 30, *Mixture Conditioning of Hot Mix Asphalt (HMA)*, prior to compaction.

The short term aging procedure should not be used on test specimens prepared from bulk mixture sampled during construction or on cores for obvious reasons (they already include short term aging).

G.3.2 Specimen Compaction

Specimens for triaxial testing are fabricated in accordance with AASHTO PP 60, *Preparation of Cylindrical Performance Test Specimens Using the Superpave Gyrotory Compactor*. This is the specimen fabrication standard developed for making specimens for the AMPT.

The target air void level for laboratory compacted test specimens using the Superpave Gyrotory Compactor shall be the average air void level expected after rolling (the expected mean air void level from construction). This value can be determined from historical records of recent construction projects.

The air void tolerance for all test specimens compacted in the laboratory using the Superpave Gyrotory shall be in accordance with AASHTO TP 79.

All triaxial test specimens shall be prepared in accordance with AASHTO TP 79; *Compaction of Triaxial Test Specimens for Dynamic Modulus and Repeated Load Permanent Deformation Tests*. The test specimen size used in the repeated load triaxial test is 100mm by 150mm. As noted above, materials should be sampled and reconstituted during the mixture design stage or bulk HMA sampled during production.

If cores of sufficient height are recovered for testing, the air voids of the test specimen should be measured in accordance with AASHTO T 269 after the test specimen has been prepared and sized in accordance with AASHTO TP 79.

G.3.3 Grouping of Test Specimens

The air void content for each test specimen should be measured and reported, as noted in sections 6.4.4 or 6.4.5.

When the multiple test temperature option is selected, sort the test specimens into three subsets of two specimens each (or the number of test specimens selected for each test temperature) so that the average air voids of the different subsets are as equal as possible. This requirement applies to laboratory compacted reconstituted mixture and bulk mixture sampled during construction, and cores of sufficient height.

Grouping of the test specimen is not required when the equivalent temperature option is selected because all test specimens are tested at the same test temperature.

G.4 REPEATED LOAD TRIAXIAL TESTING

The dynamic modulus and repeated load triaxial test shall be measured in accordance with AASHTO TP 79, *Determining the Dynamic Modulus and Flow Number for HMA Using the AMPT*, with the following exceptions.

Conditioning Cycles; 100 conditioning cycles shall be applied at the beginning of the repeated load triaxial test. The repeated axial load applied to the test specimen for the conditioning cycles is 10 psi with the use of a confining pressure of 10 psi.

Testing Condition; The repeated axial load and confining pressure for measuring the repeated load plastic strain is listed below.

- Repeated axial load applied to the test specimen is 70 psi.
- Confining pressure is 10 psi.

The plastic and total strains should be measured and stored in the data acquisition system in accordance with AASHTO TP 79. Figure G.1 shows a graphical example of the test results – cumulative plastic strain versus number of repeated axial loads or repetitions.

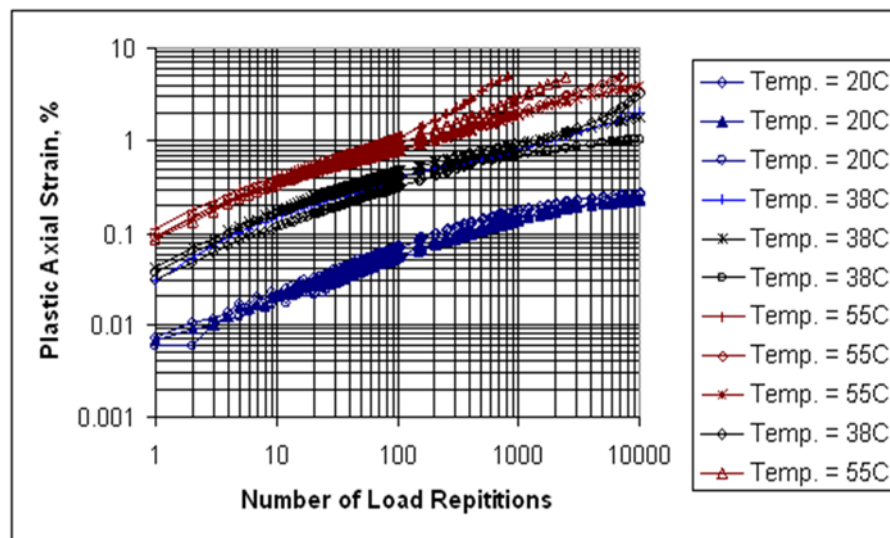


Figure G.1. Test Results from a Repeated Load Triaxial (Confined) Plastic Strain Test

G.5 DETERMINATION OF PLASTIC STRAIN COEFFICIENTS

This part of the standard explains the determination of the plastic strain coefficients for the Kaloush vertical strain rut depth transfer function.

Kaloush-Witzcak Vertical Resilient Strain Transfer Function: The following equation is the plastic strain relationship included in the MEPDG software to predict rut depth in the HMA layer increments.

$$\varepsilon_p = \varepsilon_r K_Z \beta_{r1} 10^{k_{r1}} (T)^{k_{r2} \beta_{r2}} (N)^{k_{r3} \beta_{r3}} \quad (G.1)$$

Where:

ε_p = Incremental plastic strain at the mid-depth of a thickness increment.

ε_r = Resilient strain calculated at the mid-depth of a thickness increment.

T = Temperature at the mid-depth of a thickness increment.

N = Number of axle load applications of a specific axle type and load interval within a specific time interval.

$\beta_{r1}, \beta_{r2}, \beta_{r3}$ = Local calibration coefficients, all equal to 1.0 for the global calibration effort and within NCHRP Project 9-30A.

k_{r1} = Plastic strain factor or coefficient (for the global calibration effort under NCHRP Project 1-40D, the coefficient equals -3.35412).

k_{r2} = Plastic strain factor related to the effect of temperature on the intercept (for the global calibration effort under NCHRP Project 1-40D the temperature exponent equals 1.5606).

k_{r3} = Plastic strain factor related to the effect of wheel load (for the global calibration effort under NCHRP Project 1-40D, the loading cycles exponent equals 0.4791).

K_Z = Depth function and equal to:

$$K_Z = (C_1 + C_2 D)(0.328196)^D \quad (G.2)$$

$$C_1 = -0.1039H_{HMA}^2 + 2.4868H_{HMA} - 17.342 \quad (G.3)$$

$$C_2 = 0.0172H_{HMA}^2 - 1.7331H_{HMA} + 27.428 \quad (G.4)$$

D = Depth to the mid-depth of the thickness increment, inches.

H_{HMA} = Total thickness of the asphalt concrete layer, inches.

The plastic strain factors (k_{r1} , k_{r2} , and k_{r3}) are determined from repeated load plastic strain tests conducted in the laboratory and adjusted to field conditions. The k_{r3} factor is the slope within the steady state or secondary region, while the k_{r1} is the intercept of the log-log relationship between the number of load applications and cumulative plastic strain. The k_{r2} factor is the effect of temperature on the intercept. The k_{r1} and k_{r3} coefficients are graphically illustrated in Figure G.2.

G.6 HMA MIXTURE EVALUATION PROCEDURE

The steps for determining the plastic strain coefficients from a repeated load triaxial test to evaluate the rutting resistance of asphalt concrete mixtures are included in this section. Two options are available, each of which is discussed separately.

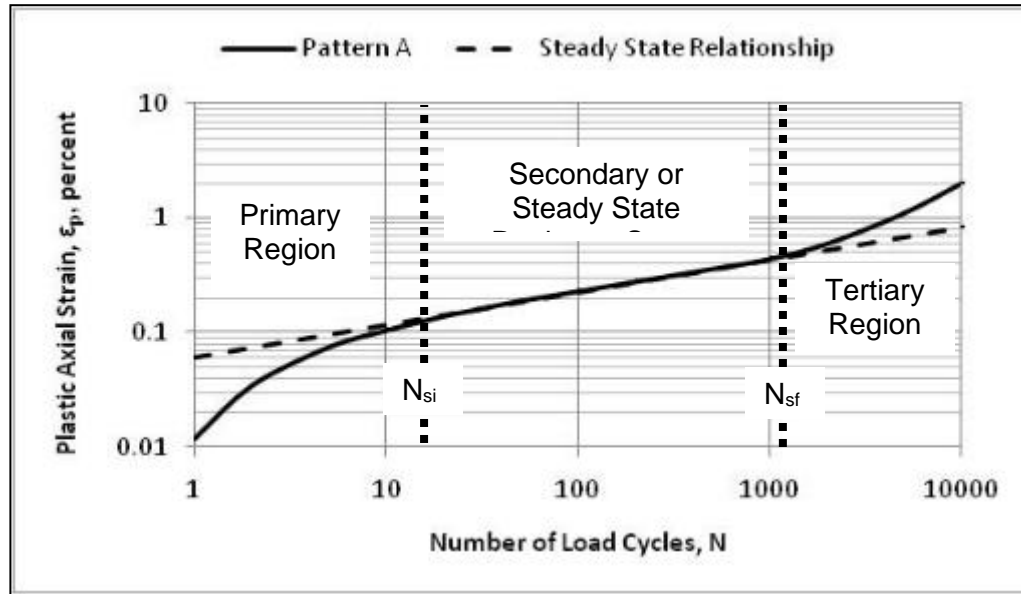


Figure G.2. Accumulation of Plastic Axial Strain Measured in the Laboratory – Defined as Pattern A (Extracted from NCHRP Report #719)

G.6.1 Option A—Multiple Temperature Option

The multiple temperature option uses three test temperatures, defined as: (1) 50 percent reliability PG high temperature minus 5°C, (2) 20°C, and (3) middle range temperature between the first two.

1. Determine the laboratory-derived slope or m-value of the steady state or secondary region for each test specimen. The steady state region is the area where the slope or m-value becomes constant between the number of loading cycles and accumulated plastic strain (refer to Figures G.2 and G.3).
 - a. The average steady state slope for laboratory repeated load tests should be determined based on a moving decade of loading cycles. [For example; 1 to 10, 2 to 20, 3 to 30, ...; 10 to 100, 20 to 200, 30 to 300, ...; 100 to 1000, 200 to 2000, 300 to 3000, ...; etc.] Once the slope becomes constant, defined as the steady state region of the laboratory test, that value represents the exponent for the load cycle term (N) of the rut depth transfer functions or m-value (Figure G.3 is an illustration of this response – Pattern B).
 - b. Two other opposite possibilities exist over the entire number of loading cycles for the laboratory repeated load tests; (1) the slope continues to decrease over the entire number of loading cycles, and (2) the slopes starts to increase at an increasing rate. Figures G.2 (Pattern A) and H.4 (Pattern C) are illustrations of these responses. Determining the slope for these conditions is discussed in the following paragraphs.

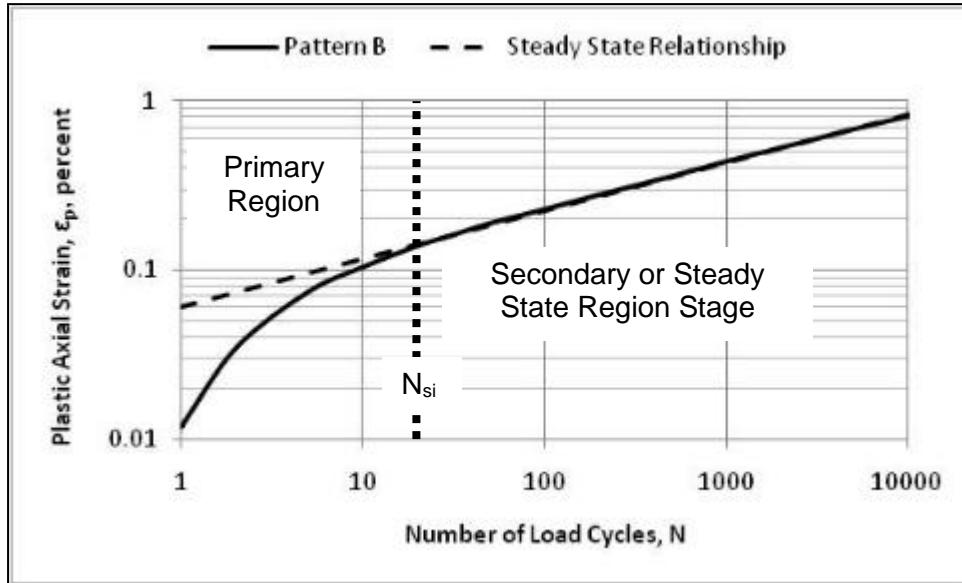


Figure G.3. Accumulation of Plastic Axial Strain Defined as Pattern B (Extracted from NCHRP Report #719)

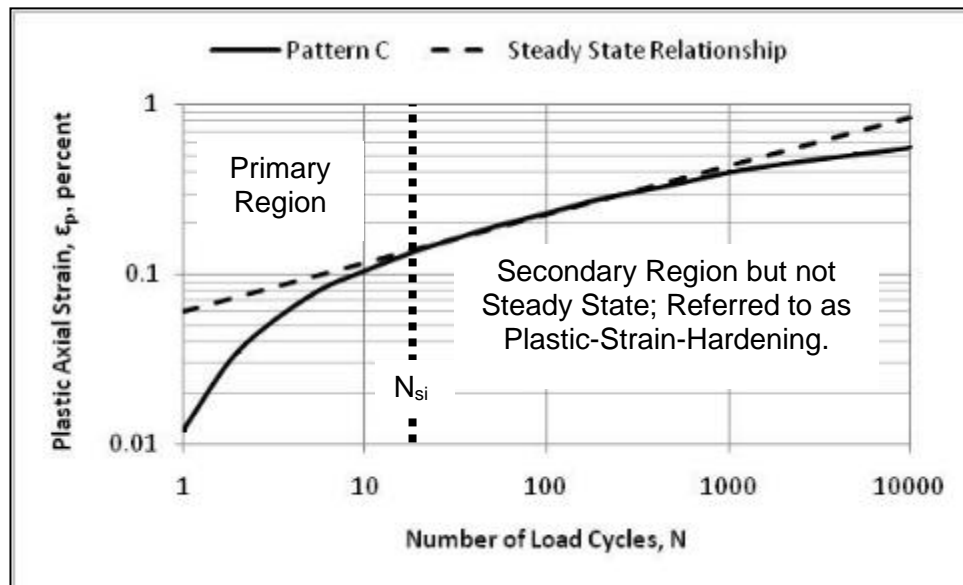


Figure G.4. Accumulation of Plastic Axial Strain Defined as Pattern C (Extracted from NCHRP Report #719)

- i. When a test specimen starts to exhibit continual decrease in plastic strains with continued loading cycles, the average slope should be determined for the region where the change in slope is relatively constant. The m-value for each test specimen is determined between 2,000 and 10,000 axial loading cycles.
- ii. When a test specimen exhibits accelerated plastic deformation (the m-value or slope continually increases at an increasing rate; typically referred to as

tertiary flow), that part of the test should be excluded from determining the m-value in the steady state region of the test.

2. Determine the laboratory-derived m-value or slope from all test specimens. The methodology included in the MEPDG assumes the steady state slope is independent of test temperature. Any change in temperature is accounted for in the temperature exponent of the transfer function and/or through the effects of temperature on dynamic modulus.
 - a. If the slope does not consistently change with test temperature, average all slopes.
 - b. If the slope consistently changes with test temperature (increasing or decreasing with test temperature), determine the representative slope at the equivalent temperature. Equivalent temperature is defined under Option B (Section G.2.2).
3. Determine the laboratory-derived intercept or I_s -value (intercept from the steady state region) for each test specimen and test temperature using equation 5 based on the m-value or slope within the steady state region determined from Step #2.

$$I_s = \log(\varepsilon_p) - m \text{Log}(N) \quad (5)$$

4. Using only the test specimens used to determine the m-value or secondary slope, determine average m-value for all test temperatures.
5. Determine the average I_s -value at each test temperature for the asphalt concrete mixture. The laboratory-derived intercept or I_s -value will be test temperature dependent.
6. Determine the temperature dependency of the intercept through the exponent of the temperature term using equation 6; the exponent to the temperature term should be determined from the laboratory test results of all test specimens and temperatures by fitting the m-value and I_s -value to the data.

$$k_{r2} = \frac{\text{Log}(\varepsilon_p) - I_s - m \text{Log}(N)}{\text{Log}(T)} \quad (6)$$

7. Determine the field matched coefficients for the asphalt concrete mixture by the following.
 - a. Figure G.5 is used to adjust the laboratory-derived average m-value or secondary slope to the “field matched” slope or k_{r3} value.
 - b. Figure G.6 is used to adjust the laboratory-derived average I_s -value or intercept from the steady state region to the “field matched” intercept or k_{r1} value.
 - c. The temperature exponent for the Kaloush transfer function, k_{r2} , is not adjusted from the laboratory measured values. In other words, the laboratory derived temperature exponent is assumed to be equal to the field adjusted temperature exponent.

8. The field matched intercept from Figure G.6 is multiplied by the thickness adjustment factors provided in Table G.1.

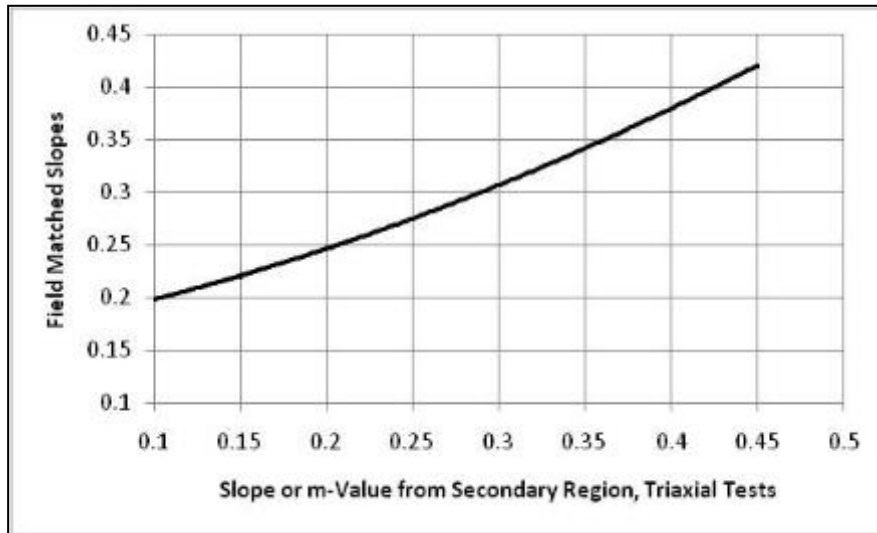


Figure G.5. Determining the Field Matched Slopes from Laboratory-Derived m-Values from Repeated Load Triaxial Tests; Kaloush Transfer Function (Extracted from NCHRP Report #719. The data for this relationship is included in the NCHRP report.)

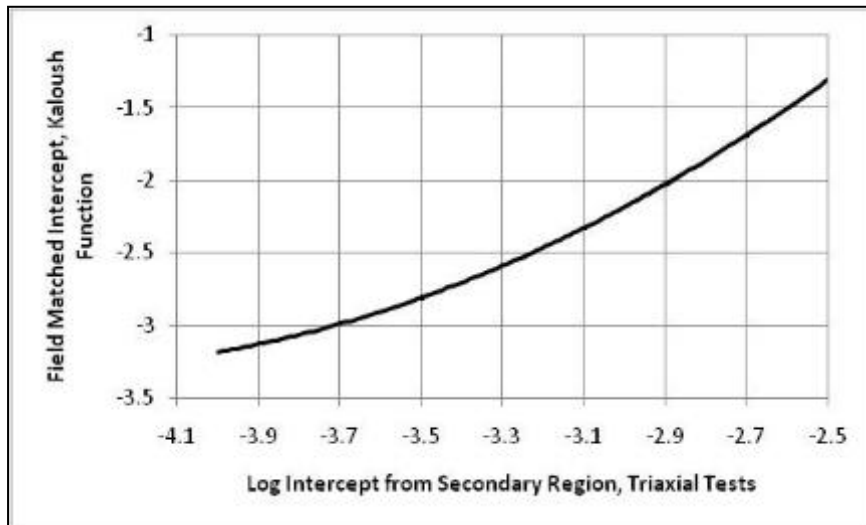


Figure G.6. Determining the Field Matched Intercept from Laboratory-Derived I_s -Values from Repeated Load Triaxial Tests; Kaloush Transfer Function (Extracted from NCHRP Report #719. The data for this relationship is included in the NCHRP report.)

Table G.1. Thickness Adjustment or Shift Factors for Determining the Field Matched Intercept Value of the Transfer Functions

HMA Mixture Application	HMA Layer Thickness, in.	Adjustment Factor for Kaloush Transfer Function
HMA Overlays of PCC or Semi-Rigid Pavements	< 3.0	0.83
	3 to 4	0.90
	> 4.0	1.0
HMA Overlays of Flexible Pavements	< 4.0	1.4
	4 to 6	1.2
	> 6.0	1.0
New Construction, Unbound Aggregate Base or Full-Depth	< 4.0	1.05
	4.0 to 6.0	1.02
	6.0 to 8.0	1.0
	> 8.0	1.0

G.6.2 Option B—Equivalent Test Temperature Option

The equivalent test temperature option uses one test temperature defined as the equivalent annual temperature, which will result in the same level of rutting at the end of the design period with the rutting predicted using temperatures defined for that climate and structure. The following lists the steps and determination of the values for the plastic strain coefficients based on the equivalent temperature concept.

1. Determine the equivalent annual or representative temperature for the climate and structure of the project. Two methods can be used to determine the equivalent or representative temperature for a specific climate and area, as listed below.
 - a. Determine the temperature for the site in accordance with LTPPBind-2.1. The temperature from LTPPBind-2.1 is entered in Figure G.7 and used to estimate the equivalent test temperature.
 - b. Use the MEPDG software to estimate the equivalent test temperature that will result in the same level of rutting for multiple roadway segments using the actual climate data within a specific site or region. This method is considered the more accurate one because it uses the MEPDG rut depth computational methodology directly in determining that temperature and can be completed during the local calibration process. The following paragraphs briefly discuss using the MEPDG software to estimate the equivalent test temperature.
 - a. Determine an initial estimate for the laboratory adjusted transfer function coefficients. The initial values can be extracted from historical data, if available, or the input level 2 values determined for the mixture being evaluated.
 - b. Execute the MEPDG to predict the rut depth over a range of constant temperatures for the trial pavement structure and design truck traffic. Constant temperatures of 10, 20, 40, and 50°C will be sufficient for most climates. These constant temperature files are available within the MEPDG Version 9-30A software. Plot

- maximum predicted rut depth at the end of the design period as a function of temperature (See Figure G.8).
- c. Execute the MEPDG software to predict the rut depth using the actual climatic files and the same default values, trial structure, and design truck traffic used in the above step.
 - d. Use the maximum rut depth predicted over the design period to determine the equivalent annual or representative temperature that results in that same value. In other words, enter Figure G.8 for the example with the predicted rut depth for the actual climatic values to find the single temperature value over the entire design period and design truck traffic. This temperature is defined as the equivalent test temperature for the specific structure, climate, and truck traffic.

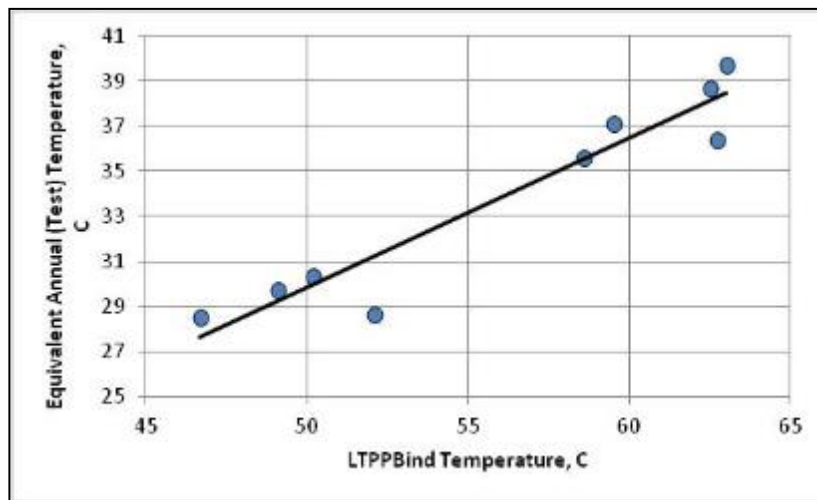


Figure G.7. Graphical Relationship between the LTPPBind2.1 Pavement Temperature and the Equivalent Test Temperature

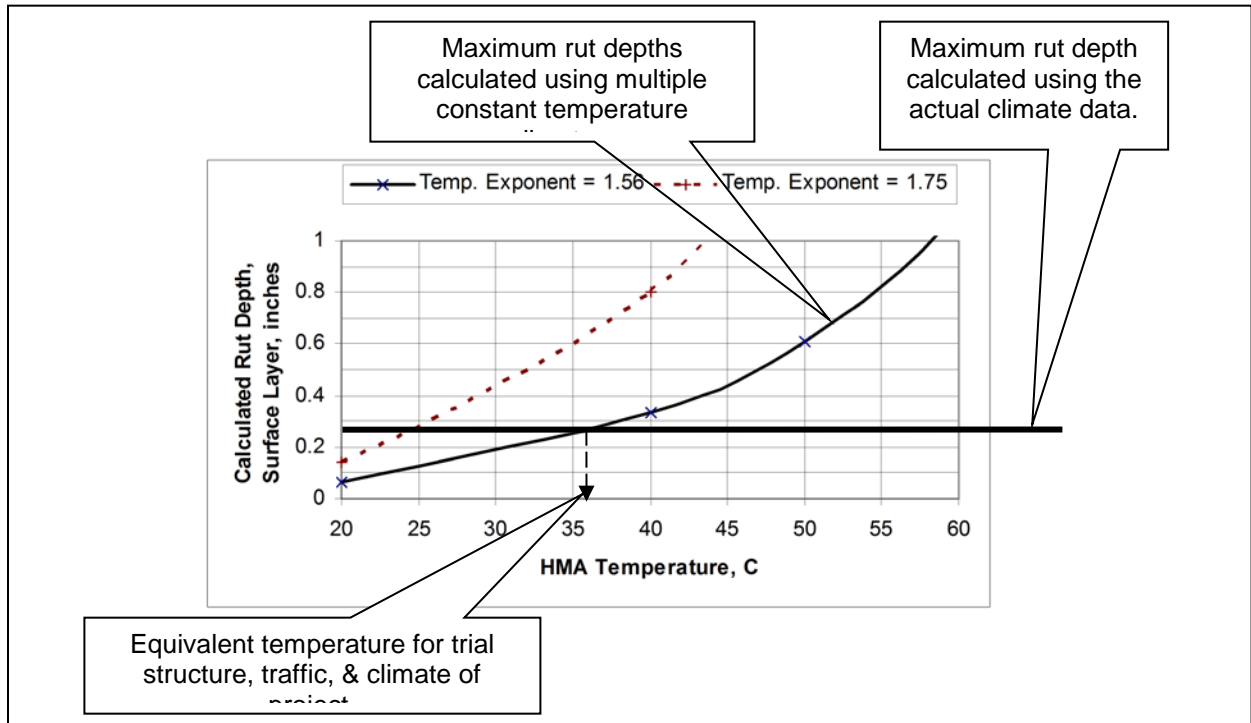


Figure G.8. Example of Rut Depths Predicted with MEPDG (Kaloush Transfer Function) using a Constant Temperature Environment to Estimate the Equivalent Test Temperature

2. Three test specimens are prepared and tested at the defined equivalent test temperature. The test specimens are compacted at the average in place air voids determined by the specifications. This value can be determined from historical records of recent construction projects.
3. Determine the laboratory-derived slope or m-value within the steady state or secondary region for each test specimen in accordance with Step #1.
4. Determine the laboratory-derived intercept or I_s -value from the steady state or secondary region for each test specimen in accordance with Step #3.
5. Determine the average m-value and I_s -value for all test specimens at the equivalent test temperature.
6. Determine the field matched coefficients for the asphalt concrete mixture by the following.
 - a. Figure G.4 is used to adjust the laboratory-derived steady state slope or average m-value to the “field matched” slope.
 - b. Figure G.5 is used to adjust the laboratory-derived intercept or average I_s -value from the steady state region to the “field matched” intercept.

- c. The temperature exponent for the Kaloush transfer function is not adjusted from the laboratory measured values (a constant value of 1.5606 is used for the equivalent temperature concept).
7. The field matched parameters for the intercept are multiplied by the appropriate thickness adjustment factor provided in Table G.1.
8. There will be cases where the equivalent annual or representative temperature for a site or layer may change because of a change in pavement structural design or other reasons. For these cases, the plastic strain coefficients determined from the repeated load triaxial tests at the equivalent test temperature can be adjusted to a higher or lower equivalent test temperature.

G.7 ESTIMATING THE PLASTIC STRAIN COEFFICIENTS FROM VOLUMETRIC PROPERTIES

This section provides a procedure to estimate the plastic strain coefficients from the volumetric properties of the asphalt concrete mixture. This procedure follows the method included in NCHRP Report #719.

G.7.1 Intercept of Transfer Function

The field adjusted, laboratory-derived intercept is required to estimate the transfer function intercept for each transfer function. The recommended relationships to estimate the laboratory-derived intercept from the secondary region of triaxial tests is provided below.

$$I_{Triaxial} = 10^{-3.6} \left(\frac{V_a}{V_{Design}} \right)^{0.52} (Log(VFA))(F_{Index})(C_{Index}) \quad (G.1)$$

Where:

- V_a = In place air voids of the HMA layer, percent.
- V_{Design} = Design air void level for selecting the target asphalt content, percent.
- VFA = Voids Filled with Asphalt, percent.
- C_{Index} = An index number related to the fine aggregate angularity (FAA) of the combined aggregate blend; refer to Table G.2 for the recommended values.
- C_{Index} = An index number related to the coarse aggregate angularity (CAA) of the combined aggregate blend; refer to Table G.2 for the recommended values.

The values from equation G.1 are entered in Figures G.5 and G.6 in the test method to estimate the field matched intercept for the Kaloush transfer function. The field matched values are multiplied by the thickness adjustment factors provided in Table G.1 within the test method for determining the inputs to the MEPDG software.

Table G.2. Aggregate Properties for Determining the Mixture Adjustment Factors

Fine Aggregate	Gradation	Fine Aggregate Angularity; AASHTO T 304				
		<45		>45		
FAA Index Value	External to Restricted Zone	1.0		0.9		
	Through Restricted Zone	1.05		1.0		
Coarse Aggregate	Gradation	Percentage Coarse Aggregate with Two Crushed Faces; AASHTO TP 61				
		0	25	50	75	100
CAA Index Value	Well Graded	1.1	1.05	1.0	1.0	0.9
	Gap Graded	1.2	1.1	1.05	1.0	0.9

G.7.2 m-Value of Transfer Functions

The relationship for estimating the m-value for dense-graded designed aggregate blends is provided in equation G.2.

$$m - Value_{Neat} = 0.265 \left(\frac{P_b}{P_{b(Opt)}} \right)^{0.75} \quad (G.2)$$

Where:

P_b = Asphalt content by weight at construction (the in place value), percent.

$P_{b(Opt)}$ = Saturation or optimum asphalt content by weight, percent. This parameter defines the asphalt content at which the VMA starts to increase or the density of the mixture starts to decrease.

For the use of modified asphalts, the m-value for neat asphalt mixtures is adjusted by equation G.3:

$$m - Value_{Modified} = m_b (m - Value_{Neat}) \quad (G.3)$$

Where:

m_b = An adjustment that accounts for the use of modified mixtures for the same aggregate blend of neat asphalt mixtures and defined below.

For m-values less than or equal to 0.2: $m_b = 1.0$.

For m-values greater than 0.2: $m_b = 0.072 + (m - Value)0.64$ (G.4)

G.7.3 Temperature Term Exponent of Kaloush Transfer Function

The Kaloush transfer function is the only one of the three recommended for use that includes temperature as a dependent variable. The temperature exponent should be set to 1.5606.

G.8 HMA PROPERTIES USED IN DETERMINING LEVEL 2 INPUTS

G.8.1 Design Air Void Content to Select Target Asphalt Content, $V_{a(\text{design})}$

This parameter is determined from mixture design charts (air voids as a function of asphalt content), and is the air void content at the target asphalt content (or the value expected during production of the mixture). Figure H.9 shows an example in determining this value or

parameter for a specific mixture. The reality of this parameter is dependent on how close the laboratory compactive effort simulates the field compaction that occurs under the rollers and truck traffic.

In most cases, the HMA mixture design will be unavailable when the structural design is completed. In this case, it is recommended that an agency's policy on design air void content be used – this will be 4 percent in most cases. However, some agencies now use 3 and 5 percent for some of their mixtures to select the asphalt content for production.

G.8.2 Saturation Asphalt Content by Weight, $P_{b(sat)}$

This parameter is determined from the mixture design charts (mixture density as a function of asphalt content), and is the asphalt content where the density begins to significantly decrease or where the VMA begins to significantly increase. This value is determined in the laboratory and is not a well-defined parameter. Figure G.10 shows an example of a sensitive HMA mixture in determining this value, while Figure G.11 shows an example for a non-sensitive mixture.

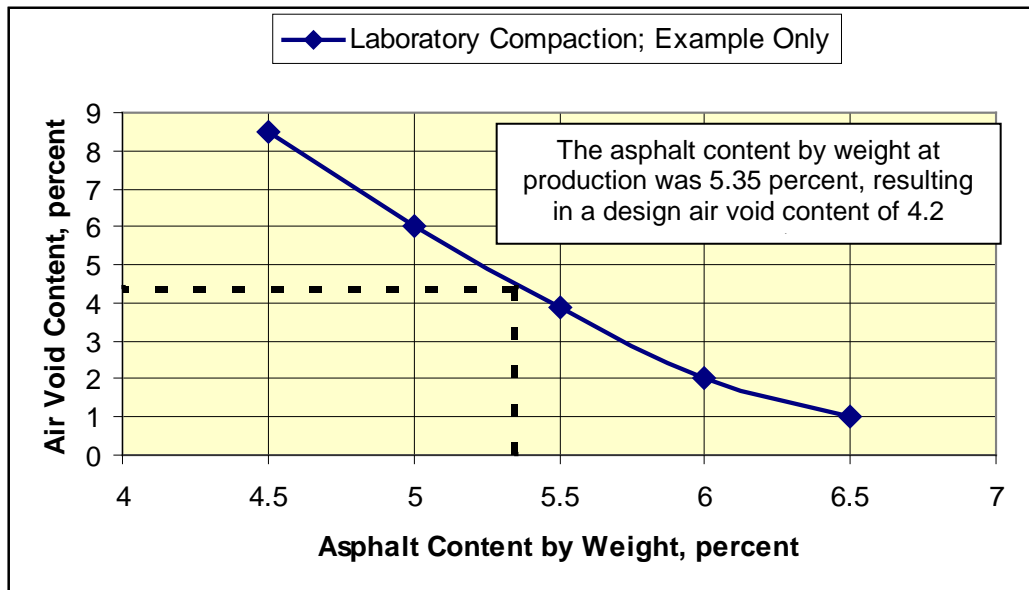
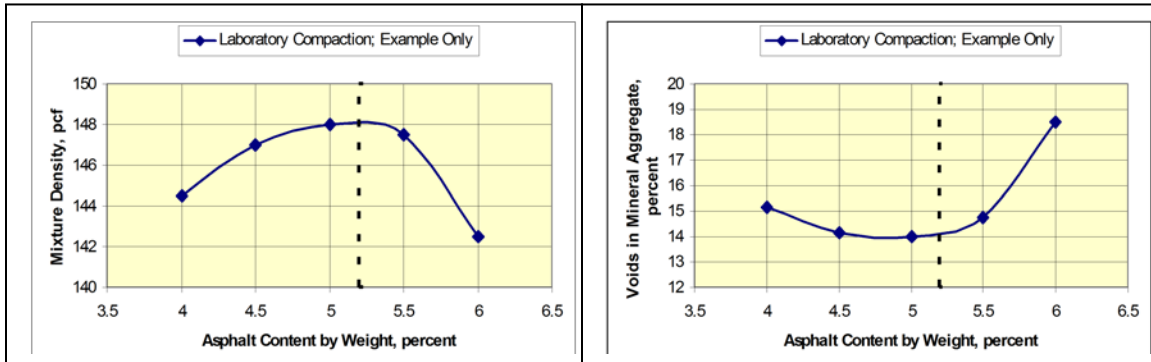


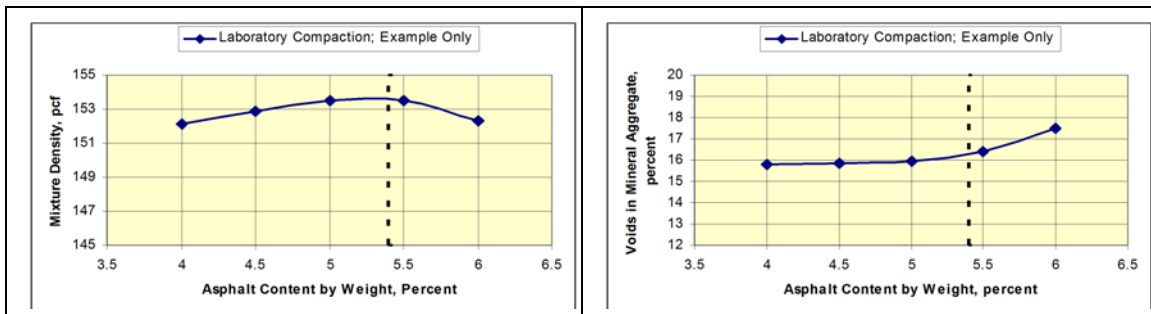
Figure G.9. Graphical Example Determining the Design Air Void Content from the Laboratory Mixture Design Chart

In most cases, the saturation asphalt content will be unknown when the structural design is completed. In this case, it is recommended that previous mixture design records be reviewed to select a reasonable ratio between the target asphalt content and saturation asphalt content by weight. This value generally varies from 0.90 to 1.0 for HMA mixtures that are resistant to rutting. The asphalt content where the density begins to significantly decrease and VMA begins to significantly increase should never be selected for mixtures to be placed on higher volume roadways.



The saturation asphalt content is defined as 5.2 percent by weight for this example, because the mixture density begins to significantly decrease and the VMA starts to increase at about that value.

Figure G.10. Graphical Example Determining the Saturation Asphalt Content from the Laboratory Mixture Design Chart for a Sensitive Mixture



The saturation asphalt content is defined as 5.4 percent by weight for this example, because the VMA starts to increase at about that value. The HMA density also starts to decrease at asphalt content slightly above that value.

Figure G.11. Graphical Example Determining the Saturation Asphalt Content from the Laboratory Mixture Design Chart for a Non-Sensitive Mixture

This parameter is dependent on the laboratory compaction device and compaction effort used in the laboratory. The assumption is that the laboratory compaction device and effort accurately simulates the compaction from the rollers and truck traffic over time.

G.8.3 Fine Aggregate Angularity Index, F_{Index}

An index number or value related to the fine aggregate angularity (FAA) of the combined fine aggregate of a mixture (refer to Table G.2). The FAA index is entered into the MEPDG software. Most agencies measure the FAA value during mixture design and for aggregate source approval (AASHTO T 304).

G.8.4 Coarse Aggregate Angularity Index, C_{Index}

An index number or value related to the coarse aggregate angularity (CAA) of the combined coarse aggregate of a mixture. Few agencies measure the CAA value in the laboratory (AASHTO T 326), but most do have required limits for the minimum amount of coarse

aggregate with two crushed faces for varying truck volumes (AASHTO TP 61). For high volume roadways, most agencies require 100 percent crushed coarse aggregate. The C_{Index} value, as used in the MEPDG, is related to the amount of crushed coarse aggregate (refer to Table G.2). The CAA index is entered into the MEPDG software.

G.8.5 Estimation of Repeated Load Plastic Deformation Parameters—Input Level 2

The following provides a few notes that should be remembered regarding use of the mixture adjustment factors in predicting rutting of HMA mixtures.

1. These mixture adjustment factors were not optimized in terms of the minimizing the residual errors of the predicted rut depths.
2. The ratio of the actual asphalt content to saturation asphalt content by weight should be less than 1.1 and greater than 0.90. It is possible that this ratio can be greater than 1.1 and less than 0.90 for some mixture designs, because of the differences in compaction devices and compaction effort used in the laboratory. It is recommended that the range of this value be limited to the values listed above because too few data outside that range were included in the initial development of this factor.
3. The design air void content based on the actual asphalt content should be within the range of less than or equal to 5.0 and greater than or equal to 3.0 percent.
4. The C_{Index} values for 0 percent coarse aggregate with two crushed faces was estimated, because all mixtures included in the original evaluation to estimate the C_{Index} value were greater than 50 percent.

G.9 PROCEDURE FOR ADJUSTING THE PLASTIC STRAIN COEFFICIENTS FOR DIFFERENT EQUIVALENT TEST TEMPERATURES

This section of Appendix G provides a procedure for making changes to the plastic strain coefficients for slightly different equivalent temperatures than were used in repeated load triaxial test. Specifically, this appendix under Option B (Equivalent Test Temperature option; Section G.8.2.2) permits the slope and intercept to be corrected based on minor temperature differences between the equivalent and actual test temperatures. The corrections should be limited to temperature differences of no more than 10 °F. The following is a step by step basis for making those corrections.

The temperature influence on the intercept of the secondary region, everything else being equal, is defined by equation H.5:

$$\text{Log}(I_s) = \text{Log}(d) + n\text{Log}(T) \quad (\text{G.5})$$

Where:

I_s = Intercept of the secondary region; see Figures G.4 and G.5.

T = Test temperature, °F.

d, n = Constants (Figure G.12 shows the relationship between d and n for a range of mixtures, test procedures, and types of test specimens.

I_s is determined from repeated load triaxial plastic strain tests at the test temperature using the equivalent test temperature Option B, while T is the test temperature.

The second step is to determine the “*d*” value, which is calculated by equation G.6.

$$\text{Log}(d) = \text{Log}(I_s) - n\text{Log}(T) \quad (\text{G.6})$$

I_s is measured from the repeated load plastic strain test and *T* is the test temperature for that test. The value of “*n*” is assumed to be the average value from similar mixtures tested at three test temperatures or Option A in the test method. Figure H.12 shows the relationship between “*n*” and “*d*” for a wide range of mixtures, test procedures, and type of test specimen. For this evaluation, a constant value of “*n*” was assumed to be 2.0, which represents the mid-range of values shown in Figure H.12 for reconstituted, laboratory compacted test specimens of the repeated load triaxial tests.

The third step is to calculate the *I_s* value for the specific equivalent annual temperature using equation G.6, but with the calculated “*d*” parameter from step b and the actual equivalent annual temperature for the specific location, design period, and HMA thickness.

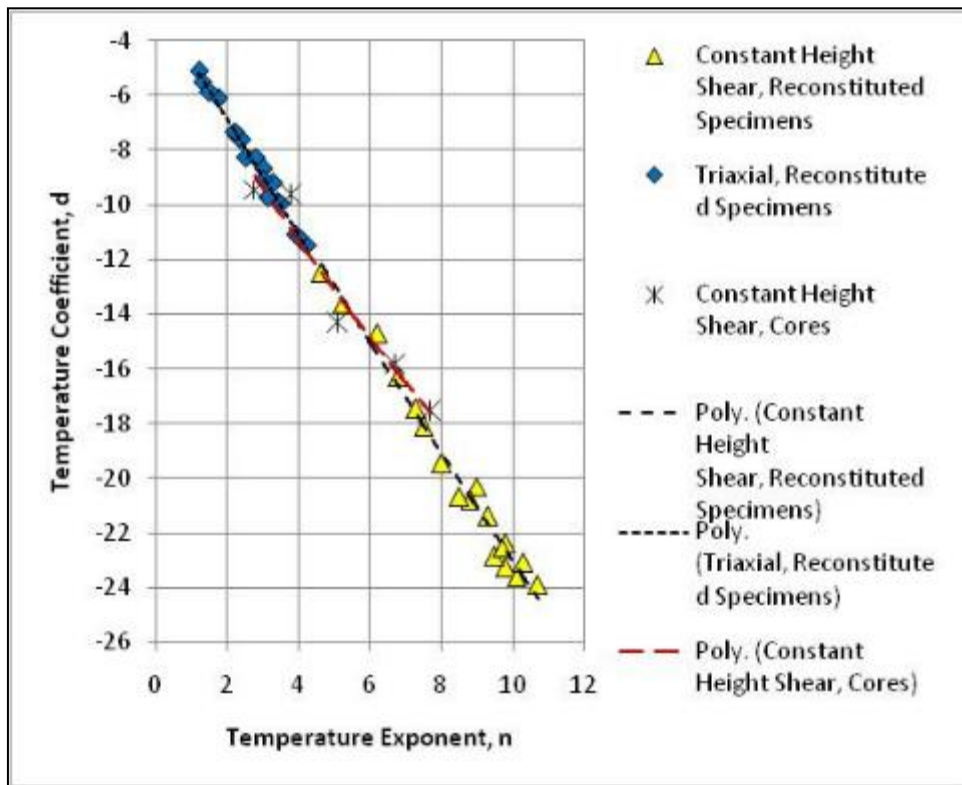


Figure G.12. Relationship of the Temperature Exponent (*n*-value) and Coefficient (*d*-value) for Different Repeated Load Tests (Extracted from NCHRP Report #719)

APPENDIX H—CALIBRATION OF FATIGUE CRACKING (BOTTOM-UP CRACKING) TRANSFER FUNCTION

This appendix covers the use of bending flexural beam tests with the Asphalt Mixture Performance Tester (AMPT) for evaluating the fatigue cracking resistance of dense-graded asphalt concrete mixtures in accordance with the Mechanistic-Empirical Pavement Design Guide (MEPDG) computational methodology.

H.1 INTRODUCTION

The occurrence of bottom-up fatigue cracks is related to the tensile strain at the bottom of the asphalt concrete layer and the stiffness of that layer. The common relationship used to estimate the number of axle load applications to a specific level of cracking is shown below and is based on laboratory repeated load flexural beam tests.

$$N = K_1(E)^{-K_3}(\epsilon_t)^{-K_2} \quad (\text{H.1})$$

The model coefficients of K_1 , K_2 , and K_3 are typically derived from laboratory flexural bending beam tests. All laboratory measured fatigue curves must be adjusted or shifted to account for the inaccuracies in simulating field conditions and crack propagation through the HMA layer. The shifting of laboratory measured fatigue curves is defined as the shift factor and is dependent on the extent and severity level of fatigue cracking that are used to define failure along the roadway. The shift factors that have been reported in the literature vary from 3 to over 100 which are applied to the K_1 coefficient or intercept of the fatigue relationship. Table H.1 summarizes some of the model coefficients that have been reported in the literature.

Flexural beam fatigue tests, however, are expensive and time consuming and rarely used to determine the model coefficients for individual mixtures. There are different relationships that can be used to estimate the fatigue coefficients from repeated load flexural beam tests. The Virginia DOT was one of the first agencies to estimate the coefficients from the indirect tensile strength test. The indirect tensile test was the primary test used to estimate the model coefficients as part of the AAMAS procedure (NCHRP Report 338) which was the precursor to the SHRP studies and NCHRP 1-37A.

H.2 RELATIONSHIPS TO DERIVE FATIGUE COEFFICIENTS

Figure H.1 shows the test results from the indirect tensile tests for many different asphalt concrete mixtures for both laboratory and field aged specimens. The following identifies some of the relationships used in the HMA mixture evaluation for fatigue strength and determining the coefficients of the fatigue model. Using results from the indirect tensile strength tests the model coefficients can be estimated.

Table H.1. Comparison of Fatigue Cracking Equation Model Coefficients

Fatigue Equation	Response Parameter	Fatigue Constants			Other Parameters in Equation	Definition of Failure, % Cracking
		Coefficient, K_1	Response Exponent, K_2	HMA Modulus Exponent, K_3		
Shell (1978)	ϵ_t	0.0685	-5.671	-2.363	Dynamic modulus	50
Asphalt Institute (DAMA, 1982)	ϵ_t	0.0796	-3.291	-0.854	Dynamic modulus Percent air voids Percent asphalt by volume, effective	20
PDMAP (Finn et al., 1973 & 1986)	ϵ_t	6.601×10^{14}	-3.291	-0.854	Flexure modulus	Lab, Crack Initiation
	ϵ_t	8.851×10^{15}	-3.291	-0.854	Flexure modulus	10
	ϵ_t	1.219×10^{16}	-3.291	-0.854	Flexure modulus	45
Cost Allocation (Rauhut et al., 1984)	ϵ_t	$f(E_t)$	$f(K_1)$	0.000	Indirect tensile resilient modulus	$f(DI)$
TRRL (Powell, 1984)	ϵ_t	1.66×10^{-10}	-4.32	0.000		---
Illinois, Full-Depth (Thompson, 1987)	ϵ_t	5.00×10^{-6}	3.00	0.000		---
Illinois (Thompson, 1987 & 1985)	Δ	5.60×10^{11}	-4.60	0.000		
Ontario	ϵ_t	8.86×10^{-14}	-5.12	0.000	Dynamic modulus	20
Virginia (Maupin et al., 1976)	ϵ_t	$f(\sigma_t)$	$f(\sigma_t)$	0.000	Indirect tensile strength @ 70F	NA

$$N_f = K_1 (\epsilon_t)^{K_2} (E)^{K_3}$$
 E_R = Repeated load resilient modulus measured by the indirect tensile test.
 Δ = Deflection; ϵ_t = Tensile Strain; ϵ_v = Vertical Strain; σ_t = Tensile Stress

AASHTO MEPDG Fatigue Relationship:

$$\text{Log}(\epsilon_f) = \frac{K_1 - K_3(\text{Log}E^*)}{K_2} \quad (\text{H.2})$$

Where:

- K_1 = 0.00227
- K_2 = 3.95
- K_3 = 1.28

FHWA Cost Allocation Fatigue Relationship:

$$\text{Log}(\varepsilon_f) = \frac{\text{Log}\left(7.87 \times 10^{-7} \left(\frac{E_T}{E_R}\right)^{-4}\right)}{1.35 - 0.252 \text{Log}\left(7.87 \times 10^{-7} \left(\frac{E_T}{E_R}\right)^{-4}\right)} \quad (\text{H.3})$$

AASHTO Fatigue Relationship from NCHRP Project 1-10B:

$$\text{Log}(\varepsilon_f) = \frac{16.48 - 0.854(\text{Log}(E^*/10^5))}{3.291} \quad (\text{H.4})$$

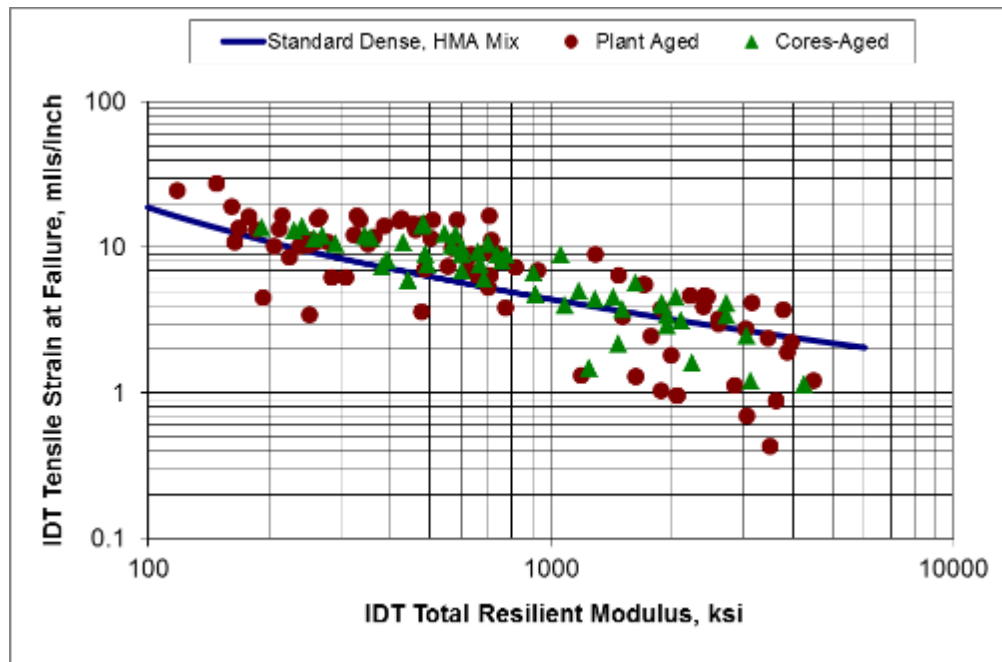


Figure H.1. Relationship between Dynamic Modulus and Tensile Strain at Failure for Estimating the Fracture Coefficients of Asphalt Concrete

Figure H.2 shows the relationship between modulus and tensile strain at failure for the three above relationships. The MEPDG relationship is the more common one used and can be used to estimate the coefficients of the fatigue relationship from the indirect tensile strength.

H.3 PROCEDURE TO DERIVE FATIGUE CRACKING MODEL COEFFICIENTS FROM THE INDIRECT TENSILE STRENGTH TEST

The following summarizes the procedure used to derive or estimate the model coefficients from the indirect tensile strength test.

1. Measure the dynamic modulus of the mixture at three different temperatures using the indirect tensile test. The three temperatures that have been used include: 40, 60, and 80 °F.
2. Measure the tensile strain at failure using the indirect tensile strength test in accordance with the procedure included in NCHRP Report 338 at the same three test temperatures using a constant loading rate of 2 inches per minute. The tensile strain at failure for the higher test temperature is determined at the 95 percent peak or maximum load of the specimen.
3. Using equation H.2, determine the model coefficients of K_1 , K_2 , and K_3 using regression analysis. The model coefficients represent an estimate from the flexural beam tests.

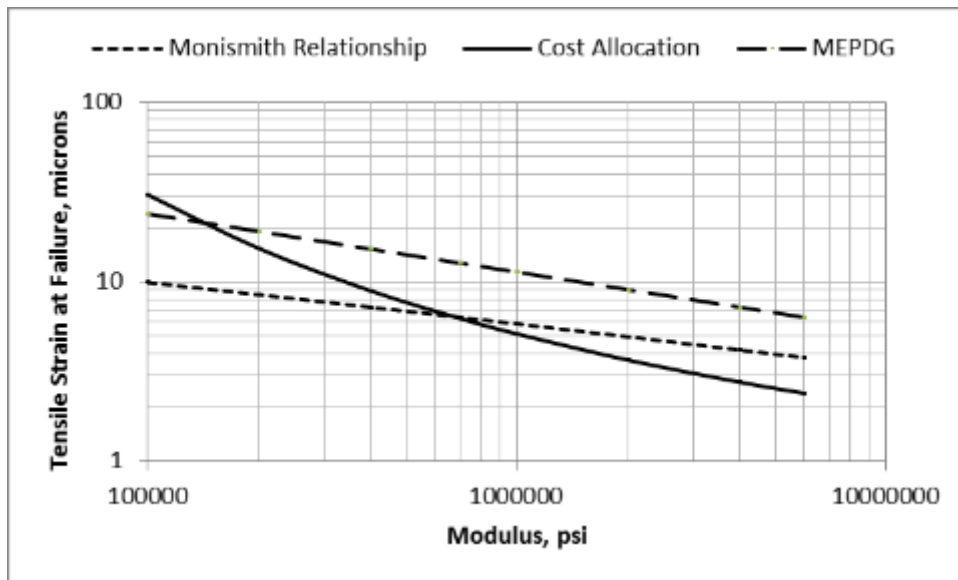


Figure H.2. Comparison of Relationship between Dynamic Modulus and Tensile Strain at Failure for Three Fatigue Equations

Examples from testing four dense-graded mixtures are shown in Figures H.3 to H.6 using the indirect tensile strength test. The data within each figure was regressed to determine the model coefficients of the MEPDG fatigue equation (see equation H.2). Table H.2 summarizes the model coefficients estimated for these four mixtures. The model coefficients listed in Table H.2 are used as the initial values, but the volumetric properties are significantly different between the different mixtures. Figure H.7 shows the comparison of

laboratory fatigue relationships after they have been normalized to the same volumetric properties.

The K_1 value is shifted or adjusted to match the measured area of fatigue cracking for the individual test sections. The shift factor is determined for each test section and analyzed or evaluated to determine if those values are dependent on any factor included in the sampling matrix or some other mixture and structural property.

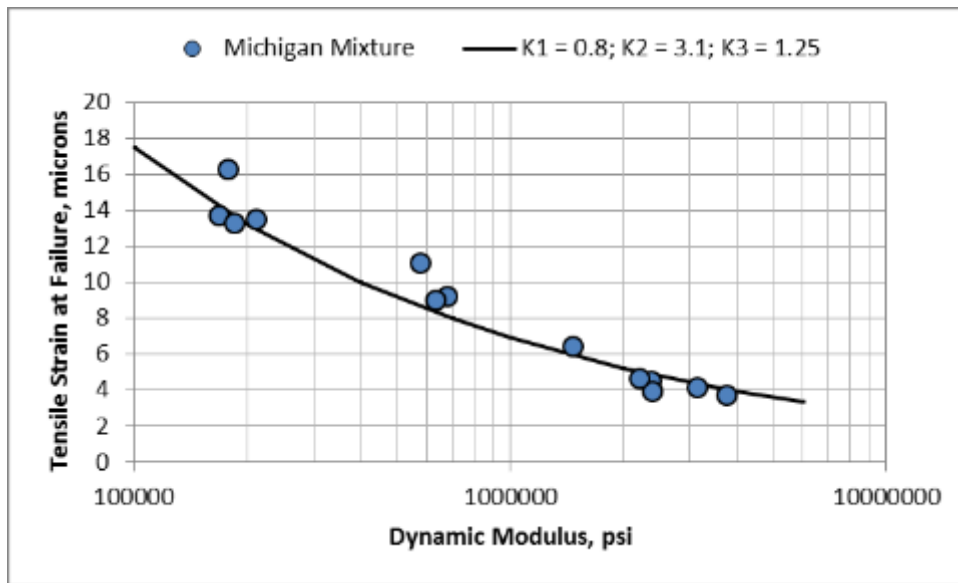


Figure H.3. Estimating Fatigue Cracking Coefficients from the Indirect Tensile Strength and Modulus Tests; Michigan Mixture

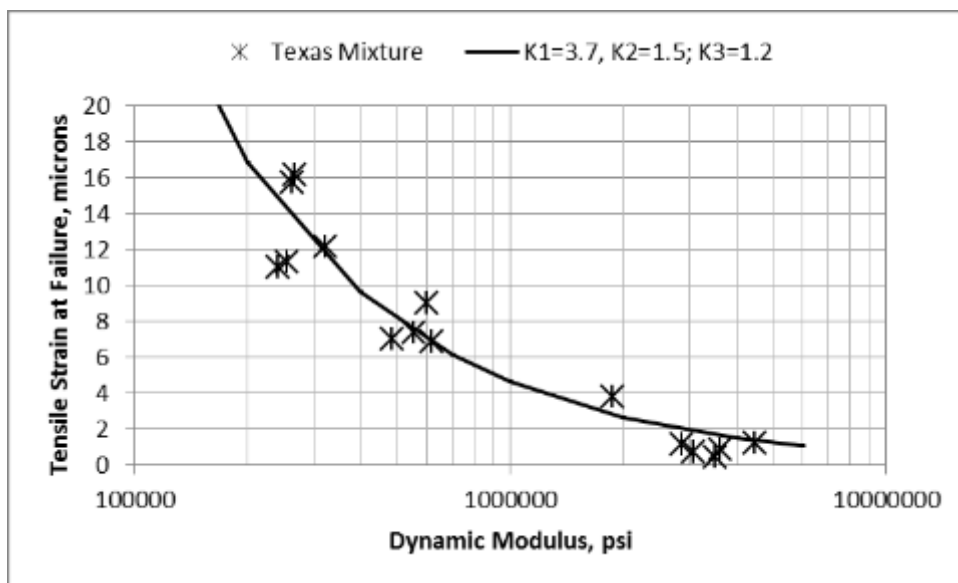


Figure H.4. Estimating Fatigue Cracking Coefficients from the Indirect Tensile Strength and Modulus Tests; Texas Mixture

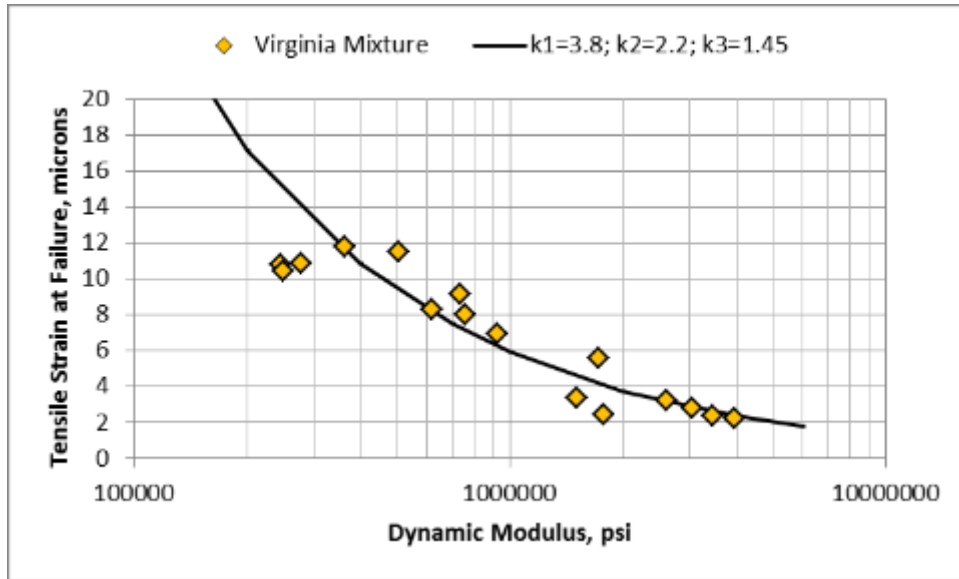


Figure H.5. Estimating Fatigue Cracking Coefficients from the Indirect Tensile Strength and Modulus Tests; Virginia Mixture

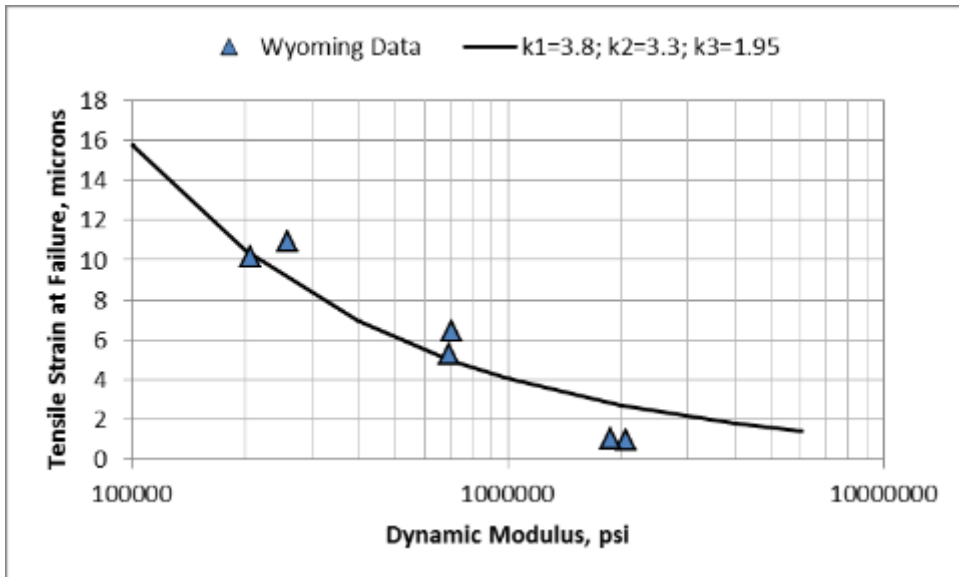


Figure H.6. Estimating Fatigue Cracking Coefficients from the Indirect Tensile Strength and Modulus Tests; Wyoming Mixture

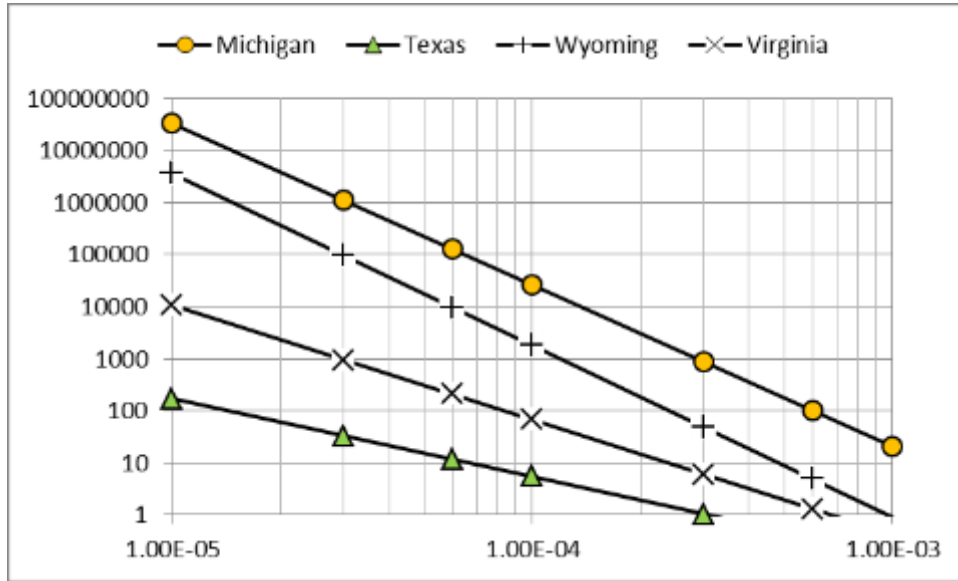


Figure H.7. Fatigue Relationships from the Indirect Tensile Strength Test and Normalized to Equal Volumetric Properties

Table H.2. Model Coefficients Regressed Using Equation H.2

Mixture	Model Coefficients; Equation H.2		
	K_1	K_2	K_3
Michigan	0.80	3.1	1.25
Texas	3.7	1.5	1.2
Virginia	3.8	2.2	1.45
Wyoming	3.8	3.3	1.95